UNIVERSITY OF PARDUBICE

FACULTY OF CHEMICAL TECHNOLOGY

Department of Physical Chemistry

Vanadium catalysts anchored on mesoporous support in oxidative dehydrogenation of *n*-butane

DOCTORAL THESIS

Author: Ing. Michal Setnička

Supervisor: Doc. Ing. Pavel Čičmanec, Ph.D.

2013

I hereby confirm that I have written this doctoral thesis independently. All the reference literature and information used in the thesis are quoted in the list of reference literature.

I hereby acknowledge that all the rights and duties resulting from Act N. 121/2000 Sb., the Copyright Act, apply to my written work, especially that the University of Pardubice has the right to make a license agreement of use of this written work as a school work pursuant to § 60 section 1 of the Copyright Act. On the condition that the written work shall be used by me or a license shall be provided to another subject for the use hereof, the University of Pardubice shall have the right to require from me a relevant contribution to reimburse the costs incurred for the making of such work including all relevant costs and total overall expenditure and expenses incurred.

I express my consent with making the work accessible in the University Library.

Dated in Pardubice on 16. April 2013

First of all, I would like to thank my supervisors Dr. Pavel Čičmanec and Dr. Roman Bulánek for their guidance, constructive scientific criticism and financial support throughout the whole period of my Ph. D. study.

I would like to thank to my colleagues from catalytic part of our department for their friendship, assistance and many fruitful discussions. Many thanks belong also to my colleagues from Jaroslav Heyrovský Institute of Physical Chemistry, ASCR for helping with samples preparation and textural characterization.

Last but not least, I would like to thanks to all members of my family and my girlfriend for their love, patience and support during my studies.

Abstract

The introduced doctoral thesis deals with the study of structural properties and catalytic performance of vanadium oxidic species (VO_X) containing high surface mesoporous silica materials in oxidative dehydrogenation of *n*-butane (C_4-ODH) to corresponding alkenes. The ODH of *n*-butane could be good alternative to classical dehydrogenation, steam cracking and fluid catalytic cracking processes which have some limitations and they are expected to be insufficient to supply increasing demand for olefins in the coming years. The thesis consists of 7 papers complemented by introduction and discussion of main results.

The main aim was investigation of the influence of VO_X species structure and their surface dispersion on silica based materials to catalytic activity in C_4-ODH reaction. Many experimental techniques were used for deep characterization of catalysts. The XRD, SEM and N_2-adsorption were used for the study of texture and H_2-TPR, DR UV–vis and Raman spectroscopy for determination of VO_X complex speciation. The most valuable method for determination of vanadium speciation seems to be a new methodology of the measurement and evaluation of DR UV–vis spectra which was developed during this thesis. The suggested methodology utilizes the benefit of the well resolved absorption bands in the UV–vis spectra of samples which were highly diluted by pure silica. By combination of the results obtained from characterization and from measurement of catalytic activity, we can conclude that the highest activity and selectivity to alkenes is reached on materials with high content of monomeric VO_X units with the tetrahedral coordination.

The second aim of this thesis was optimization of catalysts for high catalytic performance in C_4-ODH, which is necessary for using in industry. The effect of mesoporous silica support (HMS, SBA-15, SBA-16, MCM-48) differing in porous structure, the two different method for incorporation of vanadium (the wet impregnation and direct synthesis) and the effect of titanium incorporated as support modificator into silica was studied for this purpose. The best catalyst seems to be V_*SBA-15* catalysts prepared by direct synthesis, which exhibits high butenes productivity (1.9 $kg_{prod.}kg_{cat.}^{-1}h^{-1}$) and sufficient selectivity. If the productivity is used as a criterion of catalytic performance this material belongs to the three best catalytic systems reported for C_4-ODH ever.

Keywords: mesoporous silica, DR UV–vis spectroscopy, oxidative dehydrogenation (ODH), vanadium oxide species, butenes

Abstract in Czech

Tato doktorská práce se zabývá charakterizací vanad obsahujících mesoporézních silikátů a studiem jejich katalytických vlastností v oxidativní dehydrogenaci *n*-butanu (C_4-ODH) na odpovídající alkeny. Oxidativní dehydrogenace by mohla být vhodnou alternativou k dnes běžně požívané dehydrogenaci nebo fluidnímu katalytickému krakování, které mají své limity, a navíc se očekává, že stávajícími procesy nebude do budoucna možné pokrýt stále rostoucí poptávku po nenasycených uhlovodících. Tato práce se skládá ze 7 odborných publikací doplněných o úvodní text a diskusi hlavních závěrů.

Hlavním cílem této práce bylo detailní studium vlivu struktury VO_X částic a jejich disperze na povrchu silikátového nosiče na katalytickou aktivitu v C_4-ODH reakci. Pro charakterizaci materiálů byla použita řada experimentálních technik. Mezi nejčastěji používané patřily XRD, SEM a adsorpce N_2, které sloužily pro ověření struktury a morfologie připravených materiálů. Pro určení struktury a stupně disperze VO_X komplexů na povrchu nosiče bylo použito H_2-TPR, DR UV–vis a Ramanova spektroskopie. Neužitečnější metodou pro studium struktury VO_X částic se zdá být DR UV–vis spektroskopie měřená pomocí nové metodologie, která byla vyvinuta v rámci této disertační práce a je založena na měření vzorků, které jsou ředěny čistou (bílou) silikou. Takto získaná spektra mají dobře rozlišitelné jednotlivé adsorpční pásy a jejich intenzita je přímo úměrná koncentraci, což umožňuje semi-kvantitativní analýzu. Na základě kombinace výsledků získaných z charakterizace a z katalytických testů můžeme říci, že nejvyšší aktivitu a selektivitu na žádané alkeny je možné získat na materiálech s vysokým obsahem monomerních VO_X částic s tetraedrální koordinací.

Druhým úkolem této práce byla optimalizace katalyzátorů pro vysoký výkon v C_4-ODH, který je nutný pro případnou průmyslovou aplikaci. Za tímto účelem byl studován vliv struktury nosiče (HMS, SBA-15, SBA-16, MCM-48), vliv způsobu nanášení vanadu (přímá syntéza, impregnace z roztoku) a efekt přídavku titanu do silikátové matrice. Nejlepším katalyzátorem se zdá být materiál V_*SBA-15* připravený přímou syntézou, který má vysokou produktivitu (1.92 $kg_{prod.}kg_{cat.}^{-1}h^{-1}$) a dostatečnou selektivitu. Svými parametry se navíc řadí mezi tři nejlepší katalyzátory pro C_4-ODH, které byly uvedeny v literatuře.

Klíčová slova: mesoporézní silika, DR UV–vis spektroskopie, oxidativní dehydrogenace (ODH), vanadové oxo-částice, buteny

List of papers

This doctoral thesis is written in the form of commented set of scientific papers. The publications presented here were composed in years 2009-2013 at the Department of Physical Chemistry, Faculty of Chemical Technology, University of Pardubice and in collaboration with Jaroslav Heyrovský Institute of Physical Chemistry, Academy of Sciences of the Czech Republic, Prague. The corresponding author is underlined.

I) M. Setnička, P. Čičmanec, R. Bulánek
DR UV–vis and H_2-TPR characterization of the supported vanadium oxide catalysts
10th Pannonian international symposium on catalysis, Kraków, Poland, 45-51, 2010
ISBN 978-83-929430-4-4

II) R. Bulánek, L. Čapek, M. Setnička, P. Čičmanec
DR UV–vis Study of the Supported Vanadium Oxide Catalysts
The Journal of Physical Chemistry C, **115**, 12430-12438, 2011

III) R. Bulánek, P. Čičmanec, M. Setnička
Possibility of VOx/SiO_2 complexes speciation: comparative multi-wavelength Raman and DR UV–vis study
Physics Procedia, DOI: 10.1016/j.phpro.2013.04.024, 2013

IV) M. Setnička, R. Bulánek, L. Čapek, P. Čičmanec
n-Butane oxidative dehydrogenation over VO_X HMS catalyst
Journal of Molecular Catalysis A: Chemical, **344**, 1-10, 2011

V) R. Bulánek, A. Kalužová, M. Setnička, A. Zukal, P. Čičmanec, J. Mayerová
Study of vanadium based mesoporous silicas for oxidative dehydrogenation of propane and n-butane
Catalysis Today, **179**, 149-158, 2012

VI) M. Setnička, P. Čičmanec, R. Bulánek, A. Zukal, J. Pastva

V-SBA-15 prepared by direct synthesis as high performing catalyst in oxidative dehydrogenation of n-butane

Catalysis Communications, under revision

VII) M. Setnička, P. Čičmanec, R. Bulánek, A. Zukal, J. Pastva

Hexagonal mesoporous titanosilicates as support for vanadium oxide – Promising catalysts for the oxidative dehydrogenation of n-butane

Catalysis Today, **204**, 132-139, 2013

Results of our research were presented by 3 oral and 23 poster presentations on 19 international scientific meetings.

Table of Contents

List of figures

List of tables

Symbols and abbreviations

BASF	Badische Anilin & Soda Fabrik
ASCR	Academy of Sciences of the Czech Republic
BET	Brunauer-Emmet-Teller's adsorption isotherm
$C_{4\text{-deh.}}$	desired products of C_4-ODH reaction (1-butene, *cis*- and *trans*-2-butene and butadiene)
CVD	chemical vapor deposition
DH	dehydrogenation
EO	ethylene glycol
eV	electronvolt (energy equals to $1.602176565 \cdot 10^{-19}$ J)
$F(R_\infty)$	Kubelka–Munk function $F(R_\infty) = (1- R_\infty)^2/2 R_\infty$, where R_∞ denotes integral reflectivity of semi-infinite layer
FCC	fluid catalytic cracking
FT–IR	Fourier transformed infra red
HMS	hexagonal mesoporous silica
IEP	isoelectric point
IUPAC	International Union of Pure and Applied Chemistry
LCT	liquid crystal templating
LLDPE	linear low density polyethelene
LPG	liquefied petroleum gas
MCM	Mobil Composition of Matter (first series of mesoporous materials)
MEK	methyl ethyl ketone
MSU	Michigan State University material
MTBE	methyl *terc*-butyl ether
ODH	oxidative dehydrogenation
SBA	secondary butyl alcohol
SBA-15	Santa Barbara Amorphous type material – synthesis number 15
SDA	structure directing agent
TEOS	tetraethyl orthosilicate
TOF	turn over frequency
TOS	time on stream
UDD	ultradispersed diamonds

1 Introduction

The today's definition of catalyst is given by the IUPAC (International Union of Pure and Applied Chemistry) like „a substance that increases the rate of a reaction without modifying the overall standard Gibbs energy change in the reaction" [2]. However, the term catalysis was already coined by Swedish chemist Jöns Jacob Berzelius in 1835 [3] and the beginning of industrial catalyst technology was about 1875 with large-scale production of sulphuric acid on platinum catalysts. Next very important historic milestones in catalysis were Haber–Bosch process for industrial production of ammonia in the year 1913, catalytic cracking was a significant development for petroleum industry in the year 1937 or catalytic naphtha reforming led to dehydrogenation and isomerization processes in the year 1950 [3, 4]. Currently the catalysis plays an important role in up to 90% of the world's chemical processes and we can say that without catalysts our civilization as we know it today would not exist [3]. The current widespread use of catalysts does not implicate the impossibility of their further improvement. One of the main fields for catalysis investigation is the development of suitable catalysts for selective oxidation because they play the main role in more than 60% of industrial processes.

Figure 1 – J. J. Berzelius [1]

1.1 Selective oxidation of alkanes

The alkenes belongs to main building blocks of present chemical industry (next very often used are aromatics and oxygenates), mainly due to their higher reactivity relative to alkanes [5, 6]. The light alkenes are obtained mainly from catalytic or steam cracking of crude oil or natural gas and from fluid catalytic cracking (FCC) of vacuum gas oil. However, current industrial capacity for lower alkenes including ethene, propene, and butenes is expected to be insufficient in the coming years, as the demand grows for these important intermediates of the modern petrochemical industry. Even if the mentioned two routes are very well developed and widely used, the increase capacity of these processes is possible only to some extent. Hence, here appears the necessity to improve existing technologies or to develop new ones for attainment of satisfactory alkene production [6, 7].

The using of alkanes as raw materials for selective oxidations reactions could be one of the alternatives how to improve the current processes. Alkanes are, not only, cheaper

(the current cost of one metric tone of propane is 860 $/t while the cost of propene 1 105 $/t) because they are available from natural gas, but moreover they have lower impact to environment due to lower toxicity in comparison to alkenes or aromatics [6, 8-11]. These are the main reasons why the big effort is focused to use alkanes for direct synthesis of oxygenates by partial oxygenation [6] or for production of alkene by dehydrogenation or oxodehydrogenation processes [6, 10, 12] in recent years. The most extensively studied industrial processes which use alkanes feedstock in present time are: (i) methane in the presence of HCl to vinyl chloride, (ii) methane to ethene or formaldehyde, (iii) ethane to acetic acid or acetaldehyde, (iv) propane in the presence of ammonia to acrylonitrile, (v) propane to acrylic acid or acrolein, (vi) *n*-butane to maleic anhydride, (vii) *i*-butane to *i*-butene or *terc*-butyl alcohol, (viii) cyclohexane to cyclohexanone and lot of others [6, 13].

From the above mentioned reactions are commercialized only two. The direct oxidation of *n*-butane to maleic anhydride over vanadium phosphorous oxide (crystalline $(VO)_2P_2O_7$) catalysts [6-8] and the production of acrylonitrile by direct synthesis from propane and ammonia over molybdenum or antimony oxides based catalysts [6, 13]. The using of others reactions for selective oxidation of alkanes is still under scientific research or in stage of pilot plant testing. The relatively low utilization of selective oxidation of alkanes is due to several problems which have to be solved before broader industrial exploitation. The main problems are: (i) low selectivity to desired products due to formation lot of by-products or even products of total oxidation (alkenes have higher reactivity compared to alkanes feedstock and therefore they are vulnerable to subsequent reactions), (ii) some of by-products are not interesting from an economical point of view or they are dangerous for environment or for human health, (iii) some reaction feedstock could be explosive in certain range of concentration (iv) some by-products may cause corrosion of technological equipment (v) some processes require high-cost or toxic oxidizing agent (NaClO, C_6H_5IO, *terc*-BuOH) [6, 8, 14].

1.2 Economic and scientific aspect of C_4 hydrocarbons utilization

Presently, the worldwide output of C_4 fraction (recovered from LPG by distillation) is approximately 200 million metric tons (data from the year 2009) annually [15]. The main part of C_4 fractions is used as fuel and approximately 20 % (this percentage is increasing in recent years) is used in chemical industry for selective oxidation to maleic

anhydride, cracking to light olefins, dehydrogenation to butenes and butadiene *etc.* [10, 16].

Significant attention has been paid to the study of *n*-butane dehydrogenation process because of the growing demand for butenes and butadiene, respectively. While, the world production of butenes was 28.1 million tons in 1984 [17], in 2004 it was more than 44 million tons and growth of production is expected about 0.8 % per year [18]. The butadiene production is in the similar situation. The butadiene production in USA was 1.2 million tons in 1983 [17] while after ten years latter it was 1.47 million tons [10] and in 2000 it was even 2.1 million tons and similar trends we can observe around the world [19].

More than half of *n*-butenes production is used to manufacture alkylate and polymer gasoline. Around one-third is used without any conversion as fuel gas and 10% of the *n*-butenes was used in the manufacture of a variety of other chemical products like linear low density polyethylene (LLDPE) or for production of butadiene and maleic anhydride, polybutene, butylene oxide, secondary butyl alcohol (SBA), methyl ethyl ketone (MEK) and a more versatile range of polypropylene resins. *i*-Butene is used for production of methyl *terc*-butyl ether (MTBE) which is used as additive to gasoline to increase its octane rating and helping prevent engine knocking [6, 7, 20].

The importance of 1,3–butadiene production can be attributed to the enormous applications of its synthetic products. One of the well-known products is butadiene-styrene rubber – the major rubber for manufacture of automotive tyres. The other synthetic products include latex and polybutadiene rubber, plastics with special mechanical properties (*i.e.* polystyrene, ABS polymers) and of course as raw material in a wide variety of chemical synthesis [21, 22].

From the scientific point of view the *n*-butane is interesting mainly due to its higher reactivity in comparison with propane or ethane, because the *n*-butane has two secondary carbons. The cleavage of secondary C—H bonds is the first, the rate-limiting step in the oxidative reaction of hydrocarbons [12, 23]. Moreover, the number of the primary and secondary carbons is the equal what is beneficial for evaluation of obtained data. The detailed study of activation and mechanism of *n*-butane oxidation is very important for understanding very complex reaction network (see Figure 2) which leads to many different products which could be interesting for industry [6, 12].

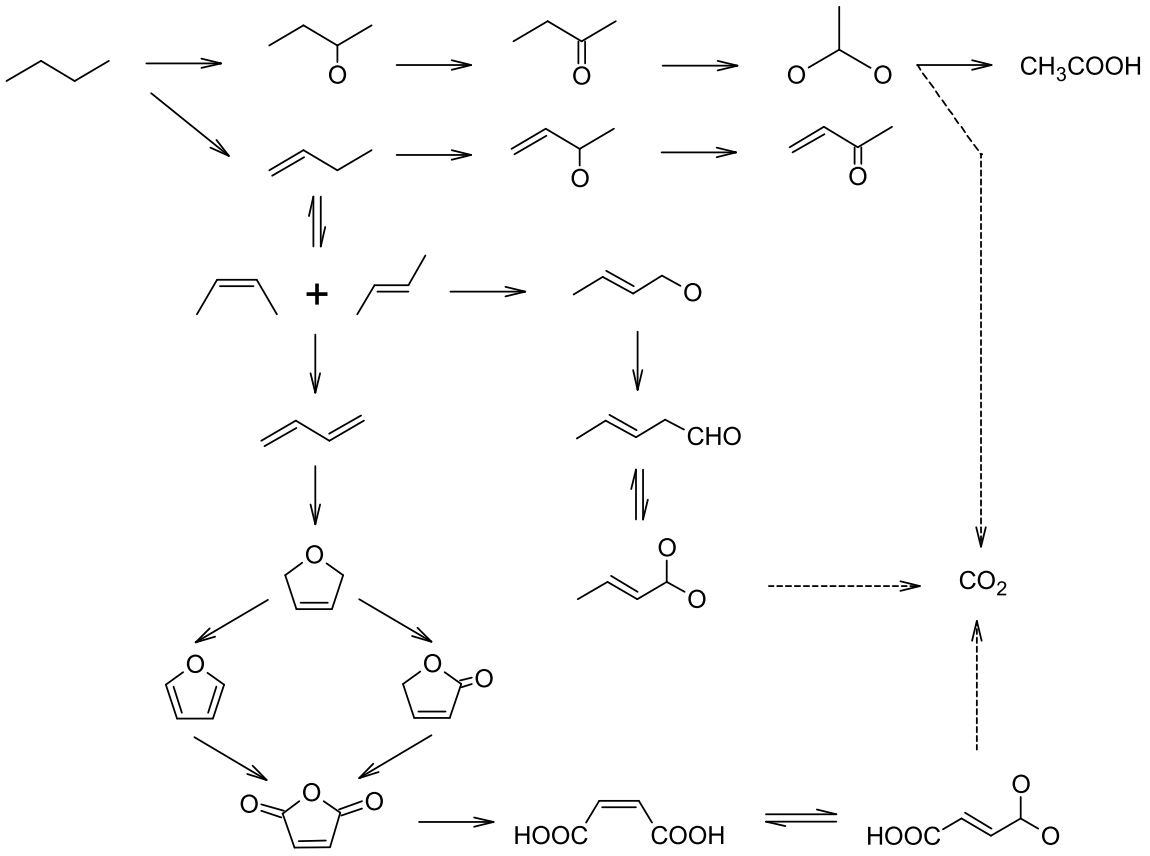

Figure 2 – Reaction network in *n*-butane oxidation on oxides [6].

1.3 Catalytic C_4 alkane to C_4 alkenes transformation

From previous chapter we can see that importance of C_4 alkenes is continuously growing up. Hence, it is necessary to find new way of their production from easy available and low price raw material. The direct catalytic oxidative dehydrogenation of *n*-butane, which is easily available from low price natural gas, to butenes and butadiene could be good alternative to classically used dehydrogenation [10].

1.3.1 Direct Dehydrogenation vs. Oxidative Dehydrogenation

The direct *dehydrogenation* (DH) of *n*-butane, which is usually used in today's industry, is carried out according to the following equation:

$$C_4H_{10} \rightarrow C_4H_8 + H_2$$

Unfortunately, the equilibrium of this reaction is shifted to alkanes in the low temperatures and at the atmospheric pressure. The reaction is endothermic (*e.g.* for *n*-butane is $\Delta H°_{r,298} = 125$ kJ·mol^{-1} [24]) and in order to shift the equilibrium to products formation, the reaction must be carried out at relatively high temperatures (for conversion

of *n*-butane about 40 % approximately 560°C was used [25]). The use of high temperature in catalytic dehydrogenation is affected by several disadvantages. The difficulty in controlling of undesirable reactions that decrease selectivity (such as cracking of hydrocarbons) and coke formation over the catalysts, which decreases activity, are the most significant of them. The chromia-alumina catalysts (used in a commercial process for conversion of alkanes) are good example of these problems, because these catalysts require regeneration after a few minutes of operation. Second disadvantage of classical dehydrogenation is the fact, that for achieve a high temperature we need to supply lot of external heat, which increases the cost of products [7, 22].

In addition, the number of molecules is higher on the product side and consequently the operation at higher pressures, which is usually preferred in industrial practice, would shift the equilibrium towards to the unfavourable direction [10, 20, 25].

Although the DH processes are, over all its drawbacks, widely used in practice, an intense research activity is taking place to develop catalysts for the oxidative dehydrogenation (ODH) of alkanes, which is promising alternative for alkenes production [14]. This reaction overcome some above mentioned drawbacks and it could be written by the following equation:

$$C_4H_{10} + \tfrac{x}{2}O_2 \rightarrow C_4H_{10-2x} + x\,H_2O$$

The formation of water as a very stable products makes this reaction very thermodynamically favourable and the conversion of *n*-butane is significantly increased due to the presence of oxygen [12, 20, 26]. Moreover, the reaction is exothermic (*e.g.* for *n*-butane is $\Delta H°_{r,298}$ = -116 kJ·mol^{-1} [24]) and it means that there is no low temperature limits for carry out this reaction. Thus, in principle, practically complete conversion can be attained at temperature about 200 °C lower than those used in DH [27] and even at high pressures, bringing enormous advantages from the economic and process engineering point of view [10]. The catalyst deactivation is also suppressed in this case, because the coke and its precursors are removed from catalysts surface by oxygen directly in reactor [10, 25].

Despite of all those advantages mentioned above, ODH has still some drawbacks, which have to be solved before putting it into the industrial practice [8]. The main problems are following:

1) Due to its exothermic character it may be required special care in reactor operation due to avoid some “hot-spot” phenomenon [10].

2) The feed composition can be explosive (explosion limits in air: *n*-butane 1.4-8.4 %, butene 1.6-9.3 %, butadiene 2.0-11.5 % [28]). It leads to limitations in feed composition or to multiple air inlets or utilization of membrane reactor

3) The molecule of *n*-butane contains four atoms of carbon which give a possibility a wide variety of products through a relatively complicated reaction network (see Figure 2). The formation of the particular products is influenced by used catalyst and by the reaction conditions [6]. The desired products must be sufficiently stable in the reaction conditions in order to be removed from the products stream before it decomposes or undergoes to other subsequent reactions. Indeed, CO and CO_2 are the most thermodynamically stable products. In general, the by-products of the ODH of alkanes have no economic interest when compared to the high value of hydrogen that is produced as a co-product in the conventional DH.

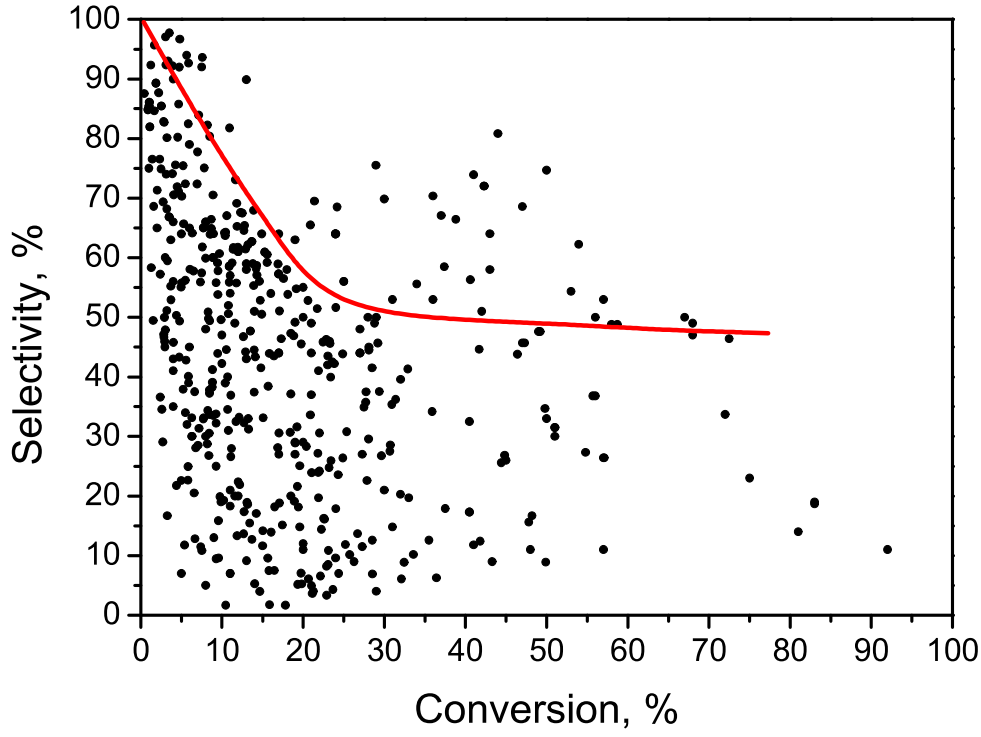

Figure 3 – The selectivity-conversion plot for oxidative dehydrogenation of *n*-butane over different catalysts and under different reaction conditions. Data from References in Table 1.

4) The main problem with most of the catalysts studied in C_4-ODH is the relatively low selectivity to desired products. This is caused by reasons discussed in previous paragraph and also due to the fact that alkenes have four–time higher reactivity in comparison with starting molecule of *n*-butane [11, 12]. This behaviour is caused

by difference in bond dissociation enthalpy of the weakest C–H bond of intermediates (*e.g.* $C–H_{butene} = 345.2\ kJ \cdot mol^{-1}$ [29]) which can be more easily cleaved than the weakest C–H bond in the molecule of *n*-butane ($C–H_{butane} = 390.8\ kJ \cdot mol^{-1}$ [29]). The Batiot et al. [29] found that if the dissociation enthalpy difference is less than $30\ kJ \cdot mol^{-1}$ a very high selectivity (limiting to 100%) is achievable at all degree of conversion, whereas for difference greater than $70\ kJ \cdot mol^{-1}$ only poor selectivity is usually recorded. The difference in dissociation enthalpy of products and reactant of C_4-ODH reaction is between two values mentioned above. This is the reason why the selectivity to $C_{4\text{-deh.}}$ (all dehydrogenated products, *i.e.* 1-butene, *cis*- and *trans*-2-butene and 1,3–butadiene) for conversion degree more than 20 % limits to 50 % and it could be clearly seen in Figure 3.

5) Reaction of alkane with oxygen could result in oxygen-containing organics products such as alcohols, ketones, aldehydes and acids. These substances could cause the corrosion and thus contribute to rapid wear of technological equipment [12].

1.3.1.1 Oxidizing agent for ODH

Gaseous oxygen from air is the most widely used oxidant, leading to the formation of very thermodynamically stable byproducts and this fact allows working at lower temperature. In addition to the oxygen from air, the pure O_2 or O_3 are sometimes used due to their higher reactivity. The main disadvantage of oxygen is the formation of products of total oxidation and that is why, the alternative dehydrogenation reagents were sought. One good example could be ODH of *n*-butane in the presence of iodine with high selectivity, known as the "Idas process", developed by Shell [30]. However, this process has not gained commercial success due to the prohibitive cost of iodine, environmental problems and corrosive nature of nascent HI [10, 31]. The ODH of ethane in the presence of HCl, H_2O and O_2 over Fe-Al catalysts could not be used from the same reason [32]. In some cases, the use of nitrogen oxides or CO_2 is also mentioned, however benefits of utilizing of these compounds are not so high in comparison with oxygen [12, 20, 33, 34]. From previous sentences is evident, that over all problems, the molecular oxygen is undoubtedly the most attractive oxidant for industrial application due to its low price and absence of environmental problems. For reasons of brevity and due to advantages of O_2, this work does not discuss the ODH of *n*-butane carried out with others oxidants.

1.3.2 Catalytic systems used in oxidative dehydrogenation of C_4-hydrocarbons

Studies regarding to ODH of alkanes started in the 1960s, when the importance of the surface nature in catalytic behaviour was emphasized. Some of the pioneering studies concerning *n*-butane ODH were performed with cobalt-molybdate which strongly favoured butadiene formation by ODH or with a Na- and/or Li-phosphomolybdate which produced 17% of butadiene and 5% of butenes at 600 °C. Nevertheless, these materials never been used in industry due to low selectivity and high temperature indispensable for their operation [10, 12, 35].

The catalysts could be generally classified according to many different criteria like: phase (homogenous or heterogeneous), catalytic active species (noble metal, transition metal), etc. We will divide catalysts to the two groups by location of active phase of catalysts.

1.3.2.1 Unsupported catalysts

The majority of the systems applied in *n*-butane ODH are solid unsupported (bulk) catalysts based on mixed oxides [10]. This group also includes the V–P–O catalyst, which is already used in industry for the production of maleic anhydride [6]. Another important member of this group of catalysts tested for *n*-butane ODH are the mixed V–Mg–O and Mo–Mg–O catalysts [12, 36, 37], which achieved 20% yield for $C_{4\text{-deh}}$ products at the conversion of *n*-butane about 40% [38]. Also nickel–molybdate catalysts have been investigated extensively [9, 11, 39, 40]. The selectivity to $C_{4\text{-deh}}$ achieved over Ni–Mo–O catalysts was 75 % [11] and over Ni–Mo–P–O the reported selectivity to 1,3-butadiene was even 83% [9].

In more recent time, the great attention was paid to the Bi–Mo–O catalysts, which were intensively studied by Jung et al. [41-43]. The selectivity to 1,3-butadiene was almost 90 % at 50 % of *n*-butane conversion. However, the big disadvantage of these catalysts is their low thermal stability, which prevents their use in industry.

This group of unsupported catalysts includes also many multi-component materials like Ni–P–O, V–K–SO_4, Ni–P–O, $ZnFe_2O_4$, $Mo_1V_{0.26}Sb_{0.13}Nb_{0.06}O_x$, $Co_9Fe_3BiMo_{12}O_{51}$ or $H_3PW_{12}O_{40}$, [10, 12, 44-47]. These systems have very often complicated structure and contain several different phases which could undergo changes under reaction conditions. The complexity of theirs structure prevents to find catalytic active centre very often, what complicates the research of these materials.

1.3.2.2 Supported catalysts

In the case of supported catalysts, the active species (most often oxides of transition metals like V, Mo or Ni) are deposited on the surface of suitable more or less inert support. Nevertheless, in these systems, besides the nature of the deposited material, the physico-chemical character of the support could also strongly affects the catalytic activity of anchored catalyst species, mainly due to their acid–base character of the support and this phenomenon will be discussed in more details latter [10].

The supported catalysts have some advantages in comparison with bulk catalysts depending on the particular support used. The main benefits could be: (i) good mechanical and thermal stability, (ii) usually high specific surface area which makes it possible to good dispersion of active species on the surface, (iii) structure of support (usually micro- or mesoporous) brings advantages in shape selectivity of these materials and last not least (iv) important point for supported model catalysts is the structural homogeneity of the support material. This allows to concentrate researcher's interest only to the active site, their relatively simple characterization by many analytical techniques and possibility to describe these systems by apparatus of theoretical chemistry (it means that they could be very easy used as model catalysts) [10, 23, 48].

Silica (SiO_2) in numerous structural modifications and alumina (Al_2O_3) belong to the most widely available supports for study of ODH reaction ever [10, 12, 20]. Among another very often used supports belong TiO_2, MgO, zeolites (crystalline alumino-silicate with an ordered structure), Nb_2O_5 or ZrO_2 and many others like result of their combination (TiO_2–SiO_2, ZrO_2–Al_2O_3) [23, 38, 49-56]. The active carbon nanotubes are also another very promising support for oxides of transition metals which have been tested in ODH of *n*-butane reaction in present time [57].

1.3.2.3 Others systems tested in ODH of *n*-butane

Téllez et al. used a membrane reactor (with an inert ceramic membrane for controlled distribution of oxygen to the bed containing traditional V–Mg–O catalyst) for catalytic oxidation of *n*-butane. This system is displaying more efficient performance than the traditionally used fixed bed reactors [58, 59].

Lemonidou et al. [60] studied oxidative pyrolysis (*i.e.* non-catalytic oxidation) of *n*-butane and concluded, that by optimizing the reaction temperature and the *n*-butane/oxygen ratio, relatively high selectivity do C_4 alkenes up to 50% at 10% of conversion can be achieved.

Recently, Malaika et al. [61] reported *n*-butane ODH over the carbon activated by hydrogen peroxide, nitric acid, ammonium peroxydisulfate or peroxyacetic acid and they reported yields to $C_{4\text{-deh}}$ products almost 13% at 450 °C.

Summary of catalysts (supported, unsupported and others) tested in oxidation reaction of *n*-butane to butenes and *1,3*-butadiene is given in Table 1. Of course, the table does not contain all tested catalysts, but only a few representative catalysts with the best results for each catalytic system. The table contains information about catalytic system (the supports are written by *italic* font and the active species or bulk catalysts are written by normal font; this method of marking will be used throughout the work.), the temperature at which the reaction was studied (T), the value of *n*-butane conversion (X), the sum of selectivity to all desired $C_{4\text{-deh}}$ products (S for 1-butene, *cis*- and *trans*-2-butene and 1,3-butadiene) and the productivity (P) to $C_{4\text{-deh}}$ (unfortunately this value is not calculated in all cases due to lack of information in literature), which is the most relevant parameter for comparison of different catalytic systems in view of potential commercial applications (the limit value of productivity which could be interesting for commercial application is 1 $kg_{product}.kg_{kat}^{-1}.h^{-1}$ [14]).

Table 1 – Summary of catalysts studied in the ODH of *n*-butane

Catalyst	T, °C	X, %	S, %	P, $g_{(C4=)}.g_{kat}^{-1}.h^{-1}$	Ref.
$Mg_3V_2O_8$	550	50	31	4.65	[62]
Fe–Zn–O	450	19	65	2.23	[63]
V_*SBA-15* (synt)	540	13	59	1.92	Paper VI
V_*TiO_2-SiO_2*	500	9	49	1.65	[52]
Zn–Cr–Fe_2O_4	470	10	61	1.06	[64]
V_*ZrO_2*	330	43	72	1.02	[65]
Zn–Fe_2O_4	470	8	51	0.76	[64]
V–MgO	550	36	73	0.74	[66]
V_*HMS* (synt)	540	36	53	0.72	Paper IV
V_Mg–*SBA-15*	520	41	56	0.69	[67]
ZnO	450	13	65	0.63	[68]
V_*SBA-15*	540	13	59	0.57	Paper V
V_*TiO_2*	500	3	51	0.56	[52]
Pt-Sn_*Al_2O_3*	450	22	20	0.48	[51]
V_*Al_2O_3*	500	21	49	0.46	[69]
V_*SBA-15*	520	57	26	0.45	[70]
V_*SiO2*	520	6	72	0.45	[71]
alfa-Fe_2O_3	450	9	32	0.43	[68]
$H_3PW_{12}O_{40}$_*clinoptilolite*	700	83	19	0.43	[46]

Catalyst	T, °C	X, %	S, %	P, $g_{(C4=)} \cdot g_{kat}^{-1} \cdot h^{-1}$	Ref.
V_*SBA-16*	540	13	58	0.41	Paper V
V–Mo_*MgO*	550	49	48	0.35	[38]
Pt–Sn_*ZrO_2-Al_2O_3*	450	20	15	0.33	[51]
V_*MCM-48*	540	13	43	0.31	Paper V
V_*MgO*	550	56	37	0.31	[38]
V_*SiO_2*	540	13	90	0.29	[15]
V_*Ti-HMS*	460	17	44	0.28	Paper VII
V_*MgO*	600	30	71	0.21	[72]
$Mg_2V_2O_7$	550	6	79	0.13	[66]
Pt_*Al_2O_3*	450	10	10	0.10	[51]
Cs-NiMoO	540	10	47	0.06	[9]
Cr_*ZrO2*	450	41	17	0.03	[50]
Cr_*Cl-ZrO_3*	450	14	48	0.03	[50]
ultradispersed diamonds (UDD)	450	11	54	0.01	[73]
V_*Al_2O_3*	550	30	21	0.01	[74]
$Mg_3V_2O_8$	550	8	5	0.01	[66]
Mo_*MgO*	600	73	46	0.01	[37]
coal	700	40	8	—	[75]
Mg-Ni-Sn-O	540	57	11	—	[35]
$MoV_{0,23}Te_{0,23}Nb_{0,14}O_X$	400	11	18	—	[47]
Nanocyl-2	500	11	21	—	[76]
none	560	45	26	—	[60]
$M_3(VO_4)_2$ (M = Mg, Zn, Ca, Pb, Cd)	540	51	32	—	[77]
V_*SnO_2–ZrO_2*	600	2	37	—	[49]
Mo-Mg_*Al_2O_3*	560	21	44	—	[78]
$Mg_3(VO_4)_2$_*ZrO_2*	500	28	45	—	[79]
Mo-V_*MCM-41*	525	6	45	—	[80]
$Mg_3(VO_4)_2$_*MgO–ZrO_2*	500	47	46	—	[81]
Mo_*MgO*	550	68	47	—	[82]
$NiMoO_4$	525	4	56	—	[40]
TiP_2O_7	530	25	56	—	[83]
TiP_2O_7	530	25	56	—	[84]
Mg-Ni-SO_4	540	18	58	—	[35]
ZrP_2O_7	530	12	61	—	[84]
SnP_2O_7	530	19	63	—	[83]
V-MgO	540	8	66	—	[60]
TiP_2O_7	570	21	70	—	[85]
Ni-Mo-P-O	540	39	72	—	[39]
Ni-Sn-P-K-O	560	37	72	—	[86]
LiCl	550	29	75	—	[87]
Ce_*MCM-41*	525	4	90	—	[80]
V_*MCM-41*	500	8	92	—	[88]
V_2O_5 (bulk)	540	11	7	—	[89]

1.4 Vanadium based catalysts

Figure 4 – Freyja

Vanadium was discovered in 1801 in Mexico by the Spanish mineralogist Andrés Manuel del Rio, and rediscovered in 1830 by the Swedish chemist Nils Gabriel Sefström, who named the element as vanadium in honour of Vanadis, the old Norse name for the Scandinavian goddess Freyja (Figure 4) – a beauty and fertility goddess – because of its beautiful multicoloured compounds [55].

Vanadium is one of the most abundant and widely distributed metals in the earth's crust (world resources of vanadium exceed 63 million tons [90]) and it is found in about 152 different minerals (*e.g.* Cavansite - $Ca(VO)Si_4O_{10} \cdot 4\,H_2O$, Patronite - VS_4, Schreyerite - $V_2Ti_3O_9$ or Sincosite - $CaV_2(PO_4)_2O_2 \cdot 5H_2O$). About 80% of the world's vanadium production (38 000 tons per year [55]) is used as steel additive. The second most dominant non-metallurgical use of vanadium is in catalysis, which represents about 5% of the annual production of vanadium. Vanadium oxides as transition metal oxides can be classified as redox catalysts. Besides the most common of V^{5+}/V^{4+} can be also find systems V^{4+}/V^{3+} and V^{5+}/V^{3+}. The simplest and longest used vanadium based catalysts are the bulk oxides of vanadium (mainly V_2O_5) which are the big reservoir of oxygen. This oxygen is highly mobile in lattice, if the oxide is in partially reduced state and it is used in many industrial applications in selective oxidation. The Table **2** summarizes some industrially important processes in which the vanadium oxides are used. Vanadium oxide based catalysts are used in the production of important chemicals (*e.g.* sulfuric acid, phthalic anhydride) and in the reduction of environmental pollutants (*e.g.* nitrogen oxides from exhaust gas of power plants) [20, 55, 91].

In the case of ODH of alkanes, carried out at higher temperatures, the using of bulk vanadium oxide leads to products of total oxidation like CO_X and H_2O. From this reason, it is better deposit the vanadium oxide on a suitable support (vanadium supported catalysts represent 28% of all supported catalysts [55]) in the form of isolated species [14, 20]. This arrangement not only prevents the overoxidation of raw hydrocarbons but also significantly improves the activity of catalysts.

Table 2 – Industrial catalytic processes using vanadium oxides [55, 92]

Industrial process	Catalyst material	Year of introduction
Oxidation of SO_2 to SO_3 in the production of sulfuric acid	V_2O_5	1920-1930
Oxidation of benzene to maleic anhydride	V_2O_5	1930-1940
Oxidation of naphthalene to phthalic anhydride	V, Mo oxides	1950-1960
Oxidation of butene to phthalic anhydride	V, P oxides	1960-1970
Oxidation of *o*-xylene to phthalic anhydride	V, Ti oxides	1960-1970
Selective reduction of NO_X with NH_3	$V_2O_5/WO_3/TiO_2$	1970-1980
n-Butane to maleic anhydride	VPO	1980-1990

VO_X catalysts are mostly deposited on the surface of an oxide support, such as SiO_2, Al_2O_3, TiO_2 and ZrO_2. The fundamental basis for the catalytic performances of supported vanadium oxides lies in the variability of geometric and electronic structure of surface vanadium oxides and in the properties of support [55]. The most profound changes are frequently observed at low vanadium loadings not exceeding the surface monolayer coverage. Species in the sub/monolayer display different activity and/or selectivity than the bulk V_2O_5 in a number of oxidation reactions, among other things in the oxidative dehydrogenation of alkanes [20, 23, 93-95].

1.4.1 Molecular structures of vanadium oxides

Supported vanadium oxides exhibit chemical and electronic properties, which are absolutely different from those found for unsupported V_2O_5. For better understanding of these differences, a brief overview of the molecular structure will be given. Vanadium has the electron configuration $3d^3\ 4s^2$. The main oxidation states are II+, III+, IV+ and V+. V^{V+} (d^0) can be present in tetrahedral (VO_4), pentahedral (VO_5) and octahedral (VO_6) coordination environment and tends to form polyoxoanions. V^{IV+} (d^1) is also stable and it is mostly present in a square pyramidal or pseudo-octahedral coordination as an isolated cation. Other oxidation states such as V^{III+} (d^2) and V^{II+} (d^3) are less stable and they exist only under reducing conditions [55].

1.4.1.1 Molecular structures of vanadium oxides in aqueous solution

The knowledge about vanadium structure in aqueous solution is important mainly during the preparation of catalysts. The most important oxidation states in aqueous solution are V^{V+} and V^{IV+}. The type of vanadium oxo-species depend on the solution pH and the vanadium concentration. This is illustrated for V^{V+} in Figure 5, which shows the different

regions in which a particular vanadium (V+) oxo-species is stable and this scheme is generally known as the Pourbaix diagram [55].

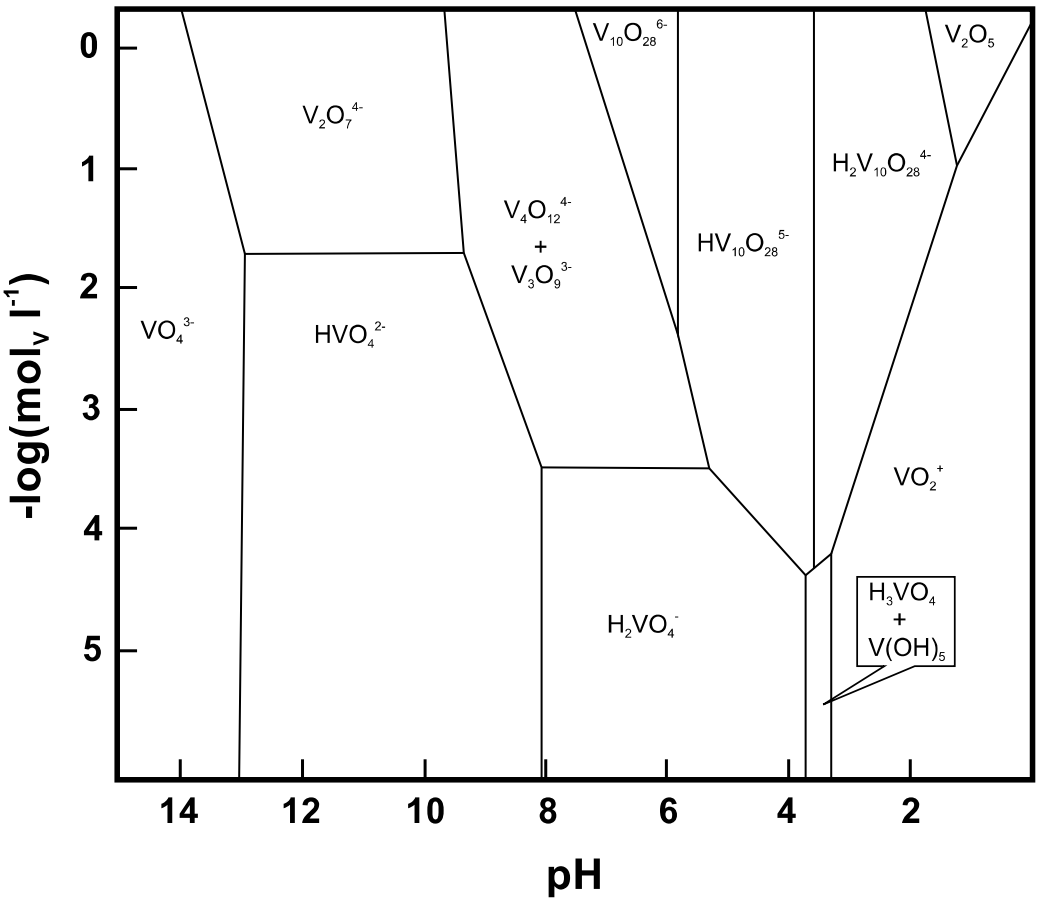

Figure 5 – Pourbaix diagram of vanadium, expressing the vanadium speciation as a function of pH and total vanadium concentration [96].

1.4.1.2 Molecular structures of vanadium oxides on the solid surface

In literature, the structure of dehydrated supported vanadia is still a matter of discussion with regard to loadings below the formation of crystalline V_2O_5. Depending on the type of preparation, the maximum amount of well dispersed vanadium oxide species corresponds to 0.5-2.3 V atoms per nm^2 [55, 97, 98]. The vanadium oxide species may be found in different coordination (tetrahedral, octahedral), in different oxidation state (0, II+ to V+) and in varying degrees of dispersion on the surface. Mix of all these properties causes the unique catalytic properties of these systems.

We can found four basic structural types of VO_X particles on the surface of the support [12, 23, 55]. If the concentration of vanadium on the surface is low (3-10 wt.% of V in dependence of used support), the particles can be dispersed in the form

of vanadium isolated tetrahedral units (group of symmetry T_d or C_{3V}) usually expected to have a structure $(sup–O)_3V=O$ under dehydrated conditions (Figure 6 A). This type of particle contains one terminal oxygen V=O with the distance $d_{(V=O)}$ = 1.58–1.62 Å. All three bonds between vanadium and bridging oxygen have an identical length approximately 1.78–1.82 Å [55]. However, this species can significantly change its structure and properties after hydration and this phenomenon will be discussed later in detail. These particles seem to be playing the key role in the ODH reactions.

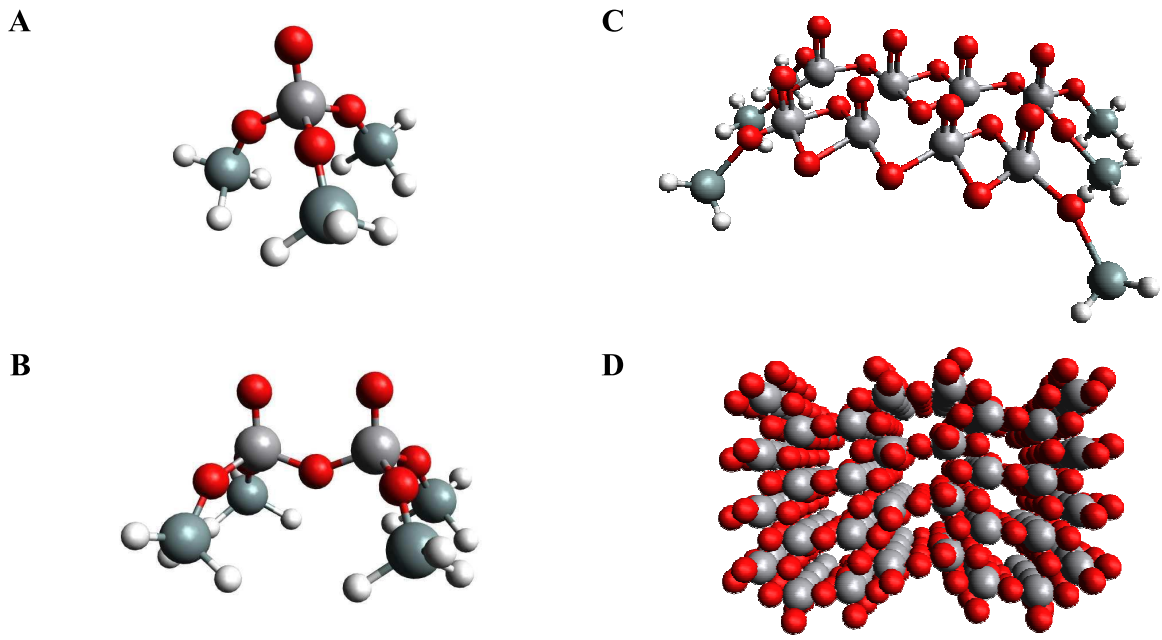

Figure 6 – Possible molecular configurations for supported vanadium oxides (red ball – oxygen, light gray ball – vanadium, dark gray – silicon and white ball – oxygen in support): A) isolated vanadium oxide species with T_d coordination; B) dimeric and 1-D oligomeric vanadium species with T_d coordination; C) 2-D vanadium oxide chains with T_d coordination; D) bulk V_2O_5 crystals with O_h coordination of vanadium atom

The increasing of vanadium concentration leads to formation of 1-D oligomeric units with tetrahedral (T_d) coordination (Figure 6 B). In this case, the vanadium is bound in chains through the bridging oxygen V–O–V. These units are combined with each other together and they create polymeric chains. The presence of V–O–V bond results in a change a T_d coordination to a deformed T_d coordination. This change is reflected as the appearance of new shifted bands in the UV–vis spectra.

Subsequent polymerizations of VO_X units lead to generation of 2-D oligomeric VO_X species with a square pyramidal structure (Figure 6 C) or with octahedral (O_h) coordination. At the highest level of VO_X concentration, O_h coordinated polycrystalline

V_2O_5 units can be created (Figure 6 D) on the surface. These particles are absolutely unselective and they are assumed to be active in the formation of total oxidation products. Distance between terminal oxygen and vanadium ion is similar to the same bond in monomeric units ($d_{(V=O)}$ = 1.58 Å) and the length of V–O bond has 1.88 Å [20, 55].

How, it was noted above, the molecular structure of the surface vanadium species supported on silica is a strongly affected not only by vanadium concentration but also by the environmental conditions. For example, the extent of catalyst hydration dramatically changes the molecular structure of the surface vanadium oxide species, and the degree of hydration plays a critical role in the determining their specific structure on the surface. Water is always formed during ODH reactions and leads to a partial or full hydration of the catalyst surface depending on reaction conditions. Hence, the knowledge about molecular structure of the hydrated supported vanadium species is very important for a better understanding of their catalytic performances during the ODH reactions.

Hydration affects mainly monomeric and low oligomeric units while the crystalline V_2O_5 species are reported to be usually unaffected by water vapor [99, 100]. Despite the importance of this issue, only a few works about hydration process of silica supported vanadium oxide catalysts have been published [97, 99, 101-103] and still there is no consensus on the structure and stability of hydrated forms. The molecular structure of the hydrated surface vanadium species is apparently a strong function of the degree of hydration. The critical factor for hydration is chemisorption of water and hydrolysis of V–O–Si bridging bonds. The gradual breaking of V–O–Si bonds and formation of V–OH groups allows the formation of the "umbrella-type" structure (*i.e.* Si–O–V=O$(OH)_2$) [99]. These particles are able to move over the surface and V–OH groups allow the polymerization of surface species *via* olation. At higher water pressures, full hydration may break all the V–O–Si bridging bonds, resulting in the maximum polymerization between VO_5 units and it leads to formation of 2D layered structure connected to the support only *via* hydrogen bonding allowing them also to move over the surface. Up to this step, the hydration is still reversible, and the isolated monomeric structure can be obtained after dehydration. However, with large quantities of water around the surface, they can compete and substitute for the Si–OH groups as the binding sites on the 2D layered structure. Once the VO_X species leave the silica surface by breaking the V···OH–Si hydrogen bonds, oxolation occurs to form $V_2O_5 \cdot nH_2O$ gels with V–O–V connections and this process is irreversible [97, 99]. This process is schematically shown in the Figure 7.

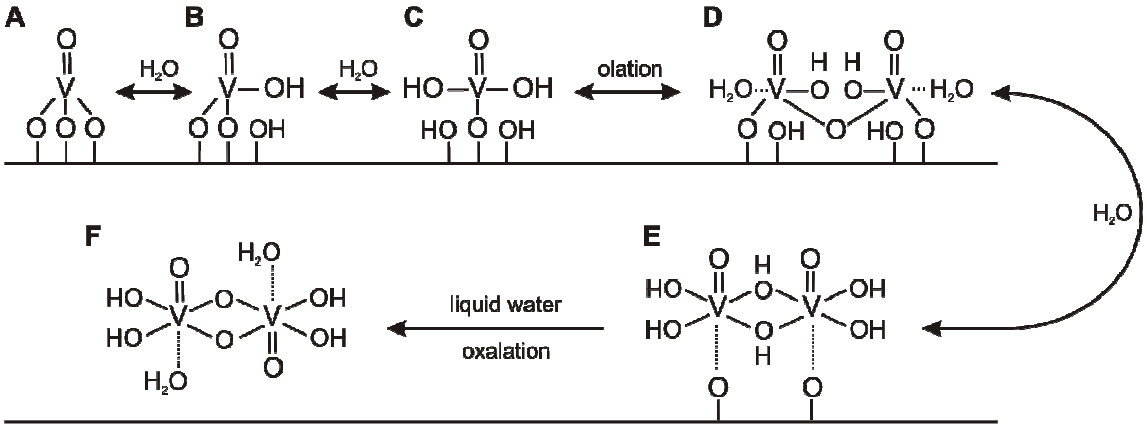

Figure 7 – Schematic dehydration/rehydration mechanism for supported vanadium oxide catalysts according to Ref. [97] A) pyramidal monomeric species, B) partially hydrated structure, C) umbrella structure, D) chain polymers, E) mobile chain and/or 2D polymers F) 2D layered structure ($V_2O_5 \cdot nH_2O$ gels)

1.5 Amorphous silica – support for vanadium catalysts

The support strongly affects the catalytic performance (activity and selectivity). The most important factors are: (i) acid–base character which influences the retention period of reactants on the surface and the dispersion of the vanadium oxides and (ii) textural properties which has influence on dispersion of vanadium oxide and on the performance. Silica is one of the most widely available supports studied in ODH reactions and it was used in presented study. Hence, the main emphasis will be placed to description of silica based supports in following paragraphs.

1.5.1 Acid-base character of support

1.5.1.1 The influence of support basicity to ODH selectivity

The molecules of alkenes with π C=C double bonds have higher electron density (nucleophilicity) than alkanes, corresponding to their higher basicity. The proton affinity of butene is 820 $kJ \cdot mol^{-1}$, which is higher than that of *n*-butane with 649 $kJ \cdot mol^{-1}$. The difference of proton affinity between butene and *n*-butane is about 1.7 eV [104-106]. Therefore, the surface acidity/basicity has an important influence on the catalytic activity, which has been widely discussed in literature. An increase in the basicity improves the desorption rate of alkenes, resulting in decrease in deeper oxidation. When the basicity of catalysts is increased, the adsorption of hydrocarbons at active sites is weaker, resulting in lower reactivity and high selectivity to mono–alkene without oxygen containing products formation. Hence, the surface basicity also explains the absence of oxygenated products

other than carbon oxides in the reaction effluent. The using of acid surfaces with high potential to adsorbed alkene leads to formation oxygen containing products (like maleic anhydride or furan) in the reaction effluent [8, 10, 107].

Blasco et al. [107] used vanadium based catalysts with different supports in ODH of *n*-butane and they found that selectivity to desired dehydrogenation products, as well as distribution of C_4-alkene, can be very well related to the acid–base character of the catalysts. Indeed, 1-butene and 1,3-butadiene selectivity decrease when the strength and number of Lewis acid sites (determined by FT–IR of adsorbed pyridine) are increased, while 2-butenes and carbon oxides show the opposite trend. It must be noted that no similar results were obtained in the case of propane or ethane ODH. However, it must be also noted, that no only the acidity of the support has the influence on the selectivity in ODH of *n*-butane. The Brønsted acid character of octahedral vanadium oxide species, which can be found in the samples with high surface density of vanadium, can play even more selectivity determining factors than acid–base character of support [10, 108]. The Figure 8 shows schematically the relationship between the dominant ODH products and catalysts acidity/basicity.

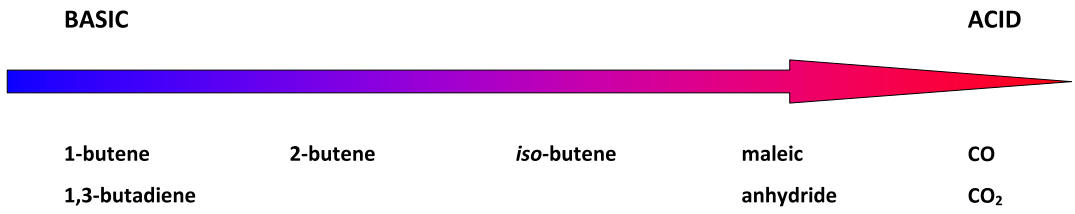

Figure 8 – Schematic illustration for the influence of acidity/basicity on products

1.5.1.2 The influence of support basicity to VO_X dispersion

The results reported in the literature indicate that the dispersion of the vanadium oxide as well as its structure can be strongly influenced by acid-base character of the different supports [23, 91, 109]. The acidity of the metal oxides is very often related to isoelectric point (IEP) (sometimes denoted zero charge point (ZCP)) and the Table 3 reports the IEP for several metal oxides which are used as supports for vanadium catalysts and the acidity of mixed metal oxides is between those of the corresponding single metal oxides. From the data in Table 3 we can see decreasing in acidity in this way: $V_2O_5 > SiO_2 > TiO_2 > ZrO_2 > Al_2O_3 > MgO$.

Table 3 – Isoelectric point at 25 °C for selected materials in water [23, 110, 111]

Material	IEP	Material	IEP
WO_3	0.2-0.5	ZrO_2	6.7
V_2O_5	1-2	CeO_2	6.75
SiO_2	1.7-3.5	Cr_2O_3	6.5-7.5
SiC	2-3.5	α-, γ-Al_2O_3	7-9
TiO_2	3.9-8.2	ZnO	8.7-9.7
MnO_2	4-5	CuO	9.5
SnO_2	4-5.5	NiO	10-11
α-Fe_2O_3	6.5-6.9	MgO	12.1-12.7

It has been observed that the tendency of VO_X species to be dispersed on the surface of the metal oxide support is related to its basicity, and decreases from MgO to SiO_2 [109, 112]. In other words, the agglomeration of vanadium oxide species to form V_2O_5 crystallites is favoured with the acid character of the support. For example, crystalline V_2O_5 structures are obtained at relatively low vanadium coverage of the theoretical monolayer (monolayer surface coverage is defined as the maximum amount of amorphous or two-dimensional vanadia in contact with the oxide support) on an acid supports like SiO_2.

Wachs and Weckhuysen [91, 113] found that vanadia monolayer surface coverage is approximately 7-8 VO_X units per nm^2 for different oxide supports (Al_2O_3, TiO_2, ZrO_2 ...) with the exception of silica supported vanadia, which exhibited a maximum surface coverage at only 0.7 VO_X units per nm^2. The much lower monolayer surface coverage on silica is (i) due to the acid character of silica and (ii) also due to the lower density and reactivity of the silica surface hydroxyls [113].

From above discussed paragraphs the MgO support (IEP *ca.* 12.5 [23]) seems to be the best support for ODH of alkane because rising alkenes (more basic then alkanes) are easy desorbed and it suppress consecutive reactions leading to CO_X. Moreover, the acid character of V_2O_5 (IEP *ca.* 1.5 [23]) facilitates good dispersion of VO_X species. These presumptions confirmed Nieto [74] who shows that the VMgO mixed oxides are the very selective catalysts for ODH of *n*-butane. Nevertheless, the MgO support has some disadvantage like specific area only about 100-150 m^2g^{-1} [107, 114] what limits vanadium loading and the formation of bulky vanadium magnesium oxide compounds also occurs on this support [48, 115] what leads to disappearance of the part of vanadium from its catalytic role. In contrary, the VO_X units supported on silica based materials, which are

theoretically least suitable, are very often reported to be efficient catalysts in the ODH of *n*-butane [10, 15, 20, 52, 67, 70, 89, 116] and hence more details about silica supports will be given in the next paragraphs.

1.5.2 Textural properties of mesoporous silica

In contrast with zeolite (crystalline alumino-silicate with pore diameter < 2 nm), the mesoporous materials are solid amorphous materials with a narrow distribution of pores. The pore diameter size is between 2 and 50 nm for mesoporous material (according IUPAC definition) and they usually exhibit the high surface area (up to *ca.* 1 000 m^2g^{-1}) which provides the space to create high amount of isolated active centers. The mesoporous materials are based on silica most often, but they could be synthesized in different chemical composition like TiO_2, Al_2O_3, sulfide, carbon or their mixture as well [117-119].

The first synthesis of an ordered mesoporous material was described in a patent in year 1971 [120]. However, due to a lack of analysis, the remarkable features of this product were not recognized. In 1992, a similar material was obtained by two groups of Japanese and American scientists from Mobil R & D Co. Both separately reported first synthesis of this novel type of silica and opened up a whole field of research of macrostructure materials [117, 119, 121, 122].

The material called MCM–41 (MCM - *"Mobil Composition of Matter"*) was one of the first prepared and characterized mesoporous materials. It consists of parallel channels which are approximately hexagonal in cross-section and are arranged in a hexagonal honeycomb structure. Size of channels depends on the method of preparation and it is between 3-4 nm with the wall thickness about 0.8-1 nm and with the surface area up to 1 400 m^2g^{-1}. This material together with other materials from the M41S family (HMS, SBA–15, MCM–48, MCM–50, FSM, PCH, MSU, KIT) are very suitable for the preparation of supported vanadium catalysts because they contain great number of weakly acidic silanol groups on the pore walls (2-3 Si–OH per nm^2 [119]), on which a large number of catalytic active centers can be incorporated. The main difference between individual materials is their structure. All materials could be separated to the three main structural groups (see Figure 9) [123]:

- **hexagonal** (H) – a one-dimensional system of hexagonally oriented pores without mutual crossing, this group contains materials labelled MCM–41.
- **cubic** (C) – a cubic structure with Ia3d symmetry and 3-dimensional pore system, with mutual crosses. The advantage of this structure is higher degree of order

however with lower hydrothermal stability. The typical example of this cubic structure is MCM–48 (sometimes is the whole cubic structured material family labeled MCM–48) or SBA-16 material.

- **lamelar** (L) – a two-dimensional system of silicate layers labeled MCM–50 (*e.g.* KIT), which are separated by double layer of organic template. MCM-50 typically collapses upon calcination, but retains large surface area, roughly 50% of the equivalent MCM-41.

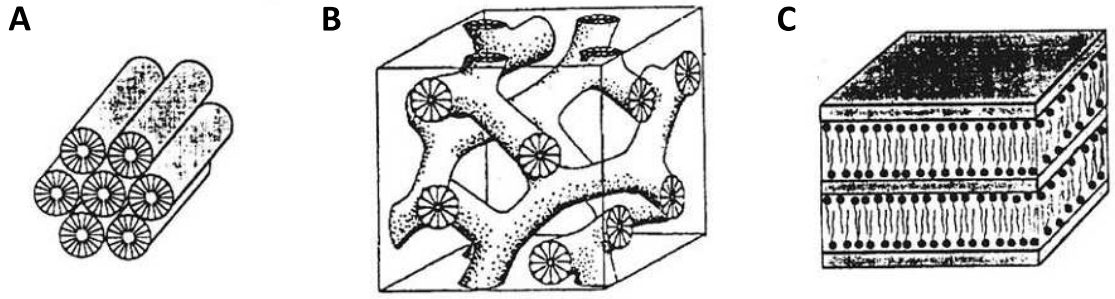

Figure 9 – M41S family of ordered mesoporous materials: A) hexagonal, B) cubic, C) lamelar Ref. [123]

1.5.2.1 Synthesis of mesoporous silica

Many papers and books [117, 119, 123-127] were written about the synthesis of mesoporous materials, hence only the short overview will be reported here. The synthesis gel contains the following reagents for the synthesis of ordered mesoporous materials based on silica usually:

– **source of silicon** - oligomeric inorganic precursors favor the formation of highly ordered mesoporous materials and almost all inorganic salts can be used as suitable precursors (*e.g.* – silica gel, SiO_2 (aerosil), sodium silicate). Tetraethyl orthosilicate - $C_8H_{20}O_4Si$ (TEOS) is other very often used source of silicon, one of the most convenient silicate precursors in the laboratory synthesis.

– **template** - often also called SDA (*Structure Directing Agent*) or surfactant plays a key factor in synthesis of mesoporous materials. The structure and nature of surfactant greatly affects the final structure (shape/topology), pore size and surface area of mesoporous molecular sieve because dissolved inorganic silicon precursors are arrange around the micellar template structure. Templates differ in size, shape, charge or in the presence of various functional groups and frequently are classified according to their polar groups into three main groups:

(i) *cationic* - quaternary alkyl ammonium salts with long aliphatic chain, (ii) *anionic* - quaternary minoslanes, carboxylic acids and (iii) *non-ionic* – amine with long aliphatic chain or triblock copolymers of BASF company.

– **suitable solvents** – the synthesis of mesoporous materials is generally carried out through a solution reaction in water or their mixture with alcohol. The pH value of the media is also a key factor which influences the structure of materials. The highly ordered structure arises under acidic or basic conditions whereas neutral solution is not suitable.

Synthesis of mesoporous materials consists of several steps and it is shown schematically in Figure 10 where is displayed the way over "liquid crystal templating" (LCT) which is one of the most often used method for preparation [117]:

1) In the first step, the template is dissolved in suitable solvent with required temperature, pH or in the presence some additives, such for example 1,2,3-trimetylbenzene for increasing of pore diameter.

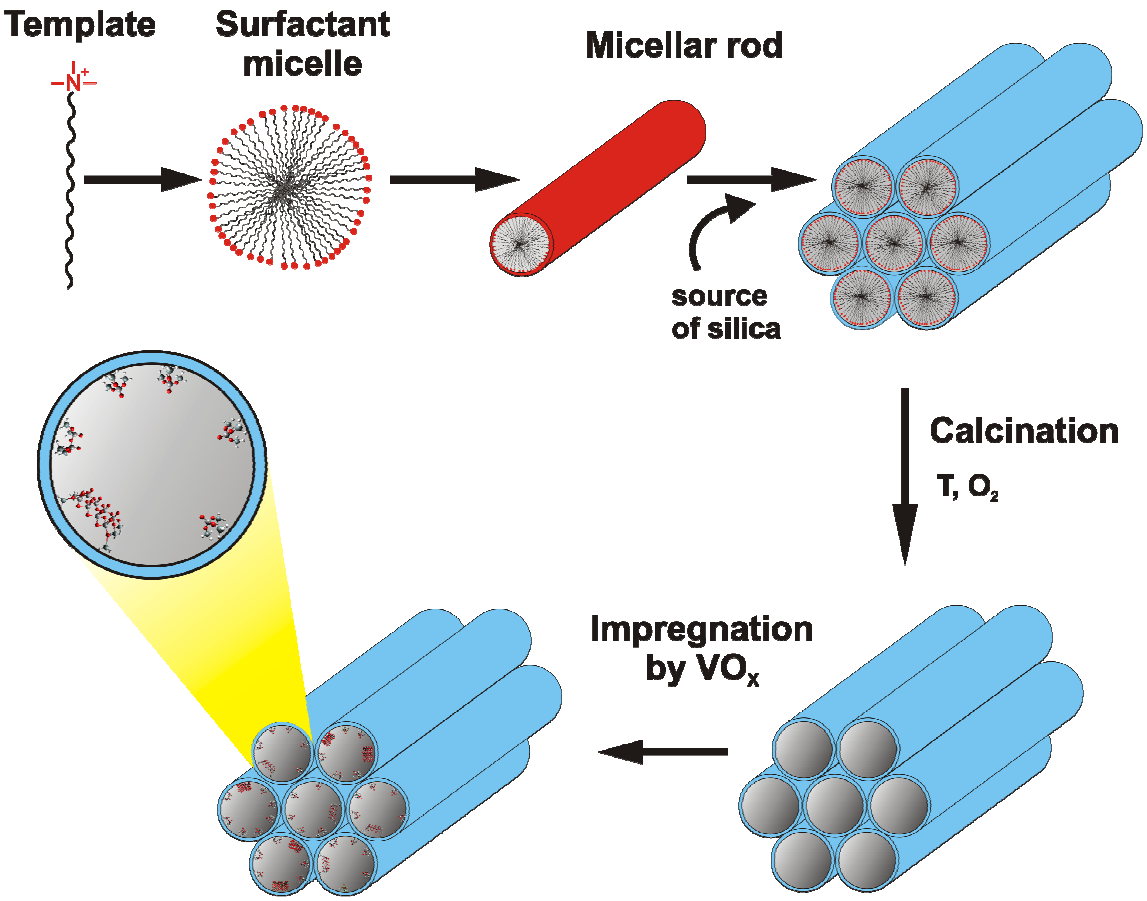

Figure 10 – Synthesis of mesoporous materials over liquid crystal templating route and theirs impregnation by vanadium

2) In the second step, the source of silica (*e.g.* TEOS) is added and it starts to hydrolyze. Sometimes, the increase of temperature (up to 100 °C) is necessary for sufficient hydrolysis.
3) The key step is condensation, which is very often carried out at higher temperature or under hydrothermal conditions which are one of the most efficient methods to improve regularity of structure of products. Duration of this step is a few hours or even a few days.
4) After condensation is necessary to separate products from the mother liquor and as-synthesized mesostructured material is obtained after washing (most often by water or by alcohol) and careful drying, because the washing step may cause the destruction of partially cross-linking frameworks.
5) The final step is the removal of templates from as-synthesized inorganic-organic composites. Different removal methods (calcination, extraction, irradiation using microwave) certainly influence the characters of mesoporous material as well. The most common method is the calcination owing to the easy operation and complete elimination. Disadvantage of this method is the total destruction of template (most often of high cost) which can not be reused.

1.5.2.2 Mesoporous materials used in this thesis

Four structures of mesoporous silica based materials, namely HMS, SBA-15, SBA-16 and MCM-48 (see Figure 11), were examined in this thesis. The most often used structure was HMS which was modified in the composition as well.

HMS – is the material with ordered hexagonal array of one-dimensional pores with a very narrow pore size distribution (35-40 Å), pore volume 0.7-1.4 $cm^3 \cdot g^{-1}$ and wall thickness about varying from 17 to 30 Å. The degree of order and thermal/hydrothermal stability are little bit worse in comparison to other used materials, but still sufficient for application in catalysis. This material is commonly prepared by using of neutral dodecylamine like SDA and tetraethyl orthosilicate like source of silica in neutral aqua/alcohol solution under ambient conditions [125, 127-129].

***SBA*-15** – this material belongs to the most often used mesoporous materials. It is very precise ordered 2D hexagonal structure which combines micro- and mesoporous structure. The volume of micropores varying between 0.06-0.1 $cm^3 g^{-1}$ and volume of mesopores from 0.8 to 1.2 $cm^3 g^{-1}$. The large pore size adjustable

between 60 and about 150 Å which facilitate mass transfer and the very high surface area allows a high concentration of active sites per mass of material. Moreover, the thick wall of 30-70 Å significantly improves the thermal and hydrothermal stability compared to others M41S materials. The SBA-15 is prepared from TEOS as source of silica and from triblock copolymer Pluronic P123 ($EO_{20}PO_{70}EO_{20}$) as SDA in the autoclave under mild acidic conditions [125, 127, 130-132].

SBA-16 – in comparison to two previous discussed structures this material exhibits 3D structure of channels with cubic cage in the channel crossing with diameter up to 176 Å (adjustable by conditions during the synthesis) and with the micropores in the wall. Opened 3D structure allows good and fast mass transport in comparison to 1D and 2D structure of HMS and SBA-15, respectively. The block copolymers with larger EO chains (*e.g.* $EO_{106}PO_{70}EO_{106}$ = F127), which favor the formation of globular structure, are used as templates under acidic conditions at room temperature for SBA-16 synthesis [127, 133, 134].

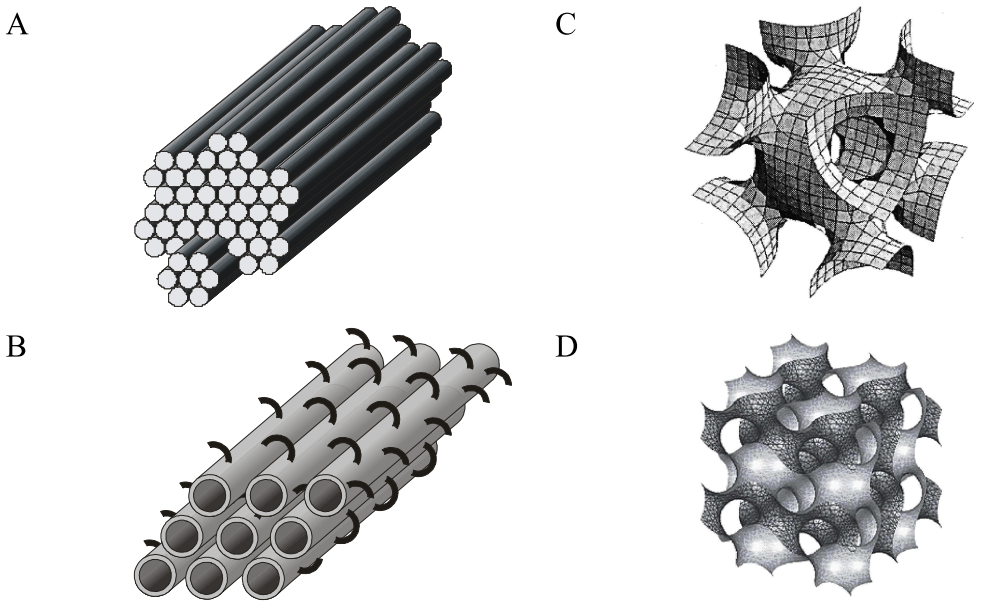

Figure 11 – Structure A) HMS, B) SBA-15, C) SBA-16 a D) MCM-48

MCM-48 – this material has a cubic 3D structure with two independent micelle system separated by the pore wall. It brings some advantages like fast mass transport. However, the wall thickness of the MCM-48 is very thin (thinner than in the case of HMS). It cause only limited chemical a hydrothermal stabilities of this support, which limits its using in catalysis and it is interesting mainly from

scientific point of view. The pore diameter varying between 25-40 Å and the pore volume is about 1-1.4 $cm^3 \cdot g^{-1}$. The Pluronic P123 and *n*-butanol dissolved in slight acid aqueous solution are used like SDA for MCM-48 synthesis. The organized MCM-48 material could be obtained only with template to silica ratios higher than 1 and TEOS is used as like the silicon source [127, 134, 135].

1.6 Preparation of supported VO_X catalysts

Supported vanadium oxide catalysts can be prepared via several methods, which can be divided to two main groups: (i) incorporation of VO_X species to the structure of support directly during the synthesis procedure or (ii) the post-synthetic dispersion of VO_X species on the support. In the following paragraphs, the most important preparation techniques will be briefly described, and their advantages and disadvantages will be discussed.

1.6.1 Direct synthesis

In this case, the source of vanadium is added directly to the synthesis gel during the preparation of mesoporous material. The vanadium species are incorporated directly to mesoporous structure, where the VO_4 units with tetrahedral coordination substitute the SiO_4 isomorphly. This interchange is possible due to similar diameter of ions and by similar coordination. The main advantage of such prepared materials is the larger surface area, better dispersion and reducibility of vanadium species and superior catalytic performances in selective oxidation reactions in comparison to material prepared by post-synthesis modification. Disadvantage of these materials is relatively low concentration of vanadium which could be deposited on the surface (maximally 15 wt. %) and moreover these materials often has lower hydrothermal stability at higher temperature [71, 136-140]. Also possible burying of part of vanadium species into the wall can be disadvantage of these materials [141].

1.6.2 Post-synthetic modification of support

Many different techniques of post-synthetic modification could be used in the preparation of supported vanadia catalysts which differ in experimental difficulty, cost of vanadium source or degree of dispersion and the amount VO_X species on the surface.

1.6.2.1 Impregnation

Impregnation is the most simple and widely used preparation technique for making supported vanadium oxide catalysts. The term impregnation denotes a procedure whereby a certain volume of an aqueous or non-aqueous solution containing a vanadium compound is adsorbed onto the surface of pores. The commonly used sources of vanadium VO_X are: (i) vanadates [33, 69, 142, 143], (ii) vanadyl acetylacetonate – $VO(C_5H_7O_2)_2$ or tripropoxyoxovanadium – $VO(OC_3H_7)_3$ [55, 91, 141, 144-147], (iii) vanadium oxalate $VO(C_2O_4)_2$ which is very often used in industry due to its high solubility in water and the absence of undesirable volatile organic solvents [55, 91, 148] and (iv) vanadyl sulfate [149-151]. The impregnation process is followed by a drying and calcination step in which the vanadium oxide compound is chemically anchored/bonded onto the support. This process is schematically showed in the Figure 10 and Figure 12. A significant disadvantage of this technique is the wide distribution of different VO_X species on the surface. It is the result of a gradual evaporating of solvent, which leads to higher concentration of vanadium complexes and their possible agglomeration (see Figure 5) already in liquid phase, as was reported in Ref. [55].

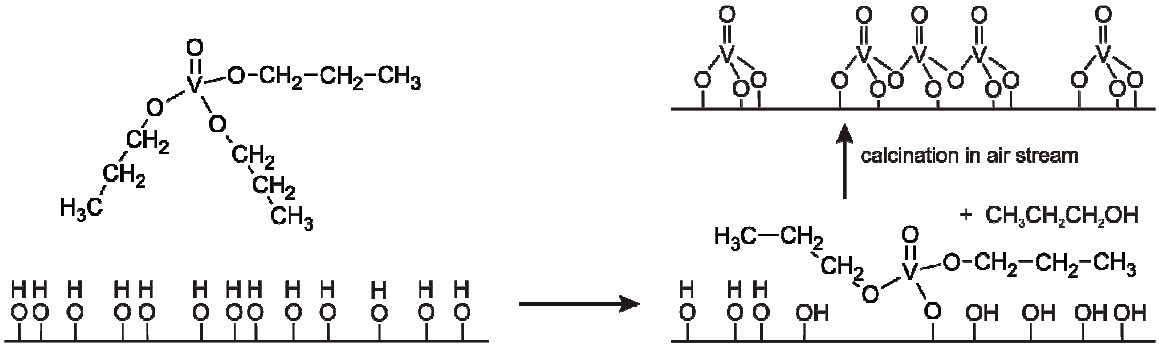

Figure 12 – Impregnation with $VO(OC_3H_7)_3$ from water/methanol solution, followed by calcination in oxygen or air and release of propanol.

1.6.2.2 Grafting

Grafting is defined as the removal of vanadium precursor from solution through interaction with Brønsted acid hydroxyl groups on the surface of an inorganic support. The using of vanadium source with a bulky anion (*e.g.* $VOCl_3$ in CCl_4 or in benzene) sterically prevents to oligomerization of vanadium particles not only on the surface, but in the solution as well. A monolayer of vanadium oxides on the surface is obtained after multiple grafting followed by calcination. The difficulty of this process together with high cost and

low final VO_X concentration on the surface are the main disadvantages which prevents to widely using of this method for preparation supported vanadium catalysts [13, 52, 55, 152]

1.6.2.3 Ion exchange

Another method of preparation of supported vanadium catalysts is based on the ion exchange, which is well known from work dealing with zeolites and in principle is very similar to grafting [123]. Ion exchange is very often performed after grafting of a suitable anion (*e.g.* 3-aminopropyltrimethoxysilane), which after treatment with aqueous HCl solution serves as an "anchor" for the deposited VO_X particles [13, 116, 153].

1.6.2.4 Chemical vapor deposition

The CVD (*chemical vapor deposition*) method combines advantages of ion exchange in solid with selective reaction (grafting). The volatile and stable inorganic or organo-metallic vanadium complexes (*e.g.* $VOCl_3$, $VO(OC_2H_5)_3$ or VCl_4) are used as source of vanadium. These complexes are transferred to the gas phase and transported to surface (tempered on higher temperature) by stream of inert gas where are deposited at the surface by reaction with the support hydroxyl groups. Such prepared catalysts have high concentration of monomeric vanadium species. These benefits are unfortunately compensated by the high costs of such prepared materials [55, 97, 154].

1.7 Aims of the study

This doctoral thesis deals with supported vanadium catalysts on mesoporous materials which are characterized by broad range of analytical techniques and tested in C_4-ODH reaction. The two main aims of this doctoral thesis are:

(**A**) Investigation of the influence of vanadium oxide species structure and their surface dispersion on silica based materials to catalytic activity in ODH of *n*-butane.

(**B**) Optimization of these materials for high catalytic performance in ODH, which is necessary for potential using in industry.

To achieve these two main objectives is necessary to answer some partial question:

- How to distinguish and quantify vanadium species in the VO_X-silica catalysts?
- Which VO_X species are the most active in n-butane ODH?
- Is it possible to influence VO_X speciation and catalytic activity by way of preparation?
- Could be the dispersion of VO_X species and performance of catalysts influenced by textural structure of used support?
- How the support chemical composition affects the VO_X dispersion and catalytic activity?

2 Summary of Papers

2.1 How to distinguish the individual vanadium species on the silica surface

Even though the supported vanadium oxide catalysts have found wide commercial application in industry (see Table 2) and many scientific groups investigate their next potential application, the detailed understanding of the mode of operation of supported vanadium-oxide catalysts is still missing. The knowledge of the prevailing molecular structure of surface vanadium species is an essential task for understanding the structure – catalytic activity relationship [14, 155] (Paper IV).

The supported vanadium oxide catalysts are very complex materials and the determination of the detailed speciation of vanadium oxide species present on the surface of the support materials is still challenging task in the process of the catalyst characterization. Nowadays the most acknowledged theory expects the existence of three or four different types (see Chapter 1.4.1.2 of this thesis) of vanadium oxide species on the surface without being exposed to reaction conditions. Despite a number of studies (Paper IV-VII and references therein) dealing with this problem the structure of VO_X species is still matter of debate. Under reaction conditions, in which the water is formed, a hydrated analogous structures of vanadium oxide species could be found on the surface (see Chapter 1.4.1.2) and this fact further complicate the understanding of vanadia based catalysts [13].

Useful characterization techniques, which can provide detailed information about the molecular structure of supported vanadium oxides, must be capable to distinguish these different vanadium oxide configurations and quantify their amount on the surface.

The presence of the various structures of the supported vanadium phase is mostly characterized by FT–IR, Raman, XANES/EXAFS, UV–vis diffuse reflectance (DR), solid state MAS ^{51}V NMR, ESR, XPS, SEM, TEM, TPR, XRD, voltammetry etc. The most used techniques are summarized in Table 4. It could be seen from Table 4 that no characterization technique is able to provide all the information needed for a complete characterization of supported vanadium species. Thus, successful characterization of vanadium oxides in heterogeneous catalysts requires a multi-technique investigation or some new approach [55].

Characterization by DR UV–vis, Raman a H_2-TPR was used as the main technique for study of vanadia dispersion and oxidation state in this thesis. However, a few problems

had to be solved before their application for study of our catalysts (Paper I-III). The main problem and benefits of combining results of DR UV–vis and Raman spectroscopy with results of H_2-TPR will be shortly discussed in following text separately and at the end the general recommendation for these techniques will be done.

Table 4 – Most often used characterization techniques for study of supported vanadium oxides

Characterization technique	Determine			
	Oxidation state	Coordination	Dispersion	Quantity
Infrared spectroscopy (IR)	+	+	-	+/-
Raman spectroscopy (RS)	+	+	+/-	-
Electron spin resonance (ESR)	+	+	+/-	+
X-ray photoelectron spectroscopy (XPS)	+	-	+	+
Nuclear magnetic resonance (NMR)	-	+	-	+
Diffuse reflectance (DR) UV–vis-NIR	+	+	-	+/-
X-ray absorption fine structure spectroscopy (XAFS)	+	+	+/-	-
Temperature programmed reduction by H_2 (H_2-TPR)	+	+/-	+/-	+
X-ray fluorescence (XRF)	-	-	-	+
X-ray diffraction (XRD)	-	+/-	-	-

2.1.1 DR UV–vis spectroscopy

Characterization by diffuse reflectance DR UV–vis spectroscopy is frequently used because it is widespread, relatively cheap and simple experimental technique which can provide information about the different oxidation states and local coordination geometry of supported vanadium oxide species. The main disadvantage of this technique is the fact that measured DR UV–vis spectra usually consist of broad, absorption bands which are overlapped with each other and it complicates their detailed interpretation (Paper I-II).

The contradictory interpretations of UV–vis spectra appeared very often in the past [98, 101, 155-162] and for clarity they are plotted in the Figure 13. Moreover, the intensities of the previously published spectra were frequently not proportional to the vanadium concentration, even for the moderately concentrated samples. This fact was reported already in the past by Catana at al. [157] and completely prohibits the quantitative or semi-quantitative analysis of spectra.

Therefore the approach which can partially overcome this problem was developed by Gao [163]. It is based on the evaluation of absorption energy edge (ε_0) from the UV–vis

spectra using the expression introduced by Davis and Mott [164] or by Tauc [165]. More details are given in Papers I–II and some examples are showed in Paper I and Papers III–V. This method allows us to obtain certain information about the speciation of vanadium on the support and through comparison with standards of known structure (Paper II and Paper V) enable the semi-quantitative analysis. Despite the fact that this method was very often used for characterization of vanadium based catalysts [141, 163, 166, 167], there are several problems that prevent wider use of this method. Firstly, it is inapplicable for samples containing the remarkable amount of octahedrally coordinated species and secondly the determination of the ε_0 value is rather subjective. These facts limit the applicability of this methodology for sets of samples with broad distribution of concentration and VO_X speciation and due to subjective determination of ε_0 make semi-quantitative analysis impossible.

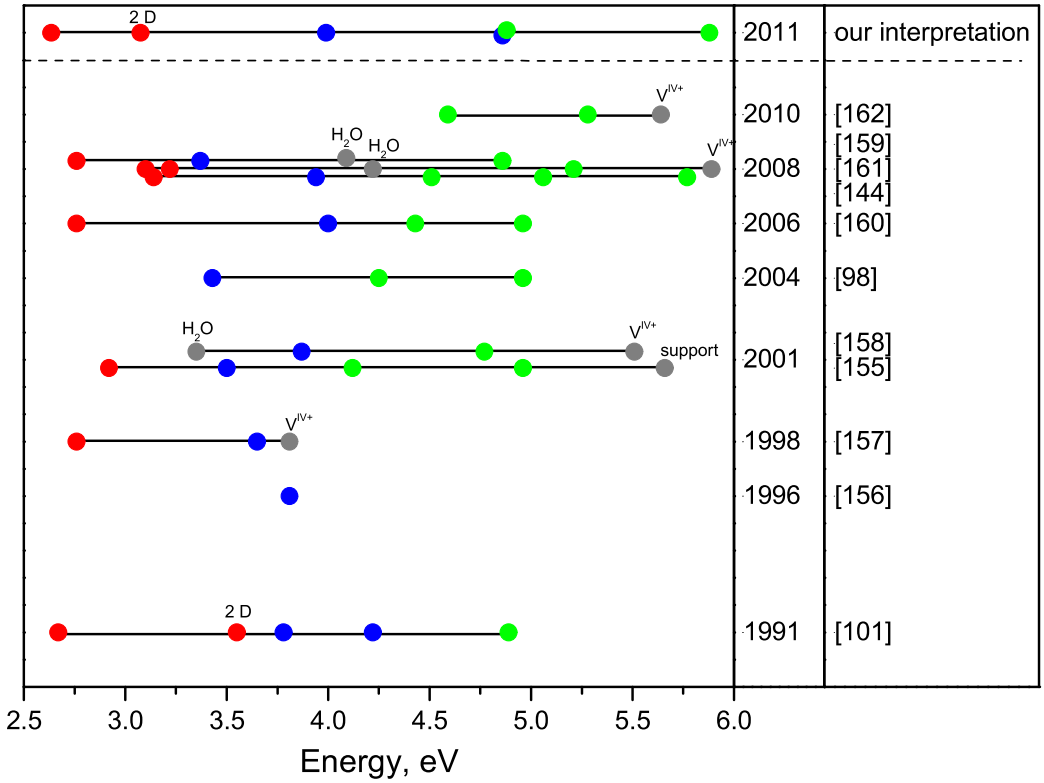

Figure 13 – Examples of previously reported absorption bands positions and their assignment. Red circle - O_h polymers or bulk V_2O_5 species; blue circle - T_d oligomeric species; green circle - T_d monomeric species; gray circle - other species described in plot

Due to above mentioned reason we tried to develop more relevant methodology for characterization of supported vanadium by UV–vis spectroscopy. In Figure 2 in Paper II we can see dependence of spectral intensity of the sample which is subsequently diluted by

pure silica (without any significant spectral signal in studied interval of wavelengths). This plot clearly indicates that linear dependence of the Kubelka–Munk function value $F(R_\infty)$ on the concentration of vanadium can be obtained only for the dilution degree higher than 50 or $F(R_\infty)$ values lower than approximately 0.5. From this reason all samples were diluted with constant ratio 1:100 by pure silica and spectra of such prepared samples you can see in Paper I–III and Paper V. The integral area values of diluted spectra are approximately proportional to the concentration of vanadium in samples, which indicates that the absorption coefficients of all supported VO_X species are approximately the same, which allows the semi-quantitative analysis of such obtained spectra. Moreover, such prepared spectra exhibit more clearly separated bands which offer the possibility to attribute observed absorption bands to individual VO_X units more reliably.

First attempt to attribute observed absorption band in diluted spectra to individual vanadium species have been published in Paper I. However, due to technical problems with UV–vis spectrometer which leads to partially deformed spectra, the interpretation was not sufficiently accurate. After removal of the problem, the second partially modified, reinterpretation has been done on the base of systematic study and analysis wide set of V_*HMS* samples, which were prepared by two different techniques. The final description of individual spectral band of vanadium oxide supported in channel of mesoporous silica is given in Paper II. On the basis of our methodology described in detail in Paper II, we deconvoluted spectra of diluted samples into five different UV–vis bands (Figure 6 and Table 1 in Paper II).

The all spectra contain three absorption bands in the region 3.0-6.5 eV and these bands can be attributed to the ligand to metal charge transfers of tetrahedrally coordinated (T_d) species. The band with maxima position approximately at 4 eV can be attributed to T_d-oligomeric species. The band at ca. 5.9 eV belongs to T_d-monomeric species and the band with maximum at approximately 5 eV is linear combination of both T_d monomeric and oligomeric species, respectively. For samples with vanadium surface density higher than monolayer coverage (for silica about 0.7 $V \cdot nm^{-2}$ [91]) the two new intensive absorption bands at the region 2.5–3.5 eV may occur. These absorption bands can be clearly ascribed (on the base referent V_2O_5 spectra measurement) to the presence of octahedrally (O_h) coordinated bulk-like VO_x units. Assignment of individual bands in UV–vis spectrum is for better illustration shown in Figure 14. Relative amount of individual VO_X species on the surface could be determined from area of corresponding bands, because the extinction coefficients of individual bands are in the first approximation the same (Paper II).

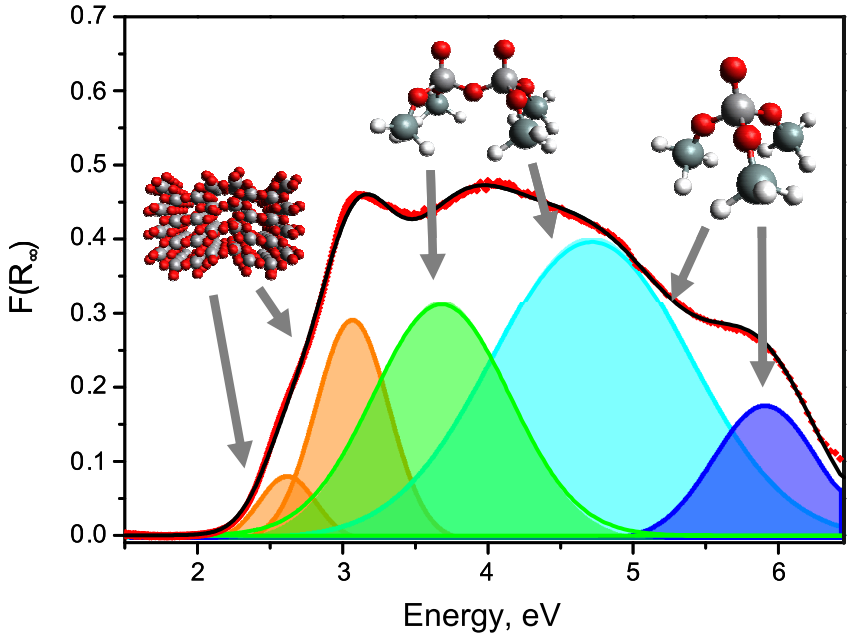

Figure 14 – Assignment of individual bands in UV–vis spectrum of V_*HMS* sample with 9.5 wt.% of V

We can say, in short conclusion of this first part dealing with DR UV–vis spectroscopy, that our new and improved methodology of characterization of vanadium oxide supported materials by DR UV–vis spectroscopy brings some benefits like: (i) the well separated absorption bands obtained by deconvolution of spectra offer detailed information about supported VO_X species, (ii) obtained spectra measured by our methodology samples are proportional to the overall amount of vanadium and allows semi-quantitative VO_X species analysis and (iii) lower sample consumption. However, this methodology has some drawbacks and constriction too. This way of sample preparation is applicable only for material which contains vanadium species inside the porous structure. In opposite way the mechanical redistribution can occur (checked on the small set of samples with VO_X supported on amorphous silica). Next disadvantage is the higher labor intensity and requirement for precision in preparation of sample. This new methodology was successfully used for evaluation of UV–vis spectra in Paper III and Paper V.

2.1.2 H_2-TPR

Temperature programmed reduction by hydrogen (H_2-TPR) is other frequently used technique for characterization of supported metal oxide [143, 145, 146, 168, 169]. It provides less information about coordination in comparison to DR UV–vis, but it is cheap and simply method which has close relation to redox properties of VO_X species under real catalytic conditions. Moreover, this method is able bring information about amount of VO_X

species accessible for redox processes [141, 170]. Nevertheless reliable assignment of individual peaks in TPR profiles to particular species is not solved yet. Our contribution to assignment of TPR peaks to specific vanadium species was done in Paper I and Paper IV.

The TPR profiles reported in literature [141, 146, 171] exhibited one, two or sometimes even three reduction peaks with temperature maximum ranging from 560 to 680 °C. The low temperature peak is usually attributed to the reduction of the isolated monomeric units whereas the high temperature peak is attributed to reduction of oligomeric units and peak with temperature maximum about 700 °C is ascribed as proof of V_2O_5 bulk-like species [143, 146, 158, 171, 172]. Nevertheless this assignment does not agree with results from the UV–vis spectroscopy as it is evident from UV–vis spectra and TPR profiles comparison in Paper I, Paper IV-V and Paper VII or in Ref. [141, 171].

On the base of deeper investigation of H_2-TPR and UV–vis spectra in Paper I and Paper IV was suggested new interpretation of individual bands in TPR profiles which is in good agreement with results obtained by DR UV–vis measurement. The Figure 15 shows representative UV–vis spectra and TPR profiles of V_*SBA-15* materials with different population of vanadium species. The first peak in the TPR profiles of vanadium oxide supported on silica materials can be definitely assigned to the reduction of all unit with T_d coordination (monomeric and oligomeric) and the second peak pertains to the vanadium species with O_h coordination (2D and 3D oligomers). The third peak with very sharp maximum at high temperature (≈ 700–900 °C) could be ascribed to large bulk-vanadium V_2O_5 crystallites with O_h coordination. Our claim is in a good agreement with interpretation suggested by Arena at al. [171].

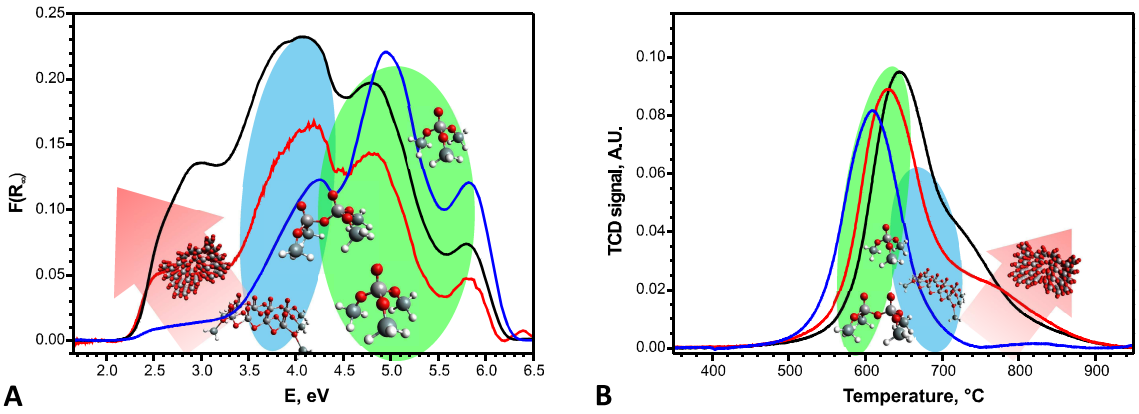

Figure 15 – A) DR UV–vis spectra and B) H_2-TPR profiles of V_*SBA-15* samples prepared by direct synthesis with different population of individual VO_X species.

In conclusion we can say that H_2-TPR is not so powerful tool for investigation detailed speciation of supported vanadium as DR UV–vis spectroscopy, but it brings some benefits too. Firstly, we are able to determine the change of oxidation state during the reduction of supported vanadium samples. Additionally, the TPR is quantitative method and that is why the results from TPR further indicate whether the vanadium species are accessible for a redox process. This is an important proof of successful synthesis of sample because during the preparation by direct synthesis some part of vanadium can be buried in silica walls (Paper IV).

2.1.3 Raman spectroscopy

Characterization of supported vanadium species is very often studied by Raman spectroscopy, in addition to widely used UV–vis spectroscopy [159, 173-178]. However, the using of Raman spectroscopy is connected with solving of some problems and restrictions for VO_X/SiO_2 characterization which could be taken into account before interpretation of Raman spectra. Firstly, the structure information is obtained only indirectly and relies on a correct assignment of the observed bands to vibrational modes. Raman spectra of vanadium supported on silica based materials are more complex and their interpretation is more difficult in comparison with other oxide supports (Al_2O_3, ZrO_2, TiO_2 or Nb_2O_5). The main reason is the strong vibrational coupling between the vanadia species and the silica support, which was reported recently [178, 179]. These vibrations cannot be separated by an easy way and hence it may be impossible to assign each of the Raman bands to a single specific bond vibration. It is main reason which makes Raman spectra of VO_X species on silica very complex and their interpretation more difficult. This subject is still under debate (Paper III and Paper V).

The second fundamental problem is the fact that Raman spectra (shape, intensity) depend on wavelength of laser which is used for the measurement of Raman spectra. This is due to the fact that different excitation wavelengths could be absorbed by different vanadium species in the sample and therefore different resonance enhancement effect control of Raman band intensities can occur (Paper III). The green laser (514-532 nm) is one of the most frequently used Raman scattering laser sources for measurement of Raman's spectra of vanadium supported samples [137, 153, 167, 173, 174, 180, 181]. In this case the resonance enhancement of V_2O_5 species vibration bands could be occurring very easy. This is the reason that most of the Raman spectra generated by this laser contain mainly very intensive signals belonging to crystalline V_2O_5 (set bands at 282, 301, 404,

520, 697 and 993 cm^{-1}). Bands belonging to other vanadium species are very broad with low intensity (expect band at *ca.* 1 035 cm^{-1}) and hence they can not be used for detailed description of vanadium speciation (Paper V). Band at 1 035 cm^{-1} is usually assigned to terminal V=O stretching vibration. Shift of this vibration band to slightly higher wavenumbers was frequently taken as proofs of changes in the extent of polymerization of the surface VO_X species on oxide supports like Al_2O_3, ZrO_2, TiO_2 etc. [167]. However, no shift of this Raman band was observed in the case of VO_X supported on silica and hence some authors predict presence only monomeric VO_4 and/or microcrystalline V_2O_5 species on the silica surface [91, 113, 167, 175]. However, this interpretation is in contradiction with our results obtained from detailed analysis of DR UV–vis spectra (Paper I and Paper II) and with conclusions reported in literature as well [97, 101, 141, 171, 173, 182].

We present deep systematic comparative study of DR UV–vis spectra and Raman spectra excited by 325 and 514 nm laser on set of dehydrated V-HMS samples with wide range of VO_X species population and distribution in Paper III. We prove that changes in population of oligomeric and monomeric VO_X species in individual samples are not manifested by significant changes in the character of Raman signals. On the other hand, the wavelength of used laser very strongly influenced the spectrum. The visible Raman spectrum is totally different from UV Raman spectrum (see Figure 5 in Paper III). This is due to the fact that both laser wavelengths are preferably absorbed by different vanadium species in the sample (see Figure 4 in Paper III) and therefore different resonance enhancement effect controls Raman band intensities. From this data, it is clearly seen that interpretation of Raman spectra is complicated and solely using of Raman spectroscopy for characterization of VO_X species on silica surface is rather problematic and it could easily lead to misinterpretation which has been published previously by Dobler [183] as well. On the other hand, Raman spectroscopy is very sensitive technique (mainly at excitation by 514 nm laser) for monitoring of microcrystalline V_2O_5 species even in such low concentration, which could not be detected by DR UV–vis or XRD techniques (Paper III).

2.1.4 Final recommendations for VO_X–SiO_2 characterization

From above discussed chapters it is clearly seen that it does not exist one universal technique for characterization of vanadium species supported on silica. It is necessary use combination of more technique for obtaining of reliable results.

As we showed in Paper II, DR UV–vis spectroscopy can provide the most detailed information about nature and population of vanadium species on silica based supports and

in addition, DR UV–vis spectra of diluted samples can be at least semi-quantitatively evaluated. The approach based on previously published edge of energy evaluation is still possible to use for such prepared samples. Moreover, we can use this method even for samples with large amount of O_h coordinated species after deconvolution and subtraction of their bands.

The Raman spectroscopy is very sensitive technique for monitoring of V_2O_5 microcrystallines but the using of several excitation wavelengths is recommended for more accurate characterization of dispersed vanadium complexes by Raman spectroscopy (Paper III).

The H_2-TPR could be used mainly for oxidation state investigation and for the verification of accessibility of vanadium particles for redox process. The quantitative information about amount of all T_d coordinated (monomeric and polymeric) and O_h coordinated vanadium species could be obtained after deconvolution of TPR profiles (Paper I).

2.2 Activity of the individual vanadium species in ODH of *n*-butane

For the development of new and efficient catalytic system it is necessary to know the relationship between catalytic activity and character of the active centre. We can found four basic structural types of vanadium oxide species on the surface of the silica support (for more information about structure see Chapter 1.4.1.2 of this thesis or Paper IV).

It is generally accepted that bulk V_2O_5 crystallites is not suitable for ODH reactions because exhibit very small activity in activation of alkanes. Moreover the bulk V_2O_5 is a big reservoir of easily available oxygen which favours subsequent reaction to the undesired total oxidation of ODH products [12, 89]. The deeper investigation of relationship between vanadium structure on the support and activity in ODH of *n*-butane was carried out in Paper IV and confirmed in Paper V.

The role of individual VO_X species supported on HMS in ODH of *n*-butane was investigated on two sets of V_*HMS* samples prepared by wet impregnation and by direct synthesis differing in amount and distribution of VO_X species. The prepared samples were characterized by set of analytical techniques and the most important was DR UV–vis spectroscopy. The population of individual VO_X units was determined on the base of edge of energy evaluation (Paper IV) or by deconvolution of DR UV–vis spectra (Paper V) according methodology described in Paper II. The relative amount of monomeric T_d coordinated units demonstrably influences both, the catalytic activity (expressed by TOF

value) and the $C_{4\text{-deh.}}$ products selectivity (see Figure 16). The all low concentrated samples exhibited approximately constant value of TOF factor (28 h^{-1} at 540 °C) until the vanadium concentration *ca.* 4–5 wt.% is reached followed by a rapid decrease of TOF value (5–7 h^{-1} at 540 °C). Decrease of apparent TOF value clearly evidences that with subsequent increasing of vanadium content the significantly less active or non active species in ODH of *n*-butane are generated.

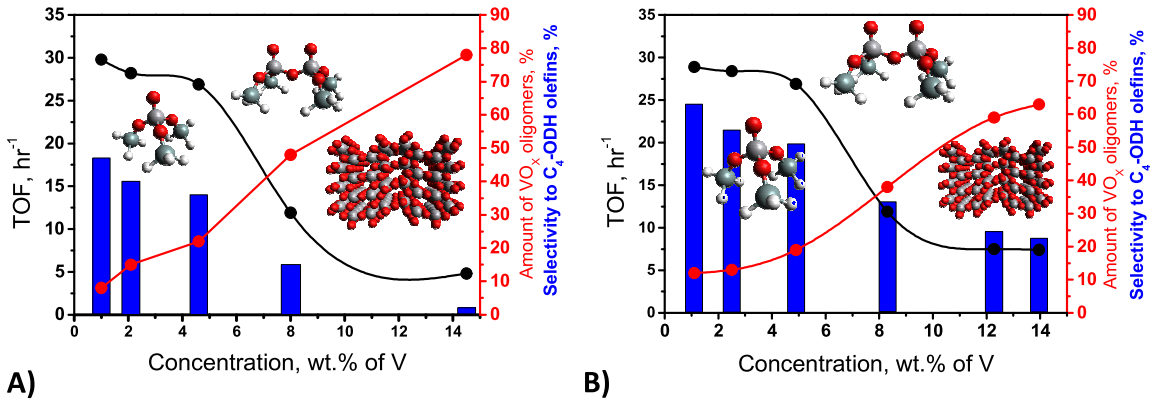

Figure 16 – The relative amount of Td oligomers (red line) as function of vanadium concentration and its impact on activity (black line) and selectivity (blue bars) for samples prepared by wet impregnation (A) and direct synthesis (B). Data originated from Paper IV.

No only activity, but also selectivity to the $C_{4\text{-deh.}}$ products rapidly decreased after reaching 4-5 wt. % of vanadium on the surface. This behaviour is probably due to increasing of abundance of oligomeric species with T_d and/or mainly O_h coordination because these species contain the V–O–V bridging oxygen atoms. According to mechanism introduced by Kung [12] the presence of this type of oxygen facilitates the formation the products of total oxidation (CO and CO_2).

Finally, we can conclude that the isolated monomeric VO_X species play the role of the most performance catalytic centre in the ODH of *n*-butane, because monomeric units are both the much more active and the selective catalytic sites than all other VO_X species. The activity and selectivity decrease continuously with increasing of polymerization degree and activity and selectivity fall almost to zero for samples with high amount of species in octahedral coordination (see Figure 16 and Paper IV).

2.3 How to influence the population of active species and performance of vanadium catalysts

The performance of active VO_X species is determined by many parameters like population of individual vanadium species, composition of support, textural properties of support, the reaction conditions and many others. Some of these parameters were systematically investigated in this thesis and they are described in details in Papers IV-VII and in briefly summarized in following paragraphs.

2.3.1 Support structure and method of VO_X species deposition

The silica based materials are very often reported to be suitable support for preparation of catalysts for ODH of alkane [10, 15, 20, 52, 67, 70, 89]. The main reason is their large surface area allowing good dispersion of active species and also good thermal and hydrothermal stability. Despite the fact, that there are many different structure of silica (for more detail see Chapter 1.5.2), only the SBA-15 and amorphous silica was investigated in ODH of *n*-butane. However, as shown by the results obtained in ODH of propane, support can affect the performance of catalysts and SBA-15 [160] and HMS [184] were reported as the best silica used support. However, it must be noted, that differences among them were not significant.

More significant differences in the catalytic behaviour could be expected in the case of *n*-butane ODH due to higher sensitivity of this reaction to the individual structure of VO_X species (Paper IV). Therefore, we compared the catalytic performance vanadium based catalysts supported on different silica structure (HMS, SBA-15, SBA-16 and MCM-48) in Paper V in order to investigate effect of silica support texture on the speciation of vanadium complexes and its impact on catalytic behaviour. More details about used support were given in Paper V and also in Chapter 1.5.2.2 of this thesis.

It was observed that in addition to structures (1D - 3D mesoporous system of channels, pore diameter, mutual crossing) materials differ mainly in the relative abundance of supported VO_X monomeric T_d-coordinated units. It was found, on the base of detailed analysis of DR UV–vis spectra of diluted samples (method described in Paper II), that the highest relative abundance of monomeric T_d-coordinated units can be found on the SBA-15 support (approximately about 85 % relative amount for sample with 3.6 wt.% of vanadium (Paper V)). We can sort tested materials, on the basis of the supports tendency to

generate the monomeric species, in the following order HMS < SBA-16 ≈ MCM-48 < SBA-15 (Paper V).

High capacity of monomeric species on SBA-15 can be given by the fact that SBA-15 silica represents mesoporous material with regular, very well defined porous system characterized by relatively high volume of mesopores [117]. Hence, the initial vanadium solution can easily homogenously penetrate to the porous system from inner space. In this case the over-concentration does not occur in comparison with worm-like (HMS) or ink-bottle (MCM-48) structure with weaker regularity and lower amount of mesopores (Paper V).

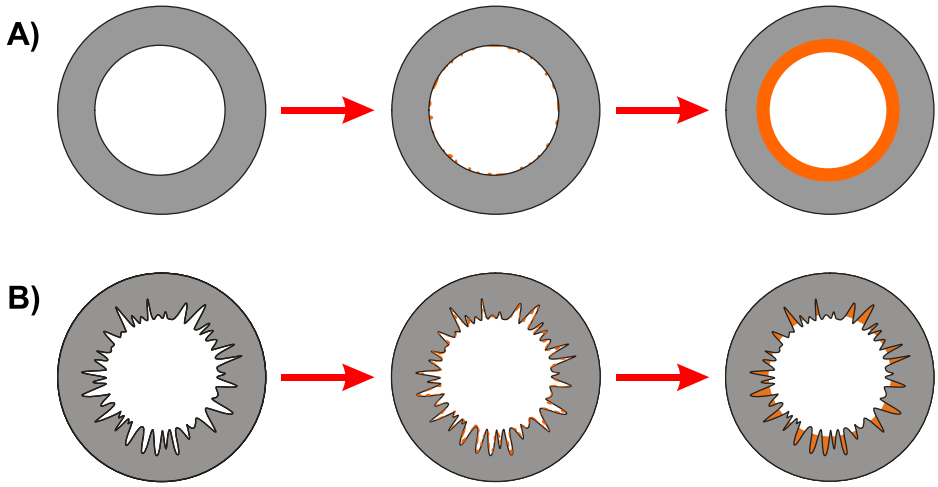

Figure 17 – The gradual filling of the corona by vanadium during the impregnation for A) very well defined structure (e.g. SBA-15) and B) worm like structure with micropore (e.g. HMS)

Previous paragraphs show that the incorporation of vanadium by impregnation may cause creation of large amount of oligomeric species in the areas of solution accumulation (i.e. in micropore and in irregularity the mesopore surface) in less defined structures (Figure 17). This problem could be solved by using different method of vanadium introduction, because the method of the deposition of active vanadium species is another very important parameter which strongly influences the degree of dispersion and coordination of VO_X units on the surface. The direct synthesis of vanadium silicate in one step is often denoted as the best method for preparation of supported catalysts [71, 136, 139, 141]. We report comparative study of two sets of V_*HMS* differing in amount and distribution of VO_X species in Paper IV. The samples with the vanadium concentration less than approximately 4–5 wt.% of V exhibit nearly the same amount of monomeric units and these species represent significant part of the VO_X species generated on the HMS surface

but the highest achievable amount of monomeric species was slightly higher for catalysts prepared by direct synthesis. The oligomeric and polymeric units with wider degree of oligomerization, which are preferentially formed in the samples prepared by the wet impregnation method, starts to generate after reaching ca. 4–5 wt.% of V. Above this concentration polymeric VO_X species with high polymerization degree and bulk like V_2O_5 are generated in the case of impregnated samples and it means rapid loss in activity and selectivity to required alkenes (Paper IV). The relative amount of oligomeric species in both sets of samples and their relationship to catalytic activity is in Figure 16 and deeper discussion was done in Paper IV.

Based on a combination of results from work presented in Paper IV and Paper V, we can suggest that the most promising catalytic system for ODH of *n*-butane could be V_*SBA-15* prepared by direct synthesis. The direct synthesis of V_*SBA-15* was done in cooperation with Jaroslav Heyrovsky institute of Physical Chemistry ASCR in Prague, because the synthesis of SBA-15 structure requires using of an autoclave unavailable in our laboratory. In the Paper VII we report simple one-pot synthesis of V_*SBA-15* catalyst according procedure reported by Gao at al. [159] and its high catalytic performance in ODH of *n*-butane.

Directly synthesized V_*SBA-15* catalysts with 6.5 wt.% of vanadium shows significantly higher apparent TOF value (45 h^{-1}) in comparison with previously published TOF value for V_*SBA-15* system prepared by impregnation (22-35 h^{-1}) which were studied in the ODH of *n*-butane (Paper V and in Ref. [67, 70]). No only high activity, but also relatively high value of selectivity to desired products ($S_{C4\text{-}deh}$ = 59 % at 13 % of *n*-butane conversion), which was equal to selectivity achieved over impregnated V_*SBA-15* with 3.6 wt. % of V (see Table 3 in Paper V). The main advantage of samples prepared by direct synthesis is the fact that the high selectivity value could be obtained even for samples with the high vanadium concentration in contrast with samples prepared by impregnation where the selectivity remains at high value only for vanadium concentration lower than 4 wt.% (Paper IV and Paper V).

The combination of high activity and relatively high selectivity resulted in very high productivity (1.9 $kg_{prod.}$ $kg_{cat.}^{-1}$ h^{-1} for directly synthesized V_*SBA-15* with 6.5 wt. % of V). The productivity is generally accepted like the best criterion for comparison of different catalytic systems tested in one reaction but under different conditions (temperature, inlet reaction mixture composition, contact time etc.) and the value of system productivity is also very important for its potential commercial applicability (the lower limit value which

is acceptable for industrial using is 1 $kg_{prod.}$ $kg_{cat.}^{-1}$ h^{-1} [14]). The productivity value obtained over our synthesized V_*SBA-15* catalyst is one of three highest $C_{4\text{-deh}}$ productivity values which were published for ODH of *n*-butane in literature (for summary see Table 1 in this thesis).

2.3.2 HMS support modified by titanium

We showed that vanadium supported on mesoporous silica could be potential catalysts for ODH of *n*-butane, in previous paragraphs. However, before introduction these materials to the current technologies of alkenes production some problems have to be resolved. The main disadvantage of vanadium oxide catalysts anchored on silica support is low value of monolayer capacity (the amount of monomeric vanadium species determine the activity and selectivity of vanado-silicates in C_4-ODH), which is only 0.7 VO_X per nm^2 [91]. The second problem is low activity of vanado-silicates due to relatively high apparent activation energies of C–H bond over VO_X_SiO_2 [185, 186].

The last problem could be solved by using of VO_X species supported on TiO_2 (anatase). This catalysts showed the highest activities in ODH reactions and this makes possible to carry out the reaction at lower temperature (due to very low apparent activation energy of C–H bond over VO_X_TiO_2 which also reduces problems with cracking of alkane [20, 52, 185, 187-190]. Nevertheless, pure TiO_2 support has also some drawbacks, such as a relatively low selectivity in comparison with silica supported materials and low specific surface area, which can be further reduced by sintering as a consequence of thermal treatments (more details in Paper IV and Paper VII and references therein). These drawbacks prevent the use of TiO_2 as conventional support for ODH catalysts.

One possibility how to solve this problem is to prepare a mixed Si–Ti support which combines suitable properties of SiO_2 and TiO_2 together in one material. The first attempts of preparation titano-silicates were done by impregnation or grafting of anatase phase to silica support [185, 187-189, 191-193] or by direct synthesis of titano-silicate [56, 192, 194-197]. However, these materials were not prepared in titanium content higher than 9 wt.% [198] which is still too low for obtaining sufficient activity in ODH of *n*-butane which is necessary for potential industrial using (Paper VII).

We report one-pot synthesis of Ti-HMS support with high content of titanium in the Paper VII. In this case we obtained hexagonal mesoporous silica support with the isomorphously exchanged titanium oxide species in tetrahedral coordination (checked by DR UV–vis and IR spectroscopy Paper VII). These units serve like an “anchor” for

vanadium active species. The main reason for this behavior is probably the difference in the isoelectric point of TiO_2 surface (IEP = 6–6.4 for Ti-OH) and SiO_2 (IEP = 1–2 for Si-OH) supports. The acidic vanadium oxide species (IEP = 1.4) are preferentially bonded to the more basic surface Ti-OH units [23].

Moreover, acid/base properties of titanium species in the support influence the strength of the bridging oxygen in Ti-O-V and therefore their reactivity. The high reactivity of V_*Ti-HMS* catalysts allows carrying out the reaction at significantly lower temperature (460 °C) then in the case of V_*HMS* catalysts. This fact prevents the reaction leading to cracking products and it increased selectivity to desired $C_{4\text{-deh.}}$ products. The Figure 8 in Paper VII shows that the selectivity to $C_{4\text{-deh.}}$ products is comparable for both catalytic systems (V_*HMS* and V_*Ti-HMS*, respectively) and it is about 50 %. However, the activity of V_*Ti-HMS* catalysts is significantly higher in comparison with V_*HMS*. The activity of V_*Ti-HMS* catalyst at 460 °C is comparable with the activity of V_*HMS* with similar vanadium content but at 540 °C (Paper IV). However, the productivity (Table 2 in Paper VII) is still too low in comparison with our most performing catalysts based on V_*SBA-15* prepared by direct synthesis (Paper VI).

3 Conclusions

The vanadium oxide species anchored on suitable support already play the important role in modern heterogeneous catalysis. Moreover, the new applications are still tested. The oxidative dehydrogenation of *n*-butane (C_4-ODH), which is studied in this thesis, is one good example of such perspective process, because the C_4-ODH reaction could be good alternative to classically used dehydrogenation. However, several problems have to be solved before introduction to industrial practice.

Determination of the active centre is very important for target preparation of catalysts with large population of this active and selective species, leads to materials with high catalytic performance in ODH. For this purpose, it is very important to find suitable characterization technique for investigation of vanadium speciation.

This doctoral thesis contributed to the general knowledge about vanadium oxide supported on silica and their using in ODH of *n*-butane and the main results can be summarized as follows:

- It is necessary use combination of more characterization techniques for proper catalyst characterization.
- DR UV–vis spectroscopy provides the most detailed information about VO_X speciation on silica based supports but for the correct results it is necessary to dilute the vanadium containing samples by pure silica (ratio 1:100). Intensity of obtained spectra of the diluted samples is proportional to overall concentration of vanadium what allows us to use deconvolution of spectra to individual spectral bands and offers the possibility to obtain more detailed and semi–quantitative information about speciation of supported VO_X species.
- The Raman spectroscopy is very sensitive technique for monitoring of V_2O_5 microcrystallines but the using of several excitation wavelengths is recommended for more accurate characterization of dispersed vanadium complexes. No information about of T_d coordinated VO_X particles speciation was founded in Raman spectra due to strong vanadium silicon vibration coupling.
- The monomeric units with T_d coordination are the most active and selective catalytic sites in n-butane ODH in comparison with all other species. Moreover C_4-ODH reaction is very sensitive to presence of isolated vanadium species and can be used as a “probe reaction” for their investigation.

- The VO_X species with higher degree of polymerization participate mainly in undesired consecutive reactions with of ODH products.
- The method of preparation influences the formation of oligomeric species. The impregnated samples contain higher amount of O_h coordinated species compared to samples prepared by direct synthesis.
- SBA-15 support is the most suitable structure for deposition of vanadium in the form of isolated T_d coordinated monomeric species.
- The V-SBA-15 material prepared by direct synthesis belongs to three catalysts with highest $C_{4\text{-deh}}$ productivity values which were published for ODH of *n*-butane in literature.
- Introduction of titanium to the silica walls led to catalysts with proper selectivity and high activity even at lower temperature (460 °C) in comparison with pure silica based materials without significantly negative effects to $C_{4\text{-deh}}$ selectivity observed on the TiO_2 based supports.

4 References

[1] E.M. Melhado, Jöns Jacob Berzelius, Vol. 2013, Encyclopedia Britannica.

[2] A.D. McNaught and A. Wilkinson, IUPAC Compendium of Chemical Terminology - the Gold Book, Blackwell Scientific Publications, Oxford, 1997.

[3] I. Chorkendorff and J.W. Niemantsverdriet, Concepts of Modern Catalysis and Kinetics, WILEY-VCH Verlag GmbH, Weinheim, 2003.

[4] J. Hagen, Industrial Catalysis, Wiley-WCH Verlag GmbH & Co. KGaA, Weinheim, Germany, 2006.

[5] A. Bielanski and J. Haber, Oxygen in Catalysis, Marcel Dekker., Inc., New York, 1991.

[6] G. Centi, F. Cavani and F. Trifiró, Selective Oxidation by Heterogeneous Catalysis, Kluwer Academic, New York 2001.

[7] H.F. Rase, Handbook of Commercial Catalysts, CRC Press, New York, 2000.

[8] S. Albonetti, F. Cavani and F. Trifiro, Catal. Rev.-Sci. Eng., 38 (1996) 413.

[9] L.M. Madeira and M.F. Portela, Appl. Catal. A-Gen., 281 (2005) 179.

[10] L.M. Madeira and M.F. Portela, Catal. Rev.-Sci. Eng., 44 (2002) 247.

[11] L.M. Madeira, M.F. Portela and C. Mazzocchia, Catal. Rev.-Sci. Eng., 46 (2004) 53.

[12] H.H. Kung, Advances in Catalysis, Vol. 40, Academic Press Inc, San Diego, 1994, p. 1.

[13] C. Hess and R. Schlögl, Nanostructured Catalysts - Selective Oxidations, Royal Society of Chemistry, 2011, p. 457.

[14] F. Cavani, N. Ballarini and A. Cericola, Catal. Today, 127 (2007) 113.

[15] Y.B. Xu, J.Y. Lu, M. Zhong and J.D. Wang, J. Nat. Gas Chem., 18 (2009) 88.

[16] S. Davis and M. Yoneyama, Butylenes, Vol. 2011, IHS, 2011.

[17] U.s.E.o.I.C.-S.e.-E. release, Ullmann´s Ecyklopedia of Industrial Chemistry, Electronic release, Vol. Sixth edition, 1999.

[18] E. Sporcic and K. Ring, Butylenes, Vol. 2009, Sri Consulting, 2005.

[19] OSHA, Vol. 2009, Occupational Safety and Health Administration, U. S. Department of Labor, 2009.

[20] E.A. Mamedov and V.C. Corberan, Appl. Catal. A-Gen., 127 (1995) 1.

[21] S. Matar, M.J. Mirbach and H.A. Tayim, Catalysis in Petrochemical Processes, Kluwer Academic Publishers, Dordrecht, 1989.

[22] A.C. Council, Butadiene - Product Stewardship Guidance manual, American Chemistry Council 2010.

[23] T. Blasco and J.M.L. Nieto, Appl. Catal. A-Gen., 157 (1997) 117.

[24] J.A. Dean, Lange´s handbook of chemistry, McGraw-Hill Inc., New York, 1999.

[25] M.M. Bhasin, J.H. McCain, B.V. Vora, T. Imai and P.R. Pujado, Appl. Catal. A-Gen., 221 (2001) 397.

[26] M.A. Chaar, D. Patel and H.H. Kung, J. Catal., 109 (1988) 463.

[27] J.L. Figueiredo and A.O. Desidrogenac, XVth Ibero-American Symposium on Catalysis, Argentina, 1996.

[28] T.E. Toolbox, Gases - Explosive and Flammability Concentration Limits, Vol. 2013, www.engineeringtoolbox.com, 2013.

[29] C. Batiot and B.K. Hodnett, Appl. Catal. A-Gen., 137 (1996) 179.

[30] K. Weissermel and H.-J. Arpe, Industrial Organic Chemistry - Third Completely Revised Edition Wiley - VCH Publishers, New York, 1997.

[31] M. Hoang, K.C. Pratt and J. Mathews, Catalysts for oxidative dehydrogenation of hydrocarbons, USA, 1998.

[32] J. Magistro, Process for the preparation of ethylene and vinyl chloride from ethane in the presence of water, 1992.

[33] J.M.L. Nieto, A. Dejoz, M.I. Vazquez, W. O'Leary and J. Cunningham, Catal. Today, 40 (1998) 215.

[34] O.V. Krylov, A.K. Mamedov and S.R. Mirzabekova, Catal. Today, 24 (1995) 371.

[35] B.J. Bertus, Nickel and cobalt catalysts including a group IIA and VIA component, in U.S.o.A.P.a.T. Office (Editor), Phillips Petroleum Company, 1975.

[36] M.A. Chaar, D. Patel, M.C. Kung and H.H. Kung, J. Catal., 105 (1987) 483.

[37] M.L. Pacheco, J. Soler, A. Dejoz, J.M.L. Nieto, J. Herguido, M. Menendez and J. Santamaria, Catal. Today, 61 (2000) 101.

[38] A. Dejoz, J.M.L. Nieto, F. Marquez and M.I. Vazquez, Appl. Catal. A-Gen., 180 (1999) 83.

[39] B.J. Bertus, Catalyst and Process for Oxidative Dehydrogenation, in U.S.o.A.P.a.T. Office (Editor), Phillips Petroleum Company, USA, 1978.

[40] L.M. Madeira, R.M. MartinAranda, F.J. MaldonadoHodar, J.L.G. Fierro and M.F. Portela, J. Catal., 169 (1997) 469.

[41] J.C. Jung, H. Kim, A.S. Choi, Y.-M. Chung, T.J. Kim, S.J. Lee and S.-H. Oh, J. Mol. Catal. A-Chem., 259 (2006) 166.

[42] J.C. Jung, H. Kim, Y.S. Kim, Y.M. Chung, T.J. Kim, S.J. Lee, S.H. Oh and I.K. Song, Appl. Catal. A-Gen., 317 (2007) 244.

[43] J.C. Jung, H. Kini, A.S. Choi, Y.M. Chung, T.J. Kim, S.J. Lee, S.H. Oh and I.K. Song, Catal. Commun., 8 (2007) 625.

[44] J.C. Jung, H. Lee, H. Kim, Y.M. Chung, T.J. Kim, S.J. Lee, S.H. Oh, Y.S. Kim and I.K. Song, Catal. Lett., 123 (2008) 239.

[45] J.C. Jung, H. Lee, J.G. Seo, S. Park, Y.M. Chung, T.J. Kim, S.J. Lee, S.H. Oh, Y.S. Kim and I.K. Song, Catal. Today, 141 (2009) 325.

[46] G. Savelieva, D. Abdukhalykov and K. Dossumov, Catal. Lett., 128 (2009) 106.

[47] B. Solsona, F. Ivars, P. Concepcion and J.M.L. Nieto, J. Catal., 250 (2007) 128.

[48] F. Arena, F. Frusteri and A. Parmaliana, Appl. Catal. A-Gen., 176 (1999) 189.

[49] G. Raju, B.M. Reddy, B. Abhishek, Y.H. Mo and S.E. Park, Appl. Catal. A-Gen., 423 (2012) 168.

[50] S.B. Wang, K. Murata, T. Hayakawa, S. Hamakawa and K. Suzuki, Energy Fuels, 15 (2001) 384.

[51] C. Larese, J.M. Campos-Martin, J.J. Calvino, G. Blanco, J.L.G. Fierro and Z.C. Kang, J. Catal., 208 (2002) 467.

[52] E. Santacesaria, M. Cozzolino, M. Di Serio, A.M. Venezia and R. Tesser, Appl. Catal. A-Gen., 270 (2004) 177.

[53] C.R. Dias, M.F. Portela and G.C. Bond, J. Catal., 157 (1995) 353.

[54] R. Grabowski, Catal. Rev.-Sci. Eng., 48 (2006) 199.

[55] B.M. Weckhuysen and D.E. Keller, Catal. Today, 78 (2003) 25.

[56] Y. Chen, Y. Huang, J. Xiu, X. Han and X. Bao, Applied Catalysis A: General, 273 (2004) 185.

[57] X.W. Chen, Z. Zhu, M. Havecker, D.S. Su and R. Schlogl, Mater. Res. Bull., 42 (2007) 354.

[58] C. Tellez, M. Menendez and J. Santamaria, Chemical Engineering Science, 54 (1999) 2917.

[59] C. Tellez, M. Menendez and J. Santamaria, Aiche J., 43 (1997) 777.

[60] A.A. Lemonidou and A.E. Stambouli, Appl. Catal. A-Gen., 171 (1998) 325.

[61] A. Malaika, K. Wower and M. Kozlowski, Acta Phys. Pol. A, 118 (2010) 459.

[62] A. Wegrzyn, A. Rafalska-Lasocha, B. Dudek and R. Dziembaj, Catal. Today, 116 (2006) 74.

[63] J.A. Toledo, H. Armendariz and E. Lopez-Salinas, Catal. Lett., 66 (2000) 19.

[64] H. Armendariz, J.A. Toledo, G. Aguilarrios, M.A. Valenzuela, P. Salas, A. Cabral, H. Jimenez and I. Schifter, Journal of Molecular Catalysis, 92 (1994) 325.

[65] D. Gazzoli, S. De Rossi, G. Ferraris, G. Mattei, R. Spinicci and M. Valigi, J. Mol. Catal. A-Chem., 310 (2009) 17.

[66] A.P.S. Dias, L.D. Dimitrov, M.C.R. Oliveira, R. Zavoianu, A. Fernandes and M.F. Portela, J. Non-Cryst. Solids, 356 (2010) 1488.

[67] W. Liu, S.Y. Lai, H.X. Dai, S.J. Wang, H.Z. Sun and C.T. Au, Catal. Today, 131 (2008) 450.

[68] H. Armendariz, G. Aguilarrios, P. Salas, M.A. Valenzuela, I. Schifter, H. Arriola and N. Nava, Appl. Catal. A-Gen., 92 (1992) 29.

[69] V. Murgia, E. Sham, J.C. Gottifredi and E.M.F. Torres, Latin Am. Appl. Res., 34 (2004) 75.

[70] W. Liu, S.Y. Lai, H.X. Dai, S.J. Wang, H.Z. Sun and C.T. Au, Catal. Lett., 113 (2007) 147.

[71] V. Murgia, E.A.F. Torres, J.C. Gottifredi and E.L. Sham, Appl. Catal. A-Gen., 312 (2006) 134.

[72] N. Kijima, M. Toba and Y. Yoshimura, Catal. Lett., 127 (2009) 63.

[73] X. Liu, B. Frank, W. Zhang, T.P. Cotter, R. Schlogl and D.S. Su, Angew. Chem.-Int. Edit., 50 (2011) 3318.

[74] J.M.L. Nieto, J. Soler, P. Concepcion, J. Herguido, M. Menendez and J. Santamaria, J. Catal., 185 (1999) 324.

[75] F.J. Maldonado-Hodar, L.M. Madeira and M.F. Portela, Appl. Catal. A-Gen., 178 (1999) 49.

[76] X. Liu and M. Gradzielski, Carbon nanotubes as catalysts in the catalytic oxidation of C4 hydrocarbons, Fritz-Haber-Institut der Max-Planck-Gesellschaft, Berlin, 2008.

[77] H.H. Kung and M.A. Chaar, Oxidative dehydrogenation of alkanes to unsaturated hydrocarbons, Northwestern University, USA, 1988.

[78] M.E. Harlin, L.B. Backman, A.O.I. Krause and O.J.T. Jylha, J. Catal., 183 (1999) 300.

[79] H. Lee, J.K. Lee, U.G. Hong, Y. Yoo, Y.J. Cho, J. Lee, H.S. Jang, J.C. Jung and I.K. Song, Journal of Industrial and Engineering Chemistry, 18 (2012) 808.

[80] S. Ahmed, F. Rahman, A.M.J. Al-Amer, E.M. Al-Mutairi, U. Baduruthamal and K. Alam, React. Kinet. Mech. Catal., 105 (2012) 483.

[81] J.K. Lee, H. Lee, U.G. Hong, Y. Yoo, Y.J. Cho, J. Lee, H. Chang and I.K. Song, Journal of Industrial and Engineering Chemistry, 18 (2012) 1758.

[82] G.E. Vrieland and C.B. Murchison, Appl. Catal. A-Gen., 134 (1996) 101.

[83] I.C. Marcu, I. Sandulescu and J.M.M. Millet, Appl. Catal. A-Gen., 227 (2002) 309.

[84] L.C. Marcu, L. Sandulescu, Y. Schuurman and J.M.M. Millet, Appl. Catal. A-Gen., 334 (2008) 207.

[85] F. Urlan, I.C. Marcu and I. Sandulescu, Catal. Commun., 9 (2008) 2403.

[86] J.B. Kimble, Oxidative dehydrogenation of paraffins Phillips Petroleum Company, USA, 1987.

[87] M.V. Landau, A. Gutman, M. Herskowitz, R. Shuker, Y. Bitton and D. Mogilyansky, J. Mol. Catal. A-Chem., 176 (2001) 127.

[88] O. Ovsitser and E.V. Kondratenko, Catal. Today, 142 (2009) 138.

[89] L. Owens and H.H. Kung, J. Catal., 144 (1993) 202.

[90] U.S.G. Survey, Vanadium, Mineral Commodity Summaries, Vol. 2013, 2012.

[91] I.E. Wachs and B.M. Weckhuysen, Appl. Catal. A-Gen., 157 (1997) 67.

[92] P. Knotek and R. Bulánek, Selektivní oxidace propanu, Faculty of Chemical Technology, Department of Physical Chemistry University of Pardubice, Pardubice, 2010.

[93] G.C. Bond and J.C. Vedrine, Catal. Today, 20 (1994) 171.

[94] G.C. Bond and S.F. Tahir, Applied Catalysis, 71 (1991) 1.

[95] I.E. Wachs, J.M. Jehng, G. Deo, B.M. Weckhuysen, V.V. Guliants, J.B. Benziger and S. Sundaresan, J. Catal., 170 (1997) 75.

[96] N.N. Greenwood and A. Earnshaw, Chemie prvků, Informatorium, Praha, 1993.

[97] X.T. Gao, S.R. Bare, B.M. Weckhuysen and I.E. Wachs, J. Phys. Chem. B, 102 (1998) 10842.

[98] C. Hess, J.D. Hoefelmeyer and T.D. Tilley, J. Phys. Chem. B, 108 (2004) 9703.

[99] D.E. Keller, T. Visser, F. Soulimani, D.C. Koningsberger and B.M. Weckhuysen, Vib. Spectrosc., 43 (2007) 140.

[100] J.M. Jehng, G. Deo, B.M. Weckhuysen and I.E. Wachs, J. Mol. Catal. A-Chem., 110 (1996) 41.

[101] M. Schramlmarth, A. Wokaun, M. Pohl and H.L. Krauss, Journal of the Chemical Society - Faraday Transactions, 87 (1991) 2635.

[102] H. Berndt, A. Martin, A. Bruckner, E. Schreier, D. Muller, H. Kosslick, G.U. Wolf and B. Lucke, J. Catal., 191 (2000) 384.

[103] C. Hess, G. Tzolova-Muller and R. Herbert, J. Phys. Chem. C, 111 (2007) 9471.

[104] V.B. Kazansky, I.N. Senchenya, M. Frash and R.A. Vansanten, Catal. Lett., 27 (1994) 345.

[105] E.P.L. Hunter and S.G. Lias, J. Phys. Chem. Ref. Data, 27 (1998) 413.

[106] P.M. Esteves, G.G.P. Alberto, A. Ramirez-Solis and C.J.A. Mota, J. Phys. Chem. A, 104 (2000) 6233.

[107] T. Blasco, J.M.L. Nieto, A. Dejoz and M.I. Vazquez, J. Catal., 157 (1995) 271.

[108] T. Blasco, A. Galli, J.M.L. Nieto and F. Trifiro, J. Catal., 169 (1997) 203.

[109] G. Deo and I.E. Wachs, J. Phys. Chem., 95 (1991) 5889.

[110] M. Kosmulski, Chemical properties of material surfaces, Marcel Dekker, New York, 2001.

[111] J.A. Lewis, J. Am. Cer. Soc., 83 (2000) 2341.

[112] A. Corma, J.M.L. Nieto, N. Parades, A. Dejoz and I. Vazquez, in V.C. Corberán and S.V. Bellón (Editors), Studies in Surface Science and Catalysis, Vol. Volume 82, Elsevier, 1994, p. 113.

[113] I.E. Wachs, Catal. Today, 27 (1996) 437.

[114] J.M.L. Nieto, P. Concepcion, A. Dejoz, H. Knozinger, F. Melo and M.I. Vazquez, J. Catal., 189 (2000) 147.

[115] A.A. Lemonidou, Appl. Catal. A-Gen., 216 (2001) 277.

[116] A.A. Teixeira-Neto, L. Marchese and H.O. Pastore, Quim. Nova, 32 (2009) 463.

[117] J. Čejka , A. Corma, H.v. Bekkum and F. Schüth, Introduction to zeolite science and practice Elsevier 2007.

[118] P. Schneider, Textura porézních látek, Ústav chemických procesů AV ČR, Praha, 2001.

[119] A. Taguchi and F. Schuth, Microporous Mesoporous Mat., 77 (2005) 1.

[120] V. Chiola, J.E. Ritsko and C.D. Vanderpool, Sylvania Electric Products, Inc., US, 1971.

[121] T. Yanagisawa, T. Shimizu, K. Kuroda and C. Kato, Bull. Chem. Soc. Jpn., 63 (1990) 988.

[122] J.S. Beck, J.C. Vartuli, W.J. Roth, M.E. Leonowicz, C.T. Kresge, K.D. Schmitt, C.T.W. Chu, D.H. Olson, E.W. Sheppard, S.B. McCullen, J.B. Higgins and J.L. Schlenker, J. Am. Chem. Soc., 114 (1992) 10834.

[123] J. Čejka and H. van Bekkum, Zeolites and ordered mesoporous materials: progress and prospects, Elsevier, 2005.

[124] J.Y. Ying, C.P. Mehnert and M.S. Wong, Angew. Chem.-Int. Edit., 38 (1999) 56.

[125] U. Ciesla and F. Schuth, Microporous Mesoporous Mat., 27 (1999) 131.

[126] F. Hoffmann, M. Cornelius, J. Morell and M. Froba, Angew. Chem.-Int. Edit., 45 (2006) 3216.

[127] V. Meynen, P. Cool and E.F. Vansant, Microporous Mesoporous Mat., 125 (2009) 170.

[128] P.T. Tanev and T.J. Pinnavaia, Science, 267 (1995) 865.

[129] P.T. Tanev and T.J. Pinnavaia, Chem. Mater., 8 (1996) 2068.

[130] D.Y. Zhao, J.L. Feng, Q.S. Huo, N. Melosh, G.H. Fredrickson, B.F. Chmelka and G.D. Stucky, Science, 279 (1998) 548.

[131] M. Kruk, M. Jaroniec, C.H. Ko and R. Ryoo, Chem. Mater., 12 (2000) 1961.

[132] P.I. Ravikovitch and A.V. Neimark, J. Phys. Chem. B, 105 (2001) 6817.

[133] D.Y. Zhao, Q.S. Huo, J.L. Feng, B.F. Chmelka and G.D. Stucky, J. Am. Chem. Soc., 120 (1998) 6024.

[134] K. Cassiers, T. Linssen, M. Mathieu, M. Benjelloun, K. Schrijnemakers, P. Van Der Voort, P. Cool and E.F. Vansant, Chem. Mater., 14 (2002) 2317.

[135] M. Bandyopadhyay, A. Birkner, M.W.E. van den Berg, K.V. Klementiev, W. Schmidt, W. Grunert and H. Gies, Chem. Mater., 17 (2005) 3820.

[136] M. Piumetti, B. Bonelli, M. Armandi, L. Gaberova, S. Casale, P. Massiani and E. Garrone, Microporous Mesoporous Mat., 133 (2010) 36.

[137] M. Piumetti, B. Bonelli, P. Massiani, S. Dzwigaj, I. Rossetti, S. Casale, L. Gaberova, M. Armandi and E. Garrone, Catal. Today, 176 (2011) 458.

[138] F. Ying, J.H. Li, C.J. Huang, W.Z. Weng and H.L. Wan, Catal. Lett., 115 (2007) 137.

[139] L.N. Zhao, Y.L. Dong, X.L. Zhan, Y. Cheng, Y.J. Zhu, F.L. Yuan and H.G. Fu, Catal. Lett., 142 (2012) 619.

[140] E.L. Sham, V. Murgia, J.C. Gottifredi and E.M. Farfan-Torres, Preparation of Catalysts Vii, 118 (1998) 669.

[141] R. Bulánek, P. Čičmanec, H. Sheng-Yang, P. Knotek, L. Čapek and M. Setnička, Applied Catalysis A: General, (2012).

[142] Y.M. Liu, Y. Cao, S.R. Yan, W.L. Dai and K.N. Fan, Catal. Lett., 88 (2003) 61.

[143] M.M. Koranne, J.G. Goodwin and G. Marcelin, J. Catal., 148 (1994) 369.

[144] L. Čapek, J. Adam, T. Grygar, R. Bulánek, L. Vradman, G. Kosova-Kucerová, P. Čičmanec and P. Knotek, Appl. Catal. A-Gen., 342 (2008) 99.

[145] L. Čapek, R. Bulánek, J. Adam, L. Smoláková, H. Sheng-Yang and P. Čičmanec, Catal. Today, 141 (2009) 282.

[146] P. Knotek, L. Čapek, R. Bulánek and J. Adam, Top. Catal., 45 (2007) 51.

[147] P. Van Der Voort, M. Baltes and E.F. Vansant, Catal. Today, 68 (2001) 119.

[148] S.A. Karakoulia, K.S. Triantafyllidis and A.A. Lemonidou, Microporous Mesoporous Mat., 110 (2008) 157.

[149] M. Mathieu, M. Baltes, P. Van der Voort and E.F. Vansant, Adsorption Science and Technology, (2000) 643.

[150] J.S. Reddy, P. Liu and A. Sayari, Appl. Catal. A-Gen., 148 (1996) 7.

[151] M. Mathieu, P. Van Der Voort, B.M. Weckhuysen, R.R. Rao, G. Catana, R.A. Schoonheydt and E.F. Vansant, J. Phys. Chem. B, 105 (2001) 3393.

[152] A. Sorrentino, S. Rega, D. Sannino, A. Magliano, P. Ciambelli and E. Santacesaria, Appl. Catal. A-Gen., 209 (2001) 45.

[153] R. Chlosta, G. Tzolova-Muller, R. Schlogl and C. Hess, Catal. Sci. Technol., 1 (2011) 1175.

[154] K. Inumaru, M. Misono and T. Okuhara, Appl. Catal. A-Gen., 149 (1997) 133.

[155] M. Baltes, K. Cassiers, P. Van Der Voort, B.M. Weckhuysen, R.A. Schoonheydt and E.F. Vansant, J. Catal., 197 (2001) 160.

[156] M. Morey, A. Davidson and G. Stucky, Microporous Mater., 6 (1996) 99.

[157] G. Catana, R.R. Rao, B.M. Weckhuysen, P. Van Der Voort, E. Vansant and R.A. Schoonheydt, J. Phys. Chem. B, 102 (1998) 8005.

[158] M.L. Pena, A. Dejoz, V. Fornes, E. Rey, M.I. Vazquez and J.M.L. Nieto, Appl. Catal. A-Gen., 209 (2001) 155.

[159] F. Gao, Y.H. Zhang, H.Q. Wan, Y. Kong, X.C. Wu, L. Dong, B.Q. Li and Y. Chen, Microporous Mesoporous Mat., 110 (2008) 508.

[160] Y.M. Liu, Y. Cao, N. Yi, W.L. Feng, W.L. Dai, S.R. Yan, H.Y. He and K.N. Fan, J. Catal., 224 (2004) 417.

[161] N. Moussa and A. Ghorbel, Appl. Surf. Sci., 255 (2008) 2270.

[162] Y.M. Liu, S.H. Xie, Y. Cao, H.Y. He and K.N. Fan, J. Phys. Chem. C, 114 (2010) 5941.

[163] X.T. Gao and I.E. Wachs, J. Phys. Chem. B, 104 (2000) 1261.

[164] E.A. Davis and N.F. Mott, Philos. Mag., 22 (1970) 903.

[165] J. Tauc, Amorphous and Liquid Semiconductors, Plenum Press, London, 1974.

[166] X.T. Gao and I.E. Wachs, J. Catal., 192 (2000) 18.

[167] H.J. Tian, E.I. Ross and I.E. Wachs, J. Phys. Chem. B, 110 (2006) 9593.

[168] N.W. Hurst, S.J. Gentry, A. Jones and B.D. McNicol, Catal. Rev.-Sci. Eng., 24 (1982) 233.

[169] C.B. Wang, G. Deo and I.E. Wachs, J. Catal., 178 (1998) 640.

[170] M. Setnička, P. Čičmanec, E. Tvarůžková and R. Bulánek, Top. Catal., in press (2013).

[171] F. Arena, F. Frusteri, G. Martra, S. Coluccia and A. Parmaliana, J. Chem. Soc.-Faraday. Trans., 93 (1997) 3849.

[172] G. Du, S. Lim, M. Pinault, C. Wang, F. Fang, L. Pfefferle and G.L. Haller, J. Catal., 253 (2008) 74.

[173] L. Burcham, G. Deo, X. Gao and I. Wachs, Top. Catal., 11-12 (2000) 85.

[174] G.G. Cortez and M.A. Banares, J. Catal., 209 (2002) 197.

[175] N. Das, H. Eckert, H. Hu, I.E. Wachs, J.F. Walzer and F.J. Feher, J. Phys. Chem. B, 97 (1993) 8240.

[176] A.E. Stiegman, J. Phys. Chem. C, 115 (2011) 10917.

[177] I.E. Wachs, Top. Catal., 8 (1999) 57.

[178] Z.L. Wu, S. Dai and S.H. Overbury, J. Phys. Chem. C, 114 (2010) 412.

[179] N. Magg, B. Immaraporn, J.B. Giorgi, T. Schroeder, M. Baumer, J. Dobler, Z.L. Wu, E. Kondratenko, M. Cherian, M. Baerns, P.C. Stair, J. Sauer and H.J. Freund, J. Catal., 226 (2004) 88.

[180] B.M. Weckhuysen, J.-M. Jehng and I.E. Wachs, J. Phys. Chem. B, 104 (2000) 7382.

[181] M.V. Martinez-Huerta, X. Gao, H. Tian, I.E. Wachs, J.L.G. Fierro and M.A. Banares, Catal. Today, 118 (2006) 279.

[182] E.V. Kondratenko, M. Cherian, M. Baerns, D.S. Su, R. Schloegl, X. Wang and I.E. Wachs, J. Catal., 234 (2005) 131.

[183] J. Dobler, M. Pritzsche and J. Sauer, J. Phys. Chem. C, 113 (2009) 12454.

[184] S.A. Karakoulia, K.S. Triantafyllidis, G. Tsilomelekis, S. Boghosian and A.A. Lemonidou, Catal. Today, 141 (2009) 245.

[185] N. Hamilton, T. Wolfram, G. Tzolova Muller, M. Havecker, J. Krohnert, C. Carrero, R. Schomacker, A. Trunschke and R. Schlogl, Catal. Sci. Technol., (2012).

[186] A. Dinse, B. Frank, C. Hess, D. Habel and R. Schomacker, J. Mol. Catal. A-Chem., 289 (2008) 28.

[187] J.H. Kwak, J.E. Herrera, J.Z. Hu, Y. Wang and C.H.F. Peden, Appl. Catal. A-Gen., 300 (2006) 109.

[188] O. Ovsitser, M. Cherian, A. Bruckner and E.V. Kondratenko, J. Catal., 265 (2009) 8.

[189] D. Shee and G. Deo, Catal. Lett., 124 (2008) 340.

[190] T. Blasco, A. Corma, M.T. Navarro and J.P. Pariente, J. Catal., 156 (1995) 65.

[191] A. Comite, A. Sorrentino, G. Capannelli, M. Di Serio, R. Tesser and E. Santacesaria, J. Mol. Catal. A-Chem., 198 (2003) 151.

[192] A. Zhang, Z. Li, Z. Li, Y. Shen and Y. Zhu, Appl. Surf. Sci., 254 (2008) 6298.

[193] W. Zhang, B.S. Zhang, T. Wolfram, L.D. Shao, R. Schlogl and D.S. Su, J. Phys. Chem. C, 115 (2011) 20550.

[194] A. Tuel, Microporous Mesoporous Mat., 27 (1999) 151.

[195] R.S. Araújo, D.C.S. Azevedo, E. Rodríguez-Castellón, A. Jiménez-López and C.L. Cavalcante Jr, J. Mol. Catal. A-Chem., 281 (2008) 154.

[196] S. Gontier and A. Tuel, Zeolites, 15 (1995) 601.

[197] W. Zhang, M. Fröba, J. Wang, P.T. Tanev, J. Wong and T.J. Pinnavaia, J. Am. Chem. Soc., 118 (1996) 9164.

[198] M. Nandi and A. Bhaumik, Chemical Engineering Science, 61 (2006) 4373.

PAPER I

DR UV-Vis and H_2-TPR characterization of the supported vanadium oxide catalysts

Michal Setnička*, Pavel Čičmanec, Roman Bulánek

Department of Physical Chemistry, Faculty of chemical technology, University of Pardubice, Studentská 573, CZ53210 Pardubice, Czech Republic,
** +420 466 037 345, Michal.Setnicka@student.upce.cz*

Introduction

The vanadium oxide supported on the surface of micro- or mesoporous materials represent a very important class of catalytic materials in modern heterogeneous catalysis. They combine unique textural and acid-base properties of support materials with redox properties of vanadium oxide species what opens possibility to activate alkanes at relatively low temperatures. In recent years, these catalysts have been investigated for applications in selective oxidation and ammoxidation of light (C_1-C_4) hydrocarbons to olefins, oxygenates and nitriles [1-2,8].

The detailed speciation of vanadium oxide species present on the surface of the support materials is challenging task in the process of the catalyst characterization. Nowadays the most acknowledged theory expects the existence of three different types of vanadium oxide species on the surface [3,12]: (i) isolated monomeric tetrahedrally coordinated VO_4 species linked by three V-O-support bonds to support at dehydrated state, (ii) oligomeric/polymeric VO_x species of distorted tetrahedral symmetry bonded by bridging V-O-V bonds to neighboring units, (iii) 2D/3D crystalline V_2O_5 nanoparticles (NPs).

The presence of the various structures of the supported vanadium phase have been extensively characterized by different techniques, especially by spectroscopic techniques (FT-IR, Raman, XANES/EXAFS, UV-Vis diffuse reflectance (DR), solid-state ^{51}V NMR, ESR, SEM, TEM etc.) [4-5,12]. However, methodology of characterization of these materials is still not sufficiently solved. Characterization by DR UV-Vis spectroscopy is frequently used because it is relatively cheap and simple experimental technique which can provide information about the different oxidation states and local coordination geometry of supported vanadium oxide species. The big disadvantage of this technique is the fact that DR UV-Vis spectra are usually broad and individual absorption bands are overlapped with each other which complicates their detailed interpretation. Another frequently used technique is temperature programmed reduction (TPR). It provides less information about coordination on the other hand it is very cheap and simply technique which has close relation to redox properties of VO_x species under real catalytic conditions. Nevertheless reliable assignment of individual bands in TPR profiles to particular species is also not solved yet.

The goal of this paper is the development of new methodology of the characterization of mesoporous silica supported VO_x catalysts based on the combination of data from both the DR UV-Vis and the H_2-TPR methods.

Experimental

Preparation of catalysts. Catalysts have been prepared in two ways (i) by impregnation and (ii) by direct synthesis. The hexagonal mesoporous silica (HMS) was used as support and it was synthesized at ambient conditions according to the procedure reported by Tanev [6] using dodecylamine (DDA, Aldrich) as a neutral structure directing template and tetraethylorthosilicate (TEOS, Aldrich) as a silica precursor. The set of impregnated V-HMS catalysts (1.24–11.69 wt.% V) was prepared by wet impregnation by solution of vanadyl(IV) acetylacetonate ($VO(acac)_2$, Aldrich) in ethanol. At the set of direct synthesized samples the $VO(acac)_2$ was added to the reaction mixture at preparation of HMS as it published by Reddy and Sayari [7]. The both sets of catalysts were calcined at 600°C in air for 8 hours after impregnation.

Characterization of catalysts. The vanadium content was determined by means of ED XRF by ElvaX (Elvatech, Ukraine) equipped with Pd anode. Samples were measured against the model samples (a mechanical mixture pure SiO_2 and $NaVO_3$) granulated to the same size as catalysts.

UV-Vis diffuse reflectance spectra of dehydrated (pure and diluted with pure silica from Aldrich) samples were measured in the range of the wavelength 200-900 nm using the Cintra 303 spectrometer (GBC Scientific Equipment, Australia) equipped with a Spectralon-coated integrating sphere using a Spectralon discs as reference material. The obtained the reflectance spectra were transformed into the dependencies of Kubelka-Munk function $F(R_\infty)$ on the absorption energy hν using the equation:

$$F(R_\infty) = \frac{(1-R_\infty)^2}{2R_\infty}$$

where the R_∞ value is the measured diffuse reflectance from a semi-infinite layer.

Hydrogen temperature programmed reduction (H_2-TPR) was used for study redox behavior and for distinguishing of individual VO_x species on the surface. Samples were oxidized in oxygen flow at 500°C (2 hours) and subsequently were reduced from ambient temperature to 900°C (10°C/min) in flow of hydrogen (5 vol.% H_2 in Ar) and the changes of hydrogen concentration were monitored by the semico TCD detector.

Results and discussion

Our UV-Vis spectra of nondiluted samples and spectra published previously [8] exhibit broad and overlapping absorption bands with strongly nonlinear dependence of Kubelka-Munk function on the concentration of VO_x species even for the moderately concentrated samples. This effect was reported already in the past [9] and very complicates even qualitative interpretation of these spectra and completely prohibits their quantitation or semi-quantitation analysis.

Wachs [10] partly eliminated this hindrance by using of methodology based on the evaluation of absorption energy edge (ε_0) from UV-Vis spectra using the expression introduced by Tauc [11] in the form:

$$\left(F(R_\infty)\cdot h\nu\right)^2 \propto \left(h\nu - \varepsilon_0\right)$$

where the ε_0 - the energy edge values were determined from obtained plots.

The ε_0 values of solid materials sodium ortho-vanadate Na_3VO_4 (by us $\varepsilon_0 = 3.83$ eV) and meta-vanadate $NaVO_3$ (by us $\varepsilon_0 = 3.16$ eV) can be used as ε_0 standard values of compounds containing only isolated monomeric tetrahedral units and linearly polymerized tetrahedrally coordinated oligomeric units respectively. Tian et al. [12]

demonstrated linear dependence of the ε_0 value on the concentration of referent compounds and suggested this method for the determination of the relative amount of VO_x monomeric units X_m. The dependence of obtained ε_0 and the X_m values on the concentration of vanadium is in the Table 1. Disadvantage of this method is that it can not be used for materials which include also the octahedraly coordinated VO_x bulk-like oxide species and must be modified to be useful for real catalyst samples.

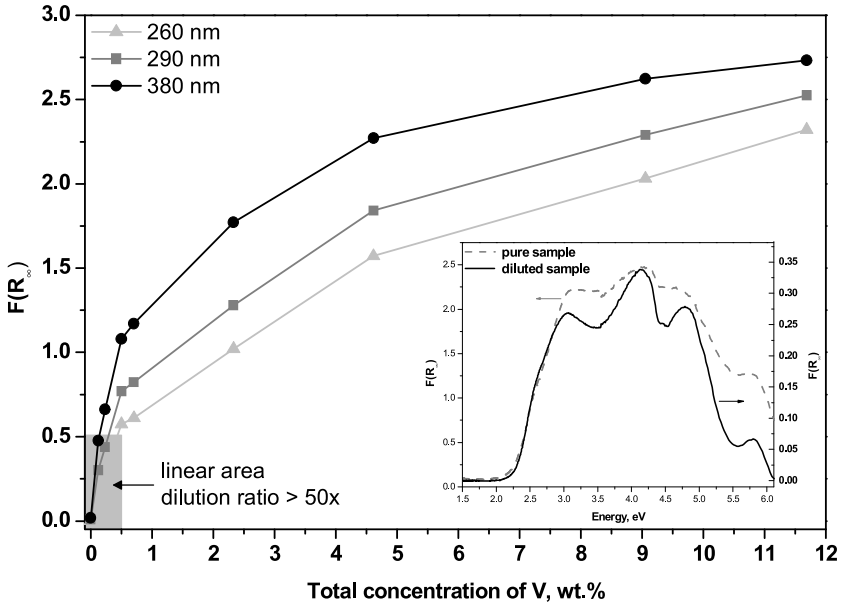

Figure 1 The dependence of spectral intensity of the sample I-VHMS-11.69 on its subsequently dilution by pure white silica. Small graf present spectrum pure and 100 x diluted samples.

The set of UV-Vis spectra of the sample I-VHMS-11.69 (see Fig. 1) subsequently diluted by the pure silica exhibit asymptotic dependence of Kubelka-Munk function $F(R_\infty)$ on concentration. This plot further clearly indicates that linear and zero-crossing dependence of the Kubelka-Munk function on the concentration of vanadium can be obtained only for the dilution degree higher than 50 or $F(R_\infty)$ values lower than approximately 0.5. Moreover the comparison of the spectra of the pure and I-VHMS-11.69 presented on small inset plot in Figure 1 uncovers the presence of clearly separated absorption bands with well defined maxima whose were cut-off in the spectra of pure samples. The maintained widths of these spectra in these spectra also demonstrate that vanadium oxide species supported in pores of support material has no tendency to redistribute himself to diluting agent.

The DR UV-Vis spectra measured in the range 1.38–6.19 eV (200–900 nm) of dehydrated VO_x-HMS samples diluted in the amorphous silica with the constant ratio 1:100 are presented in the Figure 2 and it could be seen that integral intensities of these spectra are approximately proportional to the concentration of vanadium. All spectra of the low concentrated sample consist of the three absorption bands with maximum at approximately 4.2, 4.8 and 5.8 eV. This region is usually attributed to presence of tetrahedrally coordinated VO_x species (group of symmetry T_d or C_{3v}) [3]. We can see at least two bands (denoted as A and B in Figure 3 and Table 1) with maximum at ca. 2.7 and 3.1 eV in the spectrum high concentrated sample prepared by wet impregnation. This region 2.5–3.5 eV is usually attributed to presence of two independent

octahedrally coordinated (2D and 3D) bulklike oxide [13] with group of symmetry O_h or C_{4v} and presence of these species hinders using of methodology of gap of energy mentioned above.

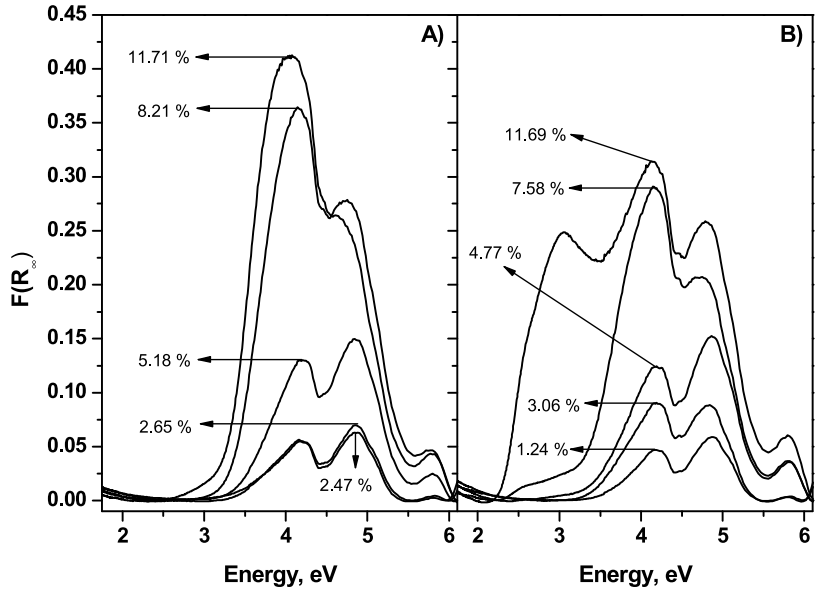

Figure 2 Spectra of diluted samples of VO_x-HMS materials with dilution ratio 1:100 where A) synthesized samples, B) impregnated samples.

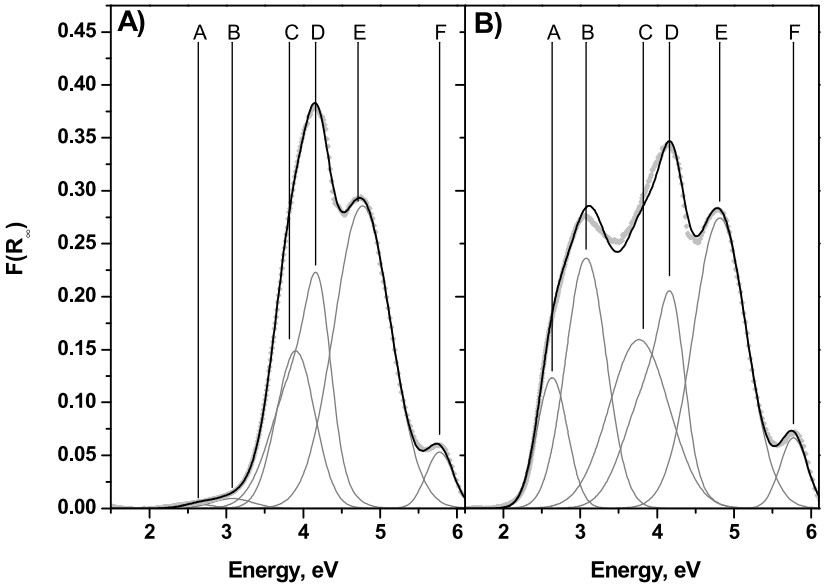

Figure 3 Result of the deconvolution of experimental spectra by suggested model for two the most concentrated samples. Grey points are experimental data, bold line is fitted envelope curve, thin grey lines are individual fitted bands. A) synthesized samples S-V-HMS-11.71 and B) impregnated samples I-V-HMS-11.67

The positions, halfwidths and areas of bands A–F (defined in Figure 3) were fitted simultaneously at all spectra by set of Gaussian curve shaped bands using the Fityk [14] software. The parameters defining the octahedral VO_x units (A, B), isolated monomeric units (D) and absorption band at ca. 5.8 eV (F) were fitted as shared for all data. The asymmetric band of isolated monomeric units (D) was described by the sum

of two Gaussians in the position ca. 3.9 and 4.2 eV with the fixed ratio of their areas. Both the band ascribed to tetrahedral oligomeric units (C) and the band at 4.8 eV (E) were fitted using the individual values of their position and halfwidth due to dependence of these parameters on the vanadium concentration. The maximum is shifted to lower energy because with increasing concentration of vanadium starts the formation of more polymerized oligomeric species.

sample name	w_V, wt.%	ε_0 [a], eV	$\varepsilon_{0\text{-}Oh}$ [b], eV	X_{mono} [c], wt.%,	X_{mono} [c], wt.%	A_1 [d], %	X_{Td}, %	X_{Oh}, %
S-VHMS-1.47	1.47	3.75	3.75	1.30	1.30	100.00	1.47	0
S-VHMS-2.65	2.65	3.74	3.76	2.30	2.38	100.00	2.65	0
S-VHMS-5.18	5.18	3.7	3.72	4.20	4.35	100.00	5.18	0
S-VHMS-8.21	8.21	3.57	3.58	5.09	5.21	100.00	8.21	0
S-VHMS-11.71	11.71	3.42	3.49	4.68	5.88	100.00	11.71	0
I-VHMS-1.24	1.24	3.74	3.75	1.08	1.10	64.91	0.87	0.37
I-VHMS-3.06	3.06	3.72	3.74	2.68	2.77	56.44	1.68	1.38
I-VHMS-4.77	4.77	3.68	3.71	3.73	3.94	76.94	3.73	1.04
I-VHMS-7.58	7.58	3.5	3.53	3.92	4.25	67.86	5.55	2.03
I-VHMS-11.69	11.69	2.45	3.34	not determined	3.30	63.90	7.53	4.16

[a] edge of absorption energy from original spectrum
[b] edge of absorption energy from spectrum after subtraction of octahedral
[c] calculated as $X = 3.148 - 0.681\ \varepsilon_0$, based on the work of Tian et al. [12]
[d] rate of the area of first TPR peak to total area TPR profiles

Table 1 Vanadium loading of samples prepared by the direct synthesis (S) and impregnation method (I) and the characteristics of samples based on the evaluation of DR-UV-Vis and H_2-TPR.

Suggested method of fitting is able to reproduce well character of experimental data including values of absorption energy gap. Hence the absorption bands of O_h coordinated species can be calculated and subtracted from spectra on the base of data obtained from fit. Subsequently it is possible to determinate the amount of T_d-monomeric species by method mentioned above (see Fig. 5 and Tab. 1).

H_2-TPR curves were measured to determine the scale dispersion and type of the present active species. The obtained TPR profiles are presented on the Figure 4 and it can be seen that samples prepared by the direct synthesis exhibit only one symmetric reduction peak at the temperature about 560-590°C and this peak can be described by one PseudoVoigt shaped curve and it has been fitted using the Fityk [14] software. The samples prepared by wet impregnation exhibit two peaks in theirs TPR profiles. The first peak has the same position as in the TPR of the synthesized samples and the second peak is at the temperature about 660-680ºC. The low temperature peak is frequently attributed to the reduction of the isolated monomeric units whereas the high temperature peak is attributed to reduction of oligomeric units [15,16]. Nevertheless this assignment does not agree with results from the UV-Vis spectroscopy. As show the UV-Vis spectra synthetised samples containing both, monomeric and polymeric, tetrahedraly coordinated units. Octahedraly coordinated units can be evidently observed only at the impregnated samples with high concentration and these samples show evidently high-temperature peak which means that the low-temperature can be assignment to both (monomeric and polymeric) T_d coordinated and the high

temperature peak can be assigned to the O_h coordinated. We can obtain amount of all T_d units (X_{Td} in Table 1) and all O_h (2D and 3D) coordinated units after subtraction area of the first peak fitted by PseudoVoigt from TPR profile.

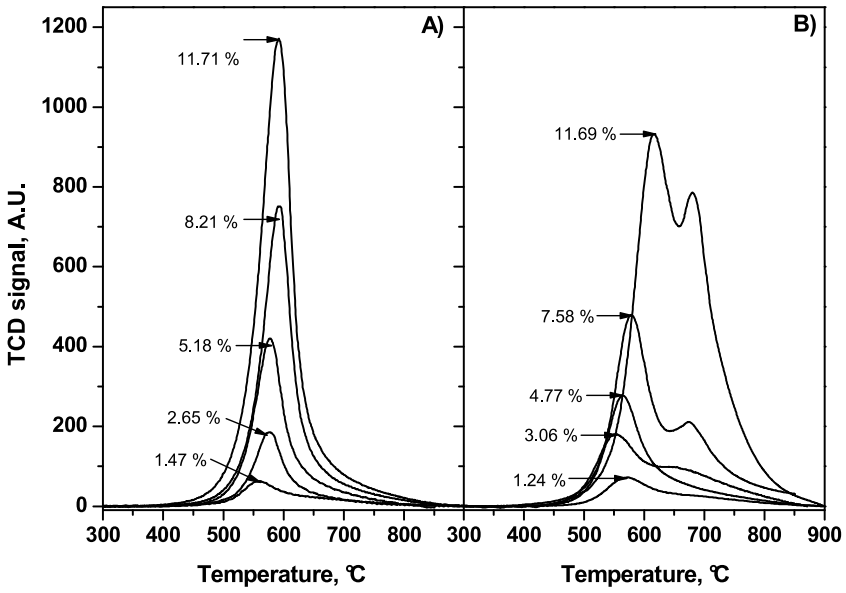

Figure 4 H_2-TPR profiles of VO_x-HMS samples where A) synthesized samples and B) impregnated samples.

By combination of results of both techniques we obtain correct information about amount and population of vanadium oxide species on the surface of HMS (see Fig. 5). From the Fig. 5 is evident that monomeric T_d coordinated units are generated only to *ca.* 5 wt.%. Exceeding this concentration it can be observed decrease of the concentration of monomeric species because the monomeric units start to polymerize (see Fig. 5)

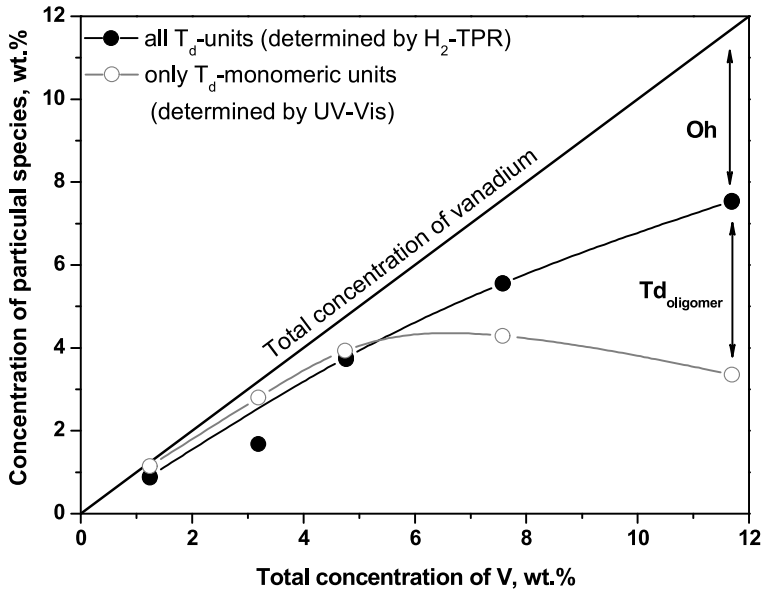

Figure 5 Correlation between the amount of T_d-monomeric units determined by UV-Vis spectroscopy, all T_d units determined by H_2-TPR and O_h units for samples prepared by impregnation.

Conclusions

The main result of this work is development of the new methodology for study vanadium oxides containing samples. The dilution of samples of V-HMS by the silica in the ratio higher than one hundred allows us to obtain the DR UV-Vis spectra containing the set of well separated absorption bands whose integral area is proportional to the vanadium concentration.

This methodology can be used to obtain the information about amount of monomer for materials containing the octahedrally coordinated species which caused failing of previously used methods with using gap of absorption energy.

The first peak in the TPR profiles of V-HMS materials can be definitely assigned to the reduction of all tetrahedraly coordinated units and the second peak pertains to the octahedrally coordinated units and quantitative analysis of TPR profiles bring complementary information for analysis of speciation of VO_x particles.

The monomeric species are formed on the support up to concentration about 5 wt.% and subsequently the oligomeric species are formed and the total of monomeric species even decrease.

The samples prepared by direct synthesis have lower tendency to formation oligomeric and octahedraly coordinated units than impregnated samples of the similar concentration.

Acknowledgements

A financial support of the Grant Agency of the Czech Republic under the project No. P106/10/0196 and Ministry of Education of Czech Republic under project No. MSM 0021627501 and LC 512 is highly acknowledged.

References

1. F. Cavani, N. Ballarini, A. Cericola, Catal. Today. 127 (2007) 113
2. M.A. Carreon, V.V. Guliants, Eur. J. Inorg. Chem. (2005) 27
3. D.E. Keller, D.C. Koningsberger, B.M. Weckhuysen, J. Phys. Chem. B. 110 (2006) 14313
4. G. Bond, S. Tahir, Appl. Cat. A 71 (2004) 1
5. Y. M. Liu, Y. Cao, N. Yi, W. L. Feng. W. L. Dai, S. R. Yan, J. Catal. 224 (2004) 417
6. P.T. Tanev, T.J. Pinnavaia, Science. 267 (1995) 865
7. J.S. Reddy, A. Sayari, J. Chem. Soc.-Chem. Commun. (1995) 2231
8. L. Capek, J. Adam, T. Grygar, R. Bulanek, L. Vradman, G. Kosova-Kucerova, P. Cicmanec, P. Knotek, Appl. Catal. A-Gen. 342 (2008) 99
9. G. Catana, R.R. Rao, B.M. Weckhuysen, P. Van Der Voort, E. Vansant, R.A. Schoonheydt, J. Phys. Chem. B. 102 (1998) 8005
10. X.T. Gao, I.E. Wachs, J. Phys. Chem. B. 104 (2000) 1261
11. J. Tauc, Amorphous and Liquid Semiconductors, Plenum Press, London, 1974
12. H.J. Tian, E.I. Ross, I.E. Wachs, J. Phys. Chem. B. 110 (2006) 9593
13. M. Schramlmarth, A. Wokaun, M. Pohl, J. Chem. Soc.-Faraday Trans. 87 (1991) 2635
14. Fityk 0.9.1, http://www.unipress.waw.pl/fityk/
15. I.E. Wachs, B.M. Weckhuysen, Appl. Catal. A: Gen. 157 (1997) 67
16. P. Knotek, L. Čapek, R. Bulánek, J. Adam, Top. Calal. 45 (2007) 1

PAPER II

THE JOURNAL OF PHYSICAL CHEMISTRY C

ARTICLE

pubs.acs.org/JPCC

DR UV−vis Study of the Supported Vanadium Oxide Catalysts

Roman Bulánek, Libor Čapek, Michal Setnička, and Pavel Čičmanec*

Department of Physical Chemistry, Faculty of Chemical Technology, University of Pardubice, Studentská 573, CZ53210 Pardubice, Czech Republic

ABSTRACT:

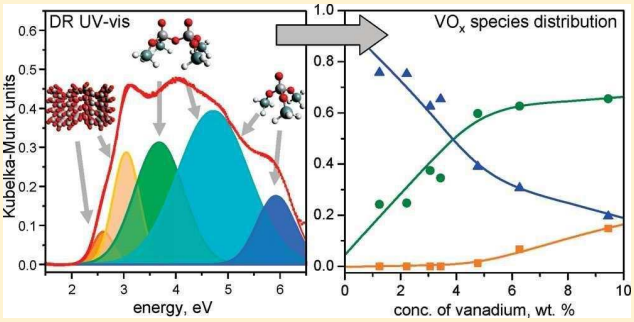

A new methodology of the measurement and evaluation of DR UV−vis spectra of VO_x species supported on hexagonal mesoporous silica was developed. The suggested methodology utilizes the benefit of the well resolved absorption bands in the spectra of highly diluted samples. Methodology was tested on two sets of V-materials prepared by the impregnation and direct synthesis method. It was observed that both types of materials consist of the same type of tetrahedrally coordinated monomeric and oligomeric species, but they differ in the population of these species. In particular, the octahedrally coordinated species and tetrahedral oligomeric units of higher polymerization degree were significantly more formed on the surface of V-materials prepared by impregnation method.

1. INTRODUCTION

Supported vanadium oxide catalysts have found wide commercial application in industry, e.g., selective oxidation of *o*-xylene to phtalic anhydride, selective catalytic reduction (SCR) of NO_x with NH_3 to N_2 and H_2O and controlling oxidation of SO_2 to SO_3 during SCR.[1−4] The vanadium oxides supported on the surface of micro- or mesoporous materials attract great interest in the scientific community[5−8] due to the ability to combine unique textural and acid−base properties of support materials with redox properties of vanadium oxide species what opens the possibility to activate alkanes at relatively low temperatures. In recent years, these catalysts have been investigated for applications in the selective oxidation and ammoxidation of light (C_1−C_4) hydrocarbons to olefins, oxygenates, and nitriles.[9−11] Moreover VO_x based catalysts can be used as model catalytic systems for fundamental investigation of supported metal oxides. Better knowledge of their behavior can be useful for understanding the mechanism of the reaction pathway, the mode of their bonding to the support, the types of supported species, and the possibility of controlling the abundance of a particular species by proper methodology of preparation.

Nowadays the most acknowledged theory expects the existence of three different types of vanadium oxide species on the surface:[2,12−14] (i) the isolated monomeric tetrahedrally coordinated VO_4 species linked by three V−O-support bonds to support at dehydrated state, (ii) the oligomeric/polymeric VO_x species of distorted tetrahedral symmetry bonded by bridging V−O−V bonds to other units, and (iii) 2D/3D crystalline V_2O_5 nanoparticles (NPs). Some authors mentioned as fourth (iv) type the mixed oxide compounds or solid solution with some oxide supports at elevated temperatures (e. g., $AlVO_4$, $V_xTi_{1-x}O_2$) on the surface.[2] Nature of support influences both population and properties of individual types of vanadium species and has significant influence to the catalytic behavior of these materials.[8,15,16]

The presence of the various structures of the supported vanadium phase has been extensively characterized by different techniques, especially by spectroscopic techniques (FT-IR, Raman, XANES/EXAFS, UV−vis diffuse reflectance (DR), solid-state ^{51}V NMR, ESR, SEM, TEM etc.);[2,17−19] however, the methodology of characterization of these materials is still not sufficiently solved. Characterization by DR UV−vis spectroscopy is frequently used because it is widespread, relatively cheap, and a simple experimental technique which can provide information about the different oxidation states and local coordination geometry of supported vanadium oxide species. This technique probes the electronic charge transfer transitions as well as the d−d transitions of vanadium ions at the catalyst surface, which are dependent on the local coordination environment, the polymerization degree, and of course on the vanadium oxidation state.[4] The big disadvantage of this technique is the fact that DR

Received: December 23, 2010
Revised: May 20, 2011
Published: May 23, 2011

UV−vis spectra are usually broad, and the individual absorption bands are overlapped with each other that complicate their detailed interpretation together with the fact that the theoretical approach which could bring relevant information is not developed yet. These facts complicate detailed speciation of vanadium oxide species present on the surface of the support. The contradictory interpretations appear very often in papers; for example Schraml-Marth et al.[20] attributed the band at 3.55 eV to 2D octahedrally coordinated species by comparison with the maxima of model compounds spectra, whereas the Gao et al.[6] ascribed the band at this region to tetrahedral oligomeric units assuming that his band at 350 nm matches to bands at 320 or 340 nm previously reported by Liu et al.[21] and Chao et al.[22]

Previously, we devoted a lot of attention to V-materials as catalysts in the ODH of ethane, propane, and butane and to the identification of the vanadium species mainly by using UV−vis, H_2-TPR, XRD, and voltammetry.[9,23−26] The analysis of previously published spectra of VO_x silica supported materials was focused on proving the presence of particular VOx species based on the evaluation of the edge of the absorption energy[2,27−29] or by the picking of an apparent maxima in obtained spectra.[3,6,30−37] Some articles also present the attempts to deconvolute the spectra by set of several Gaussian or Lorentzian shaped absorption bands,[7,20,38,39] but the spectra were usually deconvoluted in the wavelength scale and the fact that the intensity of the measured spectra is frequently not proportional to the concentration of vanadium in the samples[27,40] was neglected. The goal of this paper is the development of new methodology which would facilitate obtaining a better defined and resolved UV−vis spectra. These spectra would provide more accurate information about these systems with the possibility of assigning individual signals to the different vanadium oxide species on the surface, contributing to a deeper understanding of them. For this purpose, a set of VO_x species supported on hexagonal mesoporous silica (HMS) materials differing in the concentration of vanadium and the distribution of VO_x surface species was prepared. DR UV−vis spectra of diluted dehydrated materials were measured and investigated with the aim of obtaining more reliable information about speciation of vanadium oxide on the surface of porous support.

2. EXPERIMENTAL SECTION

2.1. Preparation of Catalysts. Catalysts have been prepared in two ways (i) by impregnation and (ii) by direct synthesis. The hexagonal mesoporous silica (HMS) was used as a support. The HMS was synthesized at ambient conditions according to the procedure reported by Tanev and Pinnavaya.[41] As a neutral structure, dodecylamine (DDA, Aldrich, purity 98%) was used as a directing agent. It was dissolved 19.3 g of DDA in the mixture of 225 mL of ethanol (purity 99%) and 200 mL of redistilled water. After 20 min homogenization by magnetic stirring, 56 mL of tetraethylorthosilicate (TEOS, Aldrich, purity 98%) was dropwise added as a silica precursor. The reaction mixture was stirred at RT for 18 h. The solid product was filtered, twice washed with 400 mL of ethanol, and calcined in nitrogen stream at 450 °C for 2 h with temperature gradient 1 °C/min and subsequently at 450 °C for 20 h in air stream. The set of impregnated VO_x-HMS catalysts (1.2 − 9.5 wt % V, denoted as I) was prepared by wet impregnation by a solution of calculated amount of vanadyl(IV) acetylacetonate ($VO(acac)_2$, Aldrich, purity 99.99%) in 75 mL of ethanol (denaturized). The solution was heated on the water bath up to evaporation of ethanol, and subsequently, the catalyst was calcined at 600 °C in air stream for 8 h with temperature gradient 5 °C/min. The set of synthesized VO_x-HMS catalysts (1.5 − 11.7 wt % of V, denoted S) was prepared by direct-synthesis method which was based on work published by Reddy and Sayari.[42] The technique was similar as in the case of the pure HMS synthesis. The solution of 75 mL of ethanol with different amounts of $VO(acac)_2$ was added to the reaction mixture of 10 mL of DDA and 66.7 mL of redistilled water. The following procedure (stirring, addition 18.7 mL of TEOS, stirring, filtration, and calcination) was the same as in the case of HMS preparation. The vanadium content was determined by means of ED XRF by ElvaX (Elvatech, Ukraine) equipped with a Pd anode. Samples were measured against the model samples (a mechanical mixture pure SiO_2 and $NaVO_3$) granulated to the same size as catalysts.

2.2. DR UV−vis Spectroscopy. The DR UV−vis spectra of dehydrated samples were measured using a Cintra 303 spectrometer (GBC Scientific Equipment, Australia) equipped with a Spectralon-coated integrating sphere using a Spectralon-coated discs as a standard. The spectra were recorded in the range of the wavelength 190−850 nm (lamps switched at 350 nm). The UV−vis spectra of samples were measured in two ways (i) in the pure form and (ii) the samples diluted with the pure silica (Fumed silica, Aldrich) in specified ratio. All samples were granulated and sieved to fraction of size 0.25−0.5 mm and dehydrated. The dehydration was carried out in the static atmosphere of oxygen in two steps: 120 °C for 30 min and 450 °C for 60 min and subsequently cooled and evacuated. Because it was recently reported that hydration of vanadium species substantially changes the character of the obtained spectra,[27,40] it was independently checked by DR UV−vis−NIR that the employed pretreatment procedure provided completely dehydrated samples. Because the main information in our spectra is in the UV region of spectra, the UV−vis−NIR spectra are not presented here for the sake of brevity. After the evacuation, the samples were transferred into a quartz optical cuvette 5 mm thick and sealed. This procedure guaranteed complete dehydration and a defined oxidation state of vanadium for all catalysts. The obtained reflectance spectra were transformed into the dependencies of Kubelka−Munk function $F(R_\infty)$ on the absorption energy $h\nu$ using the equation

$$F(R_\infty) = \frac{(1 - R_\infty)^2}{2R_\infty} \quad (1)$$

where R_∞ is the measured diffuse reflectance from a semi-infinite layer.[43] The spectrum of pure HMS material was subtracted as a baseline. The referent spectra of pure ortho-Na_3VO_4, meta-$NaVO_3$, and V_2O_5 were used for determine energy edge values ε_0 of pure monomeric, pure oligomeric, and pure bulk vanadium oxide units, respectively, by method reported in refs 2 and 29. These spectra were measured in the same way as the other samples.

It was reported by Catana et al.[3] that the dependence of the $F(R_\infty)$ function on the concentration of vanadium has nonlinear character even for a moderate concentration value. Therefore the approach which can partially solve (bypass) this problem was introduced for speciation of molybdenum oxide complexes[44] and subsequently applied for vanadium oxide species.[2,29] This methodology is based on the evaluation of absorption energy edge (ε_0) from the UV−vis spectra using the expression introduced by

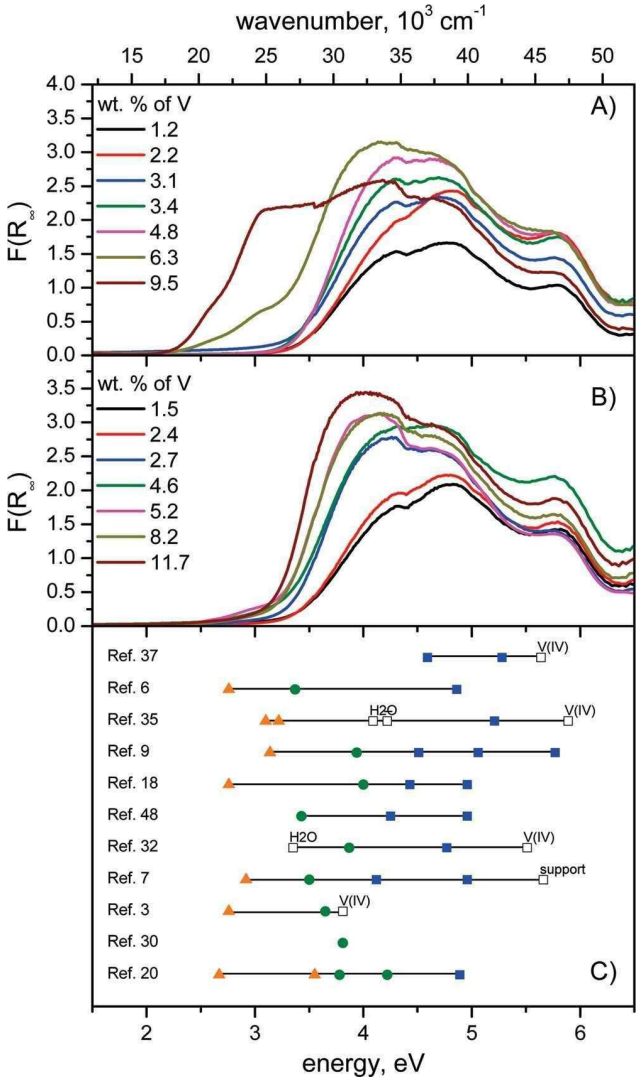

Figure 1. Spectra of dehydrated samples of VOx-HMS materials without dilution. (A) Impregnated samples, (B) synthesized samples, and (C) examples of positions previously reported absorption bands and their ascriptions. Orange triangle denotes O_h polymers or bulk V_2O_5 species; green circle, T_d oligomeric species; blue square, T_d monomeric species; hollow □, other species described in plot.

Davis and Mott[45] or by Tauc[46] in the form

$$(F(R_\infty)h\nu)^2 \propto (h\nu - \varepsilon_0) \qquad (2)$$

The ε_0 values of solid materials sodium ortho-vanadate Na_3VO_4 (3.82 eV), meta-vanadate $NaVO_3$ (3.15 eV), and V_2O_5 (2.26 eV) can be used as ε_0 standard values of compounds containing only isolated monomeric tetrahedral units, the linearly polymerized tetrahedrally coordinated oligomeric units, and polymerized octahedrally coordinated units, respectively. The described method allows us to obtain certain information about the speciation of vanadium on the HMS surface, but this method is inapplicable for samples containing the remarkable amount of octahedrally coordinated species. Moreover the determination of the ε_0 value from obtained plots is rather subjective as the wrong baseline correction can limit the applicability of this methodology.

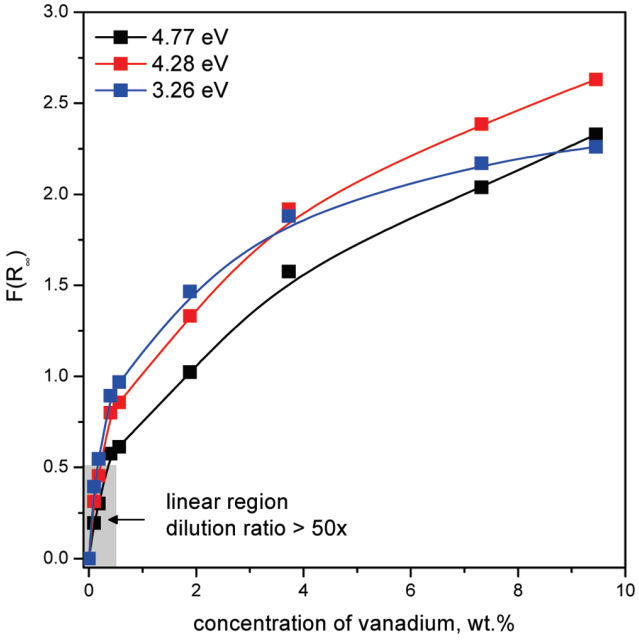

Figure 2. Dependence of spectral intensity of the sample I-VHMS-9.5 on its subsequent dilution by silica (concentration of vanadium is related to the resulting mixture).

3. RESULTS AND DISCUSSION

3.1. UV−vis Spectra of Nondiluted V-Materials. The DR UV−vis spectra measured in the range 1.46−6.5 eV (850−190 nm) of dehydrated samples of VO_x-HMS materials are presented in the Figure 1 for both sets of prepared samples. These spectra consist of several ligand to metal charge transfer absorption bands characteristic for samples containing vanadium oxide species supported on siliceous surface and represent typical UV−vis spectra of this type of material published very often in the literature.[9,39] The d−d absorption bands characteristic for the vanadium(+IV) in the region 1.55−2.07 eV[3] were not observed in the obtained spectra. This fact confirms that all vanadium atoms were successfully oxidized to oxidation state (+V) during the pretreatment procedure. The region 3.5−6 eV is usually attributed to the presence of tetrahedrally coordinated VO_x species (group of symmetry T_d), whereas the region 2.5−3.5 eV is attributed to the presence of 2D-square pyramidal or 3D-octahedrally coordinated VO_x species (group O_h). A very important factor influencing the character of the spectra and abundance of T_d and O_h species is the level of sample hydration.[27,40] Therefore, it is necessary to measure and evaluate the spectra under known and defined states. All spectra reported in this paper were recorded after complete dehydration of samples checked by monitoring of OH vibration overtones in NIR spectral region (recorded independently on UV−vis−NIR spectrometer). Therefore, all observed changes in the character of spectra (it means intensity of individual bands and shifts of absorption edges) can be attributed only to changes in the distribution of particular VOx species.

The attribution of absorption regions to particular species with the rather problematic results mentioned above is mostly based on the information obtained from the spectra of referent compounds. The results of previously published efforts to more preciously determine of the speciation of VO_x species and distinguish the

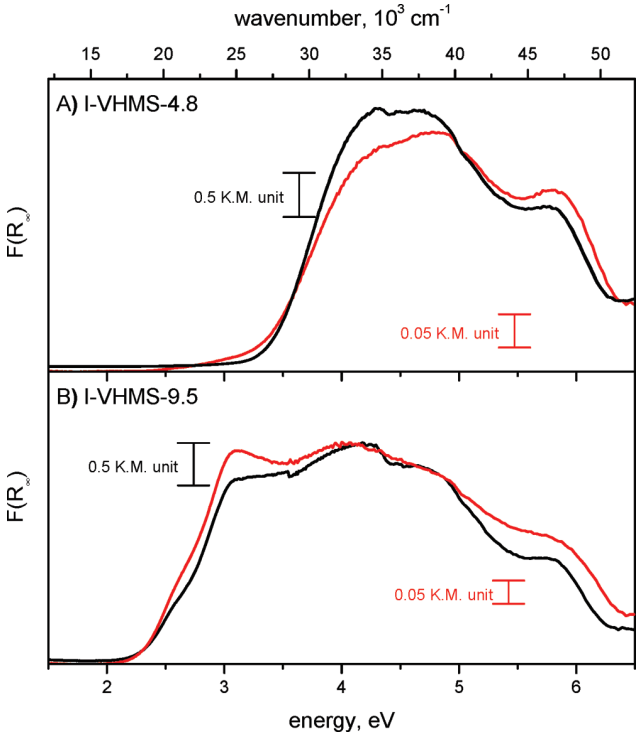

Figure 3. Comparison of spectra of pure (black line and scaler) and 100× diluted (red line and scaler) samples.

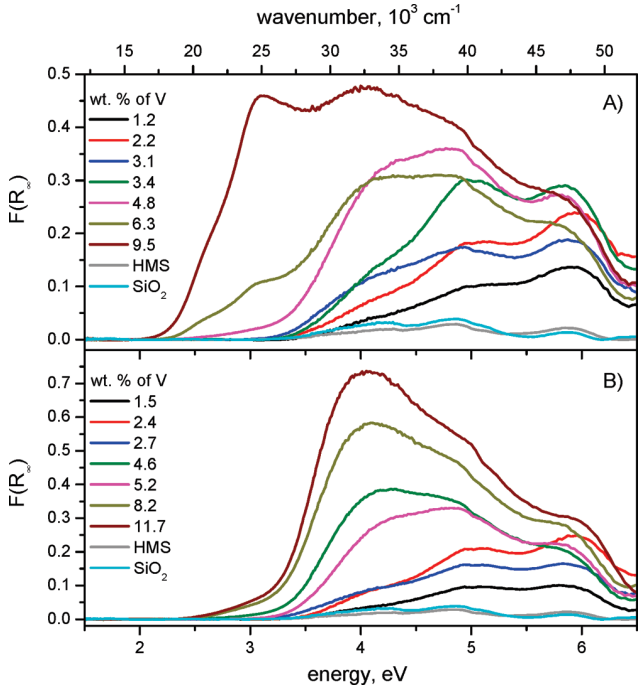

Figure 4. Spectra of diluted samples of VO_x-HMS materials with dilution ratio 1:100. (A) Impregnated samples and (B) synthesized samples.

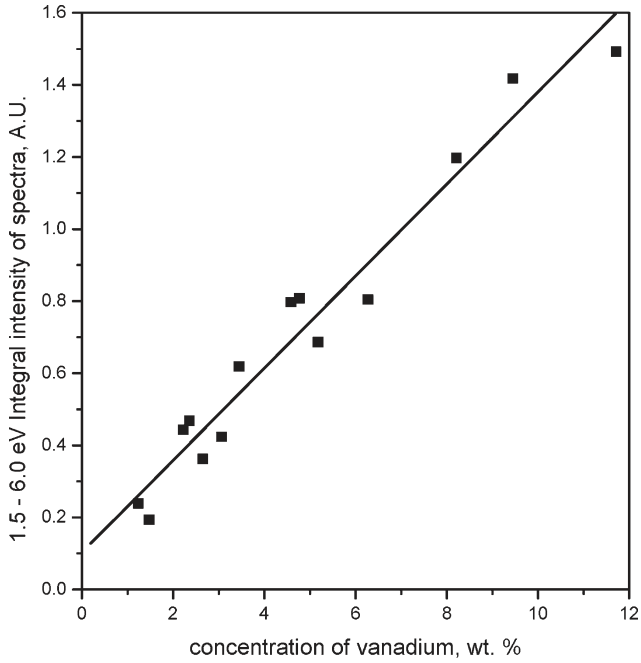

Figure 5. Dependence of the spectral integral intensity of 100 times diluted samples on the concentration of vanadium.

bands which should be attributed to T_d oligomeric and T_d monomeric species are even more ambiguous. Some examples of these ascriptions which differ not only in the positions but even in the number of bands are presented in the Figure 1.

This uncertainty of the spectra interpretation is possible due to broad and overlapping absorption bands and the strongly nonlinear dependence of the Kubelka−Munk function on the concentration of VO_x species even for the moderately concentrated samples.

3.2. UV−vis Spectra of Diluted V-Materials. The significant truncation of spectra of undiluted samples was confirmed by the measurement of the set of UV−vis spectra of the sample I-VHMS-9.5 subsequently diluted by pure silica (see Figure 2). This plot clearly indicates that linear and zero-crossing dependence of the Kubelka−Munk function on the concentration of vanadium can be obtained only for the dilution degree higher than 50 or $F(R_\infty)$ values lower than approximately 0.5. The comparison of the spectra of the pure and diluted samples I-VHMS-4.8 and I-VHMS-9.5 displayed at Figure 3 presents the retained width of these spectra. This fact demonstrates that vanadium oxide species supported in porous material has no tendency to redistribute itself to diluting agent as it can occur in the case of material supported on the external surface of nonporous SiO_2 based supports.

The DR UV−vis spectra of VO_x-HMS samples diluted in the amorphous silica with the constant ratio 1:100 are presented in the Figure 4 for both sets of VO_x-HMS samples, and the integral intensities (presented in the Figure 5) of diluted spectra are approximately proportional to the concentration of vanadium in samples. This fact indicates that the absorption coefficients of anchored VO_x species are at first approximation the same for all types of anchored VO_x species.

3.3. Interpretation of the UV−vis Spectra and Methodology of the Spectra Evaluation. Figure 4 shows the UV−vis spectra of diluted I-VHMS and S-VHMS materials with dilution ratio of 1:100. On the basis of our methodology described below, we separated spectra of diluted samples into five different UV−vis bands denoted as A−E.

dx.doi.org/10.1021/jp112206c | J. Phys. Chem. C 2011, 115, 12430–12438

Table 1. Results of UV−vis Deconvolution Procedure: Positions, Halfwidths, and Areas of Individual Bands[a]

							area of absorption band				
	c_C	c_E	c_D	hw_C	hw_D	hw_E	A	B	C	D	E
	eV	eV	eV	eV	eV	eV	A.U.	A.U.	A.U.	A.U.	A.U.
band position							2.61	3.05	c_C	c_D	c_E
halfwidth							0.23	0.30	hw_C	hw_D	hw_E
sample name											
S-VHMS-1.5	4.01	5.04	5.93	0.37	0.59	0.34	0.000	0.000	0.017	0.120	0.056
S-VHMS-2.4	4.04	5.04	6.00	0.33	0.58	0.39	0.000	0.000	0.039	0.253	0.176
S-VHMS-2.7	4.02	5.02	5.96	0.43	0.57	0.39	0.000	0.000	0.059	0.191	0.111
S-VHMS-4.6	3.97	4.75	5.86	0.38	0.66	0.40	0.000	0.004	0.174	0.488	0.131
S-VHMS-5.2	4.06	4.88	5.90	0.40	0.60	0.37	0.000	0.000	0.147	0.404	0.135
S-VHMS-8.2	3.90	4.67	5.87	0.38	0.69	0.42	0.001	0.015	0.281	0.713	0.188
S-VHMS-11.7	3.88	4.66	5.93	0.38	0.70	0.46	0.003	0.015	0.375	0.868	0.230
I-VHMS-1.2	4.09	5.06	5.96	0.38	0.56	0.39	0.000	0.000	0.022	0.120	0.097
I-VHMS-2.2	4.08	5.03	6.01	0.40	0.54	0.42	0.000	0.000	0.045	0.202	0.197
I-VHMS-3.1	3.97	4.92	5.97	0.40	0.65	0.40	0.000	0.000	0.056	0.233	0.134
I-VHMS-3.4	4.12	4.98	5.91	0.40	0.48	0.42	0.000	0.000	0.088	0.293	0.238
I-VHMS-4.8	4.03	4.88	5.91	0.43	0.61	0.38	0.001	0.008	0.184	0.441	0.173
I-VHMS-6.3	3.92	4.84	5.88	0.48	0.63	0.42	0.007	0.054	0.213	0.383	0.150
I-VHMS-9.5	3.68	4.72	5.92	0.55	0.80	0.42	0.041	0.182	0.368	0.668	0.159

[a] For assignments of bands, see the text.

Highly concentrated samples prepared by the wet impregnation method exhibit intensive absorption bands at the region 2.5−3.5 eV. The absorption bands can be clearly ascribed to the presence of octahedrally coordinated bulk-like VO_x units because only the V_2O_5 with the edge of absorption energy 2.26 eV has absorption bands in this region. Absorption in this region can be described by at least two independent absorption bands (denoted as A and B in Table 1) at ca. 2.6 and 3.1 eV due to remarkably different UV−vis absorption intensity at these energy values for various samples (see, e.g., spectra of I-VHMS-6.3 and I-VHMS-9.5 in the Figure 4B). The existence of two independent octahedrally coordinated supported VO_x species were also suggested in the past.[20,39]

All diluted VO_x-HMS samples have in the range 3.8−6.5 eV three absorption bands at positions 4.0, 5.0, and 5.9 eV in their spectra, and there is clearly observable shift of first two bands maxima to lower energy with the increasing of the vanadium concentration. These bands can be evidently attributed to the ligand to metal charge transfers of T_d-coordinated species but theirs detailed attribution to T_d monomeric and T_d oligomeric species is more complicated. Several authors attempted to ascribe one or two absorption bands in this region to T_d oligomeric units in the range 3.37−4.22 eV[3,6,7,20,32,34,39,47,48] and one, two, or three absorption bands to T_d monomeric units in the range 3.50−5.77 eV,[6,7,20,27,32,34,35,37,39,48,49] but the dispersion of these values reflects well the uncertainty of these ascriptions.

According to the ligand field theory, the vanadium (oxidation state +V) species in the field with tetrahedral symmetry should have its d^0 orbital splitted into two groups of degenerated orbitals denoted as e and t_2. This fact implies that we should expect the presence of two absorption LMCT bands in the UV−vis spectrum of the species with this symmetry. Possible energetic separation of the e and t_2 orbitals can be estimated from the position of d−d transitions in the region ca. 1.5−2.0 eV in spectra of vanadium(IV) species.[3] It can be expected that the occupancy of one vanadium d orbital increases the energetic difference between e and t_2 orbitals, and therefore, we can expect the presence of two bands in the spectra of tetrahedrally coordinated vanadium species separated no more than 1.5−2.0 eV.

Clearly separated absorption bands of diluted VO_x-HMS spectra offer the possibility to more reliably attribute observed absorption band to either T_d monomeric or T_d oligomeric units. The absorption band with the maximum at ca. 4.0 eV (in Table 1 denoted as C) is relatively broad, and it is not possible to obtain the value of the edge of absorption energy 3.82 eV obtained previously from the spectrum of the Na_3VO_4 with this band included in the UV−vis spectrum. Because the sodium orthovanadate consists of only the isolated monomeric VO_x units, we should assume the presence of only bands at approximately 5.0 and 5.9 eV (denoted as D and E in the Table 1) in the spectrum of these species. The C band at 4.0 eV hence should be attributed solely to the presence of the oligomeric tetrahedrally coordinated VO_x species.

The absorption band D at ca. 5.0 eV significantly changes its relative intensity to the band at 5.9 eV (see Figure 4B) as the concentration of the vanadium increases, and we should expect that both the monomeric and the oligomeric T_d-coordinated VO_x species contribute to the intensity of this absorption band. The absorption bands ascribed to the presence of T_d oligomeric units should be modeled by the symmetric bands whose have neither fixed position nor halfwidth due to necessity to reflect the possible shift and broadening of these absorption bands caused by the increasing of the VO_x polymerization degree.

The positions, halfwidths and areas of previously defined bands A−E were fitted to all experimental spectra by a set of Gaussian curve shaped bands using the Fityk[50] software. All experimental spectra were fitted simultaneously, and the parameters defining the octahedral VO_x units (A and B) were fitted as shared for all data sets. Bands ascribed to tetrahedral both the oligomeric and the monomeric units (C, D, and E) were fitted using the individual values of their position and halfwidth due to

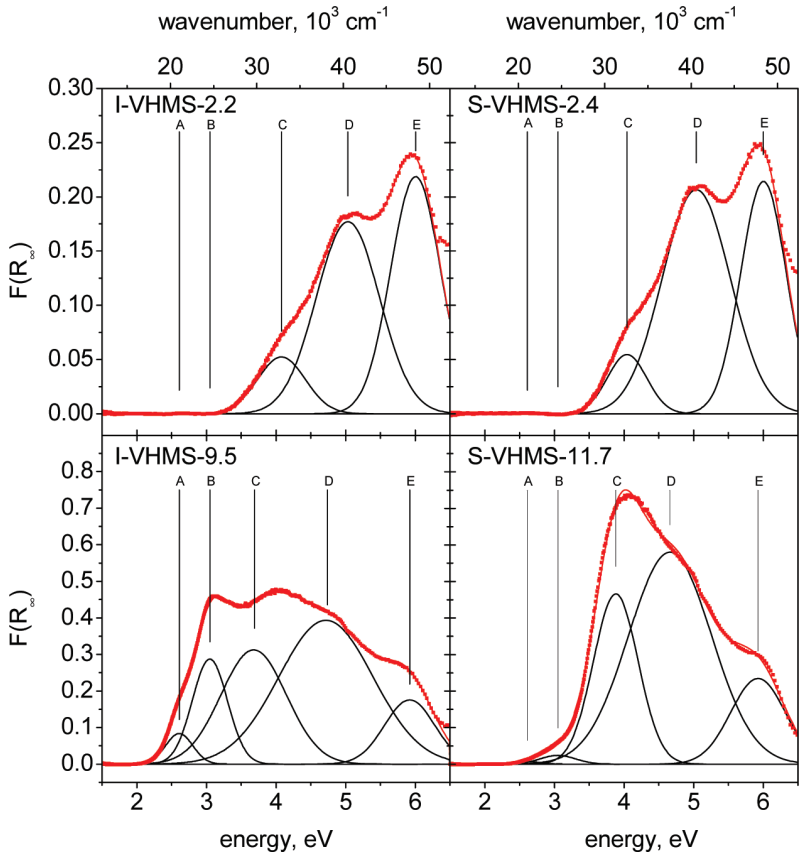

Figure 6. Results of the deconvolution of experimental spectra by suggested model for selected samples. Red points are experimental data, the red line is the fitted envelope curve, and black lines are individual spectral bands.

the expected dependence of these parameters on the vanadium concentration mentioned above.

The values of the obtained areas of model absorption bands A−E are summarized in Table 1 together with the positions and halfwidths of deconvoluted absorption bands presented in the subheader or separate columns of the table. Figure 6 presents the comparison of the experimental spectra with the model curves for the selected samples for the sake of brevity. This comparison confirms that the model suggested for the description of the experimental spectra reflects sufficiently all substantial properties of these spectra and evaluation of model parameters can be used for obtaining detailed insight into speciation of VO_x particles present on the surface of HMS support. The positions of all other fitted absorption bands correspond well with the positions and shape of clearly perceptible maxima and shoulders in experimental spectra of diluted samples.

The band attributed to the T_d oligomers (C) is shifted in its position from the 4.1 to 3.75 eV with the increasing of the concentration of vanadium. A similar shift of the position can be observed in the case of the absorption band (D) which also shifts from 5.1 to 4.6 eV with the increasing of the vanadium concentration which corresponds well with the observed effects in experimental spectra. The absorption band (E) ascribed to the isolated monomeric units does not change its position significantly; however, this value was not kept fixed during the fitting procedure. The values of the halfwidth of the absorption bands (C, D, and E) ascribed all to the tetrahedrally coordinated units increased with the increasing of the vanadium concentration for samples prepared by both methods. This effect can be ascribed to the formation of oligomeric species with higher degree of polymerization in the case of samples prepared by the wet impregnation. Nevertheless, changes in the shapes of absorption bands cannot be ascribed to only the formation of more polymerized species, because the band (E) at ca. 5.9 eV should be ascribed exclusively to the isolated monomeric species. The effect which can be responsible for the observed changes of this band halfwidth are either the long-range nonbonding adsorbate−adsorbate interactions or the interaction of vanadium oxide species with the amorphous surface of the support. Both effects can cause more distorted adsorbed VO_x complexes to be formed as the concentration of vanadium increases. The presence of several types of monomeric species with different distortion of tetrahedral structures in zeolites was reported very recently.[51]

The values of relative intensities of all bands (presented in the Figure 7) except of the band (D) in the dependence on the overall vanadium concentration follow expectable trends for the particular species to the ones they were attributed to based on the their positions. The bands (A and B) ascribed to the octahedrally coordinated species have significant intensity only for samples with a higher concentration of vanadium when the bulk-like V_2O_5 species formation is expected. The relative intensity of the band (E) ascribed to the monomeric units decreases as the vanadium concentration increases and more T_d and/or O_h oligomeric units are formed.

The relative intensity of (D) band in the dependence of vanadium concentration (area of particular band related to

dx.doi.org/10.1021/jp112206c | J. Phys. Chem. C 2011, 115, 12430–12438

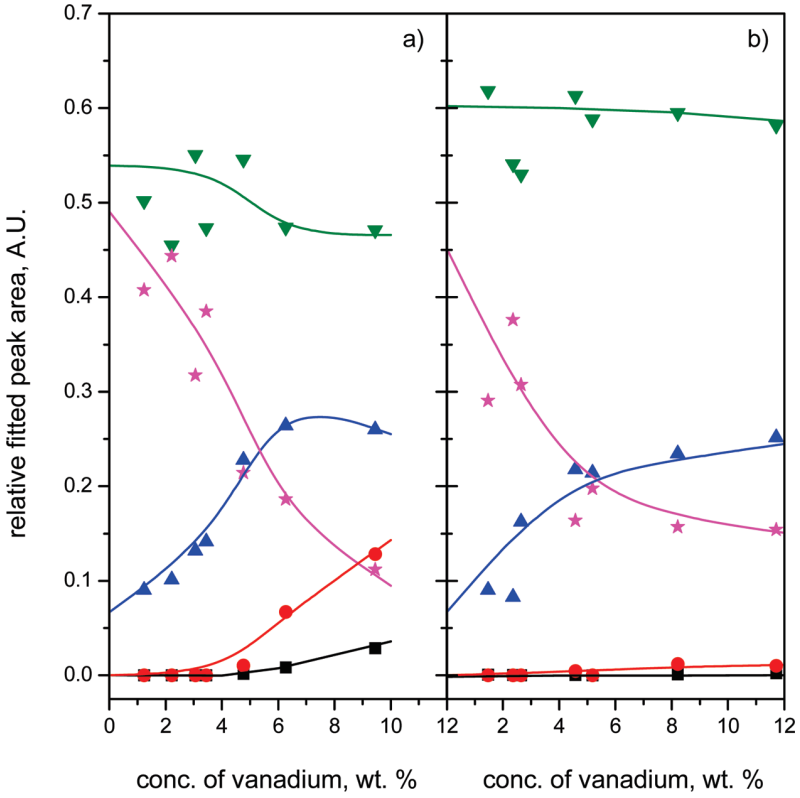

Figure 7. Relative areas of fitted absorption bands in the dependence of vanadium concentration. (A) absorption band, black square; (B) absorption band, red circle; (C) absorption band, blue triangle; (D) absorption band, green triangle; (E) absorption band, pink star. (a) Samples prepared by impregnation and (b) samples prepared by direct synthesis.

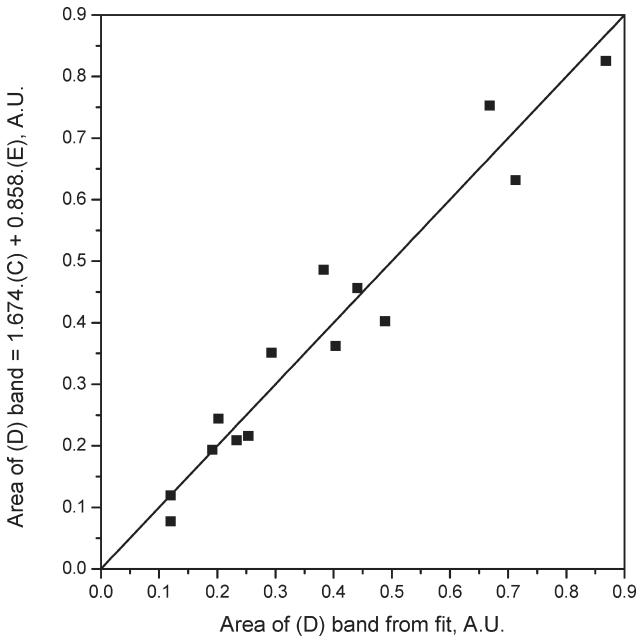

Figure 8. Demonstration of the dependence of (D) band area on the area of linear combination of bands (C and E) whose represent population of tetrahedrally coordinated units.

integral intensity of spectra) is nearly constant in the whole concentration range for samples prepared by the direct synthesis (presented in the Figure 7B). Because these samples do not contain significant bands ascribed to the octahedrally coordinated VO_x species, we can assume that this band is common for both the isolated monomeric and the oligomeric tetrahedrally coordinated VO_x species. The retained relative intensity of this absorption band suggests the same or similar absorption coefficients for both types of T_d-coordinated VO_x species in this region of spectra. The relative intensity of (D) band for the impregnated samples exhibit slight decreasing after the appearance of bands (A and B) ascribed to the octahedrally coordinated VO_x units.

3.4. Analysis of the Band at 5 eV. The area of the absorption band (D) can be hence calculated as a linear combination of the band (C) and the absorption band (E) and we can write $D = cC + eE$. Coefficients of this dependence $c = 1.674$ and $e = 0.858$ were obtained by the linear regression. The comparison of dependence of area of the (D) bands on the linear combination of bands (C and E) is presented in the Figure 8. The knowledge of the degree of contribution of both the monomeric and the oligomeric tetrahedrally coordinated species to the intensity of the band (D) together with the nearly constant absorption coefficients for all types of VO_x species offer the possibility to calculate the relative abundance of the particular species as the area of bands (A and B) to integral area of spectra for octahedrally coordinated species or the ratio $(1 + c)$C area or $(1 + e)$E area to total area of spectra for tetrahedrally coordinated oligomeric or monomeric VO_x species respectively.

The calculated values of the relative abundance of tetrahedrally coordinated T_d monomeric and T_d oligomeric units are presented in Figure 9A,B in dependence of vanadium concentration for both

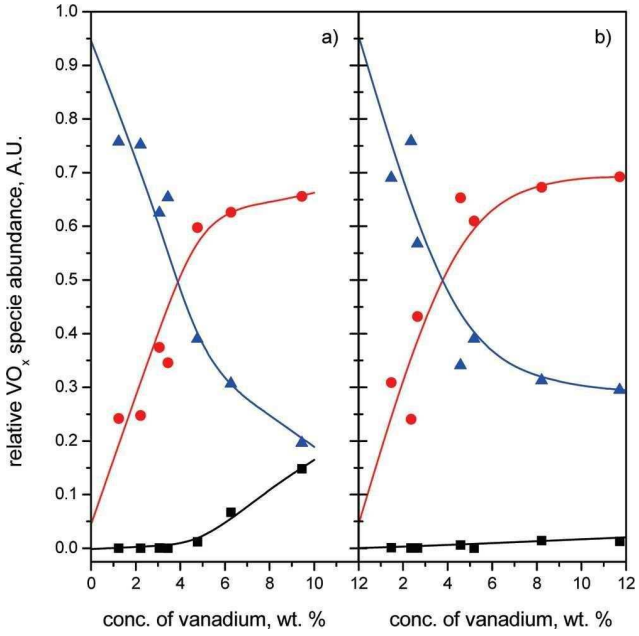

Figure 9. Relative abundance of various vanadium oxide species in the dependence of vanadium concentration. O_h-coordinated species, black square; T_d-coordinated oligomeric units, red circle; T_d-coordinated isolated monomeric units, nlue triangle. (a) Samples prepared by impregnation and (b) samples prepared by direct synthesis.

sets of prepared catalysts. It can be seen that there is no significant difference between the impregnated samples and samples prepared by the direct synthesis. Both sample sets exhibit similar dependence of the population of both tetrahedrally coordinated species on the vanadium loading. Only a small difference between both sample sets can be seen for the abundance of monomeric units in the case of samples prepared by the impregnation method which indicate that formation of the octahedrally coordinated species occurs on account of the abundance of mainly monomeric VO_x species. It can be also seen that relative abundance of oligomeric units reaches its limiting value at vanadium concentration about 5 wt % of vanadium.

Figure 9 also presents the area vs concentration dependence of the sum absorption bands (A and B) at 2.61 and 3.05 eV (ascribed to octahedral VO_x units) for both sets of samples. The intensity of the band at 3.05 eV is always higher than the intensity of the band at 2.61 eV (see Figure 7). Moreover, the band denoted A (at 2.61 eV) starts to appear at higher concentration than band (B) at 3.05 eV. We assume that two-dimensional octahedral units whose presence was suggested in the past[20] and the 3D bulk-like V_2O_5 particles that start to form at very high vanadium concentration significantly contribute to both absorption bands. The remarkable intensity of these bands (A and B) attributed to the O_h polymeric units is clearly discernible in spectra of samples prepared by the wet impregnation method in Figure 7 and the limiting concentration level when the formation of these species starts is the vanadium concentration of ca. 4%. The samples prepared by direct synthesis do not contain a substantial amount of O_h-coordinated species even at a concentration of approximately 12 wt % of vanadium.

Results of the analysis of VO_x species distribution previously reported strongly depends on both the employed experimental techniques and the methodology of preparation of samples. The Wachs's group studied VO_x materials supported on the amorphous silica by the Raman spectroscopy either at room temperature or under operando conditions.[2,27,29,49,52] The absence of V−O−V vibrations at ca. 500, 700, and 995 cm^{-1} in the Raman spectra of samples with the vanadium content less than 5−6 wt % lead them to statet that their samples contain mostly isolated tetrahedrally coordinated species in this range of concentrations.[52] When this vanadium concentration which corresponds to the vanadium surface density ca. 2.6 VO_x per nm^2 is reached, the formation of V_2O_5 on the silica surface is assumed. Similar results were also obtained by other authors,[14,15,18,48,53−55] and they usually reported the appearance of V−O−V vibrations in Raman spectra of samples with the surface density in the range 2.2−2.7 VO_x per nm^2 (above ca. 5−6 wt % of vanadium). These reported values of the limit vanadium concentration when the V_2O_5 starts to form correspond well with our value of 4−5 wt % for samples prepared by the wet impregnation method. On the other hand the differences in the preparation procedures employed by various authors can change the population of octahedrally coordinated species as it is clearly demonstrated by our set of materials prepared by direct synthesis. The presence of tetrahedrally coordinated oligomeric species over silica based supports was not reported except in the works of Hess et al.,[56,57] who detected the presence of these species by NEXAFS technique.

4. CONCLUSIONS

The main results of our attempt to develop a new and improved methodology of characterization of vanadium oxide supported materials by DR UV−vis spectroscopy are summarized in the following points:

- The dilution of samples of VO_x-HMS by the silica in the ratio higher than 100 allows us to obtain the DR UV−vis spectra whose integral area is at least in the first approximation proportional to the overall amount of the vanadium in samples within the concentration range of 0−13 wt % of vanadium.
- The particular absorption bands present in the spectra of diluted samples were attributed to individual T_d monomeric, T_d oligomeric, and O_h oligomeric VO_x species present on the support surface with high reliability. This attribution was made based on the evaluation of previously published data and the analysis of spectra of the referent compound.
- The well separated and defined absorption bands obtained by deconvolution of spectra of highly diluted samples offer the possibility of obtaining more detailed information about characteristics of supported VO_x species. This methodology also suggests the possibility of obtaining the information about their relative or absolute abundance on the surface of silica support. In addition, the correlation of this information with the results obtained by other techniques is possible.
- It was observed that the amount and distribution of tetrahedrally coordinated species to the monomeric and the oligomeric species is the same for both sets of VO_x-HMS samples prepared by the direct synthesis and wet impregnation method. The preparation method influences significantly the amount of octahedrally coordinated species and the degree of polymerization of T_d oligomeric species. Higher amount of both these species contained the samples prepared by the wet impregnation method.
- Last, but not least, the newly developed methodology needs a very low amount of the sample which allows utilization of

UV−vis spectroscopy, for example, in the postcatalytic tests, where a significantly smaller amount of material is used than the amount necessary for filling the spectroscopic cuvette.

AUTHOR INFORMATION

Corresponding Author

*Phone: +420 466 037 048. E-mail: Pavel.Cicmanec@upce.cz.

ACKNOWLEDGMENT

Financial support of the Grant Agency of the Czech Republic under Project No. P106/10/0196 and Ministry of Education of Czech Republic under Project No. MSM 0021627501 is highly acknowledged.

REFERENCES

(1) Svachula, J.; Alemany, L. J.; Ferlazzo, N.; Forzatti, P.; Tronconi, E.; Bregani, F. *Ind. Eng. Chem. Res.* **1993**, *32*, 826.

(2) Tian, H. J.; Ross, E. I.; Wachs, I. E. *J. Phys. Chem. B* **2006**, *110*, 9593.

(3) Catana, G.; Rao, R. R.; Weckhuysen, B. M.; Van Der Voort, P.; Vansant, E.; Schoonheydt, R. A. *J. Phys. Chem. B* **1998**, *102*, 8005.

(4) Weckhuysen, B. M.; Keller, D. E. *Catal. Today* **2003**, *78*, 25.

(5) Dzwigaj, S.; Gressel, I.; Grzybowska, B.; Samson, K. *Catal. Today* **2006**, *114*, 237.

(6) Gao, F.; Zhang, Y. H.; Wan, H. Q.; Kong, Y.; Wu, X. C.; Dong, L.; Li, B. Q.; Chen, Y. *Microporous Mesoporous Mater.* **2008**, *110*, 508.

(7) Baltes, M.; Cassiers, K.; Van Der Voort, P.; Weckhuysen, B. M.; Schoonheydt, R. A.; Vansant, E. F. *J. Catal.* **2001**, *197*, 160.

(8) Kondratenko, E. V.; Cherian, M.; Baerns, M.; Su, D. S.; Schlogl, R.; Wang, X.; Wachs, I. E. *J. Catal.* **2005**, *234*, 131.

(9) Capek, L.; Adam, J.; Grygar, T.; Bulanek, R.; Vradman, L.; Kosova-Kucerova, G.; Cicmanec, P.; Knotek, P. *Appl. Catal. A-Gen.* **2008**, *342*, 99.

(10) Cavani, F.; Ballarini, N.; Cericola, A. *Catal. Today* **2007**, *127*, 113.

(11) Carreon, M. A.; Guliants, V. V. *Eur. J. Inorg. Chem.* **2005**, 27.

(12) Kung, H. H. Oxidative dehydrogenation of light (C-2 to C-4) alkanes. In *Advances in Catalysis*; Academic Press Inc.: San Diego, CA, 1994; Vol. 40, p 1.

(13) Blasco, T.; Nieto, J. M. L. *Appl. Catal. A-Gen.* **1997**, *157*, 117.

(14) Keller, D. E.; Koningsberger, D. C.; Weckhuysen, B. M. *J. Phys. Chem. B* **2006**, *110*, 14313.

(15) Khodakov, A.; Olthof, B.; Bell, A. T.; Iglesia, E. *J. Catal.* **1999**, *181*, 205.

(16) Williams, T.; Beltramini, J.; Lu, G. Q. *Microporous Mesoporous Mater.* **2006**, *88*, 91.

(17) Bond, G. C.; Tahir, S. F. *Appl. Catal.* **1991**, *71*, 1.

(18) Liu, Y. M.; Cao, Y.; Yi, N.; Feng, W. L.; Dai, W. L.; Yan, S. R.; He, H. Y.; Fan, K. N. *J. Catal.* **2004**, *224*, 417.

(19) Deo, G.; Wachs, I. E.; Haber, J. *Crit. Rev. Surf. Chem.* **1994**, *4*, 141.

(20) Schramlmarth, M.; Wokaun, A.; Pohl, M.; Krauss, H. L. *J. Chem. Soc.-Faraday Trans.* **1991**, *87*, 2635.

(21) Liu, J.; Zhao, Z.; Liang, P.; Xu, C. M.; Duan, A. J.; Jiang, G. Y.; Lin, W. Y.; Wachs, I. E. *Catal. Lett.* **2008**, *120*, 148.

(22) Chao, K. J.; Wu, C. N.; Chang, H.; Lee, L. J.; Hu, S. F. *J. Phys. Chem. B* **1997**, *101*, 6341.

(23) Knotek, P.; Capek, L.; Bulanek, R.; Adam, J. *Top. Catal.* **2007**, *45*, 51.

(24) Bulanek, R.; Sheng-Yang, H.; Knotek, P.; Capek, L. *Zeolites and Related Materials: Trends, Targets and Challenges*, Proceedings of the 4th International Feza Conference 2008; Vol. *174*, p 1295.

(25) Capek, L.; Bulanek, R.; Adam, J.; Smolakova, L.; Sheng-Yang, H.; Cicmanec, P. *Catal. Today* **2009**, *141*, 282.

(26) Grygar, T.; Capek, L.; Adam, J.; Machovic, V. *J. Electroanal. Chem.* **2009**, *633*, 127.

(27) Gao, X. T.; Bare, S. R.; Weckhuysen, B. M.; Wachs, I. E. *J. Phys. Chem. B* **1998**, *102*, 10842.

(28) Male, J. L.; Niessen, H. G.; Bell, A. T.; Tilley, T. D. *J. Catal.* **2000**, *194*, 431.

(29) Gao, X. T.; Wachs, I. E. *J. Phys. Chem. B* **2000**, *104*, 1261.

(30) Morey, M.; Davidson, A.; Eckert, H.; Stucky, G. *Chem. Mater.* **1996**, *8*, 486.

(31) VanDerVoort, P.; White, M. G.; Mitchell, M. B.; Verberckmoes, A. A.; Vansant, E. F. *Spectroc. Acta Pt. A-Molec. Biomolec. Spectr.* **1997**, *53*, 2181.

(32) Pena, M. L.; Dejoz, A.; Fornes, V.; Rey, E.; Vazquez, M. I.; Nieto, J. M. L. *Appl. Catal. A-Gen.* **2001**, *209*, 155.

(33) Dzwigaj, S. *Curr. Opin. Solid State Mater. Sci.* **2003**, *7*, 461.

(34) Liu, Y. M.; Feng, W. L.; Li, T. C.; He, H. Y.; Dai, W. L.; Huang, W.; Cao, Y.; Fan, K. N. *J. Catal.* **2006**, *239*, 125.

(35) Moussa, N.; Ghorbel, A. *Appl. Surf. Sci.* **2008**, *255*, 2270.

(36) Tielens, F.; Trejda, M.; Ziolek, M.; Dzwigaj, S. *Catal. Today* **2008**, *139*, 221.

(37) Liu, Y. M.; Xie, S. H.; Cao, Y.; He, H. Y.; Fan, K. N. *J. Phys. Chem. C* **2010**, *114*, 5941.

(38) Kondratenko, E. V.; Baerns, M. *Appl. Catal. A-Gen.* **2001**, *222*, 133.

(39) Mathieu, M.; Van Der Voort, P.; Weckhuysen, B. M.; Rao, R. R.; Catana, G.; Schoonheydt, R. A.; Vansant, E. F. *J. Phys. Chem. B* **2001**, *105*, 3393.

(40) Keller, D. E.; Visser, T.; Soulimani, F.; Koningsberger, D. C.; Weckhuysen, B. M. *Vib. Spectrosc.* **2007**, *43*, 140.

(41) Tanev, P. T.; Pinnavaia, T. J. *Science* **1995**, *267*, 865.

(42) Reddy, J. S.; Sayari, A. *J. Chem. Soc.-Chem. Commun.* **1995**, 2231.

(43) Kubelka, P.; Munk, F. Z. *Thech Phys* **1931**, *12*, 593.

(44) Weber, R. S. *J. Catal.* **1995**, *151*, 470.

(45) Davis, E. A.; Mott, N. F. *Philos. Mag.* **1970**, *22*, 903.

(46) Tauc, J. *Amorphous and Liquid Semiconductors*; Plenum Press: London, 1974.

(47) Morey, M.; Davidson, A.; Stucky, G. *Microporous Mater.* **1996**, *6*, 99.

(48) Hess, C.; Hoefelmeyer, J. D.; Tilley, T. D. *J. Phys. Chem. B* **2004**, *108*, 9703.

(49) Lee, E. L.; Wachs, I. E. *J. Phys. Chem. C* **2007**, *111*, 14410.

(50) Wojdyr, M. *J. Appl. Crystallogr.* **2010**, *43*, 1126.

(51) Lewandowska, A. E.; Banares, M. A.; Tielens, F.; Che, M.; Dzwigaj, S. *J. Phys. Chem. C* **2010**, *114*, 19771–19776.

(52) Zhao, C. L.; Wachs, I. E. *J. Catal.* **2008**, *257*, 181.

(53) Hess, C.; Schlogl, R. *Chem. Phys. Lett.* **2006**, *432*, 139.

(54) Moisii, C.; Curran, M. D.; van de Burgt, L. J.; Stiegman, A. E. *J. Mater. Chem.* **2005**, *15*, 3519.

(55) Wu, Z. L.; Dai, S.; Overbury, S. H. *J. Phys. Chem. C* **2010**, *114*, 412.

(56) Cavalleri, M.; Hermann, K.; Knop-Gericke, A.; Havecker, M.; Herbert, R.; Hess, C.; Oestereich, A.; Dobler, J.; Schlogl, R. *J. Catal.* **2009**, *262*, 215.

(57) Havecker, M.; Cavalleri, M.; Herbert, R.; Follath, R.; Knop-Gericke, A.; Hess, C.; Hermann, K.; Schlogl, R. *Phys. Status Solidi B* **2009**, *246*, 1459.

PAPER III

SciVerse ScienceDirect

PHPRO

Physics Procedia 00 (2011) 000–000

www.elsevier.com/locate/procedia

10th International Conference Solid State Chemistry

Possibility of VO_x/SiO_2 complexes speciation: comparative multi-wavelength Raman and DR UV-vis study

Roman Bulánek, Pavel Čičmanec, Michal Setnička

Department of Physical Chemistry, Faculty of Chemical Technology, University of Pardubice, Studentská 573, 532 10 Pardubice, Czech Republic

Abstract

Raman spectroscopy is one of the very often used spectroscopic methods for characterization of vanadium surface species. However, Raman spectra of VO*x*-silica systems are more complex and interpretation is more difficult in comparison with other supports (like Al_2O_3, ZrO_2, TiO_2 or Nb_2O_5) because there is strong vibrational coupling between the vanadia species and the silica support. Therefore, assignment and interpretation of some vibrational bands is still subject of controversy. This fact results in incongruity of suggested molecular structure and population of individual vanadium surface complexes. In this contribution, we present systematic comparative study of DR UV-vis spectra and UV and visible Raman spectra (excited by 325 and 514.5 nm lasers) obtained on set of dehydrated VO*x*-HMS samples with vanadium loading from 2 up to 12 wt. %. We prove that changes in population of oligomeric and monomeric VO*x* species in individual samples are not manifested by significant changes in the character of Raman signals. On the other hand it is evident that with increasing of vanadium loadings the UV-vis spectra show systematic changes. Raman spectroscopy is useful characterization technique for detection presence of very small amount of V_2O_5 microcrystallites, especially if suitable wavelength of laser is used for remarkable resonant enhancement of Raman intensity of its bands (e.g. 514.5 nm).

Keywords: vanadium; catalyst; difuse-reflectance UV-vis spectroscopy; Raman spectroscopy; speciation;

1. Introduction

Supported vanadium oxide plays important role as catalysts for the selective oxidation of hydrocarbons or alcohols [1, 2]. Knowledge of the prevailing molecular structure of surface vanadium species is essential for understanding the structure – catalytic activity relationship. Supported catalysts are complex materials and the determination of active surface species and their structure is challenging task. To this

end, characterization of VO*x* species present on the surface of oxidic supports has been the subject of many spectroscopic studies including Raman, EPR, DR UV-vis, NMR, FTIR, EXAFS spectroscopy [3-19]. Raman spectroscopy is one of the most often used techniques, but structure information is obtained only indirectly and relies on a correct assignment of the observed bands to vibration modes. In the case of silica supported vanadium catalysts, recent experimental and theoretical studies indicated that there is strong vibrational coupling between the vanadia species and the silica support [20-22]. Vibrations of VO*x* species cannot be separated from those of the silica support due to coupling between bulk phonons and motions of the supported vanadium complexes which makes Raman spectra of VO*x*-silica systems more complex and interpretation is more difficult. Therefore, assignment and interpretation of some vibrational bands is controversial. For example, band at around 920 cm^{-1} was assigned to V-O-V mode of polymeric species [23, 24], V-O-support mode [20, 22, 25-27], V=O mode [28] or O-O mode [29, 30]. Band at around 1031 cm^{-1} was assigned to V=O mode and its shift was ascribed to change in polymerization degree of VO*x* surface species. Such systematic shifts to higher wavenumbers were observed in Raman spectra of VO*x* on Al_2O_3, ZrO_2, TiO_2 or Nb_2O_5 supports, but no shift of this Raman band was observed on VO*x*/SiO_2 systems. This fact was often taken as evidence of presence solely monomeric species on the silica. Contrarily, presence of oligo- and polymeric VO*x* species with distorted tetrahedral coordination (group of symmetry T_d or C_{3v}) on mesoporous silicas was recently suggested on the basis of IR study of CO and NO adsorption on reduced VO*x*-SBA-15 [16], asymmetry of NEXAFS band of O 1s core excitation of oxygen atoms centered at 531 eV [31] or shifts of CT bands in UV-vis spectra of dehydrated samples [10, 19, 23, 32-36]. Very recently, we reported systematical and significant shift of energy band gap in DR UV-vis spectra of several sets of VO*x*-HMS catalysts investigated in ODH of n-butane[9, 11] and propane[8, 9]. For evidence of tetrahedral polymeric VO*x* species we adopted methodology applied by Gao et al. [37] for supported vanadium oxide species. This methodology is based on the evaluation of edge of absorption energy ε_0 from UV-Vis spectra using the expression introduced by Davis and Mott [38] or by Tauc [39] in the form:

$$\left(F\left(R_\infty\right)\cdot h\nu\right)^2 \propto \left(h\nu-\varepsilon_0\right) \qquad (1)$$

correlating this value with the edge of absorption energy of referent compounds (such as sodium ortho- and meta-vanadate representing isolated monomeric vanadyls and polymeric species with V-O-V bond) or theirs mechanical mixtures with known composition respectively. Relative amount of monomeric and polymeric species in the sample can be evaluated from linear dependence of the ε_0 value between values obtained from spectra of model compounds.

In this contribution, we present systematic comparative study of DR UV-vis spectra and Raman spectra at 325 and 514 nm wavelength excitations obtained on set of dehydrated VO*x*-HMS samples with vanadium loading from 2 up to 12 wt. % providing wide range of VO*x* species population and distribution. We prove that changes in population of oligomeric and monomeric VO*x* species in individual samples are not manifested by significant changes in the character of Raman signals. On the other hand, Raman spectroscopy is extremely sensitive to the presence of very small amount of V_2O_5 microcrystallites, especially if suitable wavelength of laser is used for remarkable resonant enhancement of Raman intensity of its spectral bands (e.g. 514 nm).

2. Experimental

2.1. Catalysts preparation

HMS was prepared according to procedure reported by Tanev and Pinnavaia [40]. 13.6 g of dodecylamine (DDA, Aldrich) was dissolved in the mixture of 225 cm^3 ethanol and 200 cm^3 double-distilled H_2O. After stirring for 20 min, 56 cm^3 of tetraethyl orthosilicate (TEOS, Aldrich) was added dropwise and intensively stirred. The reaction was performed at 25 °C for 18 hours under stirring. The solid product was filtered and then repeatedly suspended in 500 cm^3 ethanol and stirred at 25 °C for 1 hour in order to remove major part of DDA from obtained solid. Finally, the solid was calcined in flow of air at 540 °C for 8 hours with heating rate 1 °C min^{-1}.

Vanadium oxo-complexes were doped onto silica support by standard wet impregnation procedure by appropriate amount of ethanol/H_2O solution of vanadyl acetylacetonate (Aldrich). Impregnated samples were dried at 120 °C in air overnight and then calcined at 600 °C for 8 hours in the dry air flow. Vanadium content was determined by X-ray fluorescence spectroscopy (bench-top vacuum wavelength dispersive X-ray spectrometer Spectroscan V, Spectron, Russia). Samples were denoted as S-x where x is the vanadium content in the weight percentage.

2.2. DR UV-vis spectroscopy

The UV-vis diffuse reflectance spectra of diluted and subsequently dehydrated samples were measured using Cintra 303 spectrometer (GBC Scientific Equipment, Australia) equipped with a Spectralon-coated integrating sphere using a Spectralon coated discs as a standard. The spectra were recorded in the range of the wavelength 190-850 nm. The samples were diluted by the pure silica (Fumed silica, Aldrich) in the ratio 1:100 in order to obtain better resolution of individual bands and the linear dependence of spectral area on the concentration of vanadium (for more details see ref [10]). All samples were granulated and sieved to fraction of size 0.25-0.5 mm, dehydrated before the spectra measurement and oxidized in the glass apparatus under static oxygen atmosphere (16-18 kPa) in two steps: 120 °C for 30 min and 450 °C for 60 min and subsequently cooled down to 250 °C and evacuated for 30 min. After the evacuation the samples were transferred into the quartz optical cuvette 5 mm thick and sealed under vacuum. For additional details you can see ref.[10]. This procedure guaranteed complete dehydration and defined oxidation state of vanadium for all catalysts. The obtained reflectance spectra were transformed into the dependencies of Kubelka-Munk function $F(R_\infty)$ on the absorption energy hν using the Equation 2 :

$$F(R_\infty) = \frac{(1 - R_\infty)^2}{2R_\infty} \qquad (2)$$

where R_∞ is the measured diffuse reflectance from a semi-infinite layer[41].

2.3. Raman spectroscopy

Visible Raman spectra of dehydrated catalysts were measured by a Labram HR spectrometer (Horiba Jobin-Yvon) interfaced to an Olympus BX-41 microscope. Spectra were excited by 514.5 nm line of an Ar^{+}/Kr^{+} laser (Innova 70C series, Coherent). The spectra were recorded by collecting of two scans (scan time 1200 s with resolution 2 cm^{-1}) by Peltier-cooled CCD camera detector. The laser power impinging on the dry sample was 1.2 mW. UV Raman spectra were measured using Micro-Raman Renishaw RM 1000 spectrometer equipped with CCD detection. Spectra were excited by 325 nm HeCd laser (~ 3 mW at the sample) and two scans were collected (time of scan was 100 s with resolution 4 cm^{-1}). The dehydration and oxidation protocol was the same as for DR UV-vis measurement (see above).

3. Results and Discussion

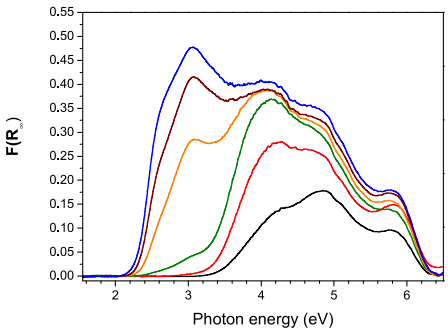

Figure 1 Diffuse reflectance UV–vis spectra of dehydrated VO*x*-HMS samples (for assignment of individual curves to the samples see Table 1)

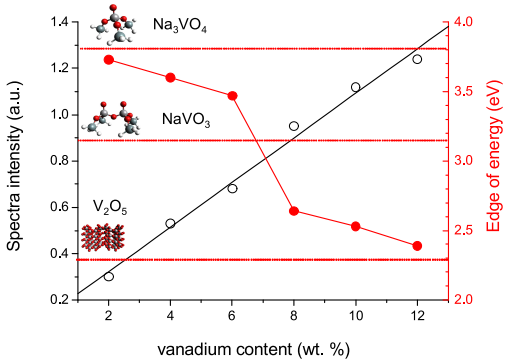

Figure 2 Plot of edge of energy value determined by means of Tauc`s law form spectra depicted in the Figure 1 and intensity of DR UV-vis spectra vs. vanadium content. Energy edges of model compounds and idealized molecular structure of surface vanadium species are inserted in the plot.

The obtained DR UV-vis spectra for investigated catalyst are presented in the Figure 1. It can be noted that parent HMS support exhibited only very low intensity spectrum without distinct signal and therefore are not reported here. Spectra of VO*x*-HMS catalysts contain several absorption bands in region 1.46-6.5 eV (850-190 nm) which are conventionally attributed to ligand to metal charge-transfer (LMCT) transitions of the O $\rightarrow V^{+V}$ type or to the d-d transitions of V^{+IV} [42]. The d–d absorption bands characteristic for the vanadium(+IV) in the region 1.55 – 2.07 eV [43] were not observed in our spectra and this fact confirms that all vanadium was successfully oxidized to oxidation state (+V) during the pretreatment procedure. The catalysts with concentration higher than 4 wt% of vanadium exhibit absorption bands in the region 2-3 eV with maxima at ca. 2.6 and 3.1 eV and they are attributed to the presence of octahedrally coordinated (group O_h) 2D/3D bulk-like VO*x* units [10, 43, 44]. Values of energy of edge (ε_0) determined by Tauc`s law (see Eq. 1) are summarized in Table 1 and plotted against vanadium content in the Figure 2. The low-loaded samples exhibit absorption only above 3 eV evidencing

VO*x* species with tetrahedral coordination. Samples with vanadium content up to 6 wt.% exhibit edge energy in the range of 3.73 – 3.47 eV (obtained accordingly to Ref. [39]), whereas edge energy of Na_3VO_4, $NaVO_3$ and V_2O_5 is 3.82, 3.13 and 2.26 eV, respectively. Taking into account this observation, it ca be concluded that both isolated VO_4 units and small VO_x aggregates that have V-O-V bonds are present on the surface of these samples (effect of partial hydration was excluded on the base of checking measurement of overtones of OH group vibration on UV-vis-NIR spectrometer, not shown for sake of brevity). Samples with vanadium content higher than 6 wt. % exhibit ε_0 below 3 eV and these values systematically decrease with increasing vanadium content and limit to the value of ε_0 of bulk oxide. This is in accordance with increasing intensity of absorption bands at 2.6 and 3.1 eV assigned to CT band of V_2O_5 microcrystallites. For quantitative analysis of all three types of surface vanadium complexes, the spectra were deconvoluted into individual bands. Parameters of individual spectral bands used in deconvolution procedure of the spectra was taken from systematic study analyzing wide set of VO*x*-HMS samples recently published [10]. The Figure 3 presents examples of the deconvolution of the experimental spectra of sample with and without octahedrally coordinated vanadium complexes. UV-vis spectra of all samples contain three absorption bands in the region 3-6.5 eV and these bands can be attributed to the ligand to metal charge transfers of tetrahedrally coordinated (T_d) species (group of symmetry T_d). The band with maxima position approximately at 4 eV can be attributed to T_d oligomeric species [45, 46]. The band at ca. 5.9 eV belongs to T_d-monomeric species [45-47] and the band with maximum at 5 eV is linear combination of the bands ascribed to both the T_d-monomeric and the T_d oligomeric species. Relative amount of individual VO*x* species on the surface was determined from area of corresponding bands (equality of extinction coefficients of individual bands is assumed based on linear dependence of spectra intensity vs. vanadium content in catalysts (see Fig. 2)) and results are given in the Table 1. The low concentrated samples contain only T_d-coordinated VO*x* species. The highest relative abundance of isolated monomeric T_d-coordinated units (33 rel. %) can be found on VO*x*-HMS with the lowest vanadium content. While relative population of oligomeric T_d-coordinated VO*x* species is almost constant (ca. 75 rel. %) , population of monomeric species decreases with increasing vanadium content from 33 rel. % to 6 rel. % and simultaneously population of octahedrally coordinated species increase from zero to 27 rel. %. This picture is consistent with results of systematic study of Wachs'group which led to conclusion that oxide microcrystallites appeared above monolayer coverage, when all the reactive hydroxyls of the support have been titrated [48, 49]. Monolayer coverage on silica is significantly lower (about 0.7 V/nm^2) in comparison to other supports like alumina, titania and zirconia (about 7–8 V/nm^2). The low surface monolayer coverage on silica is due to somewhat lower density and reactivity of the silica surface hydroxyls in comparison to other oxide supports. Surface vanadium density of our samples range from 0.3 to 24.3 V/nm^2, therefore presence of oligomeric T_d- and O_h-coordinated species is reasonable and expectable.

Table 1. List of samples, their physico-chemical characterization, results of DR UV-vis spectra deconvolution.

sample	V content (wt.%)	S_{BET} (m^2/g)	Surface density (V/nm^2)	ε_0 (eV)	Relative population of VO*x* complexes			color in Figures
					O_h	T_d^{oligo}	T_d^{mono}	
S-2	2.0	760	0.3	3.73	0.00	0.67	0.33	black
S-4	4.0	645	0.7	3.60	0.00	0.70	0.30	red
S-6	6.0	450	1.6	3.47	0.02	0.81	0.17	olive
S-8	8.0	225	4.2	2.64	0.15	0.77	0.08	orange
S-10	10.0	70	17.5	2.53	0.23	0.70	0.08	wine
S-12	12.0	60	24.3	2.39	0.27	0.67	0.06	blue

Figure 4 shows the Raman spectra of a dehydrated S-6 catalyst excited at 514.5 and 325 nm. Evidently, visible Raman spectrum is totally different from UV Raman spectrum. This is due to the fact that both excitation wavelengths are absorbed by different vanadium species in the sample and therefore different resonance enhancement effect control Raman band intensities. The Raman spectrum excited by 514.5 nm laser exhibits set of bands at 282, 301, 404, 520, 697, and 993 cm^{-1} – a typical fingerprint of V_2O_5 crystallites. Besides these bands, band at 1040 $cm^{-1}$with small shoulder at 1060 cm^{-1} can be seen. This band is usually assigned to terminal V=O stretching vibration, but this assignment has been questioned recently [28]. The shoulder at 1060 cm^{-1} was previously ascribed to silica TO vibration or $Si(-O^-)_x$ functionalities [50], but recent theoretical work suggests that it is due to V-O-Si stretching mode [20, 22, 28]. Intensity of Raman bands assigned to bulk oxide in visible Raman spectrum is strongly enhanced by resonance effect (light at 514.5 nm is absorbed by octahedrally coordinated bulk vanadium oxide clusters, see inset in Fig.4), therefore intensity of the V_2O_5 bands is much intensive than would be expected on the base of DR UV-vis spectra. The band at ~ 483, 603 and ~ 802 cm^{-1} have been assigned to the D1 and D2 defect mode of silica support, which have been attributed to tetracyclosiloxane rings produced via the condensation of surface hydroxyls, and the symmetrical Si-O-Si stretching mode, respectively [51, 52]. UV Raman spectrum is dominated by broad band at 487 cm^{-1} assigned to the D1 defect mode and band at 1024 cm^{-1} usually ascribed to V=O stretching vibration. This band is about 16 cm^{-1} lower than that observed in the visible Raman spectrum. Wu et al. attributed this difference in the frequencies to existence of two different V=O stretching vibrations (each exhibited another resonance effect). This statement induces suggestion of presence of two types of VO*x* species on silica support. For deeper investigation of this statement, we compared visible and UV Raman spectra of samples with various distributions of vanadium complexes on the silica support (see Figure 5).

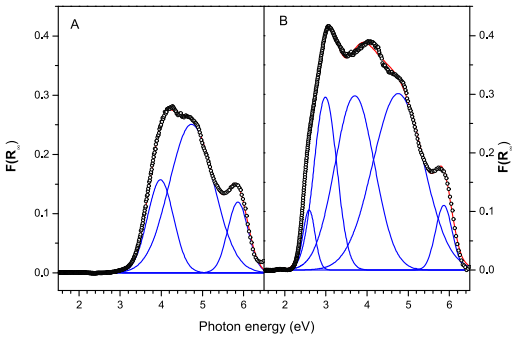

Figure 3 Deconvoluted DR UV–vis spectra of S-4 (A) and S-10 (B) samples. Black points are experimental data, red line is fitted envelope curve and blue lines are individual spectral bands.

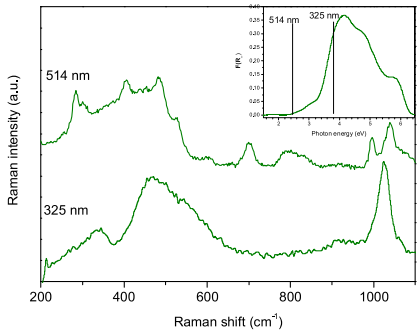

Figure 4 Raman spectra of dehydrated S-6 sample at 514.5 nm and 325 nm excitation. Inset: DR UV-vis spectrum of dehydrated S-6 sample with marked position of lights of individual lasers used for excitation of Raman spectra.

Visible Raman spectra of all investigated catalysts are depicted in the Figure 5A and B (plot A display whole spectral range from 200 to 1100 cm^{-1} and plot B display spectral features around 1000 cm^{-1} in more

details). S-2 sample, which contain lowest amount of vanadia, exhibits only one band related to vanadia species at 1040 cm^{-1}. Intensity of this band is very low and band is relatively broad (FWHM is 30 cm^{-1}). Band intensity increases with increasing vanadium loading, whereas position of band remains the same. Set of bands at 282, 301, 404, 520, 697, and 993 cm^{-1} belonging to vibration of V_2O_5 crystallites appeared in the spectrum of S-4 sample in spite of absence bands at 2.6 or 3.1 eV in the DR UV-vis spectrum of this sample (cf. Fig. 1). This is due to extremely high sensitivity of visible Raman at 514.5 nm to the presence of oxide-like species caused by resonance effect. The bands of V_2O_5 increase in intensity with vanadium loading and dominate the spectra from 8 wt. % of vanadia. This is consistent with observed shift of absorption into visible region in DR UV-vis spectra of these samples. On the other hand, band at 1040 cm^{-1} is missing in the spectra of samples with concentration of vanadia 8 wt. % and higher. Broad shoulder of the band at 995 cm^{-1} at about 1023 cm^{-1} appears instead of band at 1040 cm^{-1}. This can be caused by relatively low amount of monomeric vanadium species in the high-loaded samples, whereas amount of oligomeric species simultaneously increases. This observation is in contradiction with observation on other supports. Changes in the coordination and extent of polymerization of the dehydrated surface VO_x species on oxide supports as Al_2O_3, ZrO_2, TiO_2 or Nb_2O_5 are reflected by shift of this vibration band to slightly higher wavenumbers [3, 49]. Therefore, nature of this band is still not clear.

UV Raman spectra are shown in the Figure 5 C and D. The spectra are dominated by broad band from silica support at 487 cm^{-1} except sharp band at 1025 cm^{-1} assigned to V=O vibration. Position of later band is invariable in spectra of all samples notwithstanding increasing vanadium loading and various populations of oligomeric species determined from UV-vis spectra. Intensity of this band is increasing only up to 6 wt. % of vanadia in the sample, then intensity decreases and new band at 993 cm^{-1} appears and rises with vanadium content. It is important to note that signal at 993 cm^{-1}, characteristic for vanadium oxide clusters, appeared in the UV Raman spectra at vanadium content 8 wt. %, whereas absorption bands at 2.6 and 3.1 eV characteristic for octahedrally coordinated oxide-like species was detected by DR UV-vis spectroscopy in the spectrum of sample with 6 wt.%. It is clear from this observation that the presence of crystalline V_2O_5 can be more easily detected by visible Raman than UV Raman spectroscopy. Comparison of Raman spectra excited by both 514.5 nm and 325 nm laser in the region of stretching vibrations of V=O band led to finding out that both spectra sets provide different picture. Band at 1025 cm^{-1} is present in all UV Raman spectra and exhibits the same characteristic (FWHM is about 30 cm^{-1} as what as band at 1040 cm^{-1} in the visible Raman spectra) in contrast to visible Raman spectra in which band at 1027 cm^{-1} is detectable only in spectra of samples with the highest vanadium loading and its FWHM is significantly higher than FWHM of discussed band in UV Raman spectra. Recent experimental and theoretical investigations [20-22] shown that bands at about 1020-1050 cm^{-1} can be ascribed to normal modes with substantial contribution of both V=O and in-phase V-O-Si vibrations. Therefore interpretation of bands and its intensity dependence on excitation is not simple.

From above reported data, it is clear that interpretation of Raman spectra is complicated and using of Raman spectroscopy for characterization of VO_x species on silica surface is problematic. Dobler et al. state in their paper: „Distinguishing between monomeric and polymeric sites by vibrational spectroscopy is hardly possible because the only difference is the occurrence of new bands in spectral region covered by other (support) band“. Based on DFT calculations, these additional bands are not caused by vibration of pure V-O-V bond but they are given by normal modes consisting of contribution V-O-V (contribution to kinetics energy does not exceed 25 %), V=O and V-O-Si bonds and falling into spectral region 760-776 cm^{-1} for dimeric species and 840-870 cm^{-1} for tri- and tetrameric species. However, such bands were not detected in our spectra maybe due to their low intensity. Therefore presence/absence of particular band in the Raman spectrum cannot be clear indication of presence/absence of polymeric species. Raman spectroscopy is useful characterization technique for detection of presence of V_2O_5 microcrystallite,

especially if suitable wavelength of laser is used for resonant enhancement of Raman intensity of bands. As we showed in our recent papers, DR UV-vis spectroscopy can provide more detailed information about nature and population of vanadium species on silica based supports. In addition, DR UV-vis spectra can be at least semi-quantitatively evaluated when diluted samples are used, whereas quantitative analysis of Raman spectra is difficult owing to different resonance effects and local nature of spectral information (Raman spectrometer is usually combined with microscopy and spectrum is collected from relatively small area of sample).

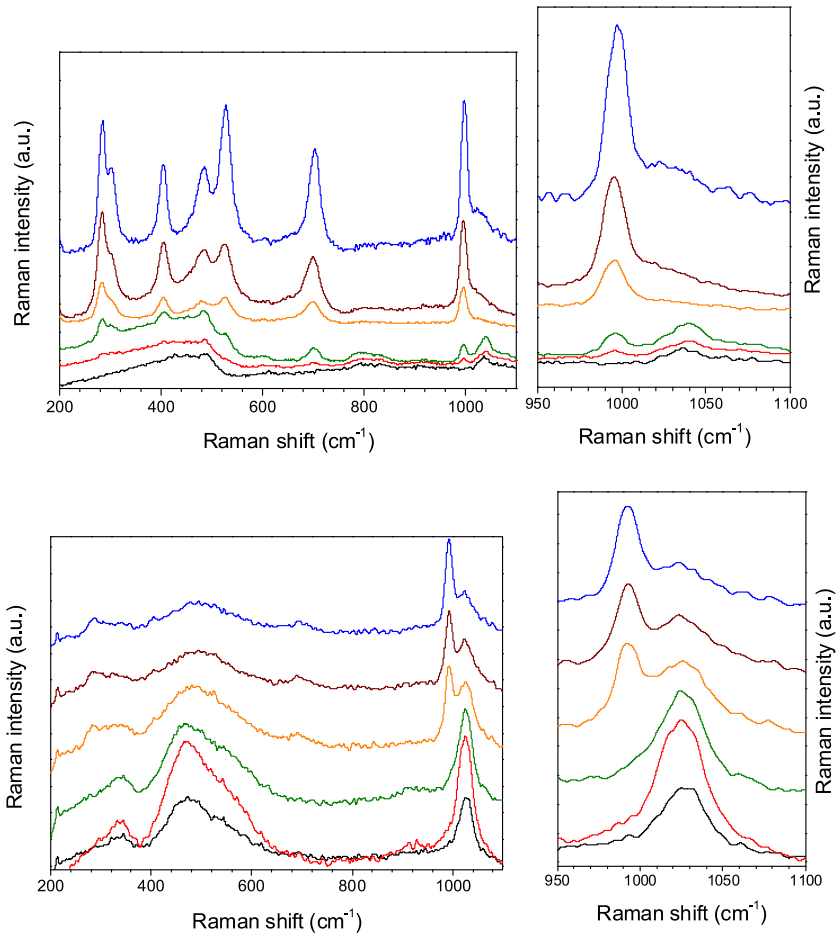

Figure 5 Visible (A and B) and UV (C and D) Raman spectra of dehydrated samples under study. Left panels depict full range of spectra, right panels display detail of spectral range of stretching vibrations around 1000 cm^{-1}. For assignment of individual curves to individual samples see Table 1.

4. Conclusion

Comparison of DR UV-vis spectra obtained on wide set of VO*x*-HMS samples differing in vanadium content in wide range and population of individual vanadium species with UV and visible Raman spectra clearly showed suitability of UV-vis spectroscopy for characterization of vanadium species spread on silica support. On the other hand, Raman spectroscopy is very sensitive technique for monitoring of V_2O_5 oxide presence. Using of several excitation wavelengths is recommended for characterization of dispersed vanadium complexes by Raman spectroscopy. It enables selective resonance enhancement that can be used for distinguishing different species.

Acknowledgement

This work was supported by the Czech Science Foundation under project P106/10/0196. In addition, the authors would like to thank to Dr. Martin Kalbáč (Heyrovský Institute of Physical Chemistry, Czech Academy of Sciences) and Martin Ledinský (Institute of Physics, Academy of Science of the Czech Republic) for their help with measurement of Raman spectra and fruitful discussion.

References

1. Cavani F, Ballarini N, Cericola A. Oxidative dehydrogenation of ethane and propane: How far from commercial implementation? *Catal Today* 2007;**127**:113-31.

2. Weckhuysen BM, Keller DE. Chemistry, spectroscopy and the role of supported vanadium oxides in heterogeneous catalysis. *Catal Today* 2003;**78**:25-46.

3. Wachs IE, Weckhuysen BM. Structure and reactivity of surface vanadium oxide species on oxide supports. *Appl Catal A* 1997;**157**:67-90.

4. Deo G, Wachs IE, Haber J. Supported vanadium-oxide catalysts - molecular structural characterization and reactivity properties. *Crit Rev Surf Chem* 1994;**4**:141-87.

5. Banares MA. Operando methodology: combination of in situ spectroscopy and simultaneous activity measurements under catalytic reaction conditions. *Catal Today* 2005;**100**:71-7.

6. Banares MA, Martinez-Huerta MV, Gao X, Fierro JLG, Wachs IE. Dynamic behavior of supported vanadia catalysts in the selective oxidation of ethane - In situ Raman, UV-Vis DRS and reactivity studies. *Catal Today* 2000;**61**:295-301.

7. Banares MA. Supported metal oxide and other catalysts for ethane conversion: a review. *Catal Today* 1999;**51**:319-48.

8. Bulanek R, Cicmanec P, Sheng-Yang H, Knotek P, Capek L, Setnicka M. Effect of preparation method on nature and distribution of vanadium species in vanadium-based hexagonal mesoporous silica catalysts: Impact on catalytic behavior in propane ODH. *Appl Catal A* 2012;**415**:29-39.

9. Bulanek R, Kaluzova A, Setnicka M, Zukal A, Cicmanec P, Mayerova J. Study of vanadium based mesoporous silicas for oxidative dehydrogenation of propane and n-butane. *Catal Today* 2012;**179**:149-58.

10. Bulanek R, Capek L, Setnicka M, Cicmanec P. DR UV-vis Study of the Supported Vanadium Oxide Catalysts. *J Phys Chem C* 2011;**115**:12430-8.

11. Setnicka M, Bulanek R, Capek L, Cicmanec P. n-Butane oxidative dehydrogenation over VOX-HMS catalyst. *J Mol Catal A - Chem* 2011;**344**:1-10.

12. Capek L, Adam J, Grygar T, Bulanek R, Vradman L, Kosova-Kucerova G, et al. Oxidative dehydrogenation of ethane over vanadium supported on mesoporous materials of M41S family. *Appl Catal A* 2008;**342**:99-106.

13. Knotek P, Capek L, Bulanek R, Adam J. Vanadium supported on hexagonal mesoporous silica: active and stable catalysts in the oxidative dehydrogenation of alkanes. *Top Catal* 2007;**45**:51-5.

14. Das N, Eckert H, Hu HC, Wachs IE, Walzer JF, Feher FJ. Bonding states of surface vanadium(v) oxide phases on silica - structural characterization by v-51 nmr and raman-spectroscopy. *J Phys Chem* 1993;**97**:8240-3.

15. Dinse A, Ozarowski A, Hess C, Schomacker R, Dinse KP. Potential of High-Frequency EPR for Investigation of Supported Vanadium Oxide Catalysts. *J Phys Chem C* 2008;**112**:17664-71.

16. Venkov TV, Hess C, Jentoft FC. Redox properties of vanadium ions in SBA-15-supported vanadium oxide: An FTIR spectroscopic study. *Langmuir* 2007;**23**:1768-77.

17. Chlosta R, Tzolova-Muller G, Schlogl R, Hess C. Nature of dispersed vanadium oxide: influence of the silica support structure and synthesis methods. *Catal Sci Technol* 2011;**1**:1175-81.

18. Hess C. Direct correlation of the dispersion and structure in vanadium oxide supported on silica SBA-15. *J Catal* 2007;**248**:120-3.

19. Hess C, Hoefelmeyer JD, Tilley TD. Spectroscopic characterization of highly dispersed vanadia supported on SBA-15. *J Phys Chem B* 2004;**108**:9703-9.

20. Magg N, Immaraporn B, Giorgi JB, Schroeder T, Baumer M, Dobler J, et al. Vibrational spectra of alumina- and silica-supported vanadia revisited: An experimental and theoretical model catalyst study. *J Catal* 2004;**226**:88-100.

21. Wu ZL, Dai S, Overbury SH. Multiwavelength Raman Spectroscopic Study of Silica-Supported Vanadium Oxide Catalysts. *J Phys Chem C* 2010;**114**:412-22.

22. Dobler J, Pritzsche M, Sauer J. Vibrations of Silica Supported Vanadia: Variation with Particle Size and Local Surface Structure. *J Phys Chem C* 2009;**113**:12454-64.

23. Liu YM, Cao Y, Yi N, Feng WL, Dai WL, Yan SR, et al. Vanadium oxide supported on mesoporous SBA-15 as highly selective catalysts in the oxidative dehydrogenation of propane. *J Catal* 2004;**224**:417-28.

24. Burcham LJ, Deo G, Gao XT, Wachs IE. In situ IR, Raman, and UV-Vis DRS spectroscopy of supported vanadium oxide catalysts during methanol oxidation. *Top Catal* 2000;**11**:85-100.

25. Ohde C, Brandt M, Limberg C, Doebler J, Ziemer B, Sauer J. V2O5/SiO2 surface inspired, silsesquioxane-derived oxovanadium complexes and their properties. *Dalton Trans* 2008;326-31.

26. Islam MM, Costa D, Calatayud M, Tielens F. Characterization of Supported Vanadium Oxide Species on Silica: A Periodic DFT Investigation. *J Phys Chem C* 2009;**113**:10740-6.

27. Wu ZL, Kim HS, Stair PC, Rugmini S, Jackson SD. On the structure of vanadium oxide supported on aluminas: UV and visible Raman spectroscopy, UV-visible diffuse reflectance spectroscopy, and temperature-programmed reduction studies. *J Phys Chem B* 2005;**109**:2793-800.

28. Moisii C, van de Burgt LJ, Stiegman AE. Resonance Raman spectroscopy of discrete silica-supported vanadium oxide. *Chem Mater* 2008;**20**:3927-35.

29. van Lingen JNJ, Gijzernan OLJ, Weckhuysen BM, van Lenthe JH. On the umbrella model for supported vanadium oxide catalysts. *J Catal* 2006;**239**:34-41.

30. Gijzeman OLJ, van Lingen JNJ, van Lenthe JH, Tinnemans SJ, Keller DE, Weckhuysen BM. A new model for the molecular structure of supported vanadium oxide catalysts. *Chem Phys Lett* 2004;**397**:277-81.

31. Cavalleri M, Hermann K, Knop-Gericke A, Havecker M, Herbert R, Hess C, et al. Analysis of silica-supported vanadia by X-ray absorption spectroscopy: Combined theoretical and experimental studies. *J Catal* 2009;**262**:215-23.

32. Fornes V, Lopez C, Lopez HH, Martinez A. Catalytic performance of mesoporous VOx/SBA-15 catalysts for the partial oxidation of methane to formaldehyde. *Appl Catal A* 2003;**249**:345-54.

33. Kustrowski P, Segura Y, Chmielarz L, Surman J, Dziembaj R, Cool P, et al. VOx supported SBA-15 catalysts for the oxidative dehydrogenation of ethylbenzene to styrene in the presence of N2O. *Catal Today* 2006;**114**:307-13.

34. Hess C, Wild U, Schlogl R. The mechanism for the controlled synthesis of highly dispersed vanadia supported on silica SBA-15. *Micropor Mesopor Mat* 2006;**95**:339-49.

35. Gruene P, Wolfram T, Pelzer K, Schlogl R, Trunschke A. Role of dispersion of vanadia on SBA-15 in the oxidative

dehydrogenation of propane. *Catal Today* 2010;**157**:137-42.

36. Arena F, Frusteri F, Martra G, Coluccia S, Parmaliana A. Surface structures, reduction pattern and oxygen chemisorption of V2O5/SiO2 catalysts *J Chem Soc - Faraday Trans* 1997;**93**:3849.

37. Gao XT, Wachs IE. Investigation of surface structures of supported vanadium oxide catalysts by UV-vis-NIR diffuse reflectance spectroscopy. *J Phys Chem B* 2000;**104**:1261-8.

38. Davis EA, Mott NF. Conduction in Non-Crystalline Systems .5. Conductivity, Optical Absorption and Photoconductivity in Amorphous Semiconductors. *Phil Mag* 1970;**22**:903-&.

39. Tauc J. Amorphous and Liquid Semiconductors. London: Plenum Press; 1974.

40. Tanev PT, Pinnavaia TJ. A Neutral Templating Route to Mesoporous Molecular-Sieves. *Science* 1995;**267**:865-7.

41. Kubelka P, Munk FZ. Ein beitrang zur optik der farbanstriche. *Tech Phys* 1931;**12**:593.

42. Keller DE, Visser T, Soulimani F, Koningsberger DC, Weckhuysen BM. Hydration effects on the molecular structure of silica-supported vanadium oxide catalysts: A combined IR, Raman, UV-vis and EXAFS study. *Vib Spectrosc* 2007;**43**:140-51.

43. Mathieu M, Van Der Voort P, Weckhuysen BM, Rao RR, Catana G, Schoonheydt RA, et al. Vanadium-incorporated MCM-48 materials: Optimization of the synthesis procedure and an in situ spectroscopic study of the vanadium species. *J Phys Chem B* 2001;**105**:3393-9.

44. Solsona B, Blasco T, Nieto JML, Pena ML, Rey F, Vidal-Moya A. Vanadium oxide supported on mesoporous MCM-41 as selective catalysts in the oxidative dehydrogenation of alkanes. *J Catal* 2001;**203**:443-52.

45. Gao F, Zhang YH, Wan HQ, Kong Y, Wu XC, Dong L, et al. The states of vanadium species in V-SBA-15 synthesized under different pH values. *Micropor Mesopor Mat* 2008;**110**:508-16.

46. Schramlmarth M, Wokaun A, Pohl M, Krauss HL. Spectroscopic investigation of the structure of silica-supported vanadium-oxide catalysts at submonolayer coverages. *J Chem Soc - Faraday Trans* 1991;**87**:2635-46.

47. Catana G, Rao RR, Weckhuysen BM, Van Der Voort P, Vansant E, Schoonheydt RA. Supported vanadium oxide catalysts: Quantitative spectroscopy, preferential adsorption of V4+/5+, and Al2O3 coating of zeolite Y. *J Phys Chem B* 1998;**102**:8005-12.

48. Tian HJ, Ross EI, Wachs IE. Quantitative determination of the speciation of surface vanadium oxides and their catalytic activity. *J Phys Chem B* 2006;**110**:9593-600.

49. Wachs IE. Raman and IR studies of surface metal oxide species on oxide supports: Supported metal oxide catalysts. *Catal Today* 1996;**27**:437-55.

50. Lee EL, Wachs IE. In situ spectroscopic investigation of the molecular and electronic Structures of SiO2 supported surface metal oxides. *J Phys Chem C* 2007;**111**:14410.

51. Morrow BA, Mcfarlan AJ. Chemical-reactions at silica surfaces. *J Non-Cryst Solids* 1990;**120**:61-70.

52. Brinker CJ, Kirkpatric RJ, Tallant DR, Bunker BC, Montez B. NMR confirmation of strained defects in amorphous silica. *J Non-Cryst Solids* 1988;**99**:418 - 25.

PAPER IV

Journal of Molecular Catalysis A: Chemical 344 (2011) 1–10

Contents lists available at ScienceDirect

Journal of Molecular Catalysis A: Chemical

journal homepage: www.elsevier.com/locate/molcata

Editor's choice paper

n-Butane oxidative dehydrogenation over VO_X-HMS catalyst

M. Setnička*, R. Bulánek, L. Čapek, P. Čičmanec

Department of Physical Chemistry, Faculty of Chemical Technology, University of Pardubice, Studentska 573, 532 10 Pardubice, Czech Republic

ARTICLE INFO

Article history:
Received 16 February 2011
Received in revised form 29 April 2011
Accepted 3 May 2011
Available online 11 May 2011

Keywords:
Vanadium oxide
Oxidative dehydrogenation
n-Butane
Hexagonal mesoporous silica
TPR
DR UV–vis

ABSTRACT

The demand for olefins increases in recent years. Oxidative dehydrogenation (ODH) of *n*-butane is possible alternative to classical dehydrogenation, steam cracking and fluid catalytic cracking processes. The role of particular VO_X species supported on hexagonal mesoporous silica (HMS) in oxidative dehydrogenation (ODH) of *n*-butane was investigated on two sets of VO_X-HMS catalysts prepared by wet impregnation and direct synthesis differing in amount and distribution of VO_X species. The materials were characterized by XRF, N_2-BET isotherms, XRD, SEM, H_2-TPR, O_2-TPO and DR UV–vis spectroscopy and tested in ODH of *n*-butane in the range of temperature from 460 to 540 °C. The highest activity and selectivity to olefins were reached on materials with high content of isolated monomeric VO_X units with tetrahedral coordination which are generated up to 4–5 wt.% of vanadium. The species with high degree of polymerization participate mainly on total oxidation reactions and those species are formed especially by wet impregnation.

1. Introduction

Main task of today's chemical industry is a production of a large amount of organic compounds. Presently it is very important to find alternative processes for production of these compounds from more economically suitable raw materials and with smaller impact to environment. For example we can use alkanes instead alkenes because alkanes are by half cheaper compared to alkenes which are easily available [1]. The global demand for C_4-olefins increases in recent years. In the year 1984 the world production of butenes was 28.1 mil. tons [2]. In the year 2004 it was already 44 mil. tons [3]. Similar situation is in the case of 1,3-butadiene whose production was 1.3 mil. tons in the year 1983 in the USA [2] and nearly 2.1 mil. tons in year 2000 [4].

Oxidative dehydrogenation (ODH) of *n*-butane is an alternative to classical dehydrogenation, steam cracking and fluid catalytic cracking processes. The ODH reaction is thermodynamically favorable and can be proceed at temperature much lower compared to a non-oxidative dehydrogenation. To a certain extent, the conditions of ODH reaction reduce the problems of coke formation and catalyst deactivation. But this reaction has still several unresolved problems whose hinder its industrial use. The molecule of butane contains four carbon atoms which enable a lot of consecutive reactions. This makes possible the formation of lot of consecutive reaction products as described in Ref. [5]. Moreover the formed alkenes are approximately four times more reactive then butane [6]. It causes the decrease of selectivity to asked products with the increasing conversion of butane. Thus the development of suitable catalyst is still important challenge.

Vanadium oxide based catalysts are very often used as catalysts in ODH reaction. Their employment offers several advantages: lower temperature for the activation of C–H bonds of reactants (limitation of cracking and combustion reactions) and suitable geometric and electron structure of VO_X (tunable with used matrix or temperature). The vanadium-oxide catalysts are hence suitable for insertion oxygen atom to molecule hydrocarbon. On the other hand vanadium oxide catalysts cannot be used in its bulk form (leads to non-selective reactions) but have to be used as the well dispersed VO_X species supported on the suitable support [6–8].

The support strongly affects the catalytic performance. The textural properties and acid–base character of the support are the most important factors [1]. The acid–base character has influence on (i) the dispersion of the vanadium oxides [7,9] (ii) their structure [7,9] and (iii) retention period of reactants and reaction intermediates on the surface [6,7,10]. From this point of view the MgO support (iso-electric point (IEP) *ca.* 12.5 [7]) seems as the best support for ODH of alkanes because rising alkenes (more basic then alkanes) are easy desorbed and it suppress consecutive reactions leading to CO_X. Moreover acid character of V_2O_5 (IEP 1.4 [7]) facilitates good dispersion of VO_X species. On the other hand MgO supports have area only about 100–150 $m^2\,g^{-1}$ [11–13] what limits attainable vanadium loading. From this reason is required to find new support materials with large surface.

The vanadium oxide (VO_X) units supported on the surface of amorphous SiO_2 or ordered mesoporous silica (SBA-15) [14–16]

* Corresponding author. Tel.: +420 466 037 345; fax: +420 466 037 068.
E-mail address: Michal.Setnicka@student.upce.cz (M. Setnička).

1381-1169/$ – see front matter © 2011 Elsevier B.V. All rights reserved.
doi:10.1016/j.molcata.2011.05.004

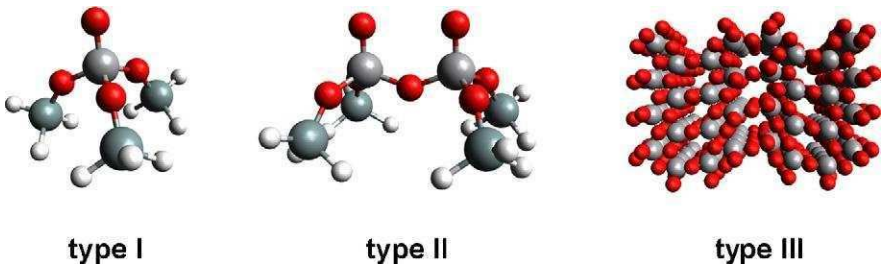

Scheme 1. Three different type of VO_X species exist on the HMS surface. Type I – isolated monomeric units with tetrahedral coordination, type II – one-dimensional oligomeric units with distorted tetrahedral coordination and type III – two- and three-dimensional polymeric units in octahedral coordination.

were reported to be potentially suitable catalysts in the ODH of *n*-butane in the past. The hexagonal mesoporous silica (HMS) is used as support in this work. Advantages of the supported catalysts on the HMS are: larger surface area (a good dispersion of active particles), thermal stability, good mechanical properties, weak acid centers, system of one dimensional open channels with 35–40 Å pore diameter (easy mass transport of products) [17,18].VO_X particle might be present at surface of catalysts in four different forms: highly dispersed isolated monomeric units with tetrahedral coordination (sup-O)$_3$V=O (sup – atom of support) (type I – see Scheme 1), one-dimensional oligomeric units connected by V–O–V bonds up to distorted tetrahedral coordination (type II – see Scheme 1), two-dimensional polymeric units in octahedral coordination called oxide-like species (type III – Scheme 1) and bulk three-dimensional V_2O_5 crystallites (type IV) [6,19].

The method of the deposition of active vanadium phase strongly influences the nature and abundance of rising VO_X species. The simple wet impregnation method of vanadium salt (NH_4VO_3, vanadyl sulfate, vanadyl acetylacetonate) is very often used for the deposition of VO_X species [14,20–23]. However, impregnation methods very often lead to materials with broad distribution of VO_X species including the VO_X units with a low degree of dispersion or bulk oxide. The direct hydrothermal synthesis of mesoporous vanadosilicate is an alternative method for incorporation of vanadium species on the silica surface by the introduction of the required amounts of metal salt to the synthesis gel. Despite of a great progress in the development of advanced method for direct synthesis of functionalized mesoporous silicas [24–26] but the exact description and mastery this synthesis is still great challenge.

In the present paper, we report for the first time the comparison of VO_X-HMS prepared by wet impregnation and direct synthesis as potential catalysts for ODH of *n*-butane and we want to contribute to understanding of relationship between vanadium structure on the HMS support and activity in ODH of *n*-butane. To analyze the effect of vanadium concentration on the type of VO_X structure, on dispersion of VO_X and their catalytic activity, the catalysts were characterized by different techniques (XRF, N_2-adsorption, XRD, DR UV–vis and H_2-TPR).

2. Experimental

2.1. Preparation of catalysts

Catalysts have been prepared in two ways (i) by impregnation and (ii) by direct synthesis. The hexagonal mesoporous silica (HMS) was used as support in both cases. The HMS was synthesized at ambient conditions according to the procedure reported by Tanev [27] by using dodecylamine (DDA, Aldrich) as a neutral structure directing agent in the mixture of ethanol and re-distilled water. After 20 min of homogenization was added tetraethylorthosilicate (TEOS, Aldrich) as a silica precursor. The reaction mixture was stirred at RT for 18 h. The solid product was filtered, washed by ethanol and calcined in air at 450 °C for 20 h (with heating rate 1 °C/min) for the template removal. The various amount (0.5–15.7 wt.% of V) of vanadium oxo-species was introduced onto the silica support by the wet impregnation from EtOH solution of vanadyl acetylacetonate for the first set of catalysts. Impregnated samples were dried at 120 °C in air overnight and then calcined at 600 °C in air for 8 h (with heating rate 5 °C/min).

The set of synthesized VO_X-HMS catalysts (1.2–14.0 wt.% of V) was prepared by direct-synthesis method which was based on work published by Reddy and Sayari [28]. The procedure was the same as in the case of the HMS synthesis when the ethanol solution with desired amount of $VO(acac)_2$ was added to the reaction mixture (DDA, H_2O and ethanol) during the synthesis. Following procedure was similar to HMS preparation. Finally, the solid was calcined in flow of air at 450 °C for 20 h (with heating rate 1 °C/min).

The investigated samples were denoted as I-VHMS-*x* and S-VHMS-*x* for impregnated and synthesized samples, respectively, where *x* is the vanadium content in weight percentage of V.

2.2. Elemental analysis

The vanadium content was determined by means of ED XRF by ElvaX (Elvatech, Ukraine) equipped with Pd anode. Samples were measured against the model samples (a mechanical mixture of pure SiO_2 and $NaVO_3$) of granulated to the same size as catalysts.

2.3. Textural properties

The N_2-adsorption isotherms were obtained at 77 K using the through-flow chromatographic method. The relative pressure of nitrogen was varied in the range of 0.01–0.30. The specific surface area (S_{BET}) was determined by the fitting of the experimental data to the BET isotherm. The surface vanadium density (VO_X surface density, VO_X nm^{-2}) was calculated according to:

$$\text{Surface density} = \frac{N_A w_V}{M_V S_{BET}} \cdot 10^{-18} \quad (1)$$

where N_A is Avogadro constant, w_V mass fraction of vanadium in V-HMS (wt.%), M_V is molecular weight of vanadium (50.94 g mol^{-1}) and S_{BET} is the specific surface area of V-HMS catalyst (m^2 g^{-1}).

The structure and crystallinity of catalysts was probed by X-ray diffraction (D8-Advance diffractometer, Bruker AXE, Germany) in the 2θ range of 2–35° with Cu Kα radiation (λ = 1.5406 Å) and scanning electron microscopy (SEM) using JSM-5500LV microscope (JEOL, Japan).

2.4. DR-UV–vis spectroscopy

UV–vis diffuse reflectance spectra were measured using the Cintra 303 spectrometer (GBC Scientific Equipment, Australia) equipped with a Spectralon™ – coated integrating sphere using a Spectralon™ discs as a standard. The spectra were recorded in

the range of the wavelength 200–850 nm. Before the spectra measurement the samples were dehydrated and oxidized in the glass apparatus under static oxygen atmosphere in two steps: 120 °C for 30 min and 450 °C for 60 min and subsequently cooled down to 250 °C and evacuated for 30 min. After the evacuation the samples were transferred into the quartz optical cuvette 5 mm thick and sealed under vacuum. For additional details you can see Ref. [22]. This procedure guaranteed complete dehydration and defined oxidation state of vanadium for all catalysts. The obtained reflectance spectra were transformed into the dependencies of Kubelka–Munk function $F(R_\infty)$ on the absorption energy $h\nu$ using the equation:

$$F(R_\infty) = \frac{(1 - R_\infty)^2}{2R_\infty} \quad (2)$$

where R_∞ is the measured diffuse reflectance from a semi-infinite layer [29].

2.5. H_2-TPR measurements

Hydrogen temperature programmed reduction (H_2-TPR) was used for study of redox behaviour and for distinguishing of individual VO_X species on the surface and the AutoChem 2920 (Micromeritics, USA) was used for the measuring. A 100 mg sample in a quartz U-tube micro reactor was oxidized in oxygen flow at 450 °C (2 h). The reduction was carried out from 30 °C to 900 °C with a temperature gradient of 10 °C/min in flow of reducing gas (5 vol.% H_2 in Ar). The changes in hydrogen concentration were monitored on TCD detector and simultaneously hydrogen consumption and water formation was detected on quadruple mass spectrometer OmniStar™ GDS 300 (Pfeiffer vacuum, Germany). The temperature programmed oxidation (TPO) experiments with the sample S-VHMS-4.9 were performed by the same apparatus. The 100 mg of sample was pre-reduced in the gas mixture (5 vol.% H_2 in Ar) as in the case of TPR. The oxidation was carried out using the gaseous mixture (2 vol.% O_2 in He) and various heating rates 8, 12 and 20 °C/min to obtain the apparent re-oxidation activation energy E_A using the Kissinger equation [30]:

$$2 \ \ln \ T_{max} - \ln \ \beta = \frac{E_A}{RT_{max}} + \text{const} \quad (3)$$

where T_{max} is the temperature of the maximum of oxidation peak determined at particular heating rate β.

2.6. Catalytic tests in ODH reaction

The *n*-butane ODH reaction was carried out in a glass plug-flow fixed-bed reactor at atmospheric pressure in the kinetic region (independently checked) and under steady state conditions of reaction. Typically 400 mg of catalyst (grains 0.25–0.50 mm) was diluted with 3 cm^3 inert SiC to avoid the catalytic bed overheating. The catalysts were pre-treated in the oxygen flow at 450 °C for 2 h before each reaction run. The input feed composition was $C_4H_{10}/O_2/He = 10/10/80$ vol.% – with a total flow rate of 100 $cm^3\ min^{-1}$. The catalytic activity was compared in the range 460–540 °C at the steady state conditions. The composition of reaction mixture analysis was made by on-line gas-chromatograph CHROM-5 (Laboratorni pristroje Praha) equipped with a thermal conductivity detector (TCD) for permanent gases and flame ionization detector (FID) for combustible products of ODH reaction. The *n*-butane and products of ODH reaction (butadiene, 1-butene, *cis*-2-butene, *trans*-2-butene, propene and propane) were separated using a packed column with n-octane on ResSil™ (Restek) at 20 °C. The packed column Porapak Q (Supelco) was used for the analysis of ethane, ethene, CO_2 and acetaldehyde. The molecular sieve 13X (Supelco) was used for the separation of permanent gases.

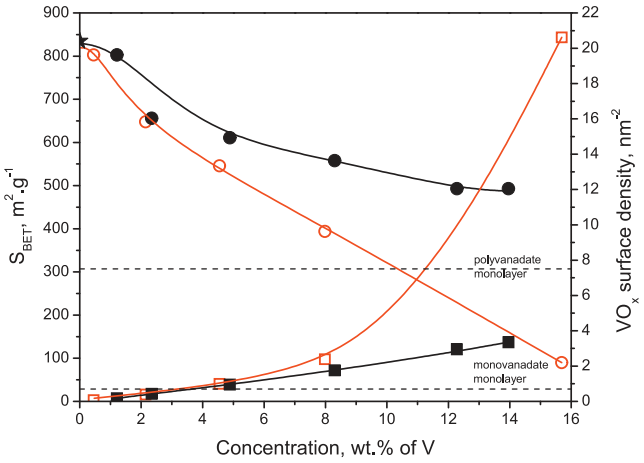

Fig. 1. Dependence of specific surface area (ring) and VO_X surface density on vanadium concentration (square) for synthesized (full symbol) and impregnated (empty symbol) V-HMS samples.

The conversion was calculated using following equation:

$$X_i = \frac{n_{i0} - n_i}{n_{i0}} \cdot 100 \quad (4)$$

where n_{i0} is amount of key component in the input feed and n_i is the amount of key component in the output from reactor.

The selectivity to products was calculated as:

$$S_j = \frac{\nu_j \cdot n_j}{\nu_i \cdot (n_{i0} - n_i)} \cdot 100 \quad (5)$$

where ν_i, ν_j is number of carbon atoms of starting compound resp. products, n_{i0} is molecular amount of key component in the input feed, n_i is the molecular amount of key component in the output and n_j is the molecular amount of product in the output from reactor.

Yield was calculated according to Sachtler [31]. The productivity and turn-over-frequency (TOF) values per V atom was calculated based on mass balance of the carbon. The TOF values were calculated as:

$$\text{TOF} = \frac{n^0_{n\text{-}C_4} X_{n\text{-}C_4} M_V}{m_{cat} w_V} \quad (6)$$

where $n^0_{n\text{-}C4}$ is mol. flow *n*-butane (mol s^{-1}), $X_{n\text{-}C4}$ conversion of *n*-butane (%), M_V is molar weight of vanadium (50.94 g mol^{-1}), m_{cat} is weight of catalyst (g), w_V is mass fraction of vanadium in catalysts.

3. Results and discussion

3.1. Characterization of catalysts

3.1.1. Textural properties

The HMS materials provide the isotherm of type IV with hysteresis loop of type H4 which is typical for combination micro- and mesoporous system of channels [20]. The average pore diameter of pure HMS support was 4.2 nm with the mesopore volume 0.68 $cm^3\ g^{-1}$ and specific surface BET 835 $m^2\ g^{-1}$. Both sets of the catalysts exhibit significant decrease of the S_{BET} value with increasing vanadium loading especially in the case of samples prepared by the impregnation method where the sample containing 15.7 wt.% of vanadium had a S_{BET} value *ca.* only 90 $m^2\ g^{-1}$. The decrease of surface for the synthesized samples was only in the range from 800 to 490 $m^2\ g^{-1}$. The dependence of surface decrease on concentration is shown in Fig. 1. This behaviour can be attributed to partial destruction of the framework [21,22] or deposition of vanadium oxo-species into mesopores which partially blocks these

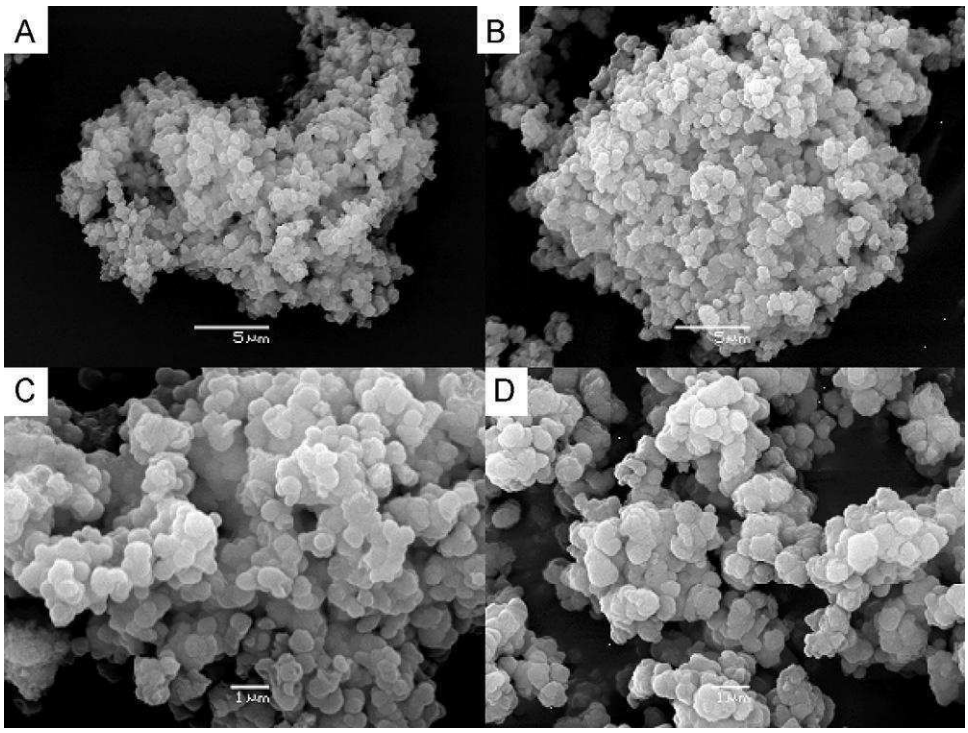

Fig. 2. SEM images of V-HMS catalysts prepared by wet impregnation (sample I-VHMS-4.6, pictures A and C) and direct synthesis (S-VHMS-4.9 sample, pictures B and D).

pores [14,22]. On the other hand decrease in surface areas can indicate that the VO_X species are located inside the channel system on the inner walls of mesoporous matrix.

The abundance of various vanadium oxide species on the surface of silica based supports was previously related to the surface concentration of VO_X species whose values are summarized in Table 1. The value of 0.7 VO_X per nm^2 [32,33] is assumed to be a limiting value for the preferential formation of isolated monomeric units. The formation of various oligomeric and polymeric species is expected after reaching this value.

This value of the surface density was reached for samples containing more than 4 wt.% of vanadium for both sets of investigated catalysts (see Fig. 1). The 3D bulk oxide species were formed after reaching the surface VO_X density higher than 10 VO_X [8] or 7–8 VO_X units per nm^2 [32]. Hence it can be seen that only impregnated samples with highest concentration of vanadium contain higher detectable concentration of these species. These results correspond well with the information obtained from DR UV–vis spectroscopy.

The representative SEM images of impregnated (I-VHMS-4.6, Fig. 2)A and C and synthesized V-HMS samples (S-VHMS-4.9, Fig. 2B and D) are presented in Fig. 2. Both types of materials exhibit similar morphology of particles. The size of the particles was analyzed using Gwyddion software based on derivation of gray-scale signal for determination of grains boundary and consecutively diameter of circle with similar area. Any significant difference in particle size distribution was not observed in individual samples. Size of particles exhibited Gaussian distribution from 0.2 to 0.8 μm. These primary particles form large aggregates with dimensions about 20–150 μm. Typical orthorhombic V_2O_5 needles were not observed in any sample. No V_2O_5 clusters were detected in SEM-EDX mapping of V content and the concentration of vanadium was spread homogeneously in all parts of catalyst grains except I-VHMS-15.7.

3.1.2. XRD analysis

Fig. 3 shows the small-angle XRD patterns, in the 2θ range of 2–35°, for pure HMS and V-HMS. The region of 2θ value higher than 35° contain no signal hence it is not showed here. Each sample exhibits one low-angle diffraction peak with line at 2–3° attributable to a d_{100} diffraction (spacing about 4.4 nm) and the very broad peak with low intensity among 15–35°. In addition, a weak broad shoulder around the 6° can be seen at synthesized samples with high concentration of vanadium and we can attribute it to d_{210} diffraction. The peaks d_{100} and d_{210} are characteristics for the SiO_2 hexagonal ordered structure and the broad low-intensity peak in range 15–35° pertains to small amount of amorphous SiO_2 which is not organized to the HMS structure [21,34]. With rise in VO_X loading the d_{100} peak weakens in intensity and gradually disappears which is results of the partial blocking of mesopores by VO_X and the decline in long-range order of hexagonal ordered structure [14]. All the synthesized V-HMS catalysts do not contain crystallites V_2O_5 in whole range of concentrations. The impregnated V-HMS cata-

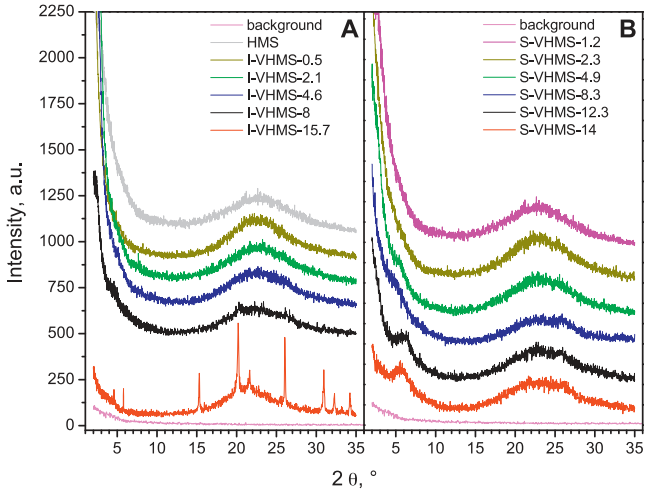

Fig. 3. X-ray diffraction patterns for V-HMS catalysts prepared by wet impregnation (A) and by direct synthesis (B).

Table 1
Chemical composition, results of physico-chemical characterization for both sets of investigated catalyst samples.

Sample name	c_V [a] (wt.%)	S_{BET} [b] ($m^2\ g^{-1}$)	VO_X [c] (nm^{-2})	ε_0 [d] (eV)	X_{mono} [e]	T_{max} [f] (°C)	Δe [g]
S-VHMS-1.2	1.2	803	0.18	3.75	0.88	557	1.70
S-VHMS-2.3	2.3	636	0.43	3.74	0.87	575	1.76
S-VHMS-4.9	4.9	611	0.95	3.70	0.81	578	1.90
S-VHMS-8.3	8.3	558	1.76	3.57	0.62	592	1.74
S-VHMS-12.3	12.3	493	2.95	3.42	0.41	594	1.74
S-VHMS-14	14	493	3.35	3.38	0.37	591	1.68
I-VHMS-0.5	0.5	803	0.07	3.78	0.97	573	1.98
I-VHMS-2.1	2.1	648	0.39	3.73	0.85	563	2.14
I-VHMS-4.6	4.6	546	0.99	3.68	0.78	565	1.83
I-VHMS-8	8	394	2.39	3.50	0.52	577 (673)	1.97
I-VHMS-15.7	15.7	90	20.62	2.45	Not determined	595 (639)	1.87

[a] Vanadium content determined by XRF method.
[b] Specific surface area calculated following BET method.
[c] VO_X surface density ($VO_X\ nm^{-2}$).
[d] Energy of absorption edge determined by Tauc [40].
[e] Relative amount of monomeric species determined from $\varepsilon_0 = 3.148 + 0.681X$.
[f] Position of first (second) maxima of H_2-TPR profile.
[g] Average change of oxidation state during H_2-TPR.

lysts up to loading of 8 wt.% of vanadium do not contain crystallites V_2O_5 as well but over this concentration reflections of bulk-like oxide VO_X species can be observed. It is represented by three main reflections at 15.4°, 20.2° and 26.1° in the XRD pattern (see Fig. 3) [14,20]. This observation is similar to results published by Karakoulia et al. [21] on V-HMS and V-MCM-41 who reported no presence bulk V_2O_5 up to 8 wt.% or on the V-SBA-15 materials studied by Liu [14]. Liu obtained the XRD signals of bulk oxides only when the concentration of vanadium was over 13.4 wt.% of vanadium. It can be said in conclusion that the presence or absence of V_2O_5 crystallites in the silica based VO_X catalysts depends on the preparation method of samples. These results are in a good agreement with the results from DR UV–vis spectroscopy as it will be discussed in next paragraph.

3.1.3. DR-UV–vis spectroscopy

Diffuse reflectance UV–vis spectroscopy provides information about the nature and oxidation state of vanadium. The spectra for both prepared sets of catalyst are presented in Fig. 4. The obtained spectra are similar to spectra published previously [20,22,26,35,36] for this catalytic system and contain several absorption bands at region 190-850 nm (6.5–1.46 eV) which are conventionally attributed to metal charge-transfer transitions of the $O \rightarrow V^{+V}$ type and d-d transitions of V^{+IV} [36].

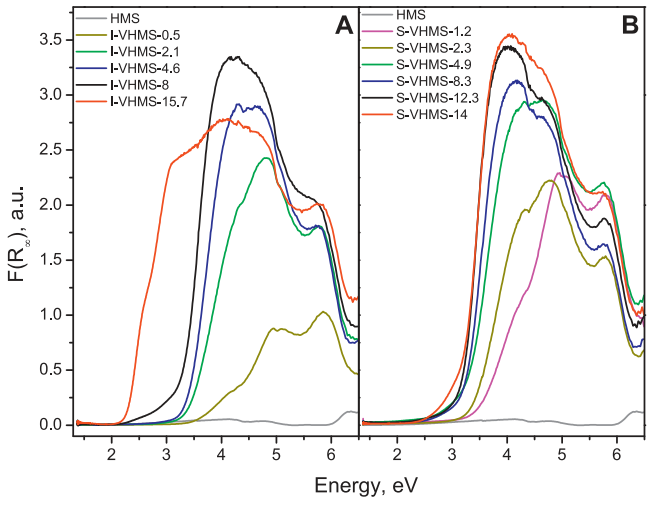

Fig. 4. Diffuse reflectance UV–vis spectra of dehydrated V-HMS samples prepared by wet impregnation (A) and direct synthesis (B). DR-UV–vis spectrum of pure HMS is displayed in both plots for comparison.

The d–d absorption bands characteristic for the V^{+IV} in the region 1.55 – 2.07 eV [35] were not observed in any spectra. The broad obtained spectrum is superposition of several individual bands with poorly defined maxima. The region 4–6 eV is usually attributed to presence of isolated monomeric tetrahedrally (T_d) coordinated VO_X species (type I denoted in introduction) [22,26,37]. The second region 3–4 eV is attributed to presence of oligomeric distorted tetrahedral VO_X units (type II) [20,22]. The impregnated catalysts with vanadium loading over 8 wt.% exhibit band bellow 3 eV and it is attributed to 3D-octahedrally coordinated VO_X species (type III) [22,26]. The exact quantitative analysis or at least relative abundance of individual species is not possible to obtain due to broad and overlapping absorption bands and due to strongly nonlinear dependence of Kubelka-Munk function on the concentration of vanadium.

The method which can partially bypass this problem was developed for speciation of molybdenum oxide [38] and subsequently applied for vanadium oxide species on surface [23]. This method is based on the evaluation of absorption energy edge (ε_0) from UV–vis spectra using the expression introduced by Davis and Mott [39] or by Tauc [40] in the form:

$$(F(R_\infty) \cdot h\nu)^2 \propto (h\nu - \varepsilon_0) \quad (7)$$

Based on the empirical linear correlation of the referent compounds structure and the value of absorption energy edge Gao [23] suggested the possibility to obtain mean value of covalent V–O–V bonds (CVB) in the coordination sphere of central $V^{(+V)}$ cation and estimate degree of the polymerization of VO_X species.

Tian et al. [41] demonstrated that mechanic mixtures of sodium ortho-vanadate Na_3VO_4 (3.83 eV, model compound for isolated monomeric T_d units) and sodium meta-vanadate $NaVO_3$ (3.16 eV, standard for linearly polymerized T_d oligomeric units) exhibited linear dependence of the ε_0 value on the concentration of referent compounds and suggested this method for the determination of the relative amount of VO_X monomeric units denoted as X_m value. The values of ε_0 and the X_m of our samples are in Table 1. Disadvantage of this method is the fact that it cannot be used for materials which include higher content of the octahedrally coordinated VO_X bulk-like oxide species (for us the sample I-VHMS-15.7).

The samples with the vanadium concentration less than approximately 4-5 wt.% exhibit nearly the same linearly decreasing trend of the ε_0 value on the VO_X concentration and it depends less on the method of their preparation. When the vanadium loading reaches the value *ca.* 5 wt.% the samples prepared by the impregnation

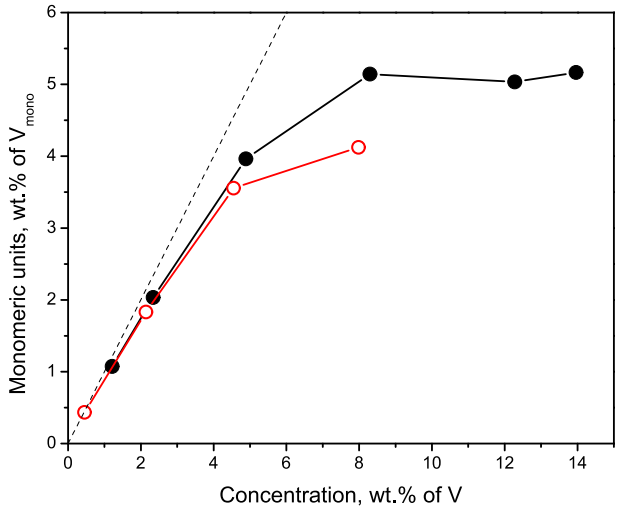

Fig. 5. The amount of monomeric species determined by Tian et al. [41] in dependence on vanadium loading for impregnated samples (open red points and red line) and for samples prepared by direct synthesis (full black points and black line). (For interpretation of the references to color in this figure legend, the reader is referred to the web version of the article.)

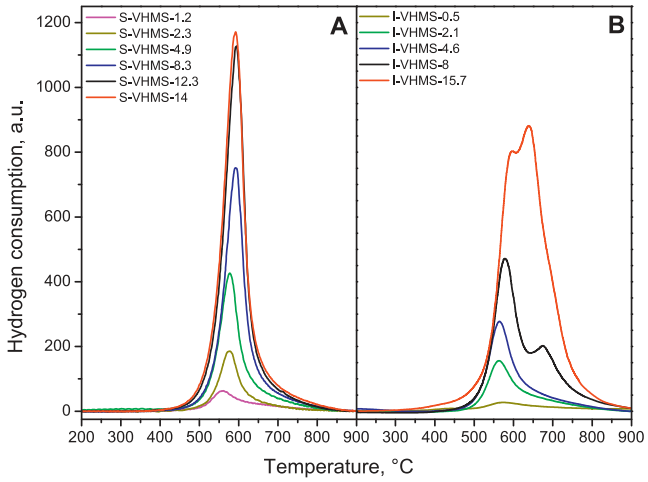

Fig. 6. H_2-TPR patterns of V-HMS samples prepared by impregnation method (A) and by direct synthesis (B).

method exhibit more rapid decrease of the ε_0 value compared to samples prepared by the direct synthesis. This effect indicates more oligomeric units formation or a wider degree of theirs oligomerization compared to samples prepared by the direct synthesis. The values presented in Table 1 indicate that samples with low VO_X concentration contain at first mostly the isolated monomeric T_d units but the relative abundance of these species decreases with the increasing of total vanadium loading. This effect can be clearly seen from Fig. 5 where is displayed the dependence of calculated amount of monomeric species on total vanadium concentration. The amount of monomeric units increases linearly and these species represent significant part of the VO_X species generated on the HMS surface but after reaching *ca.* 4–5 wt.% of vanadium there is reached their maximal concentration and the amount of these units starts to decrease. It is more important that both sets of catalysts exhibit similar maximal concentration of monomeric units and this concentration is reached at the relatively comparable level of vanadium loading.

3.1.4. H_2–TPR and TPO measurements

H_2-TPR curves were measured to determine the scale of dispersion and type of the present active species. The obtained TPR profiles are presented in Fig. 6 and results of their analysis are summarized in Table 1. From the table is visible that samples prepared by the direct synthesis exhibit only one symmetric reduction peak at the temperature about 560–590 °C whereas the samples prepared by the wet impregnation exhibit moreover the shoulder or second reduction peak at the temperature about 640-680 °C. The progressive shift of the major H_2 consumption temperature peak to higher values with increasing amount of vanadium are explained by two ways (i) either this shift can be ascribed to the kinetic or the thermodynamics of the process of VO_X reduction and it is related to the changes in H_2 to surface vanadium ratio or to ratio of (generated H_2O)/H_2 during the reduction process with the increasing of vanadium loading [30,42,43] or (ii) due to the gradual formation of polymeric vanadium species [14].

The low temperature peak can be attributed on the basis of our UV–vis spectra and according to literature either to reduction of the solely monomeric highly dispersed VO_X units (type I) [20] or rather to reduction of T_d both the monomeric and the oligomeric $(VO_4^{3-})_n$ species (type II) [44]. The second interpretation is in the good agreement with the results obtained from our DR UV–vis spectroscopy measurement. The high temperature peak most likely belongs to the reduction of O_h coordinated 2D oligomers and bulk-like 3D V_2O_5 crystallites [14,44]. The presence of V_2O_5 crystallites was clearly proven by XRD results mentioned above.

The overall hydrogen consumption was proportional to the concentration of vanadium and linearly increases with the vanadium loading and corresponds to change of oxidation state of vanadium from the V^V to V^{III}. The changes of oxidation state of vanadium cation are summarized in Table 1. The average $\Delta e/V = 1.95 \pm 0.1$ for impregnated samples corresponds to change of oxidation state of vanadium from the V^V to V^{III}. The samples prepared by the direct synthesis exhibit lower $\Delta e/V$ value 1.75 ± 0.1 and this effect can be ascribed to non-complete extraction of vanadium oxide species from the HMS lattice during the sample pretreatment.

The temperature programmed oxidation experiments were carried out using the sample S-VHMS-4.9 and obtained TPO curves consist of one oxidation peak (not shown here for sake of brevity). The variation of the heating rate β (8, 12 and 20 °C/min) in the TPO causes the changes in position of maximum of this peak to the temperatures 338, 356 and 395 °C. The apparent activation energy of the catalyst reoxidation equal to 44 ± 7 kJ mol^{-1} was calculated using the Kissinger Eq. (3).

3.2. Catalytic tests of n-butane ODH

Both synthesized and impregnated VO_X-HMS catalysts were active and selective in the ODH of *n*-butane with oxygen over the V-HMS catalysts. The reaction products identified in the reaction mixture were: methane (C_1), ethane and ethene (C_2), propane and propene (C_3), 1–butene (1-C_4), *cis*- and *trans*-2-butene (*c*-C_4 and *t*-C_4), 1,3-butadiene (1,3-C_4), carbon oxides (CO and CO_2) and traces of acetaldehyde. The carbon balance was 98 ± 3% in all the catalytic tests and no maleic-anhydride, other oxygenates or products of significant catalyst coking were not found. The activity of catalysts was stable at least for 10 hours time–on–stream (TOS) and no loss of catalyst activity during the time reported elsewhere [45] was observed. The activity of pure HMS was measured under the same conditions to check reactivity of clear support. It was not observed any activity up to 520 °C. The conversion of *n*-butane only about 3% was detected at 540 °C (for more details see Table 2). This conversion is remarkably lower in comparison to the conversions reached over all tested catalysts. Nevertheless presence of reactions in homogenous phase was proved after initialization by

Table 2
Results of catalytic tests for both sets of catalyst and pure HMS support at 540 °C (m_{cat} = 400 mg, $C_4H_{10}/O_2/He$ = 10/10/80 vol.%, total flow rate of 100 cm^3 min^{-1}).

Catalyst sample name	Conv. (%)	Selectivity (%)								1-Butene[c]	Yield,(%)	Productivity[d]	TOF (h^{-1})	Ea (kJ mol^{-1})
	C_4H_{10}	1-C_4	c-C_4	t-C_4	1,3-C_4	C_1-C_3 [a]	CO	CO_2	Dehy.[b]	i-Dehy.[b]	2-Butenes	Dehy.[b]	Dehy.[b]		
HMS	3	10	6	2	18	25	22	17	36	37	1.3	1.1	0.04		
S-VHMS-1.2	16	22	9	5	27	11	13	12	63	66	1.6	6.5	0.24	28.9	119
S-VHMS-2.3	29	15	8	4	26	5	17	26	53	63	1.2	10.0	0.38	27.4	91
S-VHMS-4.9	36	14	8	7	21	6	24	20	50	53	1.0	19.7	0.74	27.4	81
S-VHMS-8.3	29	9	5	4	15	3	28	36	33	22	1.0	9.7	0.36	11.9	62
S-VHMS-12.3	27	7	4	2	12	4	34	37	25	21	1.1	6.7	0.25	7.5	39
S-VHMS-14	30	6	4	2	11	6	38	34	22	10	1.0	6.7	0.25	7.4	23
I-VHMS-0.5	6	14	7	4	20	19	20	15	45	40	1.4	1.8	0.07	29.8	116
I-VHMS-2.1	18	10	5	5	16	13	31	20	40	45	1.1	7.1	0.27	28.2	79
I-VHMS-4.6	36	12	6	5	18	9	31	18	42	45	1.0	15.0	0.56	26.9	50
I-VHMS-8	28	7	4	3	13	5	42	25	27	15	1.0	7.6	0.29	11.9	37
I-VHMS-15.7	22	2	1	0	4	2	58	32	8	2	1.0	1.8	0.07	4.8	45

[a] C_1–C_3 is the sum of C_1–C_3 hydrocarbons and acetaldehyde.
[b] Dehy. is the sum of C_4 alkenes, i-Dehy. is the sum of C_4 alkanes at X = 7.5%.
[c] Ratio of 1-butene to (*cis*-2-butene + *trans*-2-butene).
[d] Productivity = g_{prod} g_{cat}^{-1} h^{-1}.

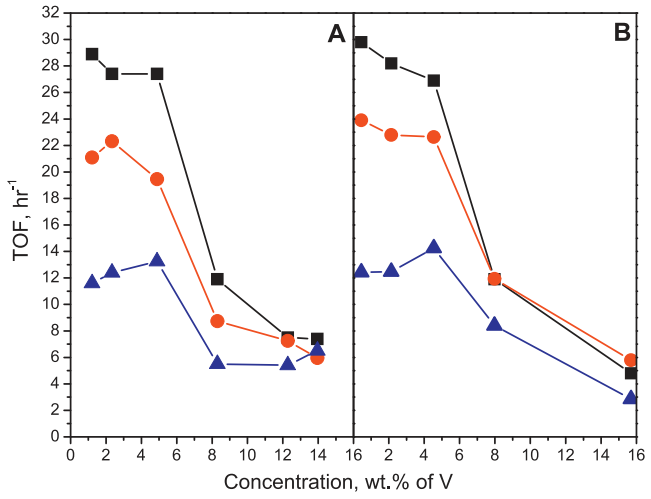

Fig. 7. The activity of synthesized (A) and impregnated (B) V-HMS catalyst in ODH of *n*-butane expressed by TOF factor at 460 °C (blue triangle and line), 500 °C (red circle and line) and 540 °C (black square and line). (For interpretation of the references to color in this figure legend, the reader is referred to the web version of the article.)

matrix which is in the compliance with previously results published [46].

3.2.1. Catalysts activity in C_4-ODH reaction

The value of turn-over-frequencies (TOF) exhibits similar dependence on the concentration of vanadium for both sets of catalysts as shown in Fig. 7. The all low concentrated samples exhibit approximately constant value of TOF factor (28 h^{-1} for 540 °C) until the vanadium concentration *ca.* 4.5 wt.% is reached followed by a rapid change of TOF to low value (5–7 h^{-1} for 540 °C). The very similar dependences of TOF *vs.* V loading were obtained for the all experiments carried out over both sets of catalysts in the temperature range 460–540 °C (see Fig. 7) regardless that at the highest temperature (540 °C) the conversion of oxygen was almost 100% for samples with the high concentration of vanadium.

The vanadium concentration when the TOF starts to decrease corresponds well with the maximal concentration of monomeric VO_X units as it is shown in Fig. 5 or reaching the level 0.7 VO_X per nm^2 for vanadium surface density previously reported [32] as limiting for obtaining the monolayer of monomeric units. Decrease of TOF value clearly evidences that with subsequent increase of vanadium content the significantly less active or non active species in ODH of *n*–butane are generated and that is why the monomeric VO_X units should be taken as the most active species in the ODH of *n*-butane.

3.2.2. Selectivity to all C_4-ODH products

The selectivity to products of C_4-ODH remained relatively constant in whole temperature range as it can be seen from Fig. 8. This character of selectivity *vs.* temperature dependence offers the possibility to compare values of selectivity at the iso-conversion conditions obtained at different temperatures of reaction, however this method is not as rigorous as comparison of iso-conversion data obtained by variation of amount of catalyst used in reaction. The values of selectivity to C_4-olefins obtained for the conversion 7.5% are summarized in Table 2. Similarity of these values with the C_4-ODH selectivity values obtained at 540 °C confirms our assumption of low dependence C_4-ODH selectivity on temperature for our materials under the given reaction conditions. Hence the both sets values can be used for the comparison of selectivity to the C_4-olefins on studied materials.

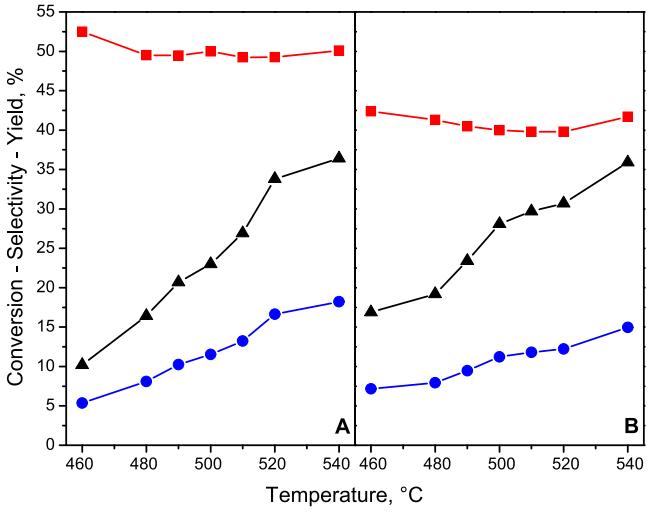

Fig. 8. The conversion (black triangle and line), selectivity (red square and line) and yield (blue circle and line) for representative sample prepared by direct synthesis (S-VHMS-4.9, A) and by wet impregnation method (I-VHMS-4.6, B). (For interpretation of the references to color in this figure legend, the reader is referred to the web version of the article.)

It can be seen the drop of C_4-olefins selectivity decreases with increasing of the vanadium content from 63% for the sample S-VHMS-1.2 to nearly non-selective catalyst I-VHMS-15.7 with selectivity only about 10% (Table 2). The yield or productivity of C4-ODH products increases with the amount of vanadium until the concentration 4–5 wt.% is reached then these values start to decrease. The maximal yield or productivity obtained was *ca.* 20% or 0.74 g C_4-olefins per gram of catalyst for one hour respectively (S-VHMS-4.9). Similar behaviour was previously published for oxidation of toluene over V-HMS prepared by similar procedure and authors explain this behaviour on the base of different amount of suitable and accessible VO_X species but they didn't propose more detailed specification of these species [47].

This behaviour is probably due to increasing of abundance of oligomeric species with T_d and mainly O_h coordination because these species contain the V–O–V bridging oxygen atoms. According to mechanism introduced by Kung [6] the presence of this type of oxygen allows the formation of alkoxide intermediate which is furthermore oxidized to the products of total oxidation (CO and CO_2).

Although both sets of catalyst exhibit similar trends of conversion on the vanadium loading the selectivity to C_4–olefins is about 10% higher for the synthesized samples than for samples prepared by impregnation method in the whole range of prepared concentrations even for samples with same value of VO_X surface density. Such difference of selectivity to C_4-ODH products can be ascribed to the VO_X species with higher level of polymerization whose are preferentially formed in the samples prepared by the wet impregnation method. These species facilitate consecutive reactions and formation of CO_X. These species cannot be detected on the basis of analysis of VO_X surface density value nor by the analysis of the DR UV–vis spectra with the sufficient accuracy. We can presume on presence of these species on the basis of TPR analysis as it was mentioned above.

3.2.2.1. Selectivity to 1,3-butadiene. When we make analysis of selectivity of individual products of C_4-olefins in detail it can be found out that approximately 40-50% belongs to 1,3-butadiene. The butadiene represents relatively high portion of C_4-ODH products in the whole range of vanadium concentration, temperature and conversion of *n*-butane and oxygen. Similar distribution of C_4-olefins was published on V-Mg-O materials by Chaar [13] and high selectivity to butadiene was ascribed to basic character of catalysts compared to silica [11,13] as well as to presence of $Mg_3(VO_4)_2$ with isolated tetrahedral species which prohibits deep oxidation [1].

However our observation is in contrast to results published previously on SiO_2 based catalysts. Owens [16] investigated vanadium anchored on amorphous silica and he described only small selectivity to butadiene. More similar results published Liu et al. [14] who studied V-SBA-15 material which exhibited selectivity about 30% (from C_4-olefins only) to butadiene.

The selectivity to dehydrogenation products as well as distribution of C_4-olefins can be related to the acid-base character of the catalysts as it was reported by Blasco et al. [12] on the base FTIR of adsorbed pyridine or Liu et al. [14] on the basis of NH_3-TPD and widely discussed in many other works [1,6,7,10,48]. In our case acid–base character of HMS support (IEP *ca.* 2) extend retention period of reaction intermediates because the olefins (electron-donating molecules with high electron densities at π bonds) are stronger adsorbed on the surface of catalysts then paraffins [1,9,12]. This confirm values of adsorption heats on silanol groups (determined by FTIR spectroscopy) 27 kJ mol^{-1} [49] for *n*-butane and 30–36 kJ mol^{-1} [49,50] for butenes, respectively. The acidity further increases with rising amount of vanadium and it implicates that vanadium species act as an acidic site on silica and that is why we need good distribution of monomeric VO_X species [51].

It seems that more basic character of MgO support predestine this support as the best support for the alkane ODH catalyst but the situation is probably more complicated because according to Albonetti et al. [10] the V/Al/O catalyst exhibit better performance for the ethane ODH than V–Mg–O catalyst. The other effects can control selectivity of ODH reaction and can prevail the influence of acid-base characteristics of support.

On the basis of this fact we can suppose that butadiene originate by direct two-step ODH reaction of the adsorbed hydrocarbon complex over one or more active centers without desorption intermediate to the gas phase. Similar mechanism was recently proposed by Marcu et al. [52] on the basis of TAP measurements over the tetravalent pyrophosphate catalysts. Moreover the large surface area of catalysts facilitates good dispersion and isolation of VO_X species. This has resulted in limiting of deep oxidation of forming intermediates to CO_X.

3.2.2.2. Selectivity to 1-butene and 2-butenes. The ratio of the selectivity of 1-butene to sum of *cis*-/*trans*-2-butene is 1.5 for samples with lowest concentration of vanadium. When we assume that the first hydrogen abstraction occur on the secondary carbon atom this value corresponds to statistical distribution of products (1-butene: *cis*-2-butene: *trans*-2-butene) 3:1:1 which can be formed by the abstraction of second hydrogen from adjacent methyl and methylene groups. Based on this assumption Chaar et al. [13] attributes this behaviour to fast radical dehydrogenation of adsorbed alkyl intermediate. Similar effect was also observed on other catalytic systems [7,11,45].

This statistical distribution ratio shifts to worth one at highest concentration for both types of samples. This shift is due to unequal participation of 1-butene in consecutive reactions and similar effect was described by Lemonidou [45]. Blasco and Nieto [7] put this shift of distribution of products to the context with acid character of catalysts which probably influences the rate of the consecutive reactions. It is known that 1-butene can isomerize to 2-butene if acid site are present on the catalyst surface [7]. With increasing VO_X loading (IEP of $V_2O_5 < SiO_2$) increases the acidity of material and that is why the distribution of products shift from statistical distribution of products to thermodynamic equilibrium. We can finally say that distribution of products is predominantly controlled by kinetic effects and not by thermodynamics of process because

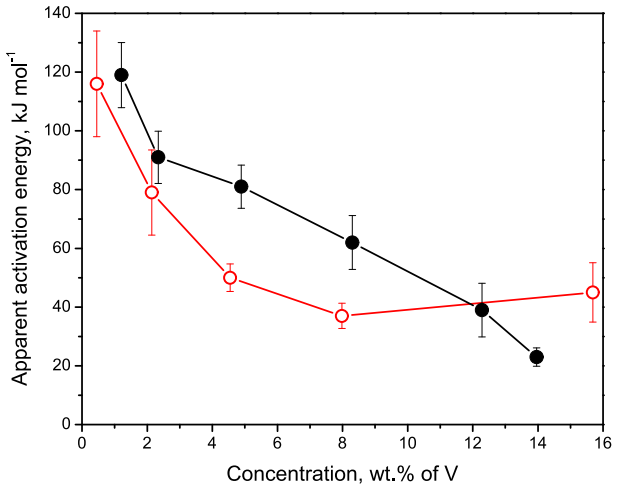

Fig. 9. The apparent activation energy in dependence on the vanadium loading for impregnated (open red points and red line) and for samples prepared by direct synthesis (full black points and black line). (For interpretation of the references to color in this figure legend, the reader is referred to the web version of the article.)

the thermodynamic control should give the product distribution (1:1:1.1) [7] and no remarkable isomerization of butenes occurs on the surface of catalysts.

3.2.3. *Apparent activation energy*

The activation energies corresponding to the transformation of *n*-butane were determined in the temperature range from 460 to 540 °C using conversion data presented in Table 2 according to Arrhenius relationship. The apparent activation energy (E_A) in dependence on the vanadium content is presented in Fig. 9. The value of apparent E_A is about 120 ± 15 kJ mol^{-1} for samples with low concentration of vanadium on the surface and it decreases to $E_A = 40 \pm 8$ kJ mol^{-1} for higher concentration. It is evident that the change of rate-limiting step in mechanism of ODH *n*-butane occurs as the vanadium loading increases. The rate-limiting step for low concentration samples is supposed to be the activation of hydrocarbon on the surface by abstraction of hydrogen from secondary carbon [5]. The value 120 kJ mol^{-1} is similar to apparent E_A for ODH of *n*-butane on VO_X–silica (110 kJ mol^{-1} [16]) or on VMgO catalysts (105 kJ mol^{-1} [45]). Because these materials have different textural properties, it can be expected that the apparent activation energy values are most likely affected only by the kinetic of ODH process for our materials as well. Therefore it can be neglected the influence of other processes *i.e.* diffusion to this value.

The value $E_A = 40 \pm 8$ kJ mol^{-1} for high concentrated samples is close to E_A of reoxidation obtained from the TPO experiments as it was mentioned above. It can be assumed that the reoxidation of active centre is rate-limiting step for samples of high vanadium concentration most likely affected by migration of oxygen atoms through the lattice of VO_X crystallites. We can find vanadium oxo-species with high degree of polymerization over these materials. These centers prefer the total oxidation reactions of *n*-butane to CO_X and thus the oxygen consumption is high for their reoxidation. This effect is very remarkable especially for samples which contain O_h coordinated vanadium species and that is why the decrease of apparent E_A is steeper for impregnated samples compared to slower decrease of E_A values for samples prepared by direct synthesis.

4. Conclusions

On the basis of this results reported in this paper the following conclusion can be made:

- The isolated monomeric VO_X species play the role of the most active catalytic centre in the ODH of *n*-butane. The catalytic behaviour of these units is similar for both sets of catalysts regardless of the method of their preparation.
- The amount of isolated monomeric species is comparable for both sets of materials up to total concentration 4–5 wt.% of vanadium but the highest achievable amount of monomeric species was slightly higher for catalysts prepared by direct synthesis.
- The VO_X species with higher degree of polymerization participate in undesired consecutive reactions with ODH products. The direct synthesis method leads to lower extent of formation of these species compared to wet impregnation.
- The method of preparation influences the formation of oligomeric species. The impregnated samples contain higher amount of octahedrally coordinated species compared to samples prepared by direct synthesis.
- The most abundant selective product was 1,3-butadiene with selectivity up to 30%. The total sum of selectivity to all C_4-olefins reached up to 65% over the catalysts prepared by direct synthesis. The samples prepared by wet impregnation exhibit 10% lower selectivity to C_4-olefins compared to catalysts prepared by direct synthesis in the whole range of vanadium concentrations. The selectivity decrease with increasing vanadium content.

Acknowledgements

A financial support of the Grant Agency of the Czech Republic under the project no. P106/10/0196 and P104/07/0214 and Ministry of Education of Czech Republic under project no. MSM 0021627501 is highly acknowledged.

References

[1] L.M. Madeira, M.F. Portela, Catal. Rev. Sci. Eng. 44 (2002) 247–286.
[2] S.-K. Lin, Butane, Wiley-VCH, 1999.
[3] E. Sporcic, K. Ring, Butylenes Sri Consulting, 2005.
[4] U.S. DHHS, 1,3-Butadiene, U.S. Department of Health and Human Services, 2005.
[5] G. Centi, F. Cavani, F. Trifiró, Selective Oxidation by Heterogeneous Catalysis, Kluwer Academic Publisher Plenum Press, Dordrecht New York, 2001.
[6] H.H. Kung, Advances in Catalysis, 40, Academic Press Inc, San Diego, 1994, pp. 1–38.
[7] T. Blasco, J.M.L. Nieto, Appl. Catal. A 157 (1997) 117–142.
[8] E.A. Mamedov, V.C. Corberan, Appl. Catal. A 127 (1995) 1–40.
[9] A. Corma, J.M.L. Nieto, N. Parades, A. Dejoz, I. Vazquez, in: V.C. Corberán, S.V. Bellón (Eds.), Studies in Surface Science and Catalysis, Elsevier, 1994, pp. 113–123.
[10] S. Albonetti, F. Cavani, F. Trifiro, Catal. Rev. -Sci. Eng. 38 (1996) 413–438.
[11] J.M.L. Nieto, P. Concepcion, A. Dejoz, H. Knozinger, F. Melo, M.I. Vazquez, J. Catal. 189 (2000) 147–157.
[12] T. Blasco, J.M.L. Nieto, A. Dejoz, M.I. Vazquez, J. Catal. 157 (1995) 271–282.
[13] M.A. Chaar, D. Patel, M.C. Kung, H.H. Kung, J. Catal. 105 (1987) 483–498.
[14] W. Liu, S.Y. Lai, H.X. Dai, S.J. Wang, H.Z. Sun, C.T. Au, Catal. Lett. 113 (2007) 147–154.
[15] E. Santacesaria, M. Cozzolino, M. Di Serio, A.M. Venezia, R. Tesser, Appl. Catal. A 270 (2004) 177–192.
[16] L. Owens, H.H. Kung, J. Catal. 144 (1993) 202–213.
[17] K. Cassiers, T. Linssen, M. Mathieu, M. Benjelloun, K. Schrijnemakers, P. Van Der Voort, P. Cool, E.F. Vansant, Chem. Mater. 14 (2002) 2317–2324.
[18] M. Kruk, M. Jaroniec, A. Sayari, Micropor. Mater. 9 (1997) 173–182.
[19] B.M. Weckhuysen, D.E. Keller, Catal. Today 78 (2003) 25–46.
[20] P. Knotek, L. Capek, R. Bulanek, J. Adam, Top. Catal. 45 (2007) 51–55.
[21] S.A. Karakoulia, K.S. Triantafyllidis, A.A. Lemonidou, Micropor. Mesopor. Mater. 110 (2008) 157–166.
[22] L. Capek, J. Adam, T. Grygar, R. Bulanek, L. Vradman, G. Kosova-Kucerova, P. Cicmanec, P. Knotek, Appl. Catal. A 342 (2008) 99–106.
[23] X.T. Gao, I.E. Wachs, J. Phys. Chem. B 104 (2000) 1261–1268.
[24] A.A. Teixeira-Neto, L. Marchese, H.O. Pastore, Quim. Nova 32 (2009) 463–468.
[25] A.A. Teixeira-Neto, L. Marchese, G. Landi, L. Lisi, H.O. Pastore, Catal. Today 133 (2008) 1–6.
[26] B. Solsona, T. Blasco, J.M.L. Nieto, M.L. Pena, F. Rey, A. Vidal-Moya, J. Catal. 203 (2001) 443–452.
[27] P.T. Tanev, T.J. Pinnavaia, Science 267 (1995) 865–867.
[28] J.S. Reddy, A. Sayari, J. Chem. Soc. -Chem. Commun. (1995) 2231–2232.
[29] P. Kubelka, F.Z. Munk, Tech. Phys. 12 (1931) 593.
[30] H.E. Kissinger, Anal. Chem. 29 (1957) 1702–1706.

[31] W.M.H. Sachtler, N.H.D. Boer, Catalytic Oxidation of Propylene to Acrolein, North-Holland Publishing Company, Amsterdam, 1964, p. 8.
[32] I.E. Wachs, B.M. Weckhuysen, Appl. Catal. A 157 (1997) 67–90.
[33] G. Centi, Appl. Catal. A 147 (1996) 267–298.
[34] C. Chen, Q.H. Zhang, J. Gao, W. Zhang, J. Xu, J. Nanosci. Nanotechnol. 9 (2009) 1589–1592.
[35] M. Mathieu, P. Van Der Voort, B.M. Weckhuysen, R.R. Rao, G. Catana, R.A. Schoonheydt, E.F. Vansant, J. Phys. Chem. B 105 (2001) 3393–3399.
[36] D.E. Keller, T. Visser, F. Soulimani, D.C. Koningsberger, B.M. Weckhuysen, Vib. Spectrosc. 43 (2007) 140–151.
[37] J. Liu, Z. Zhao, C.M. Xu, A.J. Duan, L. Zhu, X.Z. Wang, Catal. Today 118 (2006) 315–322.
[38] R.S. Weber, J. Catal. 151 (1995) 470–474.
[39] E.A. Davis, N.F. Mott, Phil. Mag. 22 (1970) 903–922.
[40] J. Tauc, Amorphous and Liquid Semiconductors, Plenum Press, London, 1974, p. 159.
[41] H.J. Tian, E.I. Ross, I.E. Wachs, J. Phys. Chem. B 110 (2006) 9593–9600.
[42] G. Du, S. Lim, M. Pinault, C. Wang, F. Fang, L. Pfefferle, G.L. Haller, J. Catal. 253 (2008) 74–90.
[43] N.W. Hurst, S.J. Gentry, A. Jones, B.D. McNicol, Catal. Rev. -Sci. Eng. 24 (1982) 233–309.
[44] F. Arena, F. Frusteri, G. Martra, S. Coluccia, A. Parmaliana, J. Chem. Soc. -Faraday. Trans. 93 (1997) 3849–3854.
[45] A.A. Lemonidou, Appl. Catal. A 216 (2001) 277–284.
[46] F. Cavani, F. Trifiro, Catal. Today 51 (1999) 561–580.
[47] T. Williams, J. Beltramini, G.Q. Lu, Micropor. Mesopor. Mater. 88 (2006) 91–100.
[48] J.M.L. Nieto, J. Soler, P. Concepcion, J. Herguido, M. Menendez, J. Santamaria, J. Catal. 185 (1999) 324–332.
[49] E. Yoda, J.N. Kondo, K. Domen, J. Phys. Chem. B 109 (2005) 1464–1472.
[50] G. Magnacca, C. Morterra, Langmuir 21 (2005) 3933–3939.
[51] Z. Zhao, Y. Yamada, A. Ueda, H. Sakurai, T. Kobayashi, Catal. Today 93–95 (2004) 163–171.
[52] I.C. Marcu, L. Sandulescu, Y. Schuurman, J.M.M. Millet, Appl. Catal. A 334 (2008) 207–216.

PAPER V

Catalysis Today 179 (2012) 149–158

Contents lists available at SciVerse ScienceDirect

Catalysis Today

journal homepage: www.elsevier.com/locate/cattod

Study of vanadium based mesoporous silicas for oxidative dehydrogenation of propane and *n*-butane

Roman Bulánek[a,*], Alena Kalužová[a,1], Michal Setnička[a,1], Arnošt Zukal[b,2], Pavel Čičmanec[a,1], Jana Mayerová[b,2]

[a] Department of Physical Chemistry, University of Pardubice, Studentská 573, CZ532 10 Pardubice, Czech Republic
[b] J. Heyrovsky Institute of Physical Chemistry Academic of Sciences of the Czech Republic, v.v.i., Dolejškova 2155/3, CZ182 23 Prague 8, Czech Republic

ARTICLE INFO

Article history:
Received 15 April 2011
Received in revised form 18 August 2011
Accepted 29 August 2011
Available online 25 September 2011

Keywords:
Vanadium
Oxidative dehydrogenation
Mesoporous silicas
Propene
Butenes

ABSTRACT

The comparative study of catalytic performance of V-containing high-surface mesoporous siliceous materials (HMS, SBA-16, SBA-15 and MCM-48) in oxidative dehydrogenation of propane and *n*-butane (C_3-ODH and C_4-ODH, respectively) was carried out. The aim of study was to investigate effect of silica support texture on the speciation of vanadium complexes and its impact on catalytic behavior in both above mentioned reactions is reported. Prepared catalysts were characterized by XRF for determination of vanadium content, XRD, SEM and N_2-adsorption for study of morphology and texture, and H_2-TPR and DR UV–vis spectroscopy for determination of vanadium complex speciation. All prepared materials were tested in propane and *n*-butane ODH reaction at 540 °C and obtained catalytic results were correlated with their structural and surface characteristics. On the basis of obtained data we conclude that the structure of mesoporous silica support plays decisive role in the case of application of catalysts in *n*-butane ODH reaction, whereas catalytic performance of investigated catalysts in propane ODH reaction is comparable for all investigated structures. Catalytic performance of investigated materials in C_3-ODH and C_4-ODH can be correlated with population of all tetrahedrally coordinated VO_x complexes and only isolated monomeric VO_x complexes, respectively.

1. Introduction

Main task of today's chemical industry is a production of a large amount of organic compounds. Presently it is very important to find alternative processes for production of these compounds from more economically convenient raw materials and with smaller impact to environment. As an example, we can use alkanes instead alkenes because alkanes are cheaper compared with alkenes (e.g. actual price of propane is 860 € per ton, while price of propene is 1105 € per ton [1]) and they are easily available. Oxidative dehydrogenation (ODH) of alkanes provides a thermodynamically accessible route to the synthesis of alkenes from alkanes. A large number of reviews dealing with the ODH of light alkanes have been published since early 1990s [2–8]. A general feature of the most catalytic systems in ODH is that the selectivity to alkenes decreases with the increasing alkane conversion. In order to avoid the over-oxidation of the primary product of alkane activation, it is necessary to develop highly structured materials with known and controlled speciation of active components. Many catalysts investigated in the ODH reaction are based on the vanadium oxides as the main component [8–30]. Bulky vanadium pentoxide, in fact, is not a good catalytic system for the selective oxidation of alkanes, but spreading the oxide on the quasi-inert matrix such as a support with the formation of centers with peculiar chemical–physical features and reactivity, leads to selective catalytic systems. The vanadium oxides supported on surface of micro- or mesoporous materials attract great interest of scientific community due to the ability to combine unique textural and acid–base properties of support with the redox properties of vanadium oxide species which opens the new possibility to activate alkanes at relatively low temperatures.

Considerable attention has been devoted to investigation of effect of micro- and mesoporous support texture on the oxidative dehydrogenation of propane (e.g. silicalite [31,32], MCM-41 [12,14,18,33–35], SBA-15 [17,34–36], MCF [34,37] and HMS [16,23,34,35]), but only few papers deal with ODH of butane over VO_x-mesoporous support of SBA-15 type [25,38,39]. Some authors rated as best support for vanadia for ODH of propane SBA-15 [17,40,41], while others denoted HMS and MCM-41 [34] as the best support. However, it must be noted, that differences were not

* Corresponding author. Tel.: +420 46 603 75 11; fax: +420 46 603 70 68.
E-mail addresses: roman.bulanek@upce.cz (R. Bulánek), jana.mayerova@jh-inst.cas.cz (J. Mayerová).
[1] Tel.: +420 46 603 75 11; fax: +420 46 603 70 68.
[2] Tel.: +420 26 605 30 55; fax: +420 28 658 23 07.

0920-5861/$ – see front matter © 2011 Elsevier B.V. All rights reserved.
doi:10.1016/j.cattod.2011.08.044

significant and direct comparison of data from various studies is very complicated due to different conditions applied to the catalytic tests by various research groups. More significant differences in the catalytic behavior could be expected in the case of *n*-butane ODH due to higher sensitivity of this reaction to the population of various types of VO_x species, as was very recently reported [42]. However, according to the best of our knowledge, such study was not published in the literature yet. Therefore, we report comparison of catalytic performance of V-containing high-surface siliceous materials of HMS, SBA-15, SBA-16 and MCM-48 structure in ODH of propane and *n*-butane in order to investigate effect of silica support texture on the speciation of vanadium complexes and its impact on catalytic behavior in both above mentioned reactions. Prepared catalysts were characterized by XRF for determination of vanadium content, XRD, SEM and N_2-adsorption for study of morphology and texture, and H_2-TPR and DR UV–vis spectroscopy for determination of vanadium complex speciation. All prepared materials were tested in propane and *n*-butane ODH reaction at 540 °C and obtained catalytic results were correlated with their structural and surface characteristics. On the basis of obtained data we conclude that structure of mesoporous silica support play decisive role in the case of application of catalysts to *n*-butane ODH, whereas catalytic performance of investigated catalysts in propane ODH reaction is comparable for all investigated structures.

2. Experimental

2.1. Catalyst preparation

HMS was prepared according to procedure reported by Tanev and Pinnavaia [43]. 13.6 g of dodecylamine (DDA, Aldrich) was dissolved in the mixture of 225 cm^3 ethanol and 200 cm^3 double-distilled H_2O. After stirring for 20 min, 56 cm^3 of tetraethyl orthosilicate (TEOS, Aldrich) was added dropwise and intensively stirred. The reaction was performed at 25 °C for 18 h under stirring. The solid product was filtered and then repeatedly suspended in 500 cm^3 ethanol and stirred at 25 °C for 1 h in order to remove major part of DDA from obtained solid. Finally, the solid was calcined in flow of air at 540 °C for 8 h with heating rate 1 °C min^{-1}.

MCM-48 samples were prepared using a mixture of triblock copolymer Pluronic P123 (Aldrich) and *n*-butanol (Aldrich, 99.4%) as a structure-directing mixture and TEOS as the silica source [44]. In the typical synthesis 20 g of Pluronic P123 and 33.5 cm^3 of hydrochloric acid (37%) are dissolved in 720 cm^3 of distilled water to form a clear solution. Then 24.66 cm^3 of *n*-butanol was added; afterwards the mixture was being stirred at 35 °C for 3 h. It was followed by addition of 46.1 cm^3 of TEOS and stirring at 35 °C for 2 h. The reaction mixture was afterwards aged without any stirring for 24 h at 35 °C and 24 h at 95 °C. The resulting solid phase was recovered by hot filtration, extensively washed out with distilled water and dried at 95 °C in Büchner funnel overnight. Calcination was carried out in air at 540 °C for 8 h with heating rate 1 °C min^{-1}.

Purely siliceous SBA-15 mesoporous molecular sieve were synthesized as reported earlier [45] using a triblock copolymer, Pluronic P123 ($EO_{20}PO_{70}EO_{20}$, BASF/Aldrich) as a structure directing agent. TEOS was used as a silica precursor yielding a typical synthesis molar ratio TEOS:HCl:P123:H_2O = 1:6.2:0.017:197. The synthesis mixture was vigorously stirred at 35 °C for 5 min and subsequently aged under static conditions for 24 h at 35 °C and 48 h at 97 °C. The resulting solid was recovered by filtration, extensively washed out with distilled water and ethanol, and dried at 100 °C overnight. The template was removed by calcination in a stream of air at 540 °C for 8 h with heating rate 1 °C min^{-1}.

SBA-16 samples were synthesized using Pluronic P123 and F127 as templates [46]. In the typical synthesis 3.27 g of Pluronic P123, 10.21 g of Pluronic F127 and 91 cm^3 of hydrochloric acid (37%) are dissolved in 550 cm^3 of distilled water to form a clear solution. After that 50 cm^3 of TEOS was added and the mixture was being stirred for 5 min. The reaction mixture was afterwards aged without any stirring for 24 h at 35 °C and 24 h at 95 °C. The resulting solid phase was recovered by hot filtration, extensively washed out with distilled water and dried at 95 °C in Büchner funnel overnight. Calcination was carried out in air at 540 °C for 8 h with heating rate 1 °C min^{-1}.

Vanadium oxo-complexes were doped onto silica support by standard wet impregnation procedure by appropriate amount of ethanol/H_2O solution of vanadyl acetylacetonate (Aldrich). Impregnated samples were dried at 120 °C in air overnight and then calcined at 600 °C for 8 h in the dry air flow. The samples with vanadium loading 3.6 and 9 wt.% were prepared representing materials with vanadium content close to monolayer and markedly exceeding this level. Surface density of vanadium on silica surface at monolayer is usually reported to be 0.7 V/nm^2 [47,48].

2.2. Catalysts characterization

The chemical composition of all investigated samples was determined by X-ray fluorescence spectroscopy by ElvaX (Elvatech, Ukraine) equipped with Pd anode. Samples were measured against the model samples (a mechanical mixture of pure SiO_2 and $NaVO_3$) granulated to the same grain size as catalysts.

The particle morphology of starting mesoporous silicas as well as modified samples was evaluated by scanning electron microscopy images using a JEOL JSM-5500LV instrument.

X-ray powder diffraction data were recorded on a Bruker D8 X-ray powder diffractometer equipped with a graphite monochromator and a position-sensitive detector (Vantec-1) using Cu Kα radiation (at 40 kV and 30 mA) in Bragg–Brentano geometry.

Nitrogen was used as adsorptive and supplied by Messer (Griesheim, Germany – purity 99.999 vol.%). Sorption isotherms of nitrogen at 77 K were determined using an ASAP 2020 instrument. In order to attain a sufficient accuracy in the accumulation of the adsorption data, this instrument is equipped with pressure transducers covering the 133 Pa, 1.33 kPa and 133 kPa ranges. Before each sorption measurement the sample was degassed to allow a slow removal of the most of preadsorbed water at low temperatures. This was done to avoid potential structural damage of the sample due to surface tension effects and hydrothermal alternation. Starting at ambient temperature the sample was degassed at 110 °C (temperature ramp of 0.5 °C min^{-1}) until the residual pressure of 1 Pa was attained. After further heating at 110 °C for 1 h the temperature was increased (temperature ramp of 1 °C min^{-1}) until the temperature of 250 °C was achieved. The sample was degassed at this temperature under turbomolecular pump vacuum for 8 h.

The UV–vis diffuse reflectance spectra of dehydrated diluted samples were measured using Cintra 303 spectrometer (GBC Scientific Equipment, Australia) equipped with a Spectralon-coated integrating sphere using a Spectralon coated discs as a standard. The spectra were recorded in the range of the wavelength 190–850 nm. The samples were diluted by the pure silica (Fumed silica, Aldrich) in the ratio 1:100. All samples were granulated and sieved to fraction of size 0.25–0.5 mm, dehydrated before the spectra measurement and oxidized in the glass apparatus under static oxygen atmosphere in two steps: 120 °C for 30 min and 450 °C for 60 min and subsequently cooled down to 250 °C and evacuated for 30 min. After the evacuation the samples were transferred into the quartz optical cuvette 5 mm thick and sealed under vacuum. For additional details you can see Ref. [49]. This procedure guaranteed complete dehydration and defined oxidation state of vanadium for all catalysts. The obtained reflectance spectra were transformed

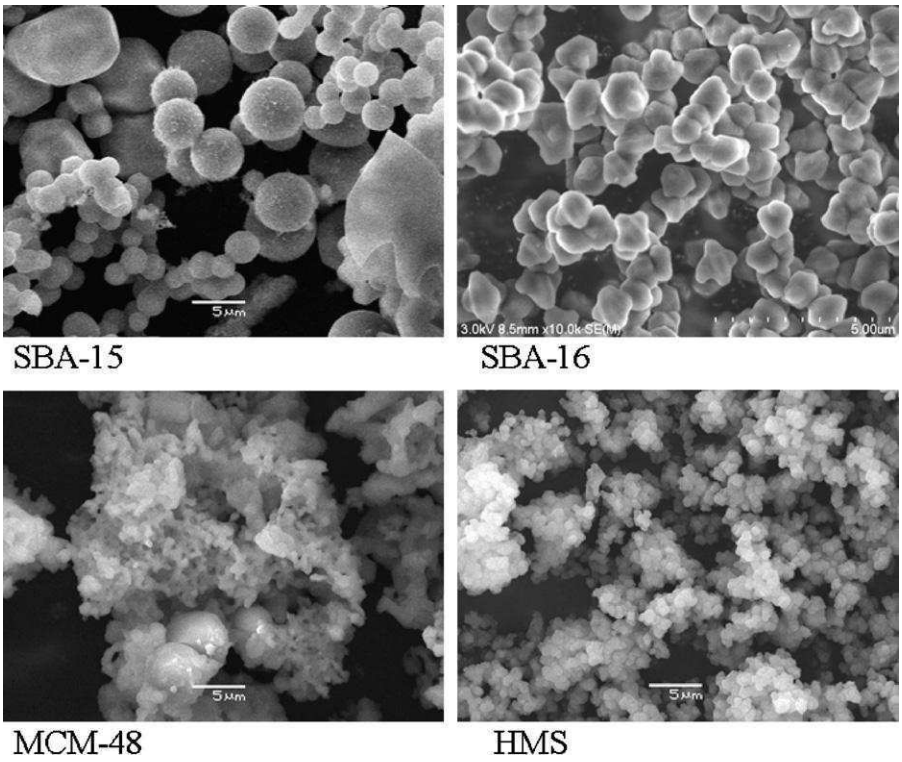

Fig. 1. SEM images of parent mesoporous silicas.

into the dependencies of Kubelka–Munk function $F(R_\infty)$ on the absorption energy $h\nu$ using Eq. (1):

$$F(R_\infty) = \frac{(1-R_\infty)^2}{2R_\infty} \quad (1)$$

where R_∞ is the measured diffuse reflectance from a semi-infinite layer [50].

All measured spectra were simultaneously fitted [49] by set of Gaussian curve shaped bands using the Fityk [51] software. Because all VO_x species exhibit the same or similar absorption coefficients [49] it is possible to make the semi-quantitative analysis of spectra.

Raman spectra of dehydrated catalysts were measured by a Labram HR spectrometer (Horiba Jobin-Yvon) interfaced to an Olympus BX-41 microscope. Spectra were excited by 514.5 nm line of an Ar^+/Kr^+ laser (Innova 70C series, Coherent). The Raman spectrometer was calibrated by using the F_{1g} line of Si at 520.5 cm^{-1}. The spectra were recorded with resolution 2 cm^{-1} by Peltier-cooled CCD camera detector. The laser power impinging on the dry sample was 1.2 mW. The dehydration and oxidation protocol was the same as for DR UV–vis measurement (see above).

Redox behavior of VO_x surface species was investigated by the temperature programmed reduction by hydrogen (H_2-TPR) using the AutoChem 2920 (Micromeritics, USA). 100 mg sample in a quartz U-tube microreactor was oxidized in oxygen flow at 450 °C (2 h) prior to the TPR measurement. The reduction was carried out from 100 °C to 900 °C with a temperature gradient of 10 °C min^{-1} in flow of reducting gas (5 vol.% H_2 in Ar). The changes of hydrogen concentration were monitored by the TCD detector.

2.3. Catalytic tests in ODH reaction

The propane and *n*-butane oxidative dehydrogenation (C_3-ODH and C_4-ODH, respectively) reaction was carried out using a plug-flow fixed-bed reactor at atmospheric pressure in the kinetic region (independently checked) and at steady state conditions of the reaction. The activity and selectivity of catalysts were tested at 540 °C in the dependence on contact time (W/F 0.03, 0.06, 0.09, 0.12 and 0.15 g_{cat} s cm^{-3}). The demanded weight of catalyst (grains 0.25–0.50 mm) was mixed with 2 cm^3 of inert SiC. The catalysts were pre-treated in a flow of oxygen at 540 °C for 2 h before each reaction run. The feed composition was $C_xH_y/O_2/He = 5/2.5/92.5$ vol.% with a total flow of 100 cm^3 min^{-1} STP (C_xH_y – C_3H_8 or C_4H_{10}). The catalytic activity was analyzed at steady state conditions and the products composition was analyzed by on-line gas chromatograph equipped with TCD and FID detectors. The feed conversion, selectivity to products and productivity were calculated based on mass balance according to Sachtler and Boer [52]. The turn-over-frequency (TOF) values per V atom were calculated using Eq. (2):

$$\mathrm{TOF}_X = \frac{n^0_{n-C} X_{n-C} M_V}{m_{cat} w_V} \quad (2)$$

where n^0_{n-C} is molar flow of hydrocarbon (mol s^{-1}), X_{n-C} conversion of hydrocarbon (%), M_V is atomic weight of vanadium (50.94 g mol^{-1}), m_{cat} is weight of catalyst (g), w_v is mass fraction of vanadium in catalysts.

3. Results and discussion

3.1. Physicochemical properties of the samples

SEM images of all four starting materials (Fig. 1) have revealed regular particle morphology without any presence of other phases. For comparison there are shown samples of SBA-15 containing different amounts of vanadium (Fig. 2) and it can be concluded that as far as particle size and morphology is concerned, no effect due to the presence of vanadium was observed.

XRD patterns of parent materials (Fig. 3A) exhibit well resolved diffraction lines, which can be associated with well-ordered pore structure of the mesoporous SBA-15, MCM-48 and SBA-16 as well as the disordered wormhole-like pore structure of HMS. After

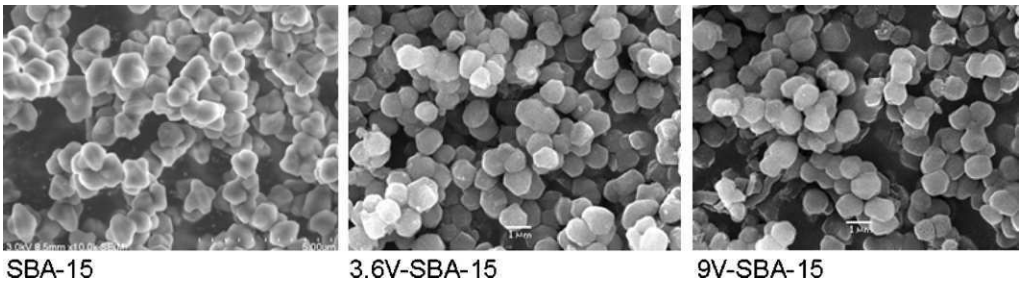

Fig. 2. SEM images of parent SBA-15 and its vanadium modified forms.

impregnation of parent materials with vanadium complex, the same diffraction lines are observed, indicating the preserved ordering of mesoporous structure as demonstrated on 3.6 and 9V-SBA-15 samples (see Fig. 3B). However, substantial decrease of intensity of diffraction lines was observed. The decrease in intensity of the peaks after post-synthesis modifications demonstrates the partial structural collapse of the mesoporous materials or the flexibility induced in the silica framework due to the strain generated from the functionalized groups [53,54].

Nitrogen adsorption isotherms of all starting and impregnated samples of selected silica SBA-15 are illustrated in Fig. 4. It was found that despite rather rough treatment of primary samples the hysteresis loop of impregnated samples remains preserved. It confirms that modification of parent samples did not significantly change the structure of these materials. In addition isotherms are characteristic of high quality of prepared materials. The BET surface area was evaluated using adsorption data in a relative pressure range from 0.05 to 0.25 (Table 1). The micropore volume (V_{MI}) was determined using *t*-plot method. The mesopore volume (V_{ME}) and mesopore distribution of silica materials were calculated using BJH algorithm (Table 1) calibrated to accurately reproduce the pore diameter and volume. In particular, the changes in S_{BET} illustrate a pronounced reduction of the surface (mainly micropore volume) which was accessible for nitrogen molecules due to the vanadium impregnation. Samples doped with the highest concentration of vanadium exhibited decrease of S_{BET} from 60% to 75% related to their parent samples. On the other hand the decrease of mesopore volumes of the same materials was only in the range from 20% to 48%. Introduction of vanadium into mesopores also affected the pore size distribution. This effect is shown on SBA-15 samples (see Fig. 5), where the higher concentration of vanadium, the lower is the peak on the distribution curve. Moreover, the pore size distribution was slightly shifted to lower values of pore diameter.

The diffuse reflectance UV–vis spectroscopy provides information about the character and oxidation state of vanadium. The obtained DR UV–vis spectra for both prepared sets of catalyst are presented in Fig. 6. It can be noted that parent silica supports exhibited only very low intensity spectrum and therefore are not reported here. All spectra were obtained by measurement of one hundred times diluted dehydrated samples with the purpose to obtain better resolution of individual bands and the linear dependence area of spectra on the concentration of vanadium (for more details see Ref. [49]). They are qualitatively similar to spectra published previously for the vanadium oxide system on the different siliceous supports [13,55,56] and contain several absorption bands in region 1.46–6.5 eV (850–190 nm) which are conventionally attributed to ligand to metal charge-transfer (LMCT) transitions of the $O \rightarrow V^{+V}$ type or to the d-d transitions of V^{+IV} [56]. The d–d absorption bands characteristic for the vanadium(+IV) in the region 1.55–2.07 eV [57] were not observed in our obtained spectra and this fact confirms that all vanadium was successfully oxidized to oxidation state (+V) during

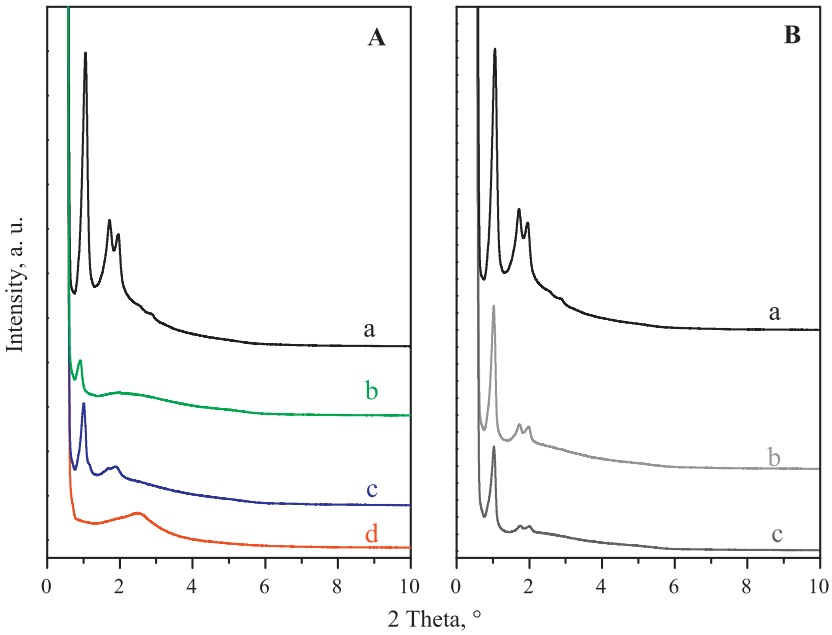

Fig. 3. (A) XRD patterns of parent mesoporous silica supports: (a) SBA-15, (b) SBA-16, (c) MCM-48, (d) HMS. (B) XRD patterns of parent SBA-15 and its vanadium modified forms: (a) SBA-15, (b) 3.6V-SBA-15, (c) 9V-SBA-15.

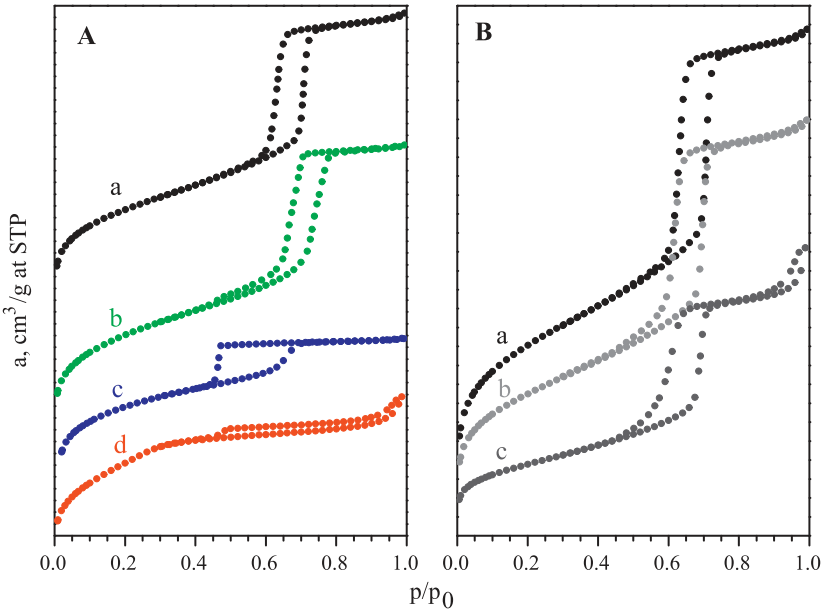

Fig. 4. (A) Nitrogen adsorption isotherms of parent mesoporous silica supports: (a) SBA-15, (b) SBA-16, (c) MCM-48, (d) HMS. (B) Nitrogen adsorption isotherms of parent SBA-15 and its vanadium modified forms: (a) SBA-15, (b) 3.6V-SBA-15, (c) 9V-SBA-15.

the pretreatment procedure. The samples with high concentration of vanadium exhibit absorption bands in the region 2–3 eV with maxima at ca. 2.6 and 3.1 eV and they are attributed to the presence of 3D-octahedrally coordinated (group O_h) bulk-like VO_x units [13,49,57]. The low-loaded samples exhibit absorption only above 3 eV evidencing VO_x species with tetrahedral coordination. Fig. 7 shows spectra of low-loaded samples together with spectra of sodium ortho-vanadate Na_3VO_4 and meta-vanadate $NaVO_3$ as standard compounds containing only isolated monomeric tetrahedral units and linearly polymerized tetrahedrally coordinated oligomeric units with V–O–V bonds respectively. Our samples with lower vanadium content exhibit edge energy 3.7–3.47 eV (obtained accordingly to Ref. [58]), whereas edge energy of Na_3VO_4 and $NaVO_3$ is 3.82 and 3.13 eV, respectively. Taking into account this observation, it is concluded that both isolated VO_4 units and small VO_x aggregates that have V–O–V bonds are present on the surface of our samples (effect of partial hydratation was excluded on the base of checking measurement of overtones of OH group vibration on UV–vis–NIR spectrometer). For quantitative analysis of all three types of surface vanadium complexes, the spectra were deconvoluted into individual bands. Parameters of individual spectral bands used in deconvolution procedure of the spectra were taken from systematic study analyzing set of VO_x–HMS samples with wide range of vanadium concentration and vanadium species distribution recently published [49]. Fig. 8 presents example of the deconvolution of the experimental spectra for the samples with low and high concentration of VO_x species anchored on SBA-15 support. UV–vis spectra of all samples (with low and high concentration) contain three absorption bands in the region 3–6.5 eV and these bands can be attributed to the ligand to metal charge transfers of T_d-coordinated species (group of symmetry T_d). The band with maxima position approximately at 4 eV can be attributed to T_d-oligomeric species [49,59,60]. The band at ca. 5.9 eV belongs to T_d-monomeric species [49,59–61] and the band with maximum at 5 eV is linear combination of the bands ascribed to both the T_d-monomeric and the T_d-oligomeric species. For more information

Table 1
Chemical composition and results of physico-chemical characterization of investigated materials.

Sample name	V[a], wt.%	S_{BET}, $m^2\ g^{-1}$	V_{MI} [b], $cm^3\ g^{-1}$	V_{ME} [c], $cm^3\ g^{-1}$	D_{ME} [d], nm	VO_x [e], nm^{-2}	X_{mono} [f]	X_{oligo} [f]	X_{O_h} [f]	T_{max} [g], °C	Δe[h]
HMS		879	0.010	0.189	6.9						
SBA-15		780	0.060	0.820	6.7						
SBA-16		710	0.073	0.510	3.9						
MCM-48		820	0.068	0.770	7.0						
3.6V-HMS	3.6	640	0.025	0.176	7.1	0.7	0.42	0.58	0	568	1.5
3.6V-SBA-15	3.6	600	0.030	0.730	5.6	0.7	0.82	0.18	0	555	1.8
3.6V-SBA-16	3.6	570	0.043	0.309	4.0	0.7	0.56	0.44	0	534	1.6
3.6V-MCM-48	3.6	670	0.045	0.678	6.0	0.6	0.55	0.45	0	562	1.9
9V-HMS	9.0	260	0.039	0.150	8.6	4.0	0.28	0.60	0.12	594	1.6
9V-SBA-15	9.0	300	0.011	0.571	6.1	3.4	0.53	0.43	0.03	572	1.7
9V-SBA-16	9.0	130	0.011	0.228	10.0	8.1	0.47	0.44	0.10	596	1.7
9V-MCM-48	9.0	350	0.018	0.545	7.0	3.1	0.46	0.47	0.07	587	1.6

[a] Vanadium content determined by XRF method.
[b] V_{MI} micropore volume determined by using the *t*-plot method.
[c] V_{ME} mesopore volume determined by Barret–Joyner–Halenda (BJH) algorithm.
[d] D_{ME} mesopore diameter determined by BJH algorithm.
[e] VO_x surface density ($VO_x\ nm^{-2}$).
[f] Relative amount of T_d-monomeric, T_d-oligomeric and O_h units.
[g] Position of maxima of H_2-TPR profile.
[h] Average change of oxidation state during H_2-TPR experiment.

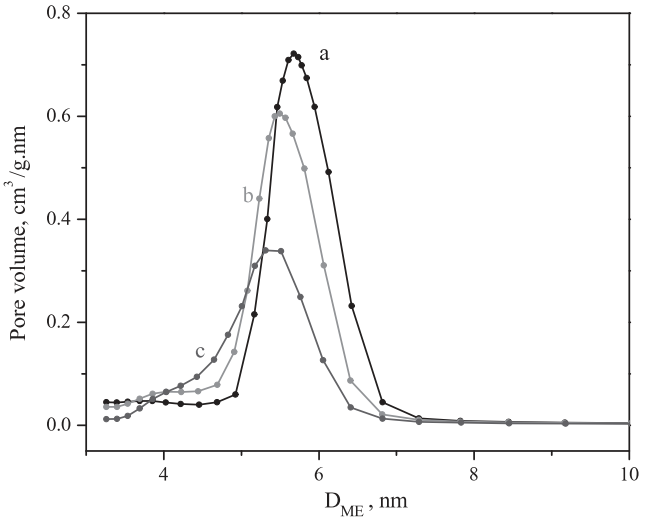

Fig. 5. Pore size distribution for parent SBA-15 and its vanadium modified forms: (a) SBA-15, (b) 3.6V-SBA-15, (c) 9V-SBA-15.

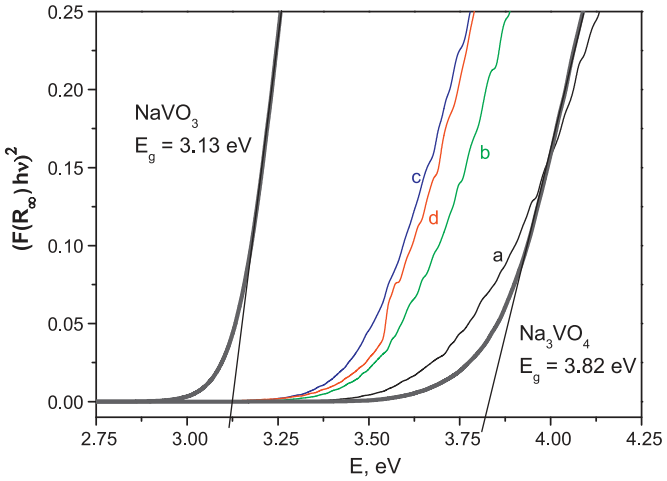

Fig. 7. Diffuse reflectance UV–vis spectra of diluted and dehydrated low-loaded VO_x catalysts (colors are the same as in Fig. 6A), ortho- and meta-vanadate with corresponding edge of absorption energy. (a) SBA-15, (b) SBA-16, (c) MCM-48, (d) HMS.

about assignment see Ref. [49]. Relative amount of individual VO_x species on the surface was determined from area of corresponding bands and results are given in Table 1. The low concentrated samples contain only T_d-coordinated VO_x species with predominantly T_d-monomeric units which are considered to be the most active particles in the light alkane ODH reactions [5,62]. The highest relative abundance of monomeric T_d-coordinated units can be found on the SBA-15 support, approximately about 85% relative amount for lower concentration of vanadium. For other low concentrated samples the amounts of monomeric units are significantly lower (about 50%). On the basis of the supports tendency to generate the T_d-oligomeric and octahedrally coordinated polymeric units we can sort tested support materials in the following order SBA-15 < SBA-16 ~ MCM-48 < HMS. We can observe this influence in samples with high concentration as well (see Table 1). High capability of SBA-15 for accommodation of well dispersed isolated monomeric vanadyl species can be given by the fact that SBA-15 silica represents mesoporous support with regular, well defined and uniform pore system characterized by very narrow pore size distribution, whereas other investigated supports exhibit worm-like (HMS) or ink-bottle (MCM-48) type of pores with wider distribution of pore diameters, which are less suitable for fine dispersion of source of vanadium during the procedure of solvent evaporation. The more regular pore system the more homogeneously is solvent removed from inner space of pore system. The Raman spectra of the dehydrated VO_x catalysts are shown in Fig. 9 (part A of Fig. 9 shows the spectra of low-loaded samples, part B of Fig. 9 shows the spectra of high-loaded samples). The catalysts possess Raman features at 282, 301, 404, ~487, 520, 697, ~802, 993 and 1031 cm^{-1}. The

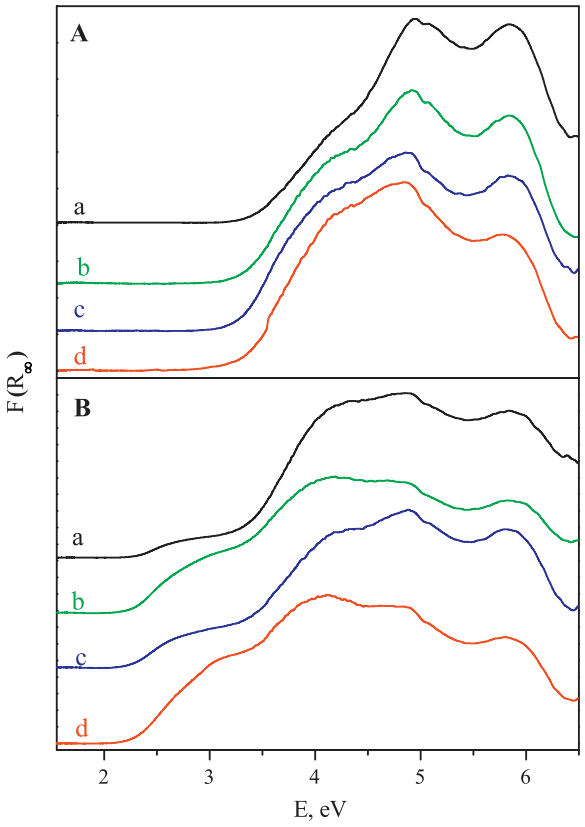

Fig. 6. Diffuse reflectance UV–vis spectra of diluted and dehydrated VO_x catalysts on different support with 3.6 (A) and 9 (B) wt.% of V: (a) SBA-15, (b) SBA-16, (c) MCM-48, (d) HMS.

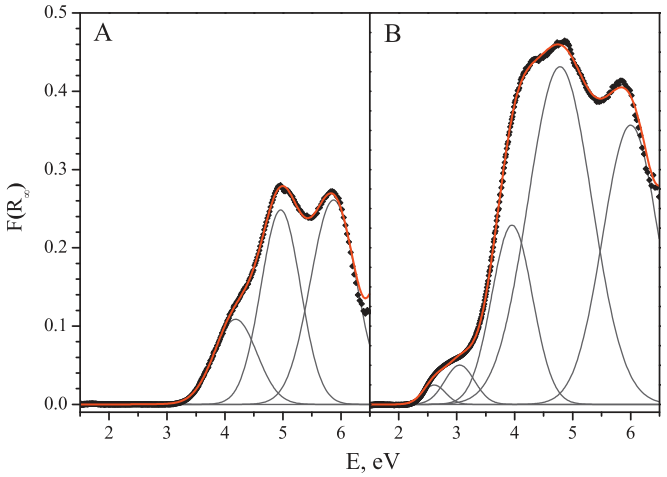

Fig. 8. Deconvoluted UV–vis spectra of V-SBA-15 with (A) 3.6 and (B) 9 wt.% of V. Black points are experimental data, red line is fitted envelope curve and dark gray lines are individual spectral bands. (For interpretation of the references to color in this figure legend, the reader is referred to the web version of this article.)

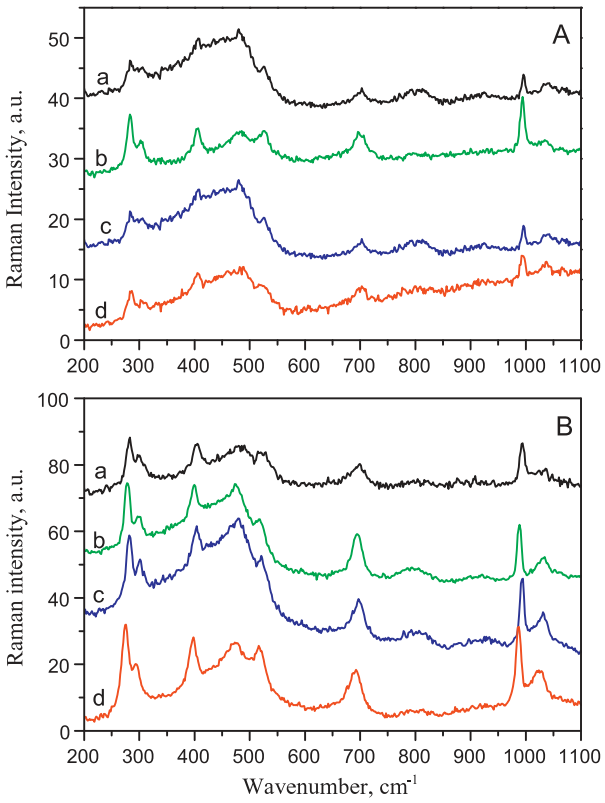

Fig. 9. Raman spectra of the dehydrated VO_x–silica samples with 3.6 (A) and 9 (B) wt.% of V: (a) SBA-15, (b) SBA-16, (c) MCM-48, (d) HMS.

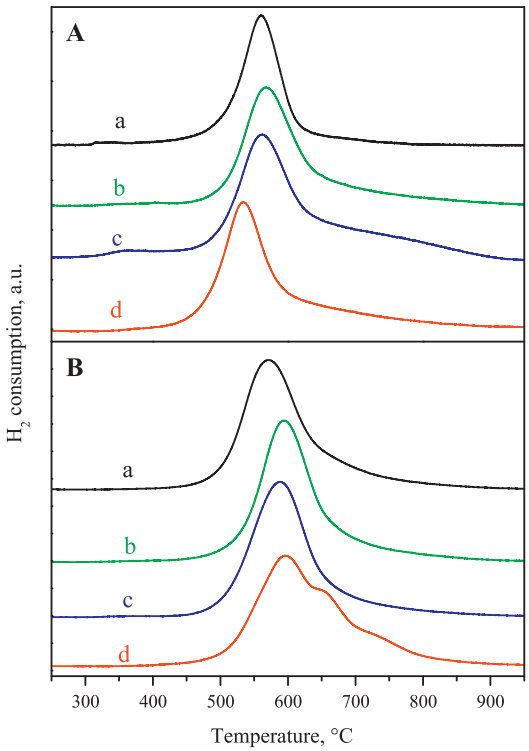

Fig. 10. H_2-TPR patterns of VO_x–silica samples with 3.6 (A) and 9 (B) wt.% of V: (a) SBA-15, (b) SBA-16, (c) MCM-48, (d) HMS.

bands at ~802 and ~487 cm^{-1} have been assigned to the symmetrical Si–O–Si stretching mode and the D1 defect mode of silica support, which have been attributed to tetracyclosiloxane rings produced via the condensation of surface hydroxyls [63,64]. All other bands can be attributed to vibration connected with presence vanadium species. It has been generally agreed that Raman bands in the range 800–1200 cm^{-1} are due to stretching modes and the bands below 800 cm^{-1} are due to bending/stretching modes of V–O [65,66]. Assignment of the Raman band is complicated by strong coupling of vanadyl stretching and silica modes, which are close in vibration energy [66,67]. However, band at 1031 cm^{-1} is usually assigned to terminal V=O stretching vibration. Shift of this vibration band to slightly higher wavenumbers was frequently taken as evidence of changes in the coordination and extent of polymerization of the dehydrated surface VO_x species on oxide supports as Al_2O_3, ZrO_2, TiO_2 or Nb_2O_5 [47,68]. However, no shift of this Raman band was observed on VO_x/SiO_2 systems [47,68,69]. This is in agreement with our observations. Position of this band is invariable notwithstanding various population of oligomeric species determined from UV–vis spectra. Recent theoretical and experimental papers dealing with vibration of vanadium species on silica surface confirmed that both monomeric and oligomeric vanadium complexes contribute to this band [59,66,67,70]. Above mentioned strong coupling of VO_x species vibration with silica skeletal vibration could be behind observed no shift of this band with progressive polymerization of VO_x species. Set of bands at 282, 301, 404, 520, 697, and 993 cm^{-1} are ascribed to V_2O_5 crystallites. It is interesting to note that above mentioned bands are present in all Raman spectra while typical bands assigned to V_2O_5 crystallites at 2.6 and 3.1 eV are detected only in DR UV–vis spectra of samples with 9 wt.% of vanadium (cf. Fig. 6). Therefore, Raman spectra prove the presence of very small amount of V_2O_5 crystallites, which cannot be detected by UV–vis spectroscopy or XRD, even in the low-loaded samples due to resonant enhance effect.

H_2-TPR curves of VO_x catalysts are depicted in Fig. 10. It can be noted that parent silica supports exhibited no reduction peaks and therefore are not reported here for the sake of brevity. Vanadium catalysts exhibit distinct reduction peaks in the temperature range from 350 to 900 °C. The average change of oxidation state (Δe) after the H_2 reduction has been calculated from the amount of H_2 consumed during the reduction process and range from 1.5 to 1.9 (see Table 1) indicating incomplete reduction of V^{+V} to V^{+III} or the presence of vanadium cations in lower oxidation states (V^{+IV} or even V^{+III}) in the samples already before starting the TPR process. The reduction peak centered at ca. 534–568 °C dominates the TPR patterns of all investigated materials. This peak is distinctly tailed on high-temperature side for samples with higher vanadium loading, especially for SBA-16 support with 9 wt.% of vanadium. Existence of other peaks at about 650 and 735 °C indicates, in accord with spectroscopic results, certain heterogeneity of vanadium complexes on the inner surface of the prepared catalysts. In previous studies reported in the literature, the low-temperature peak was tentatively attributed to the reduction of highly dispersed VO_x units with tetrahedral-like coordination [12,71–73] and the high-temperature peaks were attributed to the reduction of polymeric oxide-like VO_x species with octahedral coordination [74–78]. We reported in recent study on VO_x-HMS catalysts that presence of high-temperature reduction peak in the H_2-TPR curves of VO_x-HMS catalysts exhibited materials with presence of UV–vis bands at 2.6 and 3.1 eV in their UV–vis spectra ascribed to 2D-square pyramidal and 3D-octahedrally coordinated vanadium species [42]. Therefore, the low-temperature reduction peak could be attributed to both monomeric and oligomeric tetrahedral-like coordinated VO_x species. Generally, reducibility of bulk vanadium oxides differs from reducibility of surface species. Based on comparison of H_2-TPR and ^{51}V NMR characterization of VO_x–SiO_2 materials with various vanadium loading it was concluded that the reduction of bulk V_2O_5

Table 2
Results of catalytic tests in oxidative dehydrogenation of propane at 540 °C and iso-conversion of propane 13% ($C_3H_8/O_2/He = 5/2.5/92.5$ vol.%, total flow rate of 100 $cm^3\ min^{-1}$).

Catalyst sample name	Conv., %	Selectivity, %				Productivity[b]	TOF, h^{-1}
	O_2	C_3H_6	C_1–C_2 [a]	CO	CO_2	C_3H_6	
3.6V-HMS	65	56	1	26	17	0.22	10
3.6V-SBA-15	59	60	3	23	14	0.21	12
3.6V-SBA-16	61	57	2	26	15	0.21	12
3.6V-MCM-48	63	56	2	26	16	0.17	13
9V-HMS	74	41	0	44	15	0.23	7
9V-SBA-15	62	48	0	38	14	0.38	13
9V-SBA-16	49	50	1	35	14	0.24	6
9V-MCM-48	75	44	0	42	14	0.36	11

[a] C_1–C_2 = sum of C_1–C_2 hydrocarbons.
[b] Productivity = $g_{prod}\ g_{cat}^{-1}\ h^{-1}$.

occurred at much higher temperatures than silica supported vanadia due to increased diffusional limitations in bulk V_2O_5 [75]. On the other hand, Banares et al. observed by in situ TPR-Raman experiments formation of oxide species during heating and reduction of these species at lower temperatures than reduction of monomeric species. In addition, reducibility of individual types of vanadia species can vary in dependence on the support as was experimentally observed by systematic shifts of reduction peak position on temperature scale [78–81]. On VO_x-MCM-41 silica, investigation of reduction kinetics of surface vanadia species in hydrogen atmosphere by means of in situ UV–vis spectroscopy led to conclusion that tetrahedrally coordinated polymeric vanadia species are more reducible than monomeric species [82] similarly to VO_x–Al_2O_3 system [81]. However, position of reduction peak in our TPR curves of low-loaded samples changes within interval of 30 °C, but irrespective to population of monomeric species. Reduction of high-loaded samples is shifted by about 30 °C to higher temperature. This could be caused by increase in population of polymeric species. However, the shift of reduction peak can be influenced not only by nature of species but also by thermodynamics or kinetics limitations (e.g. changes in hydrogen and water concentration in the reduction gas owing the reduction reaction course). Therefore, it is very difficult to attribute a particular surface structure to the individual TPR peaks more reliably.

3.2. Catalytic tests of propane and n-butane ODH

Oxidative dehydrogenation of propane over investigated samples was studied at 540 °C at various contact times realized by changes of catalyst weight. Main results are presented in Table 2. The main products of C_3-ODH were propene and carbon oxides. Traces of ethene and methane were detected as cracking products. No oxygenates were detected. It is well-known that the selectivity is necessary to compare at the same degree of conversion for parallel-consecutive reaction, such as the C_3-ODH reaction. Therefore the catalytic behavior of VO_x–silica catalysts with different vanadium loading and different texture of support was compared under iso-conversion conditions at propane conversion of 13%. In addition, catalytic performance of the samples only slightly depended on time-on-stream (decline of propane conversion and propene selectivity was 1 and 2%, respectively, within 4 h in the stream). Therefore, data after 2 h in the stream were taken for catalysts comparison. The iso-conversion selectivity to propene only slightly varied in the range from 60 to 56% for lower vanadium content regardless of catalysts structure, whereas it reached only 41–50% for materials with higher vanadium loading (see Table 2). The decrease in propene selectivity was accompanied by increase in selectivity to CO. The selectivity to CO_2 was relatively constant and comparable for all catalysts ($S_{CO_2} = 15 \pm 2\%$). The activity of VO_x–silica catalysts under these conditions was expressed by so called turn-over-frequency (TOF), describing the average number of catalytic cycles at one average vanadium atom per time unit (h). The TOF factor was almost constant for catalysts with lower vanadium content (TOF equal to 12 h^{-1} except VO_x-HMS exhibiting TOF of 10 h^{-1}). The TOF for catalysts with higher loading of vanadium depended on type of mesoporous silica support. The VO_x-SBA-15 and VO_x-MCM-48 catalysts exhibited catalytic activity similar to low-vanadium ones (13 and 11 h^{-1} for SBA-15 and MCM-48, respectively), the HMS and SBA-16 supports exhibited TOF values significantly lower (7 and 6 h^{-1} for HMS and SBA-16, respectively). It must be noted that conversion of oxygen did not exceed 75% in any case and therefore both selectivity to product and activity of catalysts were not influenced by lack of reactant. Significantly lower values of TOF of 9V-SBA-16 and 9V-HMS samples corresponded very well with the enhanced population of octahedral VO_x complexes in these samples evaluated by means of deconvolution of UV–vis spectra (cf. Table 1 and Fig. 6).

Oxidative dehydrogenation of *n*-butane was studied at 540 °C at various contact times implemented by changes of catalyst weight. The main reaction products identified in the reaction mixture were: 1-butene (1-C_4), *cis*- and *trans*-2-butene (*c*-C_4 and *t*-C_4), 1,3-butadiene (1,3-C_4), methane (C_1), ethane and ethene (C_2), propane and propene (C_3), carbon oxides (CO and CO_2) and traces of acetaldehyde. The carbon balance was 98 ± 3% in all the catalytic tests and no coke deposit was observed on the catalysts. The activity of catalysts only slightly depended on the time-on-stream (TOS). Average decline of *n*-butane conversion was about 2% within 10 h in the stream. On the other hand this decrease of conversion was accompanied by the increase of C_4-ODH selectivity approximately about 4%. This small change in catalyst performance can be explained by partial redistribution of vanadium oxide species under reaction conditions [56]. Therefore the catalytic performance of VO_x-catalyst on different support and with different vanadium loading was compared under the iso-conversion conditions at *n*-butane conversion of 13% after 2 h in the stream of reaction mixture.

The TOF value strongly depended on the concentration of vanadium and decreased with the increasing VO_x concentration (for the samples with 9 wt.% of V was only 30–40% of the value obtained for samples with 3.6 wt.% V). It can be explained with higher amount of Td-oligomeric and mainly octahedral units on the support (cf. data in Tables 1 and 3, see also Figs. 6 and 8). The value of the TOF was in good agreement with relative concentration of monomeric VO_x units as it is shown in Table 1 and Fig. 11 shows TOF value of low-loaded catalysts as a function of population of monomeric VO_x units and reaction type (C_4- and C_3-ODH). The TOF values of catalysts in C_4-ODH linearly decreased with decreasing relative population of T_d monomers obtained from UV–vis spectra deconvolution, whereas TOF values obtained in C_3-ODH were rather constant irrespective of ratio between amount of T_d monomeric and T_d oligomeric species. Considering this relation the monomeric VO_x units should be taken as the most active species in the ODH of

Table 3
Results of catalytic tests in oxidative dehydrogenation of *n*-butane at 540 °C and iso-conversion of *n*-butane 13% ($C_4H_{10}/O_2/He = 5/2.5/92.5$ vol.%, total flow rate of 100 $cm^3\ min^{-1}$).

Catalyst sample name	Conv., %	Selectivity, %								Productivity[c]	TOF, h^{-1}
	O_2	1-C_4	*c*-C_4	*t*-C_4	1,3-C_4	C_1–C_3 [a]	CO	CO_2	Dehy.[b]	Dehy.[b]	
3.6V-HMS	70	23	10	12	8	5	24	19	53	0.32	16
3.6V-SBA-15	63	23	12	12	12	6	18	15	58	0.57	26
3.6V-SBA-16	63	22	11	14	11	5	20	18	58	0.41	19
3.6V-MCM-48	81	19	8	10	7	4	30	23	43	0.31	19
9V-HMS	95	11	8	10	6	3	42	22	34	0.16	5
9V-SBA-15	95	11	7	9	7	3	39	25	34	0.37	11
9V-SBA-16	87	14	7	9	5	3	37	25	35	0.16	5
9V-MCM-48	97	9	7	9	6	3	40	25	31	0.23	8

[a] C_1–C_3 = sum of C_1–C_3 hydrocarbons and acetaldehyde.
[b] Dehy. = sum of C_4 alkenes.
[c] Productivity = $g_{prod}\ g_{cat}^{-1}\ h^{-1}$.

n-butane, while both monomeric and oligomeric species with T_d coordination could act as active species in ODH of propane.

The iso-conversion selectivity to C_4-ODH is given in Table 3. They were almost independent on the structure of siliceous supports (except 3.6V-MCM-48 exhibiting significantly lower selectivity than other catalysts with 3.6 wt.% of vanadium), but they are strongly decreasing from 58% to 34% with the increasing of vanadium loading for samples with 3.6 and 9 wt.%, respectively. The decrease in C_4-ODH selectivity is accompanied by increase in selectivity to carbon oxides, mainly selectivity to CO. This fact can be explained by higher oxygen conversion over high concentrated samples where it was almost 100%. The decrease of selectivity with the increasing of VO_x concentration was most probably due to higher abundance of oligomeric species with T_d- and mainly O_h-coordination. These species contained the V–O–V bridging oxygen atoms and according to the mechanism introduced by Kung [5] the presence of these units allows the formation of alkoxide intermediates which are furthermore oxidized to the products of total oxidation. Butenes selectivity dependence on the structure of support material is not so distinct in contrast to the mentioned different activity (TOF) discussed above and this effect is due to the relatively complex mechanism of ODH of *n*-butane. The main factors affecting the selectivity are the vanadium content, the vanadium surface density, the nature of the support (structure, acidity) and the reactions temperature [11,55]. Acid character of siliceous support (iso-electric point (IEP) is ca. 2) has probably major influence on the selectivity. Increasing acidity of the catalysts extend retention period of reaction intermediate on the surface of catalyst. The alkenes (electron-donating molecules) are more basic than the corresponding alkanes and they interact more strongly with acid support [11]. This effect allows us to explain the occurrence of the consecutive reactions with neighboring VO_x species regardless on type of T_d-coordinated species. The distance of neighboring species can be related to the surface density and it is similar for all structures of support with 3.6 wt.% of vanadium (0.6–0.7 V per nm^2). In the case of high-loaded catalysts is problem more complex due to presence of significant amount of vanadium pentoxide.

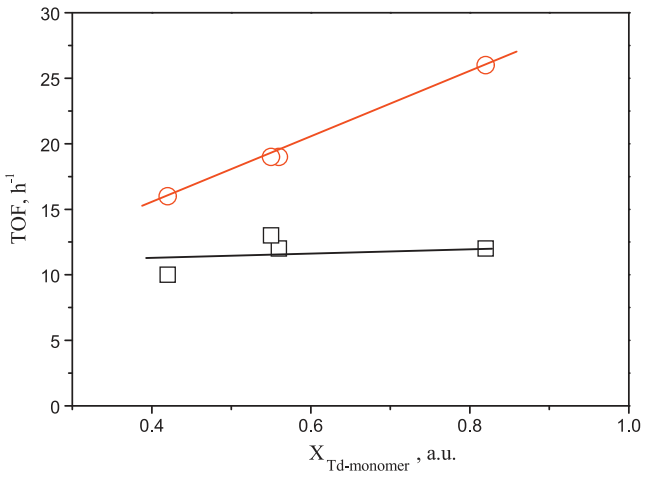

Fig. 11. Dependence of TOF factors of VO_x catalysts with 3.6 wt.% of vanadium on population of monomeric VO_x species determined by deconvolution of DR UV–vis spectra. Red circles – C_4-ODH, black squares – C_3-ODH. (For interpretation of the references to color in this figure legend, the reader is referred to the web version of this article.)

4. Conclusions

The above discussed data allow us to draw the following conclusions:

- Based on H_2-TPR, Raman and DR UV–vis results, it can be concluded that both monomeric and oligomeric species with T_d coordination exist in the all investigated samples. In addition, condensed species with O_h coordination are significantly formed in the samples with vanadium loading of 9 wt.%. Population of individual types of vanadium species is dependent on the type of silica support structure and vanadium content.
- C_3-ODH reaction is sensitive to the presence of condensed species with O_h coordination which caused lowering of catalytic activity and selectivity to propene. Nevertheless, both monomeric and oligomeric tetrahedral species are active and selective in C_3-ODH reaction as is documented by similar iso-conversion selectivity to propene and TOF factors of low-loaded catalysts without condensed VO_x species with O_h coordination, but differing in population of monomeric and oligomeric VO_x species with T_d coordination.
- On the other hand, C_4-ODH reaction is very sensitive to isolation of vanadium species, because monomeric units are much more active and selective than all other species as can be documented by differences in TOF values.
- From comparison of catalytic results of both types of reaction and from characterization of vanadium speciation it can be concluded that SBA-15 support is the most suitable structure for deposition of vanadium in the form of isolated monomeric species which are beneficial for C_3-ODH and necessary for C_4-ODH reactions.

Acknowledgements

This work was supported by the Grant Agency of the Czech Republic under project P106/10/0196 and by the University of Pardubice under project SGFChT04.

References

[1] http://www.icis.com/v2/chemicals/9076454/propylene/pricing.html.
[2] O.V. Buyevskaya, M. Baerns, Catal. Today 42 (1998) 315.
[3] F. Cavani, N. Ballarini, A. Cericola, Catal. Today 127 (2007) 113.
[4] E.A. Mamedov, V.C. Corberan, Appl. Catal. A: Gen. 127 (1995) 1.
[5] H.H. Kung, Advances in Catalysis, vol. 40, Academic Press Inc., San Diego, 1994, p. 1.
[6] M.A. Banares, Catal. Today 51 (1999) 319.
[7] R. Grabowski, Catal. Rev. Sci. Eng. 48 (2006) 199.
[8] S. Albonetti, F. Cavani, F. Trifiro, Catal. Rev. Sci. Eng. 38 (1996) 413.
[9] K. Mori, A. Miyamoto, Y. Murakami, J. Phys. Chem. 89 (1985) 4265.
[10] P.K. Rao, K. Narasimha, ACS Symp. Ser. 523 (1993) 231.
[11] T. Blasco, J.M.L. Nieto, Appl. Catal. A: Gen. 157 (1997) 117.
[12] M.L. Pena, A. Dejoz, V. Fornes, E. Rey, M.I. Vazquez, J.M.L. Nieto, Appl. Catal. A: Gen. 209 (2001) 155.
[13] B. Solsona, T. Blasco, J.M.L. Nieto, M.L. Pena, F. Rey, A. Vidal-Moya, J. Catal. 203 (2001) 443.
[14] Y. Wang, Q.H. Zhang, Y. Ohishi, T. Shishido, K. Takehira, Catal. Lett. 72 (2001) 215.
[15] Q.H. Zhang, Y. Wang, Y. Ohishi, T. Shishido, K. Takehira, J. Catal. 202 (2001) 308.
[16] R. Zhou, Y. Cao, S.R. Yan, J.F. Deng, Y.Y. Liao, B.F. Hong, Catal. Lett. 75 (2001) 107.
[17] Y.M. Liu, Y. Cao, N. Yi, W.L. Feng, W.L. Dai, S.R. Yan, H.Y. He, K.N. Fan, J. Catal. 224 (2004) 417.
[18] E.V. Kondratenko, M. Cherian, M. Baerns, D.S. Su, R. Schlogl, X. Wang, I.E. Wachs, J. Catal. 234 (2005) 131.
[19] S. Shylesh, A.P. Singh, J. Catal. 233 (2005) 359.
[20] J. Liu, Z. Zhao, C.M. Xu, A.J. Duan, L. Zhu, X.Z. Wang, Catal. Today 118 (2006) 315.
[21] J.M. Lopez, Top. Catal. 41 (2006) 3.
[22] X.J. Guo, N.H. Xue, S.M. Liu, X.F. Guo, W.P. Ding, W.H. Hou, Microporous Mesoporous Mater. 106 (2007) 246.
[23] P. Knotek, L. Capek, R. Bulanek, J. Adam, Top. Catal. 45 (2007) 51.
[24] E.V. Kondratenko, O. Ovsitser, J. Radnik, M. Schneider, R. Kraehnert, U. Dingerdissen, Appl. Catal. A: Gen. 319 (2007) 98.
[25] W. Liu, S.Y. Lai, H.X. Dai, S.J. Wang, H.Z. Sun, C.T. Au, Catal. Lett. 113 (2007) 147.
[26] T.V.M. Rao, G. Deo, AICHE J. 53 (2007) 1538.
[27] X. Rozanska, R. Fortrie, J. Sauer, J. Phys. Chem. C 111 (2007) 6041.
[28] K. Samson, B. Grzybowska-Swierkosz, Pol. J. Chem. 81 (2007) 1345.
[29] X. Rozanska, J. Sauer, Int. J. Quantum Chem. 108 (2008) 2223.
[30] T. Blasco, P. Concepcion, J.M.L. Nieto, A. Martinez-Arias, Collect. Czech. Chem. Commun. 63 (1998) 1869.
[31] G. Centi, S. Perathoner, F. Trifiro, A. Aboukais, C.F. Aissi, M. Guelton, J. Phys. Chem. 96 (1992) 2617.
[32] G. Bellussi, G. Centi, S. Perathoner, F. Trifiro, ACS Symp. Ser. (1993) 523.
[33] O.V. Buyevskaya, A. Bruckner, E.V. Kondratenko, D. Wolf, M. Baerns, Catal. Today 67 (2001) 369.
[34] S.A. Karakoulia, K.S. Triantafyllidis, G. Tsilomelekis, S. Boghosian, A.A. Lemonidou, Catal. Today 141 (2009) 245.
[35] S.A. Karakoulia, K.S. Triantafyllidis, A.A. Lemonidou, Microporous Mesoporous Mater. 110 (2008) 157.
[36] F. Ying, J.H. Li, C.J. Huang, W.Z. Weng, H.L. Wan, Catal. Lett. 115 (2007) 137.
[37] Y.M. Liu, W.L. Feng, T.C. Li, H.Y. He, W.L. Dai, W. Huang, Y. Cao, K.N. Fan, J. Catal. 239 (2006) 125.
[38] E. Santacesaria, M. Cozzolino, M. Di Serio, A.M. Venezia, R. Tesser, Appl. Catal. A: Gen. 270 (2004) 177.
[39] L. Owens, H.H. Kung, J. Catal. 144 (1993) 202.
[40] Y.M. Liu, Y. Cao, S.R. Yan, W.L. Dai, K.N. Fan, Catal. Lett. 88 (2003) 61.
[41] Y.M. Liu, Y. Cao, K.K. Zhu, S.R. Yan, W.L. Dai, H.Y. He, K.N. Fan, Chem. Commun. (2002) 2832.
[42] M. Setnicka, R. Bulanek, L. Capek, P. Cicmanec, J. Mol. Catal. A 344 (2011) 1.
[43] P.T. Tanev, T.J. Pinnavaia, Science 267 (1995) 865.
[44] T.W. Kim, F. Kleitz, B. Paul, R. Ryoo, J. Am. Chem. Soc. 127 (2005) 7601.
[45] A. Zukal, H. Siklova, J. Cejka, Langmuir 24 (2008) 9837.
[46] D.Y. Zhao, Q.S. Huo, J.L. Feng, B.F. Chmelka, G.D. Stucky, J. Am. Chem. Soc. 120 (1998) 6024.
[47] I.E. Wachs, B.M. Weckhuysen, Appl. Catal. A: Gen. 157 (1997) 67.
[48] G. Centi, Appl. Catal. A: Gen. 147 (1996) 267.
[49] R. Bulanek, L. Capek, M. Setnicka, P. Cicmanec, J. Phys. Chem. C 115 (2011) 12430.
[50] P. Kubelka, F.Z. Munk, Tech. Phys. 12 (1931) 593.
[51] M. Wojdyr, J. Appl. Crystallogr. 43 (2010) 1126.
[52] W.M.H. Sachtler, N.H.D. Boer, Proc. 3rd Int. Congr. Catalysis, Amsterdam, 1964.
[53] C.H. Lee, T.S. Lin, C.Y. Mou, J. Phys. Chem. B 107 (2003) 2543.
[54] S. Shylesh, A.R. Singh, J. Catal. 244 (2006) 52.
[55] L. Capek, J. Adam, T. Grygar, R. Bulanek, L. Vradman, G. Kosova-Kucerova, P. Cicmanec, P. Knotek, Appl. Catal. A: Gen. 342 (2008) 99.
[56] D.E. Keller, T. Visser, F. Soulimani, D.C. Koningsberger, B.M. Weckhuysen, Vib. Spectrosc. 43 (2007) 140.
[57] M. Mathieu, P. Van Der Voort, B.M. Weckhuysen, R.R. Rao, G. Catana, R.A. Schoonheydt, E.F. Vansant, J. Phys. Chem. B 105 (2001) 3393.
[58] J. Tauc, Amorphous and Liquid Semiconductors, Plenum Press, London, 1974.
[59] F. Gao, Y.H. Zhang, H.Q. Wan, Y. Kong, X.C. Wu, L. Dong, B.Q. Li, Y. Chen, Microporous Mesoporous Mater. 110 (2008) 508.
[60] M. Schramlmarth, A. Wokaun, M. Pohl, H.L. Krauss, J. Chem. Soc. Faraday Trans. 87 (1991) 2635.
[61] G. Catana, R.R. Rao, B.M. Weckhuysen, P. Van Der Voort, E. Vansant, R.A. Schoonheydt, J. Phys. Chem. B 102 (1998) 8005.
[62] B.M. Weckhuysen, D.E. Keller, Catal. Today 78 (2003) 25.
[63] B.A. Morrow, A.J. Mcfarlan, J. Non-Cryst. Solids 120 (1990) 61.
[64] C.J. Brinker, R.J. Kirkpatric, D.R. Tallant, B.C. Bunker, B. Montez, J. Non-Cryst. Solids 99 (1988) 418.
[65] E.L. Lee, I.E. Wachs, J. Phys. Chem. C 111 (2007) 14410.
[66] Z. Wu, S. Dai, S.H. Overbury, J. Phys. Chem. C 114 (2010) 412.
[67] J. Dobler, M. Pritzsche, J. Sauer, J. Phys. Chem. C 113 (2009) 12454.
[68] I.E. Wachs, Catal. Today 27 (1996) 437.
[69] N. Das, H. Eckert, H. Hu, I.E. Wachs, J.F. Walzer, F.J. Feher, J. Phys. Chem. 97 (1993) 8240.
[70] P. Gruene, T. Wolfram, K. Pelzer, R. Schlogl, A. Trunschke, Catal. Today 157 (2010) 137.
[71] J. Santamaria-Gonzalez, J. Luque-Zambrana, J. Merida-Robles, P. Maireles-Torres, E. Rodriguez-Castellon, A. Jimenez-Lopez, Catal. Lett. 68 (2000) 67.
[72] H. Berndt, A. Martin, A. Bruckner, E. Schreier, D. Muller, H. Kosslick, G.U. Wolf, B. Lucke, J. Catal. 191 (2000) 384.
[73] G. Du, S. Lim, M. Pinault, C. Wang, F. Fang, L. Pfefferle, G.L. Haller, J. Catal. 253 (2008) 74.
[74] G. Martra, F. Arena, S. Coluccia, F. Frusteri, A. Parmaliana, Catal. Today 63 (2000) 197.
[75] M.M. Koranne, J.G. Goodwin, G. Marcelin, J. Catal. 148 (1994) 369.
[76] P. Kustrowski, Y. Segura, L. Chmielarz, J. Surman, R. Dziembaj, P. Cool, E.F. Vansant, Catal. Today 114 (2006) 307.
[77] F. Arena, F. Frusteri, A. Parmaliana, Appl. Catal. A: Gen. 176 (1999) 189.
[78] J.M. Kanervo, M.E. Harlin, A.O.I. Krause, M.A. Banares, Catal. Today 78 (2003) 171.
[79] M.A. Banares, J.H. Cardoso, F. Agullo-Rueda, J.M. Correa-Bueno, J.L.G. Fierro, Catal. Lett. 64 (2000) 191.
[80] M.V. Martinez-Huerta, J.L.G. Fierro, M.A. Banares, Catal. Commun. 11 (2009) 15.
[81] M.V. Martinez-Huerta, X. Gao, H. Tian, I.E. Wachs, J.L.G. Fierro, M.A. Banares, Catal. Today 118 (2006) 279.
[82] G. Grubert, J. Rathousky, G. Schulz-Ekloff, M. Wark, A. Zukal, Microporous Mesoporous Mater. 22 (1998) 225.

PAPER VI

V-SBA-15 prepared by direct synthesis as high performing catalyst in oxidative dehydrogenation of *n*-butane

Michal Setnička[1, *], *Pavel Čičmanec*[1], *Roman Bulánek*[1], *Arnošt Zukal*[2], *Jakub Pastva*[2]

[1] Department of Physical Chemistry, University of Pardubice, Studentská 573, CZ532 10 Pardubice, Czech Republic

[2] J. Heyrovský Institute of Physical Chemistry Academy of Sciences of the Czech Republic, v.v.i., Dolejškova 2155/3, CZ182 23 Prague 8, Czech Republic

* corresponding author: Email: Michal.Setnicka@upce.cz , tel. +420 466 037 345

Abstract

The catalytic oxidative dehydrogenation (ODH) of light alkanes has great potential to be used for production of alkenes instead classically used dehydrogenation. We report successful direct synthesis of V-SBA-15 mesoporous molecular sieve ($n_{Si}/n_V \approx 10$) which could be convenient catalyst for ODH of alkane. The productivity (1.92 $kg_{prod.}$ $kg_{cat.}^{-1}$ h^{-1}) in *n*-butane ODH is 3-4 times higher in comparison to supported vanadium catalysts prepared by wet impregnation method and belongs to the three best catalytic systems which were reported for ODH of *n*-butane ever. Moreover, reported catalytic system exhibits catalytic activity stable for more than 8 hours in the stream.

Keywords - *vanadium oxide, V-SBA-15, direct synthesis, n-butane, oxidative dehydrogenation, mesoporous silica*

Highlights

- Successful direct synthesis of mesoporous V-SBA-15 with 7.4 wt.% of vanadium.
- All vanadium oxide units are on the support and accessible for redox process.
- The high activity (TOF = 45 h^{-1}) and high selectivity to C_{4}-$_{deh}$ products (60 %) at conversion of 13%.
- The productivity in *n*-butane ODH is 3-4 times higher in comparison impregnated samples.
- One from the three best catalytic systems for ODH of *n*-butane ever.

Graphical abstract

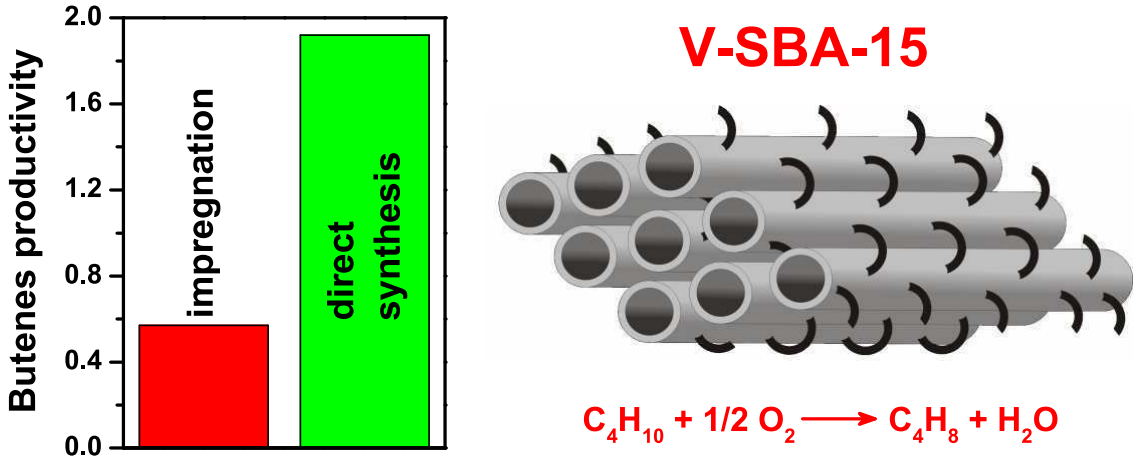

1. Introduction

The oxidative dehydrogenation (ODH) of light alkanes has great potential to be used in production of increasingly demanded alkenes instead of classically used dehydrogenation (DH) which suffers by high energy consumption and fast deactivation of catalysts requiring its frequent regeneration [1]. However, the direct using of ODH reaction over the present known and tested catalysts is still not possible due to low alkenes selectivity and productivity, not sufficient for their applicability in industrial plants. And that is why it is important to develop suitable new catalytic systems with high selectivity and productivity [2].

A wide range of catalysts have been studied in ODH of hydrocarbons as was reported in many reviews before [1-4] and most of them contained oxides of the transition metals, mainly the vanadium oxides. Vanadium oxide based catalysts are very often used as catalysts in the ODH reaction due to their lower temperature required for the activation of C-H bonds and suitable geometric and electron structure of VO_X (tunable by used matrix) [1, 5]. Nevertheless, vanadium oxide catalysts can not be used in its bulk form (leading to non selective reactions) but in the form of dispersed vanadium oxide species embedded to the matrix of practically inert material (silica, MgO, Al_2O_3, ZrO_2, TiO_2 etc.). The support strongly affects the catalytic performance of vanadium supported catalysts. The textural properties and acid-base character of the support are the most important factors, which influence dispersion of vanadium and the retention period of reactants on the surface. The MgO support was very often referred like the most suitable support for vanadium based catalysts used in ODH of *n*-butane, due its acid-base properties. Nevertheless, MgO support has area only about 100-150 m^2g^{-1} what limits attainable vanadium loading.

Another very often used supports are silica based materials with a large number of different structures. Our recent study showed that the mesoporous silica-based material with SBA-15 structure which combines high surface area, proper surface acidity and good thermal

and hydrothermal stability is suitable support for ODH of *n*-butane [6]. The method of the deposition of active vanadium species is another very important parameter which strongly influences the degree of dispersion and coordination of VO_X units on the surface. The simple wet impregnation method by vanadium salts (NH_4VO_3, vanadyl acetylacetonate) is very often used for the deposition of VO_X species. However, this method usually leads to materials with a broad distribution of VO_X species and also to formation non-selective bulk-like vanadium oxide with octahedral coordination [7, 8]. The isolated monomeric VO_X species (favorable in C_4-ODH reaction) are formed only up to 4-5 wt.% of V which is too low to achieve acceptable productivity (one of the most important parameter for industrial applicability) [2]. Above this concentration polymeric VO_X species with high polymerization degree and bulk like V_2O_5 are generated and it means rapid loss in activity and selectivity to required alkene. The direct hydrothermal synthesis of mesoporous vanadosilicate is an alternative method for incorporation of VO_X species on the silica surface or to the silica wall. This method leads to catalysts with better dispersion and with higher performance in ODH reactions [7, 9].

On the basis of our previous studies we choose the SBA-15 as the best silica support [6] and the direct synthesis as the most suitable method for deposition of vanadium to the surface [7, 9]. In the present work we report simple one-pot V-SBA-15 catalyst synthesis based on ref. [10] and its high catalytic performance in ODH of *n*-butane.

2. Experimental

The 4.0 g Pluronic P123 ($EO_{20}PO_{70}EO_{20}$) was dissolved in 30.0 g of water and stirred for 4 h. The 9.0 g tetraethyl orthosilicate (TEOS) and the appropriate amount of ammonium metavanadate (NH_4VO_3) were added directly to the homogeneous solution ($n_{Si}/n_V = 10$, *i.e. ca.* 7.4 wt.%). Then proper quantities of 0.30 M HCl were added to adjust the pH value of mixture to 3.0. The gel was stirred for 24 h and then maintained at 100°C for another 48 h.

The resultant dark-green precipitate was collected, washed thoroughly with distilled water and absolute ethanol for several times and dried at 70 °C for 12 h. The as-prepared product was then calcined in air stream at 550 °C for 6 h with a heating rate of 1 °C min^{-1} to remove the template.

The *n*-butane ODH reaction was carried out in a glass plug-flow fixed-bed reactor at atmospheric pressure in the kinetic region (independently checked) and under steady state conditions of reaction. The activity and selectivity of catalysts were tested at 540 °C in the dependence on contact time (W/F 0.03, 0.06, 0.09, 0.12 and 0.15 g_{cat} s^{-1} cm^{-3}). The demanded weight of catalyst (grains 0.25-0.50 mm) was mixed with 3 cm^3 of inert SiC. The catalysts were pre-treated in the oxygen flow at 450 °C for 2 hours before each reaction run. The input feed composition was *n*-C_4H_{10}/O_2/He = 5/5/90 vol.% - with a total flow rate of 100 cm^3 min^{-1} STP. The analysis of reaction mixture composition was made by on-line gas chromatograph.

More details about characterization techniques (XRF, N_2 adsorption-desorption isotherm measurement and H_2-TPR, analysis of reaction mixture, calculation conversion, selectivity and productivity) which were used for characterization of synthesized V-SBA-15 can be found in our previous papers [6, 7].

3. Results and discussion

3.1. Characterization

The concentration of vanadium determined from XRF was 6.5 wt.% for calcined V-SBA-15 catalysts and it means that almost 90% of vanadium from synthesis gel was incorporated to SBA-15 structure.

The N_2 adsorption-desorption isotherm resembles the isotherms for synthesized V-SBA-15 materials published previously [10, 11]. The isotherm was type IV with H1

hysteresis loop which is typical for mesoporous materials and the total surface area (S_{BET}) was 360 m^2g^{-1}. The catalyst contains negligible volume of micropores but large volume of mesopores (1.22 cm^3 g^{-1}) compared to materials prepared by impregnation. The mesopore diameter determined by BJH algorithm from desorption branch of isotherm was 8 nm. Catalysts with these parameters enable good dispersion of vanadium active species and fast diffusion of reactant and products, respectively what it is important for attainment high performance of catalyst.

The common problem of metal-silica materials catalysts prepared by direct synthesis is the fact that some part of metal can be buried in silica wall and can not participate as active species in reaction. For the check of accessibility of active vanadium species we carried out H_2-TPR experiment. The overall hydrogen consumption during H_2-TPR experiment corresponds to change of oxidation state during the reduction process and it was 1.92 of electrons per vanadium atom in this case. It indicates the fact that the most of vanadium oxo-species is accessible for redox processes (at least 96 % of vanadium, when we suppose quantitative reduction of V^{+V} to V^{+III}). Hence we can use total concentration of vanadium to calculate the value of TOF (turn-over-frequency) per one vanadium atom as the criterion for the comparison of catalytic activity of tested catalyst samples.

3.2. Catalytic activity

The oxidative dehydrogenation of *n*-butane over investigated V-SBA-15 catalyst was studied at temperature 540 °C. The results of catalytic tests are presented in Table 1 and the main reaction products identified in the reaction mixture were: 1-butene (1-C_4), *cis*- and *trans*-2-butene (*c*-C_4 and *t*-C_4), 1,3-butadiene (1,3-C_4), cracking products, *i.e.* methane, ethane, ethene, propane and propene (C_1-C_3) and carbon oxides (CO_X). No oxygenate products were observed and the carbon balance was 98 ± 3 %. The *n*-butane conversion over

empty reactor (reactor filled only by SiC) was lower than 0.5 % under the same conditions (composition of feed and temperature) therefore we can exclude participation of gas phase reaction under this reaction conditions. The stability of catalyst performance in time was almost the same as we reported for V-SBA-15 material prepared by wet impregnation method [6]. Data which will be discussed in this paper were obtained after 3 hours on-stream.

The maximum of catalytic activity of synthesized V-SBA-15 expressed by TOF value was 45 h^{-1}. This value is significantly higher then TOF value for the V-SBA-15 catalysts prepared by simple wet impregnation (TOF = 26 h^{-1} and 11 h^{-1} for sample with 3.6 and 9 wt.% of V, respectively) which were investigated under the same reaction conditions [6]. The others authors published the TOF value for V-SBA-15 system in the *n*C_4-ODH reaction ranging 22-35 h^{-1} [12, 13].

The selectivity to desired products $S_{C4\text{-}deh}$ (in this case 1-C_4, *c*-C_4, *t*-C_4 and 1,3-C_4) is next very important parameter of prepared catalysts. It is very well-known that the selectivity in parallel-consecutive reaction (such as the *n*C_4-ODH reaction) obtained over different catalytic systems must be compared at the same degree of conversion. Therefore the catalytic behaviour of synthesized V-SBA-15 catalyst was compared with previously published data for V-SBA-15 prepared by impregnation under iso-conversion conditions at *n*-butane conversion of 13%. Moreover, it must be noted that conversion of oxygen did not exceed 35% in any case and therefore selectivity value to product were not influenced by a lack of reactant. The selectivity ($S_{C4\text{-}deh}$ = 59%) of synthesized V-SBA-15 with 6.5 wt.% of V was equal to selectivity achieved over impregnated V-SBA-15 with 3.6 wt.% of V (see Table 1 and Ref. [6]) and even the distribution of individual $C_{4\text{-}deh}$ products was the same. The big advantage of direct synthesized samples is the fact that the value of high selectivity value could be obtain even over samples with the high vanadium concentration while for samples prepared by impregnation remains on high value only up to vanadium concentration around

4-5 wt.% of V. The selectivity is rapidly declining after reaching this concentration in the case of impregnated samples ($S_{C4\text{-}deh}$ = 34% for V-SBA-15 with 9 wt.% of V [6]) and the same behaviour was previously published for two sets (impregnated and synthesized) of V-HMS catalysts which were tested in ODH of *n*-butane and propane [7, 9] where the decline of selectivity was from 45% for sample with 2.1 wt.% of V to 15% or 2% for sample with 8 or 15.7 wt.% of V, respectively). This drop in selectivity of impregnated catalysts was previously attributed to the enhanced population of oligomeric vanadium species [7, 14].

The productivity ($kg_{prod.}\ kg_{cat.}^{-1}\ h^{-1}$) is generally accepted like the best criterion for comparison of different catalytic systems tested in one reaction but under different conditions (temperature, fed composition, contact time etc.) and the value of system productivity is very important for its potential commercial applicability. The lower limit (for this type of reaction) value which is acceptable for industrial using is 1 $kg_{prod.}\ kg_{cat.}^{-1}\ h^{-1}$ [2]. The maximum productivity value obtained over our synthesized V-SBA-15 catalyst was 1.92 $kg_{prod.}\ kg_{cat.}^{-1}\ h^{-1}$. This value, according best of our knowledge, is one of the five highest $C_{4\text{-}deh}$ productivity values which were published for ODH of *n*-butane in literature (for summary see Table 1). The best productivity (4.65 $kg_{prod.}\ kg_{cat.}^{-1}\ h^{-1}$ [15]) in *n*-butane ODH was shown over vanadium containing hydrotalcite with $Mg_3V_2O_8$ as active phase. However, maximum of selectivity to dehydrogenated products was only 31 % (under published conditions) and it is too low for potential industry application [2]. Second catalytic system with high productivity is mixed Fe-Zn-oxide with published $C_{4\text{-}deh}$ productivity around 2.2 $kg_{prod.}\ kg_{cat.}^{-1}\ h^{-1}$ [16] which is only a bit higher than productivity obtained over our catalyst. However, the thermal stability of this catalyst is relatively low and above 500 °C may occur phase transformation [17] what could be again problem for potential industrial using, especially when local grain overheating can occur. Next two catalysts with $C_{4\text{-}deh}$ productivity higher than 1 $kg_{prod.}\ kg_{cat.}^{-1}\ h^{-1}$ were based on the supported vanadium catalysts.

The $C_{4\text{-deh}}$ productivity achieved over vanadium oxide supported on Ti-SiO_2 matrix was 1.65 $kg_{prod.}$ $kg_{cat.}^{-1}$ h^{-1} [18] and for catalyst with vanadium oxide supported on ZrO_2 1.02 $kg_{prod.}$ $kg_{cata.}^{-1}$ h^{-1} [19]. The inconvenience of these catalysts is relatively lower area of support in comparison to SBA-15 support. The high surface area facilitates good dispersion of active vanadium species because only isolated and/or low polymeric tetrahedraly coordinated vanadium units could play the role of the active and at the same time selective species in *n*-butane ODH as was reported previously [7]. Moreover Ti-SiO_2 matrix exhibit lower thermal stability in comparison to pure silica material (SBA-15).

Our current and future research carried out on this type of material is aimed to deeper characterization of V-SBA-15 materials prepared by direct synthesis under different synthesis conditions and their relationship to catalytic properties in ODH of *n*-butane.

4. Conclusion

We have successfully prepared the mesoporous V-SBA-15 catalyst by one pot synthesis. The catalyst contains negligible volume of micropores but large volume of mesopores. Moreover this material contains VO_X species which are accessible for redox reaction what is sometimes problem in the case of samples prepared by direct synthesis.

The V-SBA-15 catalyst exhibit high activity (TOF = 45 h^{-1}) and at the same time relatively high selectivity to C_4-$_{deh}$ products which was about 60 %. The biggest advantage over previously studied catalysts is very high productivity of butenes which is about 1.9 kg_{prod} $kg_{cat.}^{-1}$ h^{-1} and it is three-times higher in comparison to the best impregnated V-SBA-15 samples and more than ten-times higher than impregnated samples with the same concentration of vanadium. This catalyst belongs to the three best catalytic systems which were reported for ODH of *n*-butane ever.

Acknowledgements

The authors thank to the project of the Czech Science Foundation No. P106/10/0196 for financial support.

References

[1] H.H. Kung, Advances in Catalysis, Vol. 40, Academic Press Inc, San Diego, 1994, p. 1.

[2] F. Cavani, N. Ballarini and A. Cericola, Catal. Today, 127 (2007) 113.

[3] R. Grabowski, Catal. Rev.-Sci. Eng., 48 (2006) 199.

[4] L.M. Madeira and M.F. Portela, Catal. Rev.-Sci. Eng., 44 (2002) 247.

[5] T. Blasco and J.M.L. Nieto, Appl. Catal. A, 157 (1997) 117.

[6] R. Bulánek, A. Kalužova, M. Setnička, A. Zukal, P. Čičmanec and J. Mayerová, Catal. Today, 179 (2012) 149.

[7] M. Setnička, R. Bulánek, L. Čapek and P. Čičmanec, J. Mol. Catal. A-Chem., 344 (2011) 1.

[8] S.A. Karakoulia, K.S. Triantafyllidis and A.A. Lemonidou, Microporous Mesoporous Mat., 110 (2008) 157.

[9] R. Bulánek, P. Čičmanec, H. Sheng-Yang, P. Knotek, L. Čapek and M. Setnička, Appl. Catal. A, (2012).

[10] F. Gao, Y.H. Zhang, H.Q. Wan, Y. Kong, X.C. Wu, L. Dong, B.Q. Li and Y. Chen, Microporous Mesoporous Mat., 110 (2008) 508.

[11] M. Piumetti, B. Bonelli, M. Armandi, L. Gaberova, S. Casale, P. Massiani and E. Garrone, Microporous Mesoporous Mat., 133 (2010) 36.

[12] W. Liu, S.Y. Lai, H.X. Dai, S.J. Wang, H.Z. Sun and C.T. Au, Catal. Lett., 113 (2007) 147.

[13] W. Liu, S.Y. Lai, H.X. Dai, S.J. Wang, H.Z. Sun and C.T. Au, Catal. Today, 131 (2008) 450.

[14] R. Bulánek, L. Čapek, M. Setnička and P. Čičmanec, J. Phys. Chem. C, 115 (2011) 12430.

[15] A. Wegrzyn, A. Rafalska-Lasocha, B. Dudek and R. Dziembaj, Catal. Today, 116 (2006) 74.

[16] J.A. Toledo, H. Armendariz and E. Lopez-Salinas, Catal. Lett., 66 (2000) 19.

[17] H. Armendariz, G. Aguilarrios, P. Salas, M.A. Valenzuela, I. Schifter, H. Arriola and N. Nava, Appl. Catal. A, 92 (1992) 29.

[18] E. Santacesaria, M. Cozzolino, M. Di Serio, A.M. Venezia and R. Tesser, Appl. Catal. A, 270 (2004) 177.

[19] D. Gazzoli, S. De Rossi, G. Ferraris, G. Mattei, R. Spinicci and M. Valigi, J. Mol. Catal. A-Chem., 310 (2009) 17.

Table 1 – Results of catalytic tests over directly synthesized V-SBA-15 and its comparison with the best catalysts published for ODH of n-butane.

Catalytic system	T, °C	w_V, wt.%	X C_4H_{10}, %	Selectivity, %						Dehy.[b]	W/F[c]	Productivity[d] to Dehy.	Ref.
				1-C_4	*c*-C_4	*t*-C_4	1,3-C_4	C_1-C_3[a]	CO_x				
$Mg_3V_2O_8$	550	3.5	50							31	0.030	4.65	[15]
Fe-Zn-O	450		19		64		1	0	35	65	0.200	2.23	[16]
V-SBA-15_synt.	**540**	**6.4**	**13**	**23**	**11**	**14**	**11**	**5**	**36**	**59**	**0.018**	**1.92**	this work
V-Ti-SiO_2	500	2.8	8.5	14	14	11	11	1	49	49	0.017	1.65	[18]
V-ZrO_2	330	6.6	43							72	0.074	1.02	[19]
V-SBA-15_impr.	540	3.6	13	23	12	12	12	6	35	59	0.057	0.57	[6]
V-SBA-15_impr.	540	9	13	11	7	9	7	3	64	34	0.052	0.37	[6]

[a] C_1-C_3 = sum of C_1-C_3 hydrocarbons

[b] Dehy. = sum of C_4 alkenes

[c] Contact time = g_{cat} cm^3 s^{-1}

[d] Productivity = $kg_{C4\text{-}deh}$ kg_{cat}^{-1} h^{-1}

PAPER VII

Catalysis Today 204 (2013) 132–139

Contents lists available at SciVerse ScienceDirect

Catalysis Today

journal homepage: www.elsevier.com/locate/cattod

Hexagonal mesoporous titanosilicates as support for vanadium oxide—Promising catalysts for the oxidative dehydrogenation of *n*-butane

Michal Setnička [a,*], Pavel Čičmanec [a], Roman Bulánek [a], Arnošt Zukal [b], Jakub Pastva [b]

[a] Department of Physical Chemistry, University of Pardubice, Studentská 573, CZ532 10 Pardubice, Czech Republic
[b] J. Heyrovský Institute of Physical Chemistry, Academy of Sciences of the Czech Republic, v.v.i., Dolejškova 2155/3, CZ182 23 Prague 8, Czech Republic

ARTICLE INFO

Article history:
Received 22 May 2012
Received in revised form 17 July 2012
Accepted 23 July 2012
Available online 10 September 2012

Keywords:
Mesoporous titanosilicate
Hexagonal mesoporous structure
Vanadium
Oxidative dehydrogenation
Butenes

ABSTRACT

The comparative study of structural properties and catalytic performance of V-containing high-surface mesoporous silica and mesoporous titanosilicate materials (HMS, Ti-HMS) in oxidative dehydrogenation of *n*-butane (C_4-ODH) was carried out. The aim of the study was to investigate effect of different titanium amount incorporated into silica support on the texture, speciation of vanadium complexes and its impact on catalytic performance. Prepared catalysts were characterized by XRF for determination of vanadium content, DTA/TG for thermal stability of matrix, XRD, SEM and N_2-adsorption for study of morphology and texture, FT-IR and DR UV–vis spectroscopy for verification of successful incorporation of Ti to the matrix and H_2-TPR and DR UV–vis spectroscopy for determination of vanadium complex speciation. All prepared materials were tested in *n*-butane ODH reaction at 460 °C. We conclude that titanium was successfully incorporated into mesoporous structure, which was preserved at least up to 600 °C. Catalytic activities of V-Ti-HMS catalysts were approximately four times higher than activity of V-HMS catalyst in spite of the fact that all samples exhibit the same amount of vanadium species with similar distribution. The selectivity to desired products was comparable for all catalysts. Enhanced catalytic activity of V-Ti-HMS materials allows activating of *n*-butane at significantly lower temperature (by 100 °C) compare with V-HMS materials.

1. Introduction

The great challenge of current chemical industry is functionalization of cheap and abundant C_2–C_4 alkanes from crude oil to corresponding olefins. For example, the oxidative dehydrogenation (ODH) of light alkanes can be used for production of alkenes instead of classically used dehydrogenation (DH) requiring very high temperatures (high energy consumption) at which additional coking and deactivation of catalyst normally occur [1–4].

Vanadium oxides are powerful redox catalysts in many industrial processes and they are taken as catalysts in oxidation reactions as well as for ODH [5,6]. However, they cannot be used in its bulk form (it leads to nonselective reactions) [4] but have to be used as the well dispersed VO_X species anchored on the suitable support [2,4,7–9]. Activity and selectivity of these catalysts strongly depend on the degree of vanadium species dispersion [3,5,10,11], method of catalyst preparation [3,10,11] and also the type of support has a dramatic effect [4,7,11,12]. Suitable supports for anchoring active species are mesoporous molecular sieves not only due to their peculiar textural properties but also due to the possibility of various modifications including different structural types and as well as different chemical compositions [13].

A large number of reviews [2,4,7,14–16] and papers dealing with the ODH of light alkanes over vanadium supported materials have been published since 1990s and most of them used different structure of silica materials (e.g. silicalite [11] or mesoporous MCM-41 [17,18], SBA-15 [9,19–22], SBA-16 [9] and HMS [3,10,23,24]). The main advantages of silica mesoporous materials are: larger surface area (a good dispersion of active particles), thermal and hydrothermal stability and good mechanical properties [3,25,26]. Next advantage of catalysts anchored on silica support (compared with Al_2O_3, TiO_2, ZrO_2, etc.) is that catalysts using silica supports are more selective to desired products [27–29]. However, they exhibit relatively low activity and C_4-ODH productivity due to high apparent activation energy of C—H bonds [27,30]. The highest activities and sufficient selectivity in ODH reaction were attained using VO_X species supported on TiO_2 (anatase) surface, which allows to carry out the reaction at lower temperatures [8,11,28,31,32]. Nevertheless, pure TiO_2 support has also some drawbacks, such as a relatively low specific surface area, which can be further reduced by sintering as a consequence of thermal treatments. Low surface area prevents dispersion of vanadium oxide species, which leads

* Corresponding author. Tel.: +420 46 603 73 45; fax: +420 46 603 70 68.
E-mail address: michal.setnicka@upce.cz (M. Setnička).

0920-5861/$ – see front matter © 2012 Elsevier B.V. All rights reserved.
http://dx.doi.org/10.1016/j.cattod.2012.07.028

to the further decrease in selectivity [3,11,31,32]. These drawbacks prevent the use of TiO_2 as conventional support for catalysts. One possibility how to solve this problem is to prepare a mixed Si–Ti support which combines suitable properties of both above mentioned SiO_2 and TiO_2 supports, respectively.

Previous studies showed that coating of silica support with anatase phase (impregnation or grafting by titanium alkoxide) as one of the frequent methods for preparing TiO_2/SiO_2 [1,31], TiO_2/MCM-41 [28,32,33] and TiO_2/SBA-15 [27,34] support. In this case it was obtined thermostable support with high specific surface (silica) and with good catalytic performance (TiO_2). These materials were doped by vanadium and obtained materials were studied in C_2-ODH [31,35], C_3-ODH [1,27,31] and only in one case in C_4-ODH [11] reaction. The disadvantage of materials prepared in this way is their complicated synthesis with multiple synthesis and calcination steps. Moreover, these postsynthetic methods sometimes lead to the blocking of the channels by the formation of bulk metal oxide clusters [36]. To avoid these problems, several attempts have been made to incorporate titanium into the silica framework directly. This problem could be overcome using direct synthesis method as was published previously for Ti-SBA-15 [37,38], Ti-HMS [37,39–41], Ti-MCM-41 [33,40,42] and Ti-MCM-48 [43] but according to our knowledge these materials were not prepared in titanium content higher than 9 wt.% [44].

In the present paper we report on one-pot synthesis of Ti-HMS support with high content of titanium. In this case we obtain hexagonal mesoporous silica support with the isomorphously exchanged titanium oxide species and they serve as an "anchor" for vanadium active species. The reason for this behavior is the difference in the isoelectric point of TiO_2 (IEP = 6–6.4) and SiO_2 (IEP = 1–2) supports. The acidic vanadium oxide species (IEP = 1.4) are preferentially bonded to the more basic TiO_2 [7]. Moreover, acid/base properties of Ti species in the support influence the basicity of the bridging oxygen in sup-O-V (sup = Si, Al, Ti, etc.) and therefore their reactivity [6,27]. The part of the surface composed of silica positively affects selectivity to desired ODH products. We prepared three HMS support with different content of titanium (0, 6 and 19 wt.%, respectively). These materials were investigated by DTA/TG, FT-IR, N_2-BET, SEM, XRD and DR UV–vis spectroscopy for the physico-chemical characterization of the mesoporous support structure. After impregnation of these matrices by vanadium we verified preservation of mesoporous structure. We used DR UV–vis spectroscopy and H_2-TPR for investigation of vanadium dispersion and for the study of catalytic activity we used ODH of *n*-butane which is interesting for the industry as well as very suitable model reaction at the same time [3,11].

2. Experimental

2.1. Catalysts preparation

The hexagonal mesoporous silica (HMS) and hexagonal mesoporous titanosilica (Ti-HMS), were synthesized under ambient conditions according to the procedure reported by Tanev and Pinnavaia [45] with their modification for Ti-HMS. In a typical preparation, dodecylamine (DDA, Aldrich) as a neutral structure directing agent was added to the mixture of ethanol and re-distilled water. After 20 min of homogenization tetraethylorthosilicate (TEOS, Aldrich) was added as silica precursor in the case of HMS preparation or TEOS and tetraethylorthotitanate (TEOT, Aldrich) as a titanium precursor was added simultaneously in the case of Ti-HMS preparation. The reaction mixture was stirred at room temperature for 18 h. The solid product was filtered, washed by ethanol and calcined in air at 450 °C for 20 h (with heating rate 1 °C/min) for the template removal.

The vanadium oxo-species (1.5 wt.% of V) were introduced onto the support by the wet impregnation method from EtOH solution of vanadyl acetylacetonate. Impregnated samples were dried at 120 °C in air overnight and then calcined at 600 °C in air for 8 h (with heating rate 5 °C/min).

The investigated samples were denoted as *x*Ti-HMS, where *x* is the titanium content in support in the weight percentage. V-*x*Ti-HMS is used for materials after impregnation of vanadium.

2.2. Catalysts characterization

The content of titanium was determined by means of ICP-OES by Integra XL 2 (GBC Dandenog, Australia) for both prepared Ti-HMS supports. The vanadium content was determined by means of ED XRF by ElvaX (Elvatech, Ukraine) equipped with Pd anode [46]. Samples were measured against the model samples (a mechanical mixture pure SiO_2 and $NaVO_3$) granulated to the same size as catalysts.

The structure and crystallinity of catalysts were probed by scanning electron microscopy (SEM) using JSM-5500LV microscope (JEOL, Japan) and by X-ray diffraction (D8-advance diffractometer, Bruker AXE, Germany) in the 2θ range of 2–35° with Cu Kα radiation ($\lambda = 1.5406$ Å).

Specific surface area and texture of investigated samples were measured by means of nitrogen adsorption/desorption at temperature of liquid nitrogen for verification of mesoporous structure by using ASAP 2020 equipment (Micromeritics, USA). Prior to adsorption isotherm measurement, the samples were degassed at 300 °C under turbomolecular pump vacuum for 8 h. The specific surface area was calculated according to BET method. The mesopore volume was determined by DFT by using of "N2 @ 77K" model for cylindrical pores and oxide surface.

Thermal stability of prepared matrix was studied using Jupiter STA 449C (Netzsch, Germany) thermobalance. Around 40–50 mg of matrix were heated in corundum TG–DTA-crucibles under a flow of air at a heating rate of 10 °C/min up to 1200 °C and the α-Al_2O_3 was used as a reference material.

For verification of successful incorporation of titanium to the HMS matrix the infrared spectra were collected on Nicolet 6700 FTIR spectrometer equipped with DTGS detector. Samples were diluted using dry KBr, pressed into pellets and scanned in the range 1400–400 cm^{-1} with a resolution of 2 cm^{-1} (32 scans). The spectrum of blank KBr pellet was also measured to allow background subtraction.

The UV–vis diffuse reflectance spectra of dehydrated diluted samples were measured by using Cintra 303 spectrometer (GBC Scientific Equipment, Australia) equipped with a Spectralon-coated integrating sphere using a Spectralon coated discs as a standard. The spectra were recorded in the range of the wavelength 190–850 nm. The samples were diluted by the pure silica (Fumed silica, Aldrich) in the ratio 1:100 for avoid spectra detection limits overflow and to give better resolution of individual bands. All samples were granulated and sieved to fraction of size 0.25–0.5 mm, dehydrated before the spectra measurement and oxidized in the glass apparatus under static oxygen atmosphere in two steps: 120 °C for 30 min and 450 °C for 60 min and subsequently cooled down to 250 °C and evacuated for 30 min. After the evacuation the samples were transferred into the quartz optical cuvette 5 mm thick and sealed under vacuum. Additional details about diluting and measuring can be seen in Refs. [47,48]. The obtained reflectance spectra were transformed into the dependencies of Kubelka–Munk function $F(R_\infty)$ on the absorption energy $h\nu$ using the equation:

$$F(R_\infty) = \frac{(1 - R_\infty)^2}{2R_\infty} \quad (1)$$

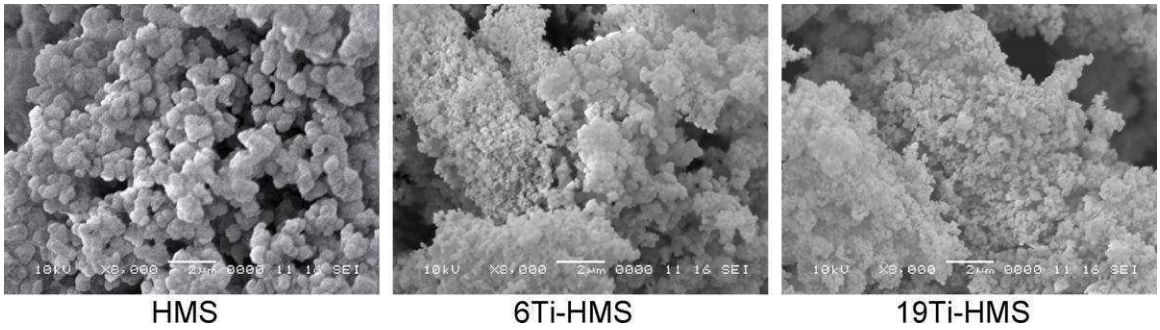

Fig. 1. SEM images of mesoporous HMS and Ti-HMS supports.

where R_∞ is the measured diffuse reflectance from a semi-infinite layer [49].

Hydrogen temperature programmed reduction (H_2-TPR) was used for the study of redox properties and AutoChem 2920 (Micromeritics, USA) was used for the measuring. A 100 mg sample in a quartz U-tube micro reactor was oxidized in oxygen flow at 450 °C (for 2 h). The reduction was carried out from 35 °C to 850 °C with a temperature gradient of 10 °C/min in flow of reducing gas (5 vol.% H_2 in Ar). The changes in hydrogen concentration were monitored by online connected TCD detector.

2.3. Catalytic tests

The *n*-butane ODH reaction was carried out in a glass plug-flow fixed-bed reactor at atmospheric pressure in the kinetic region (independently checked) and under steady state conditions of reaction. Typically 400 mg of catalyst (grains 0.25–0.50 mm) was diluted with 3 cm^3 inert SiC to avoid the catalytic bed overheating. The catalysts were pre-treated in the oxygen flow at 450 °C for 2 h before each reaction run. The input feed composition was $C_4H_{10}/O_2/He = 10/10/80$ vol.% – with a total flow rate of 100 cm^3 min^{-1} STP. The catalytic activity was measured at 460 °C under the steady state conditions. The analysis of reaction mixture composition was made by on-line gas-chromatograph CHROM-5 (Laboratorní přístroje Praha) equipped with thermal conductivity detector (TCD) and flame ionization detector (FID). The *n*-butane and products of ODH reaction (butadiene, 1-butene, *cis*-2-butene, *trans*-2-butene, propene and propane) were separated using a packed column with *n*-octane on ResSil (Restek) at 20 °C. The packed column Porapak Q (Supelco) was used for the analysis of ethane, ethene and CO_2. The molecular sieve 13 X (Supelco) was used for the separation of permanent gases (O_2, CO and traces of N_2). For details about calculation conversion, selectivity, yield and productivity please see our previous work [3].

3. Results and discussion

3.1. Characterization of materials

SEM images of prepared supports (Fig. 1) show poorly defined morphology of every studied sample. Particles exhibit uneven shapes of sub-micrometer size. Size of particles of Ti-HMS supports is significantly (approximately three-times) smaller than particles of pure silica HMS support. Similar observation has been described by Comite et al. [1] who prepared TiO_2/SiO_2 support by grafting and they assign this behavior to modification in calcination step. SEM–EDX mapping of Ti content led to the conclusion that Ti is spread homogeneously in all parts of support and no TiO_2 clusters were detected. Moreover mapping of vanadium content in the catalysts prepared by impregnation of supports shows that vanadium is distributed uniformly in all parts of catalysts and no V_2O_5 clusters and typical orthorhombic needles were observed in any sample (not shown here).

XRD patterns of supports and catalysts show (see Fig. 2) characteristic broad low-angle diffraction peak at $2\theta = 2$–$2.5°$ attributable to a d_{100} diffraction typical for hexagonal lattice structure of mesoporous materials [40,45]. The value of d_{100} spacing slightly changed for individual support in the range from 3.3 to 3.9 nm in correspondence with literature [42,50]. This result corresponds to the changes in pore size distribution obtained from N_2 adsorption/desorption isotherm NLDFT analysis (see inset in Fig. 3). In addition, very broad peak with low intensity among 15–35° was detected in the X-ray powder patterns of all samples. This signal is usually assigned to the presence of amorphous SiO_2 wall [51,52]. Similar patterns were reported for hexagonal mesoporous materials in literature [10,40–42,50,53]. Absence of diffraction lines belongs to TiO_2 (anatase and/or rutile) crystallites or V_2O_5 crystallites in the XRD patterns of all supports and catalysts confirm results from SEM; titanium is incorporated into HMS framework and do not form separated crystallites of TiO_2 and vanadium species are finely spread on the surface of supports without creation of oxide-like clusters or separated V_2O_5 crystallites.

BET specific surface area of parent materials and catalysts are summarized in Table 1. S_{BET} of parent supports slightly decreases with increasing content of titanium and ranges from 880 m^2 g^{-1} for pure HMS to 800 m^2 g^{-1} for 19Ti-HMS and these values are in a good agreement with data published previously for similar type of materials with lower content of Ti in matrix [37,40]. Such high values of specific surface area together with type IV isotherms with capillary condensation step and H4 hysteresis loop indicate

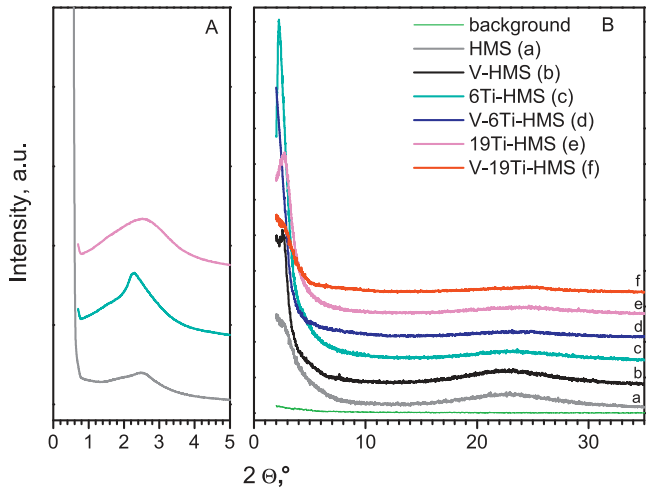

Fig. 2. (A) Low-angle diffraction patterns for parent supports and (B) X-ray diffraction patterns for parent supports and supports after impregnation by vanadium (XRD patterns were offset for clarity).

Table 1
Chemical composition and results of physico-chemical characterization of investigated materials.

Sample	$Ti_{(matrix)}$ [a] (wt.%)	V [a] (wt.%)	S_{BET} ($m^2\ g^{-1}$)	V_P [b] ($cm^3\ g^{-1}$)	D_{ME} [c] (nm)	T_{onset} [d] (°C)	T_{max} [e] (°C)	Δe [f]	E_g [g](eV)
HMS	0.00	0.0	880	0.560	2.4–3.1	–	–	–	–
V-HMS	0.00	1.5	650	–	–	397	562	2.1	3.73
6Ti-HMS	6.0	0.0	890	0.532	2.6–3.2	–	–	–	3.78
V-6Ti-HMS	6.0	1.5	690	–	–	376	586	2	3.66
19Ti-HMS	12.0	0.0	800	0.495	2.4–3.0	–	–	–	3.72
V-19Ti-HMS	12.0	1.5	770	–	–	376	609	1.6	3.65

[a] Titanium resp. vanadium content determined by XRF method (error: ±0.2 wt.%).
[b] V_P total pore volume determined at $p/p_0 = 0.97$.
[c] D_{ME} mesopore diameter determined by NLDFT.
[d] Onset temperature of H_2-TPR profile.
[e] Position of maxima of H_2-TPR profile.
[f] Average change of oxidation state during H_2-TPR experiment.
[g] Energy of absorption edge determined by Tauc's method [60].

mesoporous character of solids (Fig. 3). Pore size distribution for all three matrices exhibits distribution of pore diameter in the range from 2 to 4 nm (see inset in the Fig. 3 and Table 1). S_{BET} of catalyst modified by vanadium is significantly lower, as is very often observed for impregnated catalysts [3,10,28]. Surface area loss ranges from ca. 25% for V-HMS sample to 44% for V-6Ti-HMS sample. This surface area loss is attributed in the literature to partial destruction of the framework [32] or rather by blocking of pores by oxide nanoclusters (in this case not detectable by XRD) because our previous works showed systematic surface degree with increasing vanadium content [3,10,32].

The IR spectra of powder supports and catalysts in KBr pellets before and after reaction are reported in Fig. 4 in the 1300–400 cm^{-1} range, where the skeletal vibrational modes occurs. The bands at 1228, 1091, 963, 798 and 470 cm^{-1} perceptible in all spectra are characteristic for the silica network. The broad feature at 1228 and 1091 cm^{-1} is assigned to inter-tetrahedral and intra-tetrahedral asymmetric stretch vibrations of T—O—T, respectively. Bands at 798 and 470 cm^{-1} can be assigned to symmetric stretching modes of T—O—T vibration and T—O bending modes, respectively. Finally, the feature at 950 cm^{-1} can be assigned to two overlapping peaks of ν(Si—O—H) and ν(Ti—O—Si) vibration [1,33,44,54]. In any case, no spectral feature of crystalline TiO_2 (anatase and/or rutile) with characteristic dominant broad band at 600–650 cm^{-1} [55–57] was detected in the spectra of KBr pellets of both Ti-HMS supports. This is another indication that titanium is relatively homogeneously incorporated into framework. All catalysts after reaction condition treatment have the same spectral characteristics as the fresh catalysts; no changes in the band intensity or occurrence of new band were detected. Therefore, it can be concluded that catalysts are stable under reaction conditions.

Thermal stability of supports was investigated by DTA in the temperature range from ambient temperature to 1200 °C (see Fig. 5). DTA curves of all three supports exhibit weak endothermic process at about 130 °C, which is ascribed to removal of physisorbed molecules of water and long time drift of baseline caused by different values of thermal heat capacity of samples and α-Al_2O_3 standard referent respectively. No other process was detected for pure silica HMS support. On the contrary, exothermic processes are observed above 650 °C for Ti-HMS supports (peak maxima are at 750, 900 and 1040 °C for 19Ti-HMS and at 1050 and 1080 °C for 6Ti-HMS). These signals can be assigned to destruction of mesoporous titanosilicate framework and separation of SiO_2 and TiO_2 phase [55]. Similar behavior was published by Morey et al. [43] for material Ti-MCM-48 which is stable up to 800 °C. On the other hand some authors reported stability of titanium mesoporous silica materials even up to 1000 °C [58].

DR UV–vis spectra of both supports and vanadium catalysts under study are presented in Fig. 6. All samples exhibit absorption bands in the range of photon energies from 3 to 6 eV attributed to ligand to metal charge-transfer (LMCT) transitions of the $O \rightarrow V^{+V}$ and/or $O \rightarrow Ti^{+IV}$ type. HMS support exhibits only very low intensity spectrum, whereas spectra of Ti-HMS supports exhibit very intense absorption bands with maxima at 4.29, 4.70 and 5.74 eV (289, 264 and 216 nm, respectively), which overlap absorption bands

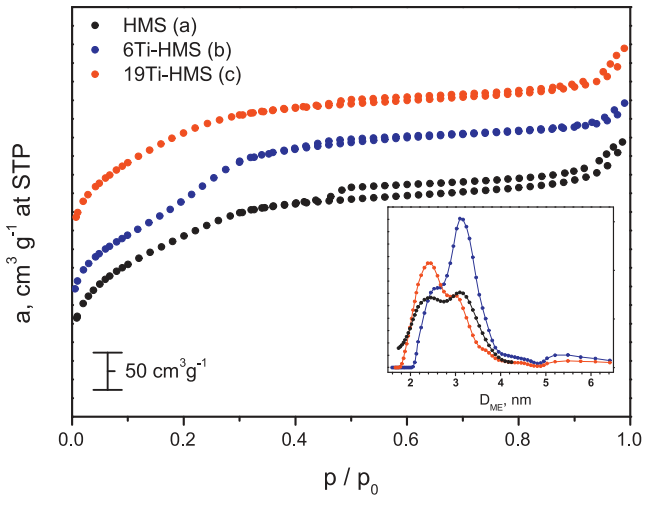

Fig. 3. Nitrogen adsorption isotherms of bare supports (isotherms were offset for clarity). Inset: pore size distribution of bare supports determined by DFT method for cylindrical pores and metal oxide surface.

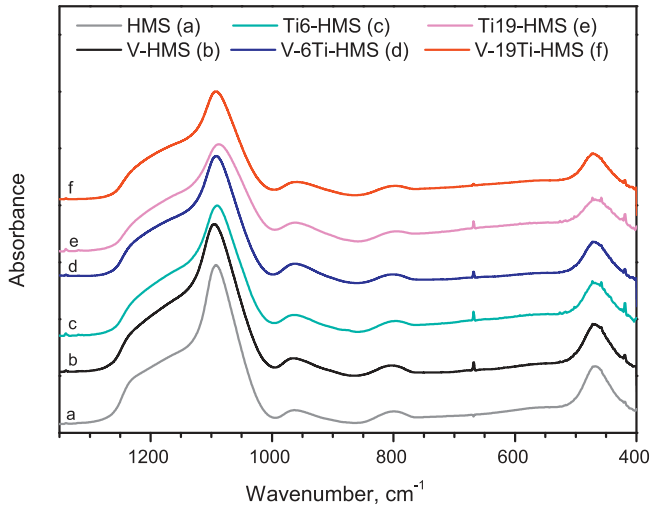

Fig. 4. FT-IR spectra of KBr pellets of supports and supports after impregnation by vanadium (spectra were offset for clarity).

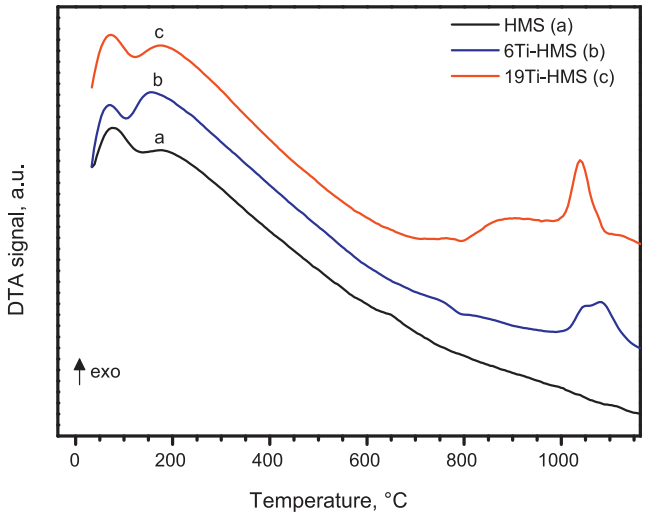

Fig. 5. Thermal analysis pattern of HMS and Ti-HMS supports (curves were offset for clarity).

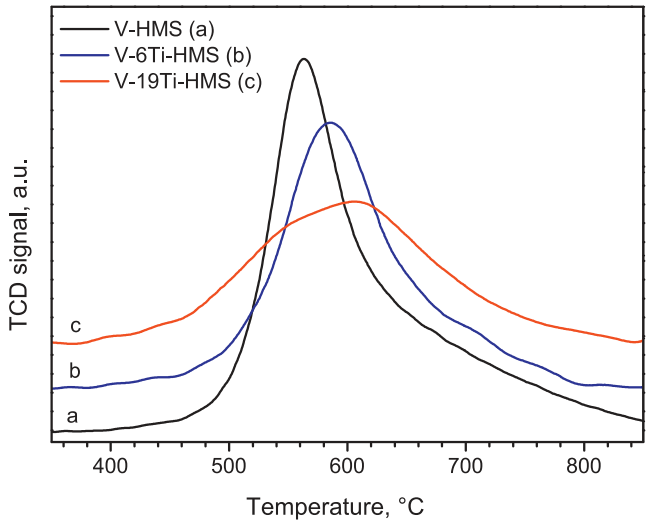

Fig. 7. H_2-TPR patterns of V-HMS and V-Ti-HMS samples (curves were offset for clarity).

belonging to vanadium species in the spectra of vanadium catalysts. This is in a good agreement with spectra published previously for mesoporous titanosilicate support [27,37,40]. LMCT transitions are strongly influenced by the type and number of ligands surrounding the central metal ion in the first coordination sphere and, therefore, provide information on its local coordination environment. The absorption edge energy (E_g) of the spectra is usually employed for this purpose [6,59,60]. The values of E_g of all samples are listed in Table 1. Comparison of our Ti-HMS samples spectra with spectra of referent materials (TS-1 representing isolated titanium atoms surrounded by SiO_4 tetrahedra and rutile representing bulk Ti—O—Ti network) displayed in the $[F(R_\infty)\ h\nu]^2$ vs. $h\nu$ coordinates (see inset in Fig. 6) led to conclusion that titanium in our samples is predominantly present in the form of isolated TiO_4 tetrahedra, because values of energy edges of our samples is 3.78 eV and 3.72 eV for 6Ti-HMS and 19Ti-HMS, respectively. These values are very close to the value of energy edge of TS-1 silicalite (E_g = 3.82 eV) whereas rutile/anatase exhibits lower energy edge (E_g = 3.11 eV) [40,61]. Small differences in energy edge value of TS-1 and our

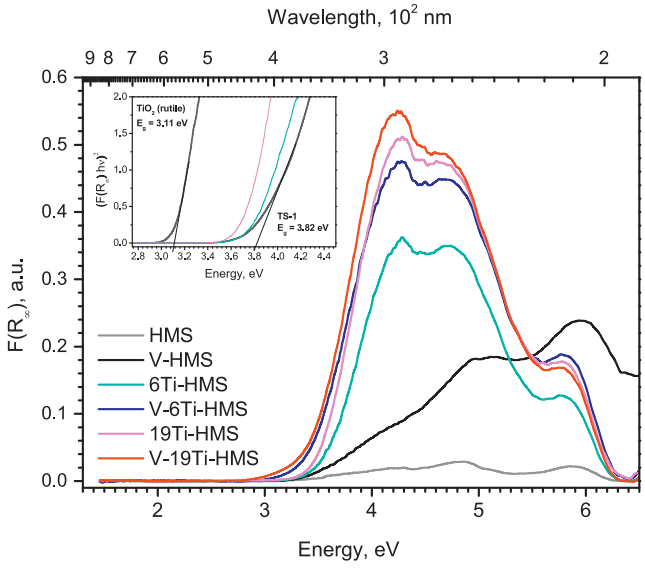

Fig. 6. Diffuse reflectance UV–vis spectra of diluted and dehydrated supports and supports after impregnation by vanadium.

materials (lower value of E_g) is probably due to small amount of titanium species coordinated in an octahedral coordination or Ti-O-Ti clustering in the framework, which are not detected by XRD [40,62]. Presence of vanadium complexes in the sample leads to increase in intensity of spectra and slight red-shift of energy edges to the lower value. Energy edges of all vanadium catalysts fall to very narrow interval from 3.73 to 3.65 eV indicating very similar distribution of vanadium species. Based on the empirical correlation of these values with the structure of referent compounds and absorption edge energies of their UV–vis spectra (sodium ortho-vanadate Na_3VO_4 with E_g = 3.83 eV and meta-vanadate $NaVO_3$ E_g = 3.16 eV as compounds containing only isolated monomeric tetrahedral units and linearly polymerized tetrahedral units [47]) can be concluded that all vanadium species in our investigated catalysts are in tetrahedral coordination (no spectral signals under 3.16 eV). Unfortunately, we cannot determine the amount of monomeric and polymeric species, as was published previously [3,10]. Determination prevents overlapping absorption bands belonging to vanadium species by the intensive bands belonging to titanium. On the other hand we can say that most of the species are in isolated or low-polymeric form.

H_2-TPR curves of VO_X catalysts are depicted in Fig. 7 and values of onset temperature and temperature of reduction peak maxima are summarized in Table 1. It should be noted that parent supports exhibited no reduction peaks and therefore they are not reported here for the sake of brevity. TPR curves of all samples exhibit only one reduction peak in the temperature range from 400 to 800 °C. The overall hydrogen consumption corresponds to change of oxidation state during the reduction. The change of oxidation state varies from 1.6 to 2.1 of electrons per vanadium atom (see Table 1) indicating reduction from V^{+V} to V^{+III} or in some case partially only to V^{+IV}. Maximum of the reduction peak shifts to higher temperature with increasing titanium content. V-HMS catalysts exhibit reduction peak with maximum at 562 °C, whereas maxima of reduction peaks of V-Ti-HMS catalysts are at 586 and 609 °C for V-6Ti-HMS and V-19Ti-HMS, respectively. In addition, the reduction peak becomes broader with increasing titanium content. However, it is contrary to investigation of redox behavior of vanadium species on pure titanium oxide or pure silica support reported in the literature. Most authors present that vanadium complexes on TiO_2 are more reducible (reduction of vanadium on the TiO_2 proceed at a temperature about 100 °C lower) than vanadium on silica support [63,64]. But we can see this behavior only at V-titanosilicates where the support is prepared by impregnation of pure silica by

Table 2
Results of catalytic tests for bare supports and support with impregnated vanadium at 460 °C (m_{cat} = 400 mg, $C_4H_{10}/O_2/He$ = 10/10/80 vol.%, total flow rate of 100 cm^3 min^{-1}).

Sample	Conv. (%)	Selectivity							Yield (%)	Productivity[c]
	C_4H_{10}	1-C_4	*c*-C_4	*t*-C_4	1,3-C_4	C_1-C_3 [a]	CO_x	$\sum C_4$ [b]	$\sum C_4$	$\sum C_4$
HMS	1	10	6	2	18	25	39	36	0.4	0.01
V-HMS	4	17	7	3	19	8	45	46	2.3	0.08
6Ti-HMS	5	8	7	10	4	4	67	28	1.5	0.06
V-6Ti-HMS	14	8	7	3	20	2	61	37	5.0	0.18
19Ti-HMS	6	10	9	13	5	4	59	37	2.1	0.08
V-19Ti-HMS	17	9	8	4	23	2	53	44	7.7	0.28

[a] Sum of C_1–C_3 hydrocarbons and acetaldehyde.
[b] Sum of C_4 alkene selectivity, yield or productivity, resp.
[c] g_{prod} g_{cat}^{-1} h^{-1}.

titanium [28]. Reiche et al. [64] who investigated V-titaniumsilicate aerogels prepared by direct synthesis and impregnated by vanadium showed the same results as in our work and this observation proves successful synthesis of titanosilicate with Ti—O—Si bonds. However, we must take into account that redox behavior of supported vanadium species is very complex problem and can be affected by structural changes during heating of the sample, nature of vanadia complex (monomer/polymer/oxide) or nature of support and interaction of vanadia with support [3,65,66]. In addition, we must take into account that only part of vanadia species is probably coordinated to surface in close vicinity of titanium. Shift of TPR onset to lower temperature with increasing titanium content clearly indicates interaction of vanadium complexes with titanium (see Table 1).

3.2. Catalytic tests of n-butane ODH

Oxidative dehydrogenation of *n*-butane over investigated samples was studied at 460 °C. Main results for both prepared supports and vanadium impregnated catalysts are presented in Fig. 8 and Table 2. The main reaction products identified in the reaction mixture were: 1-butene (1-C_4), *cis*- and *trans*-2-butene (*c*-C_4 and *t*-C_4), 1,3-butadiene (1,3-C_4), methane (C_1), ethane and ethene (C_2), propane and propene (C_3), carbon oxides (CO_X) and traces of acetaldehyde. The carbon balance was 98 ± 3% in all catalytic tests and no coke deposit was observed on the catalysts. The activity of catalysts only slightly depended on the time-on-stream (TOS) and changes in conversion degree were less than 1% during 10 h.

All prepared supports exhibited measurable activity in the activation of *n*-butane. The catalytic activity of both titanosilicate matrices was significantly higher when compared to the pure silica material, and ca. 5% conversion degree of *n*-butane was obtained over these materials. The ability of titanosilicate matrix to activate alkanes was also reported in ODH of propane by TS-1 catalyst [67]. Because the activity of supports cannot be neglected, it must be taken into account in the evaluation of the activity of prepared vanadium based catalyst. The catalytic activity of obtained vanadium impregnated materials was higher for all catalysts than activity of pure support material. The highest change of catalytic activity was obtained for sample of V-19Ti-HMS for which the *n*-butane conversion increased from 6 to 17% after VO_X impregnation.

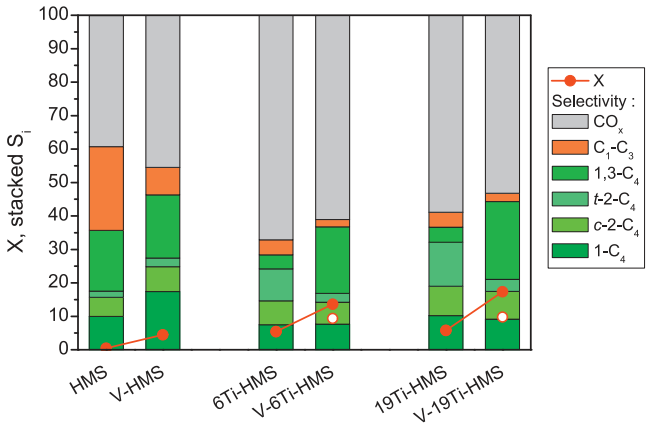

Fig. 8. The conversion (full red circle and line), hypothetic conversion (hollow red circle point) and selectivity (stacked bar) of bare supports and support with impregnated vanadium in ODH of *n*-butane at 460 °C. (For interpretation of the references to color in this figure legend, the reader is referred to the web version of the article.)

The degree of *n*-butane conversion obtained over our samples did not exceed 20%, hence it can be assumed that the value of conversion is at first approximation proportional to the reaction rate. The summation of conversion values obtained on the Ti-HMS and V-HMS materials can be under this assumption taken as a proportional to hypothetic reaction rate occurring on the system of two independent active sites. These sum of conversion values on Ti-HMS and V-HMS material (in Fig. 8 presented as hollow red circle point) are for both V-Ti-HMS materials lower than experimentally obtained values of conversion of *n*-butane. Therefore, some synergy effect can be observed. The V/TiO_2 based catalysts are reported [11,27,31,32,68] as materials with significantly higher activity in partial oxidation or oxidative dehydrogenation of alkanes in comparison to V/SiO_2 based materials. Hence, the observed enhancement of catalytic activity over the mesoporous titanosilicate supported vanadium oxide catalysts is an evidence of the interaction of vanadium atoms with titanium oxide species on the surface of these materials.

The selectivity to sum of C_4-ODH products obtained over prepared samples of catalysts was below 50% and highest selectivity to these products (46%) was obtained over the sample V-HMS. Selectivity to C_4-ODH products was in all cases lower over pure matrices and the impregnation of vanadium increased the selectivity to ODH products and decreased the selectivity to products of *n*-butane cracking. The presence of titanium in catalysts slightly decreased the selectivity to C_4-ODH products, but the lowering of this value does not exceed 10% for the sample V-6Ti-HMS. It can be seen that V-19Ti-HMS sample exhibited comparable selectivity to C_4-ODH products (44%) comparable to selectivity which was achieved on the sample V-HMS.

To the best of our knowledge, the only reported results on C_4-ODH over VO_X–titanosilicate catalysts were presented by Santacesaria et al. [11] who also published only small changes in selectivity to C_4-ODH products over VO_X–TiO_2/SiO_2 based catalyst in comparison to the VO_X/SiO_2 samples. The comparison of our results with data from this paper also clearly shows significant differences in distribution of individual C_4-ODH products. The 1,3-butadiene was the most abundant product in our C_4-ODH products over all vanadium containing catalysts with the selectivity ca. 20% and similar high selectivity to 1,3-butadiene was published

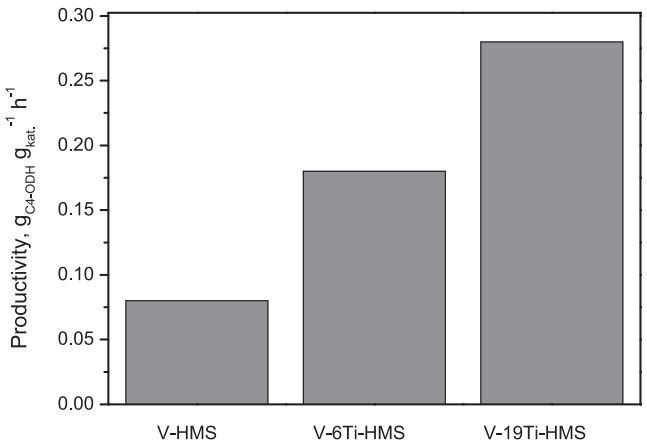

Fig. 9. Productivity to C_4 dehydrogenation products in *n*-butane ODH over V-HMS and V-Ti-HMS catalysts.

previously [3] over the other set of V-HMS materials, whereas the Santacesaria et al. [11] published nearly equimolar selectivity to 1-C_4, *t*-2-C_4 and *c*-2-C_4 with only a small amount of 1,3-C_4 (less than 12%) for catalysts with similar vanadium concentration. Moreover the similar distribution of C_4-ODH products which was obtained in mentioned paper was obtained also over both of our Ti-HMS supports. Differences in the selectivity to C_4-ODH products between catalysts cannot be ascribed to one simple effect, but more likely to the superposition of two effects. The significantly lower contact times were used in mentioned article, which is also indicated by the lower reported conversion values (less than 10%) compared to conversion values reached over our VO_X catalysts. It could be one effect which suppresses the occurrence of subsequent ODH reactions which can be a source of 1,3-butadiene. Nevertheless, solely this effect cannot explain the difference between the 1,3-C_4 selectivity over our Ti-HMS supports and VO_X–Ti-HMS catalysts. The higher selectivity to 1,3-butadiene over our VO_X containing catalysts in comparison to the Ti-HMS support materials is hence most likely caused by one-step subsequent ODH reaction of butenes occurring without the desorption to the gas phase, facilitated by the more acidic nature of VO_X active sites which prolongs the time of alkene retention on the surface as it was recently suggested [7,69]

The productivity of C_4-ODH products over prepared vanadium containing catalysts is presented in Fig. 9. It can be clearly seen that productivity to desired C_4-ODH products increases with increasing amount of titanium mesoporous support. When we compare the results obtained for vanadium catalysts impregnated on Ti-HMS support with our recently published data [3] it is evident that the presence of titanium in the mesoporous HMS matrix has significant promoting effect to the catalytic activity of V-Ti-HMS materials. The activity of V-19Ti-HMS catalyst at 460 °C is comparable with the activity of previously reported material I-VHMS-2.1 at 540 °C retaining the selectivity to C_4-ODH products, except for slightly higher selectivity to 1,3-butadiene. The improvement of activity of VO_X catalyst impregnated on mesoporous titanosilicate support hence offers the possibility to carry the reaction at lower temperature or to use catalysts with lower loading of vanadium.

4. Conclusion

Here presented results indicate successful one-pot synthesis of mesoporous titanosilicate with high titanium content (up to 19 wt.%) isomorphously incorporated into framework. No method of characterization detected signals attributable to bulk TiO_2 phase either for neither fresh materials nor catalysts after reaction conditions (460 °C for at least 10 h). These materials seem to be promising supports for vanadium oxide-based catalysts allowing their good dispersion. Advanced properties of these materials were demonstrated in C_4-ODH reaction. Productivity to desired C_4-ODH products was four times higher for titanosilicate materials compared with silica-based V-HMS materials and reached value up to 280 g of C_4 alkenes per 1 kg of catalyst per hour.

Acknowledgement

The authors thank to project of the Czech Science Foundation No. P106/10/0196 for financial support.

References

[1] A. Comite, A. Sorrentino, G. Capannelli, M. Di Serio, R. Tesser, E. Santacesaria, Journal of Molecular Catalysis A-Chemical 198 (2003) 151.
[2] L.M. Madeira, M.F. Portela, Catalysis Reviews-Science and Engineering 44 (2002) 247.
[3] M. Setnicka, R. Bulanek, L. Capek, P. Cicmanec, Journal of Molecular Catalysis A-Chemical 344 (2011) 1.
[4] H.H. Kung, Advances in Catalysis, vol. 40, Academic Press Inc., San Diego, 1994, p. 1.
[5] B.M. Weckhuysen, D.E. Keller, Catalysis Today 78 (2003) 25.
[6] H.J. Tian, E.I. Ross, I.E. Wachs, Journal of Physical Chemistry B 110 (2006) 9593.
[7] T. Blasco, J.M.L. Nieto, Applied Catalysis A-General 157 (1997) 117.
[8] E.A. Mamedov, V.C. Corberan, Applied Catalysis A-General 127 (1995) 1.
[9] R. Bulanek, A. Kaluzova, M. Setnicka, A. Zukal, P. Cicmanec, J. Mayerova, Catalysis Today 179 (2012) 149.
[10] R. Bulánek, P. Čičmanec, H. Sheng-Yang, P. Knotek, L. Čapek, M. Setnička, Applied Catalysis A-General (2012).
[11] E. Santacesaria, M. Cozzolino, M. Di Serio, A.M. Venezia, R. Tesser, Applied Catalysis A-General 270 (2004) 177.
[12] S. Albonetti, F. Cavani, F. Trifiro, Catalysis Reviews-Science and Engineering 38 (1996) 413.
[13] R.M. Martin-Aranda, J. Cejka, Topics in Catalysis 53 (2010) 141.
[14] F. Cavani, Journal of Chemical Technology and Biotechnology 85 (2010) 1175.
[15] A.A. Teixeira-Neto, L. Marchese, H.O. Pastore, Quimica Nova 32 (2009) 463.
[16] I.E. Wachs, B.M. Weckhuysen, Applied Catalysis A-General 157 (1997) 67.
[17] E.V. Kondratenko, M. Cherian, M. Baerns, D.S. Su, R. Schloegl, X. Wang, I.E. Wachs, Journal of Catalysis 234 (2005) 131.
[18] Q.H. Zhang, Y. Wang, Y. Ohishi, T. Shishido, K. Takehira, Journal of Catalysis 202 (2001) 308.
[19] W. Liu, S.Y. Lai, H.X. Dai, S.J. Wang, H.Z. Sun, C.T. Au, Catalysis Letters 113 (2007) 147.
[20] P. Gruene, T. Wolfram, K. Pelzer, R. Schlogl, A. Trunschke, Catalysis Today 157 (2010) 137.
[21] Y.M. Liu, Y. Cao, N. Yi, W.L. Feng, W.L. Dai, S.R. Yan, H.Y. He, K.N. Fan, Journal of Catalysis 224 (2004) 417.
[22] F. Ying, J.H. Li, C.J. Huang, W.Z. Weng, H.L. Wan, Catalysis Letters 115 (2007) 137.
[23] L. Capek, R. Bulanek, J. Adam, L. Smolakova, H. Sheng-Yang, P. Cicmanec, Catalysis Today 141 (2009) 282.
[24] P. Knotek, L. Capek, R. Bulanek, J. Adam, Topics in Catalysis 45 (2007) 51.
[25] K. Cassiers, T. Linssen, M. Mathieu, M. Benjelloun, K. Schrijnemakers, P. Van Der Voort, P. Cool, E.F. Vansant, Chemistry of Materials 14 (2002) 2317.
[26] M. Kruk, M. Jaroniec, A. Sayari, Microporous Materials 9 (1997) 173.
[27] N. Hamilton, T. Wolfram, G. Tzolova Muller, M. Havecker, J. Krohnert, C. Carrero, R. Schomacker, A. Trunschke, R. Schlogl, Catalysis Science and Technology (2012).
[28] O. Ovsitser, M. Cherian, A. Bruckner, E.V. Kondratenko, Journal of Catalysis 265 (2009) 8.
[29] E. Kondratenko, M. Cherian, M. Baerns, Catalysis Today 112 (2006) 60.
[30] A. Dinse, B. Frank, C. Hess, D. Habel, R. Schomacker, Journal of Molecular Catalysis A-Chemical 289 (2008) 28.
[31] D. Shee, G. Deo, Catalysis Letters 124 (2008) 340.
[32] J.H. Kwak, J.E. Herrera, J.Z. Hu, Y. Wang, C.H.F. Peden, Applied Catalysis A-General 300 (2006) 109.
[33] A. Zhang, Z. Li, Z. Li, Y. Shen, Y. Zhu, Applied Surface Science 254 (2008) 6298.
[34] W. Zhang, B.S. Zhang, T. Wolfram, L.D. Shao, R. Schlogl, D.S. Su, Journal of Physical Chemistry C 115 (2011) 20550.
[35] M.A. Bañares, X. Gao, J.L.G. Fierro, I.E. Wachs, in: S.T.O.A.M.G.R.K. Grasselli, J.E. Lyons (Eds.), Studies in Surface Science and Catalysis, vol. 110, Elsevier, 1997, p. 295.
[36] F. Bérubé, F. Kleitz, S. Kaliaguine, Journal of Materials Science 44 (2009) 6727.
[37] A. Tuel, Microporous and Mesoporous Materials 27 (1999) 151.
[38] Y. Chen, Y. Huang, J. Xiu, X. Han, X. Bao, Applied Catalysis A-General 273 (2004) 185.
[39] R.S. Araújo, D.C.S. Azevedo, E. Rodríguez-Castellón, A. Jiménez-López, C.L. Cavalcante Jr, Journal of Molecular Catalysis A-Chemical 281 (2008) 154.
[40] W. Zhang, M. Fröba, J. Wang, P.T. Tanev, J. Wong, T.J. Pinnavaia, Journal of the American Chemical Society 118 (1996) 9164.
[41] S. Gontier, A. Tuel, Zeolites 15 (1995) 601.

[42] T. Blasco, A. Corma, M.T. Navarro, J.P. Pariente, Journal of Catalysis 156 (1995) 65.
[43] M. Morey, A. Davidson, G. Stucky, Microporous Materials 6 (1996) 99.
[44] M. Nandi, A. Bhaumik, Chemical Engineering Science 61 (2006) 4373.
[45] P.T. Tanev, T.J. Pinnavaia, Science 267 (1995) 865.
[46] M. Pouzar, T. Kratochvil, L. Capek, L. Smolakova, T. Cernohorsky, A. Krejcova, L. Hromadko, Talanta 83 (2011) 1659.
[47] R. Bulanek, L. Capek, M. Setnicka, P. Cicmanec, Journal of Physical Chemistry C 115 (2011) 12430.
[48] L. Capek, J. Adam, T. Grygar, R. Bulanek, L. Vradman, G. Kosova-Kucerova, P. Cicmanec, P. Knotek, Applied Catalysis A-General 342 (2008) 99.
[49] P. Kubelka, F.Z. Munk, Technical Physics 12 (1931) 593.
[50] Y. Liu, K. Murata, M. Inaba, N. Mimura, Applied Catalysis A-General 309 (2006) 91.
[51] C. Chen, Q.H. Zhang, J. Gao, W. Zhang, J. Xu, Journal of Nanoscience and Nanotechnology 9 (2009) 1589.
[52] S.A. Karakoulia, K.S. Triantafyllidis, A.A. Lemonidou, Microporous and Mesoporous Materials 110 (2008) 157.
[53] J. Santamaria-Gonzalez, J. Luque-Zambrana, J. Merida-Robles, P. Maireles-Torres, E. Rodriguez-Castellon, A. Jimenez-Lopez, Catalysis Letters 68 (2000) 67.
[54] G.W. Wallidge, R. Anderson, G. Mountjoy, D.M. Pickup, P. Gunawidjaja, R.J. Newport, M.E. Smith, Journal of Materials Science 39 (2004) 6743.
[55] Y. Djaoued, S. Badilescu, P.V. Ashrit, D. Bersani, P.P. Lottici, J. Robichaud, Journal of Sol–Gel Science and Technology 24 (2002) 255.
[56] M. Ocana, V. Fornes, J.V.G. Ramos, C.J. Serna, Journal of Solid State Chemistry 75 (1988) 364.
[57] P.M. Kumar, S. Badrinarayanan, M. Sastry, Thin Solid Films 358 (2000) 122.
[58] M. Chatterjee, H. Hayashi, N. Saito, Microporous and Mesoporous Materials 57 (2003) 143.
[59] X.T. Gao, I.E. Wachs, Journal of Physical Chemistry B 104 (2000) 1261.
[60] J. Tauc, Amorphous and Liquid Semiconductors, Plenum Press, London, 1974.
[61] C. Li, G. Xiong, Q. Xin, J.K. Liu, P.L. Ying, Z.C. Feng, J. Li, W.B. Yang, Y.Z. Wang, G.R. Wang, X.Y. Liu, M. Lin, X.Q. Wang, E.Z. Min, Angewandte Chemie-International Edition 38 (1999) 2220.
[62] W.H. Zhang, J.Q. Lu, B. Han, M.J. Li, J.H. Xiu, P.L. Ying, C. Li, Chemistry of Materials 14 (2002) 3413.
[63] A. Sorrentino, S. Rega, D. Sannino, A. Magliano, P. Ciambelli, E. Santacesaria, Applied Catalysis A-General 209 (2001) 45.
[64] M.A. Reiche, E. Ortelli, A. Baiker, Applied Catalysis B-Environmental 23 (1999) 187.
[65] B.E. Handy, A. Baiker, M. Schraml-Marth, A. Wokaun, Journal of Catalysis 133 (1992) 1.
[66] F. Arena, F. Frusteri, G. Martra, S. Coluccia, A. Parmaliana, Journal of the Chemical Society-Faraday Transactions 93 (1997) 3849.
[67] W. Schuster, J.P.M. Niederer, W.F. Hoelderich, Applied Catalysis A-General 209 (2001) 131.
[68] I.E. Wachs, J.M. Jehng, G. Deo, B.M. Weckhuysen, V.V. Guliants, J.B. Benziger, S. Sundaresan, Journal of Catalysis 170 (1997) 75.
[69] L.C. Marcu, L. Sandulescu, Y. Schuurman, J.M.M. Millet, Applied Catalysis A-General 334 (2008) 207.